Oxford Brookes University
Faculty of Health and Life Sciences
Department of Biological and Medical Sciences

Functional Characterisation of Aphid, *Myzus persicae*, Nicotinic Acetylcholine Receptors and Identification of a Novel Biogenic Amine-Gated Ion Channel from the Honeybee, *Apis mellifera*.

Eleanor Louise Mitchell

Collaborating Establishments:
Syngenta

A thesis submitted in partial fulfilment of the requirement of Oxford Brookes University for the degree of Doctor of Philosophy

PhD Thesis

December 2022

Declaration

I hereby declare that this thesis was written in full by myself and all research present is my own original work and has not been submitted in fulfilment for any other previous application for a degree. All sources of information have been acknowledged.

Acknowledgements

My gratitude goes to the BBSRC and Syngenta for funding this PhD. My PhD was part of the Oxford Interdisciplinary Bioscience Doctoral Training Programme, so my thanks goes to them for the training provided and the support from my fellow students. I must thank the University of Oxford for the use of library resources. Thank you to Syngenta for providing the *Myzus persicae*.

Thank you to my primary supervisor, Dr Andrew Jones, for all his support and feedback and unfailing enthusiasm for any result however bizarre or seemingly insignificant. I am grateful to Prof Isabel Bermudez for assistance and troubleshooting the electrophysiology work. Thanks is also given to my industrial supervisor James Goodchild at Syngenta for feedback on my work and supervising my industrial placement.

I want to thank everyone who has supported me at Oxford Brookes University, especially the technicians who kept everything running. My gratitude to all my colleagues in the laboratory and office, in particular everyone involved in oocyte preparation. I want to also thank everyone at the university who has given feedback on my research.

I would like to thank Mum and Dad for all their encouragement and help over the years. Thanks is also given to wider family and friends for their support and interest.

Contents

Chapter 1 Introduction 21

1.1 Neurotransmitters in Insects 21

1.2 Nicotinic Acetylcholine Receptors 21

1.3 Nicotinic Acetylcholine Receptors in Insects 25

1.4 The Insect α5 nAChR Subunit 28

1.5 The Heterologous Expression of Insect nAChRs 28

1.5.1 NACHO 32

1.5.2 UNC-50 33

1.5.3 TMX3 33

1.5.4 RIC-3 33

1.6 Insecticides and Crop Protection 35

1.7 Insecticides and Insect Populations 35

1.8 Neonicotinoids and Spinosad 38

1.9 Knockout Studies of nAChR in Insects 40

1.10 *Myzus persicae* 42

1.11 *Apis mellifera* 44

1.12 Aim of Thesis 46

Chapter 2 Methods 48

2.1 Reagents 48

2.2 Animals 48

2.3 DNA sequencing 49

2.4 Molecular Biology 49

2.4.1 RNA Extraction and Reverse Transcription 49

2.4.2 Cloning Protocol 49

2.4.3 Midipreps 56

2.4.4 Maxipreps 56

2.4.5 *In vitro* Transcription 56

2.4.6 Site-Directed Mutagenesis 57
2.4.7 Acquiring *M. persicae* β1 R81T Mutant from Twist Bioscience 58
2.4.8 Sequence Analysis 58
2.5 Electrophysiology 58
2.5.1 Preparing Oocytes 58
2.5.2 Injecting DNA or RNA 59
2.5.3 Two-Electrode Voltage-Clamp Electrophysiology 61
2.5.4 Dose-Response Curves 62
2.5.5 Testing Chemicals 62
2.6 Statistical Analysis 62
Chapter 3 Cloning of *Myzus persicae* Nicotinic Acetylcholine Receptor Subunits and Chaperones 64
3.1 Introduction 64
3.1.1 Cloning of Insect Nicotinic Acetylcholine Receptor Families 64
3.1.2 Cloning of Insect Nicotinic Acetylcholine Receptor Chaperones 65
3.2 Aim 66
3.3 Results 67
3.3.1 Sequence Predictions 67
3.3.2 Cloning of *M. persicae* β1 and β2 Subunits 67
3.3.3 Sequences of Cloned *M. persicae* Nicotinic Acetylcholine Receptor Subunits 70
3.3.3 Description of Cloned *M. persicae* Nicotinic Acetylcholine Receptor Chaperones ... 80
3.3.5 Phylogenetic Analysis of the Cloned *M. persicae* Nicotinic Acetylcholine Receptor Subunits 85
3.4 Discussion 87
3.4.1 *M. persicae* nAChR Subunits 87
3.4.2 *M. persicae* nAChR Chaperones 89
3.5 Conclusion 91

Chapter 4 Functional Expression of Nicotinic Acetylcholine Receptors from *Myzus persicae* with the Assistance of Protein Chaperones....92

4.1 Introduction....92

4.1.1 The Expression of nAChRs Containing the Insect α6 Subunit....92

4.1.2 The Expression of Ionotropic Acetylcholine Receptors from Nematodes in *X. laevis* Oocytes using RIC-3, UNC-50 and TMX3....93

4.1.3 The Expression of nAChRs from Insects and Crustaceans in *X. laevis* Oocytes using RIC-3, UNC-50 and TMX3....93

4.2 Aims....95

4.3 Results....95

4.3.1 Expression of a nAChR Composed of the *M. persicae* α6 and α7 Subunits with NACHO and RIC-3 by Injection of DNA.....95

4.3.2 Expression of a nAChR Composed of the *M. persicae* α1, α3, α8 and β1 Subunits with RIC-3, UNC-50 and TMX3 by Injection of DNA.....95

4.3.3 Expression of a nAChR Composed of the *M. persicae* α1, α2, α8 and β1 Subunits with RIC-3, UNC-50 and TMX3 by Injection of DNA.....96

4.3.4 Expression of a nAChR Composed of the *M. persicae* α1, α3, α8 and β1 Subunits with RIC-3, UNC-50 and TMX3 by Injection of RNA.....97

4.3.5 Expression of a nAChR Composed of the *M. persicae* α1, α2, α8 and β1 Subunits with RIC-3, UNC-50 and TMX3 by Injection of RNA.....98

4.3.6 Expression of a nAChR Composed of the *D. melanogaster* α1 and *M. persicae* α3, α8 and β1 nAChR Subunits with *M. persicae* RIC-3, UNC-50 and TMX3 by Injection of DNA..99

4.3.7 Expression of a nAChR Composed of the *D. melanogaster* α1 and *M. persicae* β1 with *M. persicae* RIC-3, UNC-50 and TMX3 by Injection of DNA.....101

4.4 Discussion....106

4.4.1 Expression of *M. persicae* nAChRs with Chaperones....106

4.4.2 Expression of nAChRs Composed of *D. melanogaster* and *M. persicae* Subunits with Chaperones....107

4.4.3 The Interactions of Neonicotinoids with the nAChR Composed of the *D. melanogaster* α1 and *M. persicae* β1 Subunits....109

4.4.4 Further Work 109

4.5 Conclusion 111

Chapter 5 Functional Characterisation of the Homomeric *Apis mellifera* α5 Nicotinic Acetylcholine Receptor 112

5.1 Introduction 112

5.1.1 Expression of α5, α6 and α7 Insect Nicotinic Acetylcholine Receptors 112

5.1.2 The Insect α5 Nicotinic Acetylcholine Receptor Subunit 114

5.2 Chapter Aim 115

5.3 Results 115

5.3.1 Phylogenetic analysis of the *A. mellifera* α5 nicotinic acetylcholine receptor subunit 115

5.3.2 Cloning the *A. mellifera* α5 Nicotinic Acetylcholine Receptor Subunit 119

5.3.3 Expression of the *A. mellifera* α5 Nicotinic Acetylcholine Receptor Subunit in *X. laevis* Oocytes 119

5.3.4 Co-expression of the *A. mellifera* α5 Nicotinic Acetylcholine Receptor Subunit with other *A. mellifera* Nicotinic Acetylcholine Receptor Subunits 122

5.3.5 Actions of Insecticides and Other Nicotinic Acetylcholine Receptor Targeting Compounds on the *A. mellifera* α5 Nicotinic Acetylcholine Receptor 124

5.4 Discussion 128

5.4.1 The Non-Dipteran α5 Subunits are a Phylogenetically Distinct Group from Other Insect Nicotinic Acetylcholine Receptor Subunits. 128

5.4.2 The Properties of the *A. mellifera* α5 as a Homomeric Nicotinic Acetylcholine Receptor 129

5.5 Conclusion 138

Chapter 6 The Functional Characterisation of the *Apis mellifera* α5 nAChR with Biogenic Amines and Other Neurotransmitters 139

6.1 Introduction 139

6.1.1 Cys-loop Ligand Gated Ion Channels Activated by Other Biogenic Amines 139

6.1.2 Biogenic Amines in the Honeybee Brain 142

6.1.3 Biogenic Amines and Honeybee Behaviour 143
6.2 Chapter Aim 145
6.3 Results 146
6.3.1 Response of the *A. mellifera* α5 nAChR to 5-HT 146
6.3.2 Response of the *A. mellifera* α5 nAChR to Dopamine 148
6.3.3 Response of the *A. mellifera* α5 nAChR to Octopamine 149
6.3.4 Response of the *A. mellifera* α5 nAChR to Tyramine 151
6.3.5 Response of the *A. mellifera* α5 nAChR to Histamine 153
6.3.6 Response of the *A. mellifera* α5 nAChR to GABA, Glycine and Glutamate 154
6.3.7 Comparing the Responses of the *A. mellifera* α5 nAChR to Different Neurotransmitters 154
6.4 Discussion 156
6.4.1 The *A. mellifera* α5 nAChR is Primarily a Dopamine Receptor with Other Biogenic Amines Showing Agonist Actions 156
6.4.2 Amitraz Does Not Act on the *A. mellifera* α5 nAChR 158
6.5 Conclusion 158
Chapter 7 Final Discussion 159
7.1 The Heterologous Expression of Insect nAChRs in *X. laevis* oocytes 159
7.2 The Potential Functions of an Ionotropic Dopamine Receptor in *A. mellifera* 159
7.3 The Possibility of Reclassifying the *A. mellifera* α5 as an Ionotropic Dopamine Receptor 160
Chapter 8 References 162
Chapter 9 Appendix 187

List of Figures

Figure 1.1 Structure of the nAChR. Schematic representation of a heteromeric receptor consisting of two α (dark grey) and three non-α subunits (light grey). The polypeptide layout of two subunits are shown highlighting the cys-loop (two white circles connected by a white double line), the two vicinal cysteines in loop C defining α subunits and four transmembrane domains (TM1-4) with a large intracellular loop between TM3 and TM4. The six binding loops (A-F) that contribute to ligand binding are shown and two acetylcholine (ACh) molecules are bound to this particular nAChR. The five subunits that make up the receptor are arranged around a central cation-permeable channel modified from (Jones and Sattelle, 2010). ----------24

Figure 1.2 Structure of the human α7 nAChR. Figure S4 from (Noviello et al., 2021). A–C. Side views of each model. ECD, extracellular domain. TMD, transmembrane domain. ICD, intracellular domain. The coupling region is boxed. D. A subunit interface labelled to indicate loops, domains, helices and glycans. Deletion of disordered residues in the EM construct and insertion of bRIL are indicated. ----------25

Figure 1.3 Tree showing the nAChR gene families of A. gambiae, A. mellifera, B. mori, D. melanogaster and T. castaneum. Based on their high amino acid sequence homology, several insect nAChR subunits cluster into groups. Each insect possesses at least one divergent subunit that does not fall into any of these groups. From (Jones and Sattelle, 2010) ----------27

Figure 1.4 Chemical structure of nithiazine and neonicotinoid insecticides. Nithiazine is a synthetic compound with insecticidal activity on nAChRs which was a lead compound for the development of neonicotinoid insecticides. The neonicotinoid insecticides include chloronicotinyl compounds (imidacloprid, nitenpyram, acetamiprid and thiacloprid), thianicotinyl compounds (thiamethoxam and clothianidin) and the furanicotinyl compound (dinotefuran) from (Millar and Denholm, 2007). ----------39

Figure 1.5 M. persicae David Cappaert, Bugwood.org.----------43

Figure 2.1 A flowchart of the cloning process for M. persicae nAChR subunits. ----------50

Figure 2.2 1 kb plus ladder used for gels from https://international.neb.com/products/n3200-1-kb-plus-dna-ladder#Product%20Information ----------54

Figure 2.3 Circuit diagram of the two-electrode voltage clamp system. Mitchell personal figure. ---------61

Figure 3.1 Schematic representation of the alternatively spliced A. mellifera RIC-3 variants. Adapted from (Brunello et al., 2022). ----------66

Figure 3.2 Example agarose gels showing amplification products after reverse transcription and PCR. Well numbers in table correspond to labelled well numbers on gel. Gel images of amplification products of M. persicae β1 and β2 nAChR subunits before and after band excision. The photograph of the top gel was taken with low UV before excision on a Transilluminator Model MUV2020-312 (Major Science, Saratoga, CA, USA). The bottom gel photograph was taken, after excision using a Bio-rad Gel imager (Hercules, CA, USA). The 1kb NEB plus ladder (Figure 2.2.) was used.----------68

Figure 3.3 Agarose gel of colony PCR to detect the cloning of M. persicae β1 and β2 nAChR subunits from transformed E. coli colonies. Well numbers in table correspond to labelled well numbers on gel. The top

row shows β1 colonies and the bottom row β2 colonies. The image taken using a Bio-rad Gel imager. The 1kb NEB plus ladder (Figure 2.2) was used.----------69
Figure 3.4 An agarose gel showing the digest of the minipreps of M. persicae β1 and β2 with XhoI and XbaI. Well numbers in table correspond to labelled well numbers on gel. Both the pCI plasmid (~3 kb) and insert (1-1.8 kb) can be seen. The image taken using a Bio-rad Gel imager and the red bands were a result of overexposure. The 1 kb plus ladder (Figure 2.2) was used. ----------70
Figure 3.5 Peptide sequences of cloned M. persicae α3 and α8 nAChR subunits, which are identical to accession numbers AJ236786 and AJ236787 when translated respectively. The predicted signal peptide is in lowercase, predicted transmembrane helices in bold, the cys-loop cysteines underlined and the consecutive cysteines present in α subunits double underlined. ----------71
Figure 3.6 The aligned sequences of two clones (a1c22 and a1c21) of M. persicae α1 nAChR subunits. The predicted signal peptide is in lowercase, predicted transmembrane helices in bold, the cys-loop cysteines underlined, the consecutive cysteines present in α subunits double underlined and putative phosphorylation sites that differ between the two isoforms circled, predicted using NetPhos 3.1 (https://services.healthtech.dtu.dk/service.php?NetPhos-3.1). ----------72
Figure 3.7 The aligned sequences of the predicted sequence and three clones (a2c2o, α2c31 and a2c37) of M. persicae α2 nAChR subunits. Predicted transmembrane helices are shown in bold, the cys-loop cysteines underlined and the consecutive cysteines present in α subunits double underlined.----------74
Figure 3.8 Alignment of the predicted sequence and two clones (a4c7 and a4c5) of M. persicae α4 nAChR subunits. The predicted signal peptide is in lowercase, predicted transmembrane helices in bold, the cys-loop cysteines underlined and the consecutive cysteines present in α subunits double underlined. --------75
Figure 3.9 The aligned sequences of two clones (a6c3 and a6c6) of M. persicae α6 nAChR subunits. The predicted signal peptide is in lowercase, predicted transmembrane helices in bold, the cys-loop cysteines underlined and the consecutive cysteines present in α subunits double underlined. Exon 8a is highlighted in light grey and exon 8b is highlighted in dark grey. ----------76
Figure 3.10 The aligned sequences of two clones (a7c10 and a7c12) of M. persicae α7 nAChR subunits. The predicted signal peptide is in lowercase, predicted transmembrane helices in bold, the cys-loop cysteines underlined and the consecutive cysteines present in α subunits double underlined. Exon 6a is highlighted in light grey shading. Exon 7a is highlighted in medium grey shading with white text and exon 7b in dark grey shading with white text. ----------77
Figure 3.11 The aligned sequences of two clones (β1c6 and β1c4) of M. persicae β1 nAChR subunits. The predicted signal peptide is in lowercase, predicted transmembrane helices in bold and the cys-loop cysteines underlined. R81, which has been found mutated in strains of M. persicae resistant to neonicotinoids (Bass et al., 2011), is highlighted in grey.----------78
Figure 3.12 The aligned sequences of two clones (a9c7 and a9c2) of M. persicae α9 nAChR subunits. The predicted signal peptide is in lowercase, predicted transmembrane helices in bold and the consecutive cysteines present in α subunits double underlined. Single amino acid changes between the α9 clones are highlighted in grey.----------79

Figure 3.13 The cloned sequence of the M. persicae α10 subunit. The predicted signal peptide is in lowercase, predicted transmembrane helices in bold and the consecutive cysteines present in α subunits double underlined. ----------*79*
Figure 3.14 The aligned predicted sequence and sequences of two clones (β2c18 and β2c13) of M. persicae β2 nAChR subunits. The predicted signal peptide is in lowercase, predicted transmembrane helices in bold and the cys-loop cysteines underlined. ----------*80*
Figure 3.15 The aligned sequences of NACHO from M. persicae and A. mellifera (UKN32600) (Hawkins, Mitchell and Jones, 2022). The predicted signal peptide is in lowercase and predicted transmembrane helices in bold. ----------*81*
Figure 3.16 The cloned sequence of M. persicae UNC-50. Predicted transmembrane helices are in bold.81
Figure 3.17 The cloned sequence of M. persicae TMX3. The predicted signal peptide is in lowercase and predicted transmembrane helices in bold. ----------*82*
Figure 3.18 The aligned sequences of three clones (RIC3c23, RIC3c25 and RIC3c21) from M. persicae, DmRIC-3[6,7,9] from D. melanogaster (Lansdell et al., 2008) (AM902271 translated using ExPASy https://web.expasy.org/translate/), also from (Ihara et al., 2020) and Amel RIC-3 from A. mellifera (Ihara et al., 2020) (BCD56240.1). Bold shows predicted transmembrane helices, underlined predicted coiled-coil domains and boxed putative A to I editing. Dmel RIC-3 and Amel RIC-3 transmembrane helices predicted with MemBrain 3.1 (Feng et al., 2020), coiled-coil domains predicted with DeepCoil (Zimmermann et al., 2018; Gabler et al., 2020; Ludwiczak et al., 2019). ----------*84*
Figure 3.19 A section of the chromatogram of the PCR product of M. persicae RIC-3, showing potential A to I editing. AB1 file displayed using Chromas (Technelysium, South Brisbane, Australia). ----------*85*
Figure 3.20 Tree showing the relationship of M. persicae (Mper) subunits with those of A. pisum (Apis), A. mellifera (Amel) and D. melanogaster (Dmel), ELIC was used as an outgroup. For accession numbers for A. pisum, D. melanogaster and A. mellifera see Figure 5.1 in Chapter 5. ----------*86*
Figure 4.1 Representative current traces showing the response to different concentrations of acetylcholine (10 -300 µM) of X. laevis oocytes injected with M. persicae α1, α3, α8 and β1 nAChR subunit cDNAs and M. persicae RIC-3, UNC-50 and TMX3 cDNAs. ---------- ***Error! Bookmark not defined.***
Figure 4.2 Traces showing the response to 1 mM acetylcholine of X. laevis oocytes injected with M. persicae α1, α2, α8 and β1 nAChR subunit cDNAs and M. persicae RIC-3, UNC-50 and TMX3 cDNAs. ***Error! Bookmark not defined.***
Figure 4.3 Representative current traces showing the response to different concentrations of acetylcholine (100 pM -300 µM) of X. laevis oocytes injected with M. persicae α1, α3, α8 and β1 nAChR subunit RNA and M. persicae RIC-3, UNC-50 and TMX3 RNA. ----------*98*
Figure 4.4 Representative current traces showing the response to different concentrations of acetylcholine (100 pM -1 mM) of X. laevis oocytes injected with M. persicae α1, α2, α8 and β1 nAChR subunit RNA and M. persicae RIC-3, UNC-50 and TMX3 RNA. ---------- ***Error! Bookmark not defined.***
Figure 4.5 Reponses to acetylcholine in X. laevis oocytes injected with the D. melanogaster α1 nAChR subunit and M. persicae α3, α8 and β1 nAChR subunits with M. persicae RIC-3, UNC-50 and TMX3. A.

Representative current traces showing responses to different concentrations of acetylcholine (1–1000 µM). The first trace shows the effect of applied SOS only indicating a response to pressure. B. Acetylcholine concentration response curve. Data are normalised to the maximal response (300 µM acetylcholine) and have a mean EC_{50} of 122.8 (78.09-193.2) µM from 5 oocytes from 3 different batches of oocytes. ---------- *100*

Figure 4.6 Reponses to acetylcholine in X. laevis oocytes injected with the D. melanogaster α1 nAChR subunit and M. persicae α3, α8 and β1 nAChR subunits with M. persicae RIC-3, UNC-50 and TMX3. Acetylcholine concentration response curves plotted separately of the data from Figure 4.5 (B). Data are normalised to the maximal response (300 µM acetylcholine). ---------- *101*

Figure 4.7 Reponses to acetylcholine in X. laevis oocytes injected with the D. melanogaster α1 nAChR subunit and M. persicae β1 nAChR subunits with M. persicae RIC-3, UNC-50 and TMX3. A. Representative current traces showing responses to different concentrations of acetylcholine (1–1000 µM). The first trace shows the response of an oocyte injected with water alone whilst the remaining traces show responses from oocytes injected with nAChR subunits. B. Acetylcholine concentration response curve. Data are normalised to the maximal response (300 µM acetylcholine) and have a mean EC_{50} of 91.05 (67.69-122.5) µM from 5 oocytes from 3 different batches of oocytes. ---------- *102*

Figure 4.8 Reponses to acetylcholine in X. laevis oocytes injected with the D. melanogaster α1 subunit and M. persicae β1 subunit with M. persicae RIC-3, UNC-50 and TMX3. Acetylcholine concentration response curves plotted separately of the data from Figure 4.7 (B). Data are normalised to the maximal response (300 µM acetylcholine). ---------- *103*

Figure 4.9 Traces showing the nAChR composed of D. melanogaster α1 and M. persicae β1 with M. persicae RIC-3, UNC-50 and TMX3 expressed in X. laevis oocytes in response to 300 µM acetylcholine (ACh), then the response to 300 µM acetylcholine and 1 µM atropine following pre-incubation with 1 µM atropine for 3 min 29 s followed by the response to 300 µM acetylcholine only after a wash with SOS solution for 5 min. ---------- *104*

Figure 4.10 Traces showing the nAChR composed of D. melanogaster α1 and M. persicae β1 with M. persicae RIC-3, UNC-50 and TMX3 expressed in X. laevis oocytes in response to 300 µM acetylcholine (ACh), then 100 µM imidacloprid, then 300 µM acetylcholine after 3 min, then 300 µM acetylcholine after over 1 hour washing. ---------- *105*

Figure 4.11 Traces showing the nAChR composed of D. melanogaster α1 and M. persicae β1 with M. persicae RIC-3, UNC-50 and TMX3 expressed in X. laevis oocytes in response to 300 µM acetylcholine (ACh), then 100 µM thiacloprid, then 300 µM acetylcholine after 3 min. ----- ***Error! Bookmark not defined.***

Figure 4.12 The aligned peptide sequences of the α1 subunits from D. melanogaster and M. persicae. Identical amino acids highlighted in grey. The predicted signal peptide is in lowercase, predicted transmembrane helices in bold, the cys-loop cysteines underlined and the consecutive cysteines present in α subunits double underlined. Structural motifs were predicted as in Chapter 2.4.8. ---------- *110*

Figure 5.1 Tree showing relationships of insect and vertebrate α7–10 nAChR subunit protein sequences as well as vertebrate 5-HT3 subunits. Numbers at each node signify bootstrapping 1000 times

represented as a percentage of trees in which the associated taxa clustered together and the scale bar represents substitutions per site. ELIC (Accession number P0C7B7), from Dickeya chrysanthemi, a bacterial ancestor of cysLGICs, was used as an outgroup. Species subunit sequences used in the tree are as follows: Agam (A. gambiae) see (Jones, Grauso and Sattelle, 2005); Amel (A. mellifera) α5 (AJE70263) otherwise see (Jones et al., 2006); Apis (A. pisum) see (Dale et al., 2010); Bmor (B. mori) see (Shao, Dong and Zhang, 2007); Bter (B. terrestris) see (Sadd et al., 2015); Dmel (D. melanogaster); Pame (P. americana) see (Jones et al., 2020); Tcas (T. castaneum) see (Jones and Sattelle, 2007); Ggal (Gallus gallus) α7 (NP989512), α8 (CAA36544), α9 (NP990091), α10 (NP001094506), 5-HT3A (XP040508006); Hsap (Homo sapiens) α7 (CAA69697), α9 (NP060051), α10 (CAC20435), 5-HT3A (NP998786), 5-HT3B (NP006019.), 5-HT3C (AF459285), 5-HT3D (AY159812), 5-HT3E (AY159813); Mmus (Mus musculus) α7 (AAF35885), α9 (NP001074573), α10 (NP001074893), 5-HT3A (6Y59_A), 5-HT3B (NP064670). ----------116

Figure 5.2 Gene duplications from the phylogenetic tree in Figure 5.1, blue squares indicate a gene duplication event, created in MEGA X (Kumar et al., 2018). ----------117

Figure 5.3 Exon composition of a selection of insect α5, α6 and α7 nAChR subunits. Transmembrane regions are indicated as grey boxes, a star marks the adjacent cysteines denoting an α subunit and triangles the GEK sequence preceding TM2 that is important for cation selection (Corringer, Novère and Changeux, 2000; Jensen, Schousboe and Ahring, 2005). Exon boundaries are in blue. Exon boundaries shared between most α6, α7 and Dipteran α5 but not a majority of non-Dipteran α5 are indicated by a green arrow ----------118

Figure 5.4 Reponses to acetylcholine in X. laevis oocytes expressing the A. mellifera α5 nAChR subunit. A. Representative current traces showing responses to different concentrations of acetylcholine (0.1–10 mM). The first trace shows the response of an oocyte injected with water alone whilst the remaining traces show responses from oocytes injected with α5. B. Acetylcholine concentration response curve. Data are normalised to the maximal response (5 mM acetylcholine) and have a mean EC_{50} of 2.653 (2.405-2.926) mM from 15 oocytes from 7 different batches of oocytes. ----------120

Figure 5.5 Traces showing A. mellifera α5 nAChR expressed in X. laevis oocytes in response to 5 mM acetylcholine (ACh), then with 1 µM atropine following pre-incubation with 1 µM atropine for 5 min followed by ACh only again after a wash with SOS solution for 5 min. ----------121

Figure 5.6 Reponses to choline in X. laevis oocytes expressing the A. mellifera α5 nAChR subunit. A. Representative current traces showing responses to different concentrations of choline (0.3–12 mM). B. Choline concentration response curve. Data are normalised to the response to 12 mM choline and have a mean EC_{50} of 9.070 (4.482-18.35) mM from 5 oocytes from 4 different batches of eggs. ----------122

Figure 5.7 A. Responses to acetylcholine in X. laevis oocytes injected with A. mellifera α5 + α3 + α8 nAChR DNA. B. Acetylcholine concentration response curves for all A. mellifera nAChR combinations tested. Data are normalised to the maximal response (5 mM acetylcholine). ----------124

Figure 5.8 Traces of effects of spinosad on A. mellifera α5 subunit expressed in X. laevis oocytes. A. 10 µM spinosad applied 3 min after 5 mM acetylcholine (ACh) B. Co-application of 10 µM spinosad + 5 mM acetylcholine, 5 µM spinosad + 5 mM acetylcholine, 1 µM spinosad + 5 mM acetylcholine C. 2 mM

acetylcholine compared to 2 mM acetylcholine + 10 µM spinosad and 1 mM acetylcholine compared to 1 mM acetylcholine + 10 µM spinosad. 3 min wash between applications. ---------- *125*
Figure 5.9 Traces of effects of neonicotinoids on A. mellifera α5 subunit expressed in X. laevis oocytes. A. Imidacloprid (IMI) showed no agonist actions when 100 µM was applied 3 min after 5 mM acetylcholine (ACh). Imidacloprid showed antagonistic actions when coapplied with 2 mM acetylcholine (EC_{50} concentration) in a dose dependent manner. B. Thiacloprid (THI) showed no agonist actions when 100 µM was applied 3 min after 5 mM acetylcholine. Thiacloprid showed antagonistic actions when 100 µM was coapplied with 2 mM acetylcholine. ---------- *126*
Figure 5.10 Current traces showing responses to high concentrations of nicotine (nic) applied 3 min after 5 mM acetylcholine (ACh) from X. laevis oocytes expressing the A. mellifera α5 nAChR subunit. --------- *127*
Figure 5.11 Representative traces showing responses from X. laevis oocytes expressing the A. mellifera α5 nAChR subunit to 2 mM acetylcholine (ACh) (EC_{50} concentration), 2 mM acetylcholine coapplied with 0.1 µM α-bungarotoxin (α-bgt) after 3 min 20s incubation with 0.1 µM α-bungarotoxin, normal response to 2 mM acetylcholine restored after 26 min washing with SOS. ---------- *128*
Figure 5.12 An alignment showing the N-terminal domain (where acetylcholine binding occurs) for the A. mellifera nAChR α5 subunit and subunits from Table 2: the α7 subunit from chicken, the α4 subunit from chicken, AChBP from A. californica, γ subunit from T. californica, δ subunit from T. californica, α subunit from T. californica, α1 subunit from mouse, γ subunit from mouse, δ subunit from mouse, α1 subunit from human, α4 subunit from human. Aligned using ClustalW Identical amino acids in A. mellifera α5 from Table 2 are circled in green whilst non-matching amino acids are circled in red. Binding loops are indicated by an orange line. ---------- *135*
Figure 6.1 Reponses to 5-HT in X. laevis oocytes expressing the A. mellifera α5 nAChR subunit. A. Representative current traces showing responses to different concentrations of 5-HT (1–1000 µM). The lack of response from a control oocyte injected with water only is included. B. 5-HT concentration response curve. Data are normalised to the response to 1 mM 5-HT and have a mean EC_{50} 121.6 (110.7-133.5) µM from n = 7, N = 5. C. Sample traces comparing the response to maximal concentrations of acetylcholine (5 mM), 5-HT (1 mM) or 1 mM acetylcholine from the same oocyte, 3 min between applications. ---------- *147*
Figure 6.2 Trace showing that quipazine and mCPBG have no agonist actions when 100 µM was applied to X. laevis oocytes expressing the A. mellifera α5 nAChR 3 min after 5 mM acetylcholine application. 148
Figure 6.3 Response to dopamine (DA) in X. laevis oocytes expressing the A. mellifera α5 nAChR subunit. A. Representative current traces showing responses to different concentrations of dopamine (0.3-300 µM). The lack of response from a control oocyte injected with water only is included. B. Dopamine concentration response curve. Data are normalised to 100 µM dopamine and have an EC_{50} = 3.371 (2.926-3.885) µM n = 5, N = 3. C. Sample traces comparing the response to maximal concentrations of acetylcholine (5 mM) and DA (100 µM). ---------- *149*
Figure 6.4 Response to octopamine (OA) in X. laevis oocytes expressing the A. mellifera α5 nAChR subunit. A. Representative current traces showing responses to different concentrations of octopamine

(10-3000 µM). The lack of response from a control oocyte injected with water only is included. B. Octopamine concentration response curve. Data are normalised to 1 mM octopamine and have an EC_{50} = 378.1 (354.3-403.5) µM n = 6, N = 3. C. Sample traces comparing the response to maximal concentrations of acetylcholine (5 mM) and OA (1 mM).----------150

Figure 6.5 Traces showing that amitraz has no agonist actions when 10 µM was applied to X. laevis oocytes expressing the A. mellifera α5 nAChR 3 min after 5 mM acetylcholine (ACh) application and that amitraz has no antagonist actions when 10 µM was coapplied with 2 mM acetylcholine or 400 µM octopamine (OA).----------151

Figure 6.6 Response to tyramine (TA) in X. laevis oocytes expressing the A. mellifera α5 nAChR subunit. A. Representative current traces showing responses to different concentrations of tyramine (1-3000 µM). The lack of response from a control oocyte injected with water only is included. B. Tyramine concentration response curve. Data are normalised to 1 mM tyramine and have an EC_{50} = 91.12 (78.31-106.0) µM n = 5, N = 3. C. Sample traces comparing the response to maximal concentrations of acetylcholine (5 mM) and TA (1 mM).----------152

Figure 6.7 Response to histamine (HA) in X. laevis oocytes expressing the A. mellifera α5 nAChR subunit. A. Representative current traces showing responses to different concentrations of histamine (0.1-6 mM). The response from a control oocyte injected with water only is included. B. Histamine concentration response curve. Data are normalised to 5 mM histamine and have an EC_{50} = 3.355 (2.278-4.941) mM n = 5, N = 4. C. Sample traces comparing the response to maximal concentrations of acetylcholine (5 mM) and HA (5 mM). ----------153

Figure 6.8 Traces showing that GABA (A), glycine (B) and glutamate (C) have no agonist actions when 1 mM was applied to X. laevis oocytes expressing the A. mellifera α5 nAChR 3 min after 5 mM acetylcholine application. ----------154

Figure 6.9 A concentration response graph comparing the responses of the A. mellifera α5 nAChR expressed in X. laevis oocytes to acetylcholine, choline, 5-HT, dopamine, octopamine, tyramine and histamine.----------156

Figure 7.1 Homology modelling of the A. mellifera α5 nAChR based on the human α7 crystal structure (Zhao et al., 2021). Binding conformations generated by Autodock Vina with the interactions between acetylcholine (yellow) and serotonin (magenta) and the main binding site amino acids (red = hydrogen bond, orange = cation-π, and pale cyan = π-π) for A. mellifera α5 (A, and B, C) and human α7 (D, E, and F) from (Mitchell et al., 2022).----------161

List of Tables

Table 1.1 A summary of insect and crustacean (Lepeophtheirus salmonis) nAChRs expressed in X. laevis oocytes. Unless specified chaperones are from the same species as subunits.----------29
Table 1.2 A summary table of the results of knocking out nAChR subunits in D. melanogaster. Both the α4 and β1 homozygous knockouts appear to be lethal so any information about these subunits has to be deduced from heterozygous knockouts or other mutants (Perry et al., 2021; Lu et al., 2022). In the case of the β1 subunit this was a somatic knockout using a GAL4-UAS driver (Perry et al., 2021).----------40
Table 1.3 The sublethal effects of neonicotinoids on bees----------45
Table 2.1 Primers used for cloning, restriction sites underlined. Primers are written in the 5' to 3' direction.----------51
Table 2.2 PCR protocol ----------53
Table 2.3 Colony PCR protocol ----------55
Table 2.4 The sequences for site-directed mutagenesis. ----------57
Table 2.5 Primers for site-directed mutagenesis ----------57
Table 2.6 Concentrations of A. mellifera nAChR subunits in pCI injected into X. laevis oocytes ----------59
Table 2.7 Concentrations of M. persicae nAChR subunits and chaperones in pCI injected into X. laevis oocytes ----------60
Table 3.1 The percentage identity of UNC-50 and TMX3 amino acid sequences cloned from M. persicae to the UNC-50 and TMX3 cloned from D. melanogaster, A. mellifera and B. terrestris (Ihara et al., 2020).--90
Table 5.1 Effect of acetylcholine on membrane currents from X. laevis oocytes expressing A. mellifera α5 and other A. mellifera nAChR subunits. EC_{50} and Hill coefficient values are displayed as the mean ± 95% confidence limits. ----------123
Table 5.2 Table of Amino Acids Important for Agonist Binding in nAChRs, Method of Identification and if the Amino Acid is Present in A. mellifera α5. Amino acid numbers refers to an amino acid sequence alignment of all the sequences constructed using ClustalW (Kumar et al., 2018).----------131
Table 6.1 A summary of cys-loop ligand gated ion channels gated by biogenic amines or with multiple neurotransmitter agonists. ----------140
Table 6.2 Comparing the responses of the A. mellifera α5 nAChR expressed in X. laevis oocytes to different neurotransmitters. EC_{50} values and Hill coefficients are displayed as the mean ± 95% confidence limits and maximum responses displayed as percentages ± 95% confidence limits calculated using a two-tailed t test. ----------155

List of Abbreviations

Abbreviation	Definition
5-HT	5-hydroxytryptamine
$5HT_3R$	5-HT 3 receptor
α-bgt	α-bungarotoxin
A. californica	*Aplysia californica*
A. gambiae	*Anopheles gambiae*
A. gossypii	*Aphis gossypii*
A. mellifera	*Apis mellifera*
A. pisum	*Acyrthosiphon pisum*
ACh	acetylcholine
AChBP	acetylcholine binding protein
AChE	acetylcholine esterase
ACR-16	acetylcholine receptor-16
ACR-23	acetylcholine receptor-23
ACR-8	acetylcholine receptor-8
APFBzCho	4-azido-2,3,5,6-tetrafluorobenzoylcholine
Arf-GEF	guanine-nucleotide exchange factors for ADP-ribosylation factor GTPases
B. germanica	*Blattella germanica*
B. impatiens	*Bombus impatiens*
B. mori	*Bombyx mori*
B. terrestris	*Bombus terrestris*
C. elegans	*Caenorhabditis elegans*
C. histolyticum	*Clostridium histolyticum*
Cho	choline
COPI	coat protein I
cys-LGIC	cys-loop ligand gated ion channels
D. melanogaster	*Drosophila melanogaster*
DA	dopamine
DEFRA	Department for Environment, Food and Rural Affairs

DEG-3	degeneration of certain neurons 3
DES-2	degeneration suppressor 2
DMSO	dimethyl sulfoxide
E. coli	*Escherichia coli*
EC_{50}	half maximal effective concentration
EDTA	ethylenediaminetetraacetic acid
ELIC	Erwinia ligand-gated ion channel
GABA	γ-amino butyric acid
G. gallus	*Gallus gallus* (chicken)
Glu	glycine
Gly	glutamate
GMH1	Gea1-6 membrane-associated high-copy suppressor
GPCR	G-protein coupled receptor
H. contortus	*Haemonchus contortus*
HA	histamine
HEPES	4-(2-hydroxyethyl)-1-piperazineethanesulfonic acid
HisClB	histamine-gated chloride ion channel B
IMI	imidacloprid
L. migratoria	*Locusta migratoria*
L. salmonis	*Lepeophtheirus salmonis*
L-AChR	levamisole sensitive acetylcholine receptor
LB	Luria-Bertani
LEV-1	levamisole resistant-1
LEV-8	levamisole resistant-8
M. domestica	*Musca domestica*
M. musculus	*Mus musculus* (mouse)
M. persicae	*Myzus persicae*
mAChR	muscarinic acetylcholine receptor
mCPBG	1-(m-chlorophenyl)-biguanide
NACHO	novel acetylcholine receptor chaperone

nAChR	nicotinic acetylcholine receptor
nH	Hill coefficient
nic	nicotine
O. bicornis	*Osmia bicornis*
OA	octopamine
Octβ2R	octopamine β2 receptor
P. americana	*Periplaneta americana*
PNAS	Proceedings of the National Academy of Sciences
RIC-3	resistance to inhibitors of cholinesterase 3
S. spinosa	*Saccharopolyspora spinosa*
SOS	standard oocyte solution
T. californica	*Torpedo californica*
T. castaneum	*Tribolium castaneum*
T. marmorata	*Torpedo marmorata*
TA	tyramine
THI	thiacloprid
TMX3	thioredoxin related transmembrane protein 3
UNC-29	uncoordinated-29
UNC-38	uncoordinated-38
UNC-50	uncoordinated-50
UNC-63	uncoordinated-63
UNC-74	uncoordinated-74
V. destructor	*Varroa destructor*
X. laevis	*Xenopus laevis*

Abstract

Nicotinic acetylcholine receptors (nAChRs) are cysteine-loop ligand-gated ion channels that are the targets of effective insecticides, including neonicotinoids and spinosad. The heterologous expression of nAChRs, in *Xenopus laevis* oocytes, has enabled the study of functional and pharmacological properties of these receptors by two-electrode voltage clamp electrophysiology.

Myzus persicae, the peach potato aphid, is a major global pest of multiple crop species. The nAChR subunits and several protein chaperones from *Myzus persicae* have been cloned. It was difficult to achieve robust and frequent expression of a nAChR consisting entirely of subunits from *Myzus persicae* with the chaperones RIC-3, UNC-50 and TMX3. However, use of the α1 subunit from *Drosophila melanogaster* allowed nAChRs containing *Myzus persicae* α3, α8 and β1 subunits to be expressed and characterised with an EC_{50} for acetylcholine of 123 μM. The *Drosophila melanogaster* α1 and *Myzus persicae* β1 subunits formed a functional nAChR with an EC_{50} for acetylcholine of 91.1 μM, upon which neonicotinoids acted as partial agonists.

The *Apis mellifera*, European honeybee, α5 subunit formed a homomeric nAChR in oocytes without any chaperones. This was sensitive to 0.1 μM α-bungarotoxin and responded to both acetylcholine and choline but with low affinity, as shown by EC_{50} values in the millimolar range (2.65 mM and 9.07 mM respectively). Further testing revealed that the α5 nAChR responded to dopamine (EC_{50} 3.37 μM), 5-hydroxytryptamine (EC_{50} 122 μM), octopamine (EC_{50} 378 μM), tyramine (EC_{50} 91.1 μM) and histamine (EC_{50} 3.36 mM) but not to GABA, glycine or glutamate. Dopamine, 5-hydroxytryptamine, octopamine and tyramine all acted as superagonists relative to acetylcholine and had higher affinities than acetylcholine, as shown by EC_{50} values in the micromolar range, with dopamine having the highest efficacy and affinity. Histamine was a low-affinity, partial agonist. Phylogenetic analysis indicated that the non-Dipteran α5, including from *Apis mellifera*, form a distinct group from the Dipteran α5.

This thesis contributes to the rapidly growing field of knowledge gained from expressing insect nAChRs in heterologous systems. This is especially useful as a nAChR from a pest species has not been robustly expressed yet. The characterisation of a novel nAChR from the beneficial species, *Apis mellifera*, potentially indicates a new class of receptor, with unusual pharmacological properties.

Chapter 1 Introduction

1.1 Neurotransmitters in Insects

In order to be a neurotransmitter a chemical must fulfil certain criteria: it must act on a receptor to cause nerve stimulation, the effect must end on a physiologically realistic timescale by a specific inactivation mechanism, the neurotransmitter and the relevant biosynthetic enzymes must be present in nervous tissue, the release of the neurotransmitter must be stimulated by an increase in cytoplasmic calcium ion concentration and the chemical has an effect on behaviour (Osborne, 1996). In insects there is good evidence that acetylcholine, dopamine, octopamine, 5-hydroxytryptamine (5-HT) (serotonin), histamine, glutamate, γ-amino butyric acid (GABA) and tyramine fulfil these criteria (Osborne, 1996; Roeder, 1994; Prescott *et al.*, 1977; Breer, 1981; Dewhurst *et al.*, 1972; Orchard, 1990; Morton and Evans, 1984). Dopamine is the only one of the catecholamines found at sufficient concentrations in insects to be a neurotransmitter (Mercer *et al.*, 1983; Osborne, 1996). The equivalent roles of epinephrine and norepinephrine in vertebrates are often presented as being filled by the monohydroxylic analogues; octopamine and tyramine in insects (Schilcher *et al.*, 2021; Roeder, 1994).

1.2 Nicotinic Acetylcholine Receptors

Acetylcholine acts on two classes of receptors, ionotropic nicotinic acetylcholine receptors (nAChRs) and G-protein coupled receptors (GPCRs), the muscarinic acetylcholine receptors (mAChRs), which are present in both vertebrates and invertebrates (Albuquerque *et al.*, 2009). nAChRs are distinguished by being activated by nicotine and blocked by curare whereas mAChRs are activated by muscarine and blocked by atropine (Dale, 1914). However, atropine can also have some inhibitory effects on nAChRs but does not produce a complete block (Zwart and Vijverberg, 1997). The snake venom component, α-bungarotoxin, was used in early experiments to investigate nAChRs (Changeux, 2012). It was found to block neuromuscular transmission in vertebrates and block the response to nicotinic agonists in extracted membranes containing nAChRs without interacting with acetylcholine esterase (AChE) (Changeux, 2012). A similar α-toxin was used to separate nAChRs from AChE, using affinity

chromatography, this confirmed they were separate proteins (Changeux, 2012). In insects, nAChRs have subsequently been divided into α-bungarotoxin sensitive and insensitive groups (Courjaret and Lapied 2001; Buckingham *et al.*, 1997; Lansdell and Millar, 2000b).

nAChRs are cys-loop ligand-gated ion channels (cys-LGICs) (Jones and Sattelle, 2010). These receptors open in response to ligands to allow sodium or calcium ions to enter the cell, thus initiating an action potential (Jones and Sattelle, 2010; Changeux, 2012). The cys-LGIC superfamily also includes: GABA chloride channels in vertebrates and insects; glycine chloride channels and 5-HT sodium channels in vertebrates; histamine, glutamate and pH sensitive chloride channels in invertebrates (Jones and Sattelle, 2010; Jones, 2018; Feingold *et al.*, 2019; Changeux, 2012).

The complete quaternary structure of nAChRs consists of five subunits around a central pore, they can be homomeric or heteromeric but must contain at least two α subunits to be activable (Sattelle *et al.*, 2005; Bouzat, 2012; Corringer, Novère and Changeux, 2000). Each subunit has the same structure; a large N-terminal extracellular domain, four transmembrane helices and an intracellular domain formed by a highly variable loop between the third and fourth helices (Figure 1.1). The N-terminal domain possesses a disulfide bond between two cysteines separated by 13 amino acids; 'the characteristic cys-loop' (Jones and Sattelle, 2010; Corringer, Novère and Changeux, 2000). The acetylcholine binding site is situated at the interface between two subunits and is formed by six binding loops in the extracellular domain; loops A, B and C from the principle subunit and loops D, E and F from the complementary subunit (Figure 1.1) (Jones and Sattelle, 2010). Two adjacent cysteines in loop C are required for acetylcholine binding and these two cysteines define the α subunit, the principle subunit must be an α subunit, the complementary subunit can be a non-α subunit or another α subunit in homomeric nAChRs (Jones and Sattelle, 2010). Various amino acids involved in acetylcholine binding and activation of the receptor have been identified by a variety of methods (see Chapter 5 Table 5.2), including photoaffinity labelling, studying point mutations and structural studies (Tomizawa *et al.*, 2007; Nirthanan *et al.*, 2005; Morales-Perez, Noviello and Hibbs, 2016; Osaka, Sugiyama and Taylor, 1998; Corringer *et al.*, 1995; Galzi *et al.*, 1991). There are several important aromatic amino acids that can form cation-π interactions with the positive amine of acetylcholine (Corringer, Novère and Changeux, 2000). These include tryptophan in loop D and loop B (54 and 148 in chicken α7 respectively) (Corringer *et al.*, 1995; Galzi *et al.*, 1991) and tyrosine including the important YXCC motif in loop C (187 in chicken α7), as well as others in loop A and loop C (92 in chicken α7 and 198 in mouse α1 respectively) (Galzi *et al.*, 1991; Sine *et al.*, 1994). There are also negatively charged aspartates in loops B

and C that seem to have an electrostatic contribution to acetylcholine binding (Corringer, Novère and Changeux, 2000; Osaka, Sugiyama and Taylor, 1998). The GEK peptide motif preceding the second transmembrane domain is thought to be important for cation selectivity (Corringer, Novère and Changeux, 2000; Jensen, Schousboe and Ahring, 2005). The second transmembrane helix of each subunit lines the pore (Corringer, Novère and Changeux, 2000). In the resting state the extracellular half of the pore is too narrow to allow ions to pass through, constricted at the L16', V13' and L9' positions, the L9' position is highly conserved in cysLGICs (the prime numbers refers to the position of the amino acid from the cytosolic end of the pore (L277, V274 and L270 in the human α7 subunit)) (Noviello *et al.*, 2021; Zhao *et al.*, 2021). In the open state the pore is wider at this section due to a rotation of the helix so L16', V13' and L9' no longer constrict the pore allowing the passage of ions (Noviello *et al.*, 2021; Zhao *et al.*, 2021). It is uncertain that the activation and gating mechanisms are conserved between cysLGICs (Noviello *et al.*, 2021). Here is a brief description of the activation mechanism of the human α7 receptor, a homomeric receptor. Connections between the N-terminal ligand-binding domain and the transmembrane domain form the coupling region, which is coordinated by the cys-loop. When the ligand is bound loop C moves to create the aromatic cage around the ligand. This movement and others causes changes in the coupling region; salt bridges and hydrophobic interactions between the β1-β2 loop, β8-β9 loop, TM2-TM3 loop, pre-TM1 linker and cys-loop are altered causing the second transmembrane domain to rotate and move out of the membrane opening the pore (Figure 1.2) (Noviello *et al.*, 2021; Zhao *et al.*, 2021).

The protein structures of several nAChRs in different states have been solved including the nAChR from the electric organs of *Torpedo marmorata* at 4 Å resolution (Unwin, 1995; Unwin, 2005), the human $\alpha4_3\beta2_2$ at 3.9 Å resolution (Morales-Perez, Noviello and Hibbs, 2016) and the human α7 (Figure 1.2) resolutions 2.7-3.6 Å (Noviello *et al.*, 2021; Zhao *et al.*, 2021).

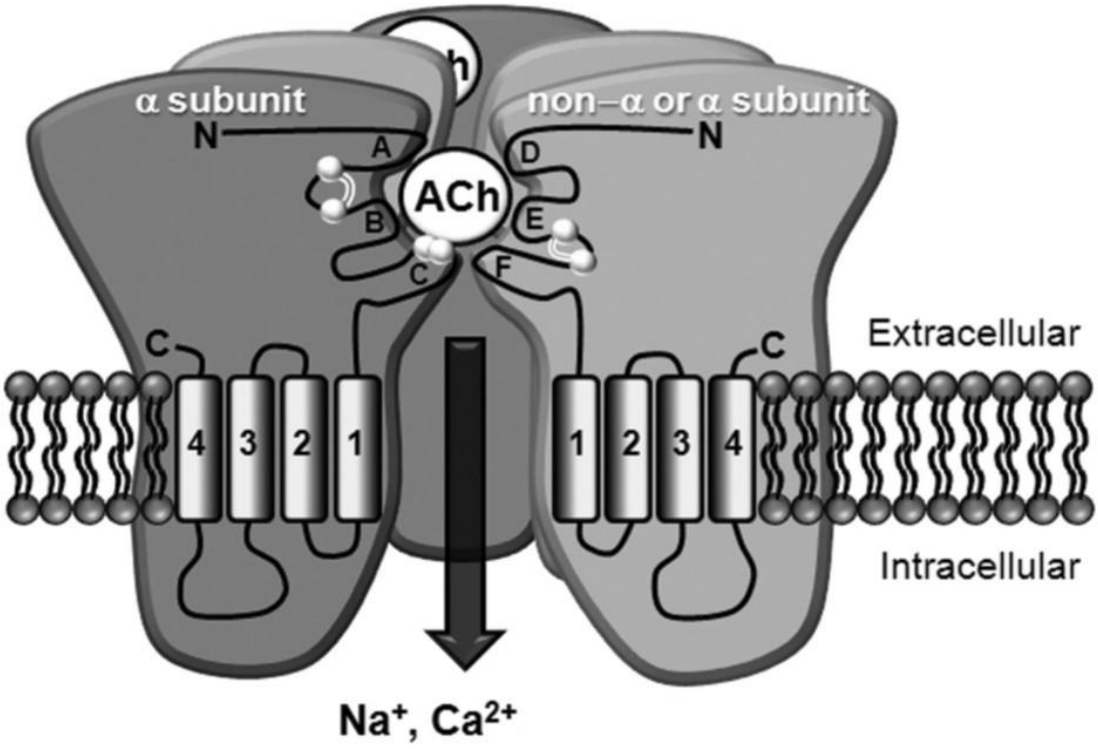

Figure 1.1 Structure of the nAChR. Schematic representation of a heteromeric receptor consisting of two α (dark grey) and three non-α subunits (light grey). The polypeptide layout of two subunits are shown highlighting the cys-loop (two white circles connected by a white double line), the two vicinal cysteines in loop C defining α subunits and four transmembrane domains (TM1-4) with a large intracellular loop between TM3 and TM4. The six binding loops (A-F) that contribute to ligand binding are shown and two acetylcholine (ACh) molecules are bound to this particular nAChR. The five subunits that make up the receptor are arranged around a central cation-permeable channel modified from (Jones and Sattelle, 2010).

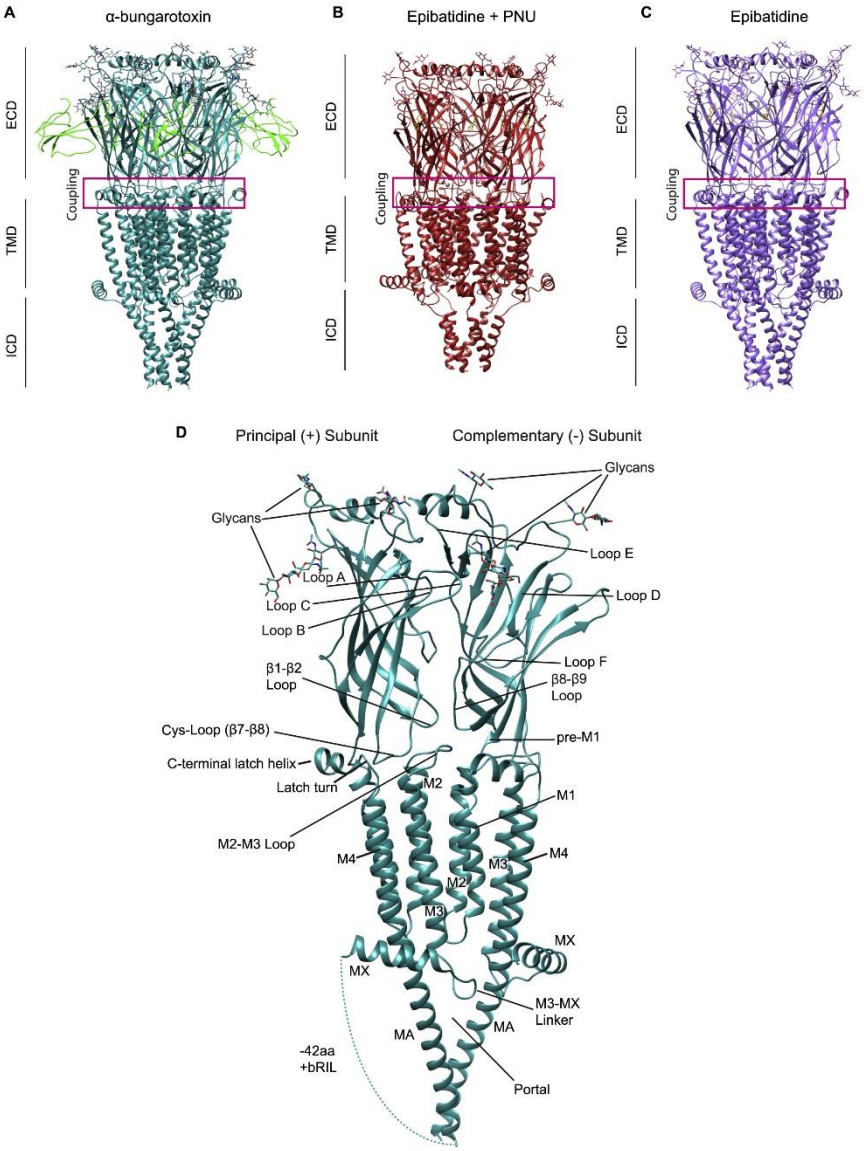

Figure 1.2 Structure of the human α7 nAChR. Figure S4 from (Noviello et al., 2021). A–C. Side views of each model. ECD, extracellular domain. TMD, transmembrane domain. ICD, intracellular domain. The coupling region is boxed. D. A subunit interface labelled to indicate loops, domains, helices and glycans. Deletion of disordered residues in the EM construct and insertion of bRIL are indicated.

1.3 Nicotinic Acetylcholine Receptors in Insects

Acetylcholine is the primary neurotransmitter in insects, the insect nervous system is richer in nAChRs than any other tissue, except the electric organs of fish (Sattelle, 1980). Unlike in vertebrates, nAChRs are not present at neuromuscular junctions in insects, glutamate receptors have this function (Millar and Denholm, 2007). Compared to vertebrates (mammals have 16 nAChR subunit genes (Pedersen, Bergqvist and Larhammar, 2019)) and nematodes

(*Caenorhabditis elegans* have at least 30 nAChR subunit genes (Treinin and Jin, 2021)), the nAChR subunit families of insects are compact, with the fruit fly *Drosophila melanogaster*, honeybee *Apis mellifera*, mosquito *Anopheles gambiae*, aphids *Myzus persicae* and *Acyrthosiphon pisum*, silkworm *Bombyx mori*, red flour beetle *Tribolium castaneum*, bumblebee *Bombus terrestris* and locust *Locusta migratoria* all having 10-12 subunit-encoding genes (Jones and Sattelle, 2010; Dale *et al.*, 2010; Wang *et al.*, 2015; Shao, Dong and Zhang, 2007), although, the cockroaches *Periplaneta americana* and *Blattella germanica* have larger families consisting of 19 and 17 subunits respectively (Jones *et al.*, 2020). There are seven core groups of highly conserved nAChR subunits with clear orthologous relationships between insect species. Thus, insects clearly possess α1, α2, α3, α4, α5, α6, α7, α8 (or β2 in some Dipteran species) and β1 subunits. In addition, each insect contains at least one divergent subunit which is less closely related to subunits from other species (Figure 1.3) (Jones and Sattelle, 2010). The peptide sequences of subunits in the *D. melanogaster* α5-α7 group are notably similar to vertebrate α7 (and α8) nAChRs, thus these subunits are thought to be evolutionarily ancient (Jones and Sattelle, 2010; Corringer, Novère and Changeux, 2000; Grauso *et al.*, 2002). Apart from the α5-α7 subunits, there are no other clear orthologous relationships between vertebrate and insect nAChRs (Jones and Sattelle, 2010).

Variation in nAChR receptors can be achieved through alternative splicing and A-to-I editing (Jones and Sattelle, 2010; Dale *et al.*, 2010; Jones *et al.*, 2006; Jones *et al.*, 2009; Sattelle *et al.*, 2005; Lansdell and Millar, 2000a; Jones *et al.*, 2020; Seeburg, 2002). For example, the *D. melanogaster* α4 subunit has alternative splicing that changes the N-terminal domain, which leads to a difference in receptor assembly efficiency in S2 cells (Lansdell and Millar, 2000a). Also, in *D. melanogaster* the α6 subunit was found to have five potential A-to-I editing sites, potentially altering the amino acid sequence in the ligand-binding domain (Grauso *et al.*, 2002; Jones and Sattelle, 2010).

Information on the *in vivo* subunit composition of insect nAChRs is limited; with assumptions either drawn from colocalisation (Ihara *et al.*, 2020; Thany *et al.*, 2005) or from heterologous expression experiments (see Table 1.1) (Watson *et al.*, 2010; Lansdell *et al.*, 2012; Ihara *et al.*, 2020).

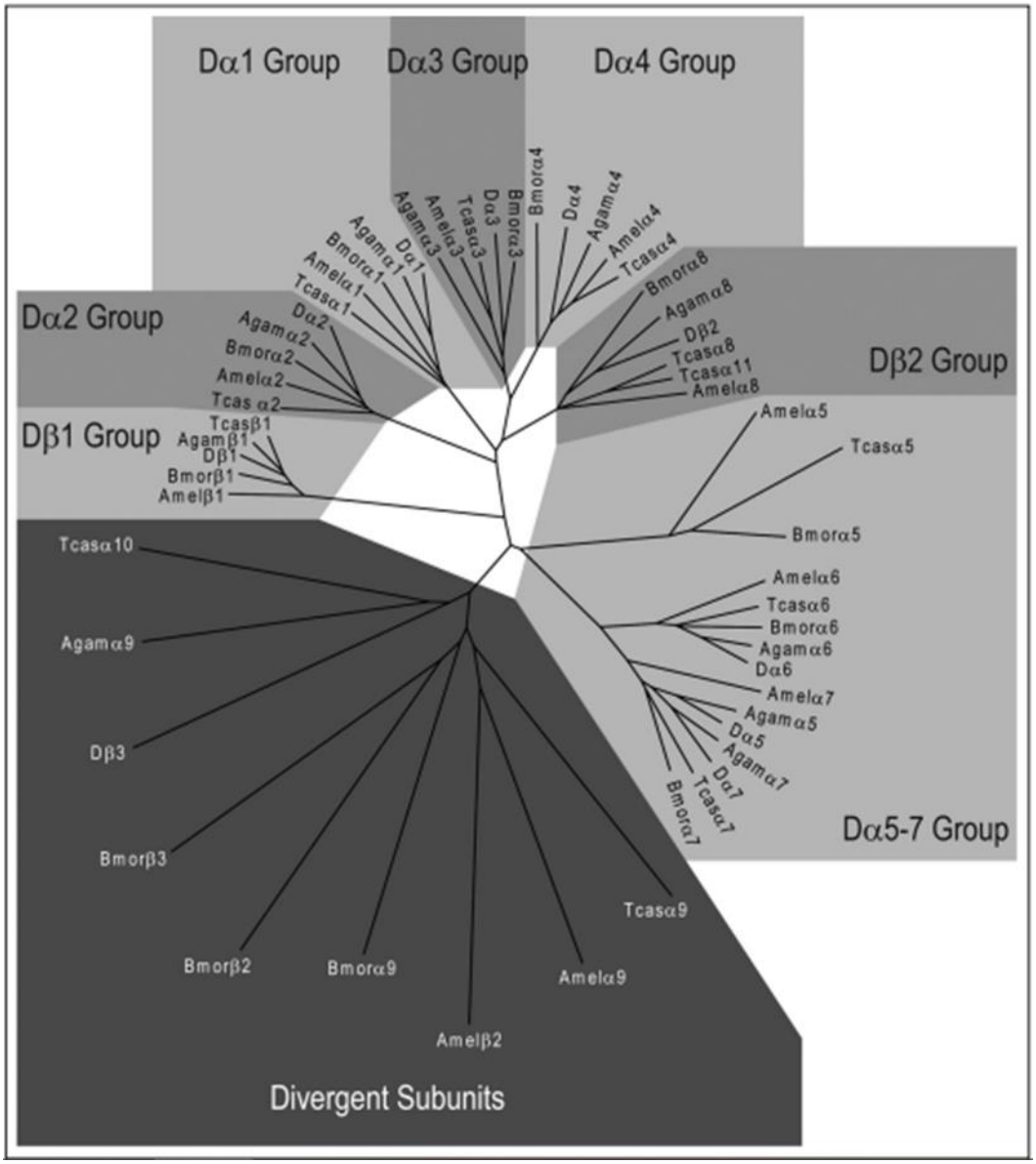

Figure 1.3 Tree showing the nAChR gene families of A. gambiae, A. mellifera, B. mori, D. melanogaster and T. castaneum. Based on their high amino acid sequence homology, several insect nAChR subunits cluster into groups. Each insect possesses at least one divergent subunit that does not fall into any of these groups. From (Jones and Sattelle, 2010)

1.4 The Insect α5 nAChR Subunit

The insect α5 nAChR subunit has always been phylogenetically grouped with the α6 and α7 subunits (Jones *et al.*, 2010; Jones and Sattelle, 2010), even though non-Dipteran α5 subunits (e.g. from *A. mellifera*, *B. mori* and *T. castaneum*) do not appear to be as closely related to the α7 subunit as those from Dipteran species such as *D. melanogaster* and *A. gambiae* (Jones and Sattelle, 2010) (Figure 1.3). Interestingly, aphids do not have an α5 subunit (Dale *et al.*, 2010), see Chapter 3. This is speculated to be because the α5 subunit evolved recently after the divergence of aphids and other insects, possibly from gene duplication of the α7 subunit (Dale *et al.*, 2010; Wang *et al.*, 2015). Based on phylogenetic analysis, the α5 subunit of Diptera (flies and mosquitoes) and non-Diptera (cockroach, bee, beetles and butterflies) may belong to distinct subgroups (Cartereau *et al.*, 2020). Further phylogenetic analysis followed by functional characterisation would help resolve this.

1.5 The Heterologous Expression of Insect nAChRs

Heterologous expression of nAChRs, commonly in *Xenopus laevis* oocytes, has enabled the study of functional and pharmacological properties of nAChRs by two-electrode voltage clamp electrophysiology (Buckingham, Pym and Sattelle, 2006). This measures the change in current across the membrane due to the opening of the nAChR, allowing sodium (and calcium) ions to move inside the cell, while the voltage is maintained at a constant level. This has proved particularly instructive for studying the pharmacological and functional properties of vertebrate nAChRs, however insect nAChRs have proven extremely recalcitrant to heterologous expression (Millar, 2009). Some success has been achieved by co-expressing insect nAChRs with vertebrate nAChR subunits, usually an insect α subunit with a vertebrate β2 subunit (Millar, 2009; Shimomura *et al.*, 2005; Ihara *et al.*, 2018; Schulz *et al.*, 1998) but this is not as relevant a model for the study of native insect nAChRs as expressing insect nAChRs alone.

Some nAChRs compromising of only insect subunits have been expressed in *X. laevis* oocytes although not always with robust enough expression or frequent enough expression to permit study of their functional properties (Table 1.1) (Marshall *et al.*, 1990; Cartereau *et al.*, 2020; Sgard *et al.*, 1998; Sawruk *et al.*, 1990; Brunello *et al.*, 2022). The addition of chaperone

proteins has proved essential or useful in the expression of several insect nAChRs in *X. laevis* oocytes (Hawkins, Mitchell and Jones, 2022; Brunello *et al.*, 2022; Ihara *et al.*, 2020; Rufener *et al.*, 2020; Lansdell *et al.*, 2012; Watson *et al.*, 2010) (Table 1.1). A summary of insect nAChRs that have been expressed in *X. laevis* oocytes without the use of vertebrate subunits is shown in Table 1.1. In some studies acetylcholine was not tested or the response to acetylcholine was too small to calculate an EC_{50} so nicotine was tested instead (Marshall *et al.*, 1990; Cartereau *et al.*, 2020; Sawruk *et al.*, 1990). A more expansive description of studies expressing α5, α6 and α7 subunits is provided in Chapter 5 and a more detailed description of studies expressing subunit combinations including the β1 subunit with the chaperones RIC-3, UNC-50 and TMX3 in Chapter 4. The chaperone proteins that have proven key to assist in the heterologous expression of insect nAChRs are summarised in the following sections. Detailed information on the structure and cloning of these chaperones are included in the introduction to Chapter 3.

Table 1.1 A summary of insect and crustacean (Lepeophtheirus salmonis) nAChRs expressed in X. laevis oocytes. Unless specified chaperones are from the same species as subunits.

Species	**Subunits**	**Chaper-ones**	**Acetyl-choline**	**Nicotine**	**Frequency of Expression**	**Reference**
D. melanogaster	α2	None	Yes	Yes EC_{50} 10-15 mM		(Sawruk *et al.*, 1990)
Schistocerca gregaria	α1 (ortholo-gous insect α2)	None	Not tested	Yes		(Marshall *et al.*, 1990)
M. persicae	α1 (ortholo-gous insect α2)	None	Yes EC_{50} 40 µM	Yes EC_{50} 0.5 µM	Infrequent	(Sgard *et al.*, 1998)

M. persicae	α2 (ortholo-gous insect α1)	None	Yes	Yes	Very infrequent	(Sgard *et al.*, 1998)
D. melanogaster	α5 + α6	RIC-3	Yes	Yes		(Watson *et al.*, 2010)
D. melanogaster	α5	RIC-3	Yes EC_{50} 8.8 µM	Not tested	Infrequent 33%	(Lansdell *et al.*, 2012)
D. melanogaster	α7	RIC-3	Yes EC_{50} 6.7 µM	Not tested	Infrequent 33%	(Lansdell *et al.*, 2012)
D. melanogaster	α5 + α6 + α7	RIC-3	Yes EC_{50} 13.5 nM	Not tested	Infrequent 33%	(Lansdell *et al.*, 2012)
P. americana	α7	None	Yes	Yes EC_{50} 790 µM		(Cartereau *et al.*, 2020)
D. melanogaster	α1 + β1	RIC-3, UNC-50, TMX3	Yes EC_{50} 7.59 µM	Not tested		(Ihara *et al.*, 2020; Takayama *et al.*, 2022)
D. melanogaster	α1 + α2 + β1	RIC-3, UNC-50, TMX3	Yes EC_{50} 51.3 µM	Not tested		(Ihara *et al.*, 2020)
D. melanogaster	α1 + β1 + β2	RIC-3, UNC-50, TMX3	Yes EC_{50} 15.1 µM	Not tested		(Ihara *et al.*, 2020)
D. melanogaster	α1 + α2 + β1 + β2	RIC-3, UNC-50, TMX3	Yes EC_{50} 6.03 µM	Not tested		(Ihara *et al.*, 2020)

A. mellifera	α1 + α8 + β1	RIC-3, UNC-50, TMX3	Yes EC_{50} 1.15 µM	Not tested		(Ihara *et al.*, 2020) (Brunello *et al.*, 2022)
A. mellifera	α1 + α2 + α8 + β1	RIC-3, UNC-50, TMX3	Yes EC_{50} 1.91 µM	Not tested		(Ihara *et al.*, 2020)
B. terrestris	α1 + α8 + β1	RIC-3, UNC-50, TMX3	Yes EC_{50} 1.58 µM	Not tested		(Ihara *et al.*, 2020)
B. terrestris	α1 + α2 + α8 + β1	RIC-3, UNC-50, TMX3	Yes EC_{50} 2.19 µM	Not tested		(Ihara *et al.*, 2020)
L. salmonis	α1 + α2 + β1 + β2	RIC-3, UNC-50, TMX3	Yes EC_{50} 1.96 µM	Yes 3.95 µM		(Rufener *et al.*, 2020)
L. salmonis	α3 + β1 + β2	RIC-3, UNC-50, TMX3	Yes EC_{50} 1.83 µM	Yes 9.98 µM		(Rufener *et al.*, 2020)
A. mellifera	α6	NACHO	Yes EC_{50} 0.88 µM	Not tested	Infrequent 33%	(Hawkins, Mitchell and Jones, 2022)
A. mellifera	α7		Yes	Not tested	Very infrequent	(Brunello *et al.*, 2022)
A. mellifera	α7	RIC-3, UNC-50, TMX3 (*C. elegans*)	Yes	Not tested		(Brunello *et al.*, 2022)

A. mellifera	α1 + α8 + β1	RIC-3 (*C. elegans*)	Yes	Not tested		(Brunello *et al.*, 2022)
A. mellifera	α2 + α8 + β1	None	Yes	Not tested	Very infrequent	(Brunello *et al.*, 2022)
A. mellifera	α2 + α7 + α8 + β1	NACHO	Yes	Not tested	Very infrequent	(Brunello *et al.*, 2022)

1.5.1 NACHO

NACHO (novel acetylcholine receptor chaperone) was discovered by genomic screening of human cDNA libraries for proteins essential for α7 assembly in HEK293T cells, where it would not normally express (Gu *et al.*, 2016). Knockouts of the NACHO gene in mice show it is necessary for α7 expression (Matta *et al.*, 2017). There are orthologs of NACHO in vertebrates and invertebrates and NACHO from *D. melanogaster* that can augment human α7 expression (Gu *et al.*, 2016). NACHO also is necessary for the expression of the human α3β2 nAChR in HEK293T cell lines and enhances the expression of α4β2, α3β4 and α6β2β3 nAChRs (Matta *et al.*, 2017). NACHO promotes the expression of the $(\alpha4)_2(\beta2)_3$ stoichiometry at the cell membrane over the expression of the $(\alpha4)_3(\beta2)_2$ stoichiometry (Mazzaferro *et al.*, 2020).

As described in the introduction to Chapter 5, NACHO was necessary for the expression of the *A. mellifera* α6 nAChR in *X. laevis* oocytes (Hawkins, Mitchell and Jones, 2022). In another study, the *A. mellifera* NACHO was also cloned (Brunello *et al.*, 2022), this increased the acetylcholine current from human α4β2 nAChRs expressed in *X. laevis* oocytes but did not facilitate the expression of the *A. mellifera* α7 nAChR. Expression was found in one oocyte out of 82 for a combination of *A. mellifera* α2, α7, α8 and β1 with *A. mellifera* NACHO (Brunello *et al.*, 2022) (Table 1.1).

NACHO has only been located to the endoplasmic reticulum, compared to RIC-3 which has also been located in the Golgi body (Rex *et al.*, 2016). NACHO associates with the oligosaccharidetransferase machinery and calnexin in the endoplasmic reticulum; these are required for nAChR surface expression (Kweon *et al.*, 2020).

1.5.2 UNC-50

UNC-50 (uncoordinated-50) is an orthologue of Gea1-6 membrane-associated high-copy suppressor (GMH1) in yeast and is an evolutionarily conserved integral membrane protein, located in the Golgi body (Eimer *et al.*, 2007). UNC-50 was identified in a screen for levamisole-resistance mutations in *C. elegans* (Lewis *et al.*, 1980). The mammalian orthologue UNCL has also been found to bind RNA in the inner nuclear membrane (Fitzgerald *et al.*, 2000). In humans, arthrogryposis multiplex congenita in a consanguineous family was found to be caused by a frameshift deletion of functional UNC-50 (UNCL) (Abiusi *et al.*, 2017). UNC-50 influences coat protein I (COPI) -mediated trafficking by recruiting guanine-nucleotide exchange factors for ADP-ribosylation factor GTPases (Arf-GEF) to the Golgi body, preventing targeting to the lysosome (Eimer *et al.*, 2007; Selyunin *et al.*, 2017).

1.5.3 TMX3

TMX3 (thioredoxin related transmembrane protein 3) was initially identified as UNC-74 in the screen for levamisole-resistance mutations in *C. elegans* (Lewis *et al.*, 1980). TMX3 is a thiol-disulfide oxidoreductase from the protein-disulfide isomerase family (Haugstetter, Blicher and Ellgaard, 2005). It has been located to the endoplasmic reticulum membrane by subcellular fractionation, identification of attached glycans unmodified by the Golgi body and immunofluorescence microscopy (Haugstetter, Blicher and Ellgaard, 2005). TMX3 catalyses the formation of disulfide bonds, which are critical for nAChR subunit assembly, and in nematodes UNC-74 is a cofactor for reconstituting levamisole-sensitive nAChRs (Boulin *et al.*, 2008; Boulin *et al.*, 2011).

1.5.4 RIC-3

RIC-3 (resistance to inhibitor of cholinesterase 3) was first identified in a screen for acetylcholinesterase resistances in *C. elegans* (Miller et al., 1996). It is a highly conserved chaperone mostly of nAChRs in the wider α7 group (Lansdell *et al.*, 2005) but can also influence the surface expression of other vertebrate neuronal nAChRs depending on the cell

type (Lansdell *et al.*, 2005; Bao *et al.*, 2018; Halevi *et al.*, 2003; Treinin, 2008). In *C. elegans* it interacts with multiple nAChRs (Halevi *et al.*, 2003; Treinin, 2008; Lansdell *et al.*, 2005). Human RIC-3 can be co-immunoprecipitated with human α3, α4, α7, β2 and β4 subunits (Lansdell *et al.*, 2005). Similarly RIC-3 isoforms from *D. melanogaster* can be co-immunoprecipitated with the α2, α3, α6 and β3 subunits from *D. melanogaster* (Lansdell *et al.*, 2008). RIC-3 was found to decrease the acetylcholine induced current of *X. laevis* oocytes injected with human α4β2 and α3β4 nAChRs (Halevi *et al.*, 2003). RIC-3 can also influence the composition of nAChRs, expressed at the surface of *X. laevis* oocytes, preferentially promoting the maturation of degeneration of certain neurons 3 (DEG-3) rich DEG-3/degeneration suppressor 2 (DES-2) receptors (Ben-Ami *et al.*, 2005). The effects of RIC-3 also depend on cell type (Bao *et al.*, 2018); in *D. melanogaster* cell lines RIC-3 from *D. melanogaster* enhanced nAChR maturation to a greater extent than human RIC-3 but the converse was the case in human cell lines (Lansdell *et al.*, 2008). RIC-3 can affect expression of other cys-LGICs where it was found to enhance the expression of homomeric $5HT_{3A}R$ in human cells (Walstab *et al.*, 2010). RIC-3 has been localised to the endoplasmic reticulum and Golgi body (Rex *et al.*, 2016) and has multiple isoforms arising from alternative splicing in many species but so far it appears only the transmembrane and N-terminal regions (proline-rich domain) are required to enhance human α7 expression (Lansdell *et al.*, 2008; Castelán *et al.*, 2008). Expression of RIC-3 changes the proteins in the human α7 nAChR interactome, with 39 proteins only associating with human α7 when RIC-3 is expressed (Mulcahy *et al.*, 2015). RIC-3 is an obligatory chaperone for the maturation, assembly and surface trafficking of the vertebrate α7 nAChR but does not actually increase expression of the subunits (Dau *et al.*, 2013; Williams *et al.*, 2005). At very high concentrations RIC-3 can prevent the α7 nAChRs from leaving the endoplasmic reticulum (Alexander *et al.*, 2010). However, it appears that RIC-3 alone is not sufficient for the surface expression of human α7 nAChRs, with only a small proportion of α7 subunits reaching the surface (Rex *et al.*, 2016; Mukherjee *et al.*, 2009). RIC-3 has synergistic effects with NACHO, suggesting they act in different parts of the nAChR assembly pathway (Gu *et al.*, 2016; Shelukhina *et al.*, 2017).

The heterologous expression of insect nAChR has allowed quantification of the interactions between some nAChRs and insecticides (Watson *et al.*, 2010; Ihara *et al.*, 2020; Hawkins, Mitchell and Jones, 2022), confirming the importance of nAChRs as insecticide targets.

1.6 Insecticides and Crop Protection

It is thought by some that insecticides are required to achieve global food security (Holt *et al.*, 2016). With 20-30% of crops being lost to pests and pathogens globally (Savary *et al.*, 2019), we are heavily reliant on pesticides to protect crops. In situations where certain pesticides have been banned this has led to difficulties in food production. In 2018, three N-nitroguanidine neonicotinoids (imidacloprid, clothianidin and thiamethoxam) were banned from outdoor use in the European Union (Lämsä *et al.*, 2018) due to the risk they pose to bee populations. Several neonicotinoid products have had registrations cancelled in the United States as part of a settlement with environmental groups (Hou, 2019). The banned neonicotinoids have mostly been replaced by pyrethroids, which is an older class of insecticide, to which pests have developed resistance (Bass *et al.*, 2014). The ban on neonicotinoids in the European Union has proven problematic in the production of oilseed rape due to resistance to the replacement pesticides, pyrethroids (Scott and Bilsborrow, 2019). In 2022 an emergency application to the Department for Environment, Food and Rural Affairs (DEFRA) from the National Farmers Union and British Sugar allowed the use of the neonicotinoid, thiamethoxam on sugar beet in certain conditions to prevent the spread of the beet yellow virus carried by aphids (*Statement of reasons for the decision on the application for emergency authorisation for the use of Cruiser SB on sugar beer crops in 2022*, 2022). However this has been criticised in the media as being against expert advice (Dalton, 2022). This highlights the requirement for novel crop protection agents, including insecticides that have a higher selectivity toward pest species than beneficial insects.

1.7 Insecticides and Insect Populations

There are major concerns that the use of insecticides has contributed to a decline in insect populations, particularly pollinators on which agriculture relies (Sánchez-Bayo and Wyckhuys, 2019; Wagner *et al.*, 2021; van Klink *et al.*, 2020a; van Klink *et al.*, 2020b). It is difficult to assess changes in insect populations against natural generational background fluctuations (Wagner, 2020; Wagner *et al.*, 2021). The global status of insect populations is also extremely complex, with a lack of data from pre-industrial times and many regions outside Europe (Wagner, 2020; Thomas, Jones and Hartley, 2019). Species and ecosystem level detail is also lost when data is aggregated together to draw general conclusions (Wagner *et al.*, 2021). This

is currently an area of much study with large metareviews of many datasets underway, such as EntoGEM (Grames and Montgomery, 2022). Below is a summary of the current state of research in changes to insect populations and the probable causes.

In 2021, the journal The Proceeding of the National Academy of Sciences (PNAS) dedicated a special issue to the global status of insects after a symposium of the Entomological Society of America in 2019 (Wagner *et al.*, 2021). The introduction gives a good general overview of the state of the field: there is much variation between studies into the changes in insect abundance with some insect populations decreasing and others increasing, however there is a large decline in previously abundant species. There is also a common finding that the populations of specialists have declined faster than the populations of generalists (Wagner *et al.*, 2021). A review of 73 reports (Sánchez-Bayo and Wyckhuys, 2019) concluded over 40% of insect species are threatened with extinction. The main driver of this was proposed to be habitat loss (including the intensification of agriculture) but pollution from pesticides and fertilisers was also thought to be a major contributing factor and therefore a reduction in pesticide usage in order to halt population declines was recommended. This paper received much media coverage (Carrington, 2019). However, this paper has been criticised for methodological flaws due to bias in the literature search, the difficulty of combining diverse data sets and assigning the importance of different factors to the decline using an unreliable method, so these conclusions may be unreliable (Komonen, Halme and Kotiaho, 2019). There was criticism of extrapolating global extinction rates of insects from data from individual sites, mostly in Europe (Thomas, Jones and Hartley, 2019). Overall, this paper received 6 rebuttals (Wagner *et al.*, 2021), however it was the catalyst for the initiation of many more studies (Thomas, Jones and Hartley, 2019; Crossley *et al.*, 2020). A meta-analysis of 116 long-term surveys came to the conclusion that globally there had been a decline in terrestrial insect abundance but an increase in freshwater insect abundance (van Klink *et al.*, 2020a). There was, however, a lot of variation between sites and the trends were mostly driven by Europe and North America. There was a small association between increased urbanisation and decreasing terrestrial insect abundance but there were some other strong trends illustrating the possible drivers of changes in terrestrial insect abundance such as changes in agricultural practices (van Klink *et al.*, 2020a). There were some errors in the analysis where the wrong numbers and duplications were analysed but removing these did not change the overall results (van Klink *et al.*, 2020b). So far this is considered the most expansive and definitive study of insect population change (Wagner *et al.*, 2021). A study combining data from long-term surveys in the USA was conducted to try and fill a data gap for insect populations outside

Europe (Crossley *et al.*, 2020). This study concluded there was no net change in insect populations across the USA (Crossley *et al.*, 2020). However, these conclusions have been criticised as they relied on the assumption that sampling was consistent across the surveys which was flawed (Welti *et al.*, 2021).

It is difficult to assign direct causes to declines in insect populations as there are many factors involved that act synergistically (Outhwaite, McCann and Newbold, 2022; Wagner *et al.*, 2021; Wagner, 2020). It is particularly difficult to distinguish the effects of pesticides as they are often not separate from the other aspects of agricultural intensification, including loss of habitat on both a local and a large scale (Outhwaite, McCann and Newbold, 2022; Wagner *et al.*, 2021; Wagner, 2020). However, in terms of neonicotinoids, declines predate their use and occur in areas with little pesticide usage (Wagner, 2020). There are many stressors affecting insect populations, the most important stressors have been considered climate change, habitat loss and degradation as well as agriculture but there is uncertainty to their relative contributions (Wagner *et al.*, 2021). In Europe and California, the increase in agricultural intensification is probably the primary cause of loss of insects (Wagner, 2020). However, the contributions of climate change may increase, insects are particularly vulnerable to desiccation so changes in precipitation might be considerably influential (Wagner, 2020). According to analysis the primary driver of global changes in biodiversity is a combination of land-use changes (habitat loss and intensification of agriculture) and climate change acting synergistically (Outhwaite, McCann and Newbold, 2022), with a decline of 50% in abundance and 27% in the number of species relative to less disturbed habitats with lower warming. Tropical species are more sensitive to climate change than temperate species as they have narrower thermal niches (Outhwaite, McCann and Newbold, 2022). These conclusions were drawn from analysis of the PREDICT database with 6,094 locations and 264 studies (Outhwaite, McCann and Newbold, 2022).

So in conclusion, there seems to be an overall decline in insect populations and this decline is due to various factors, with no evidence that populations are decreasing for inexplicable reasons (Wagner, 2020). However, it is difficult to disentangle the contributions of insecticides to changes in insect populations and in terms of neonicotinoids in particular declines predate their use, so any contribution they make to population declines is likely not uniquely extraordinary compared to other insecticides (Wagner, 2020).

1.8 Neonicotinoids and Spinosad

Neonicotinoids are insecticides which act as agonists and antagonists at nAChRs, causing insect death by prolonged excitation of the nervous system (Millar and Denholm, 2007; Sparks *et al.*, 2021). The first neonicotinoid, imidacloprid, was introduced in 1991, followed by several other neonicotinoids from the 1990s to the early 2000s, including thiacloprid and clothianidin (Millar and Denholm, 2007; Matsuda, Ihara and Sattelle, 2020) (Figure 1.4). Neonicotinoids have a large share of the insecticide market with imidacloprid being the first insecticide to achieve US$1 billion annual sales (Ihara *et al.*, 2008). Neonicotinoids have traditionally been divided into N-nitroguanidine neonicotinoids (imidacloprid, clothianidin and thiamethoxam among others) and N-cyanoamidine neonicotinoids (thiacloprid among others) (Millar and Denholm, 2007). N-cyanoamidine neonicotinoids have been found to be much less toxic to bees than N-nitroguanidine neonicotinoids (Kumar, Singh and Pramod Kodigenahalli Nagarajaiah, 2020), due to the highly efficient metabolism of N-cyanoamidine neonicotinoids by CYP9Q enzymes, rather than any difference in effect at the target site (Manjon *et al.*, 2018). Neonicotinoids bind to the same site as acetylcholine and loops D, E and G contribute to neonicotinoid sensitivity (Ihara *et al.*, 2017). In studies to determine the involvement of various nAChRs in insecticide resistance using knockouts of nAChR subunits in *D. melanogaster* (Table 1.2), the knockout combinations that were resistant to different neonicotinoids seemed to be dependent on the neonicotinoid ring size and the R_2 substituents rather than the N-nitroguanidine/ N-cyanoamidine pharmacophore (Table 1.2) (Lu *et al.*, 2022). Thus, the N-nitroguanidine and N-cyanoamidine groups determine how the neonicotinoids are metabolised but the shape and other chemical substituents of the neonicotinoid determines the target site. The fourth generation of neonicotinoids, for example sulfoxaflor, has recently been developed (Wang *et al.*, 2018), this is in category 4C of the IRAC classification compared to the neonicotinoids which are 4A (Sparks *et al.*, 2021). Slowly, some resistance has developed to neonicotinoids in the field, for example in the aphid *M. persicae* resistance has developed both through target site alteration (Bass *et al.*, 2011) and from enhanced metabolism (Puinean *et al.*, 2010) (see section 1.11).

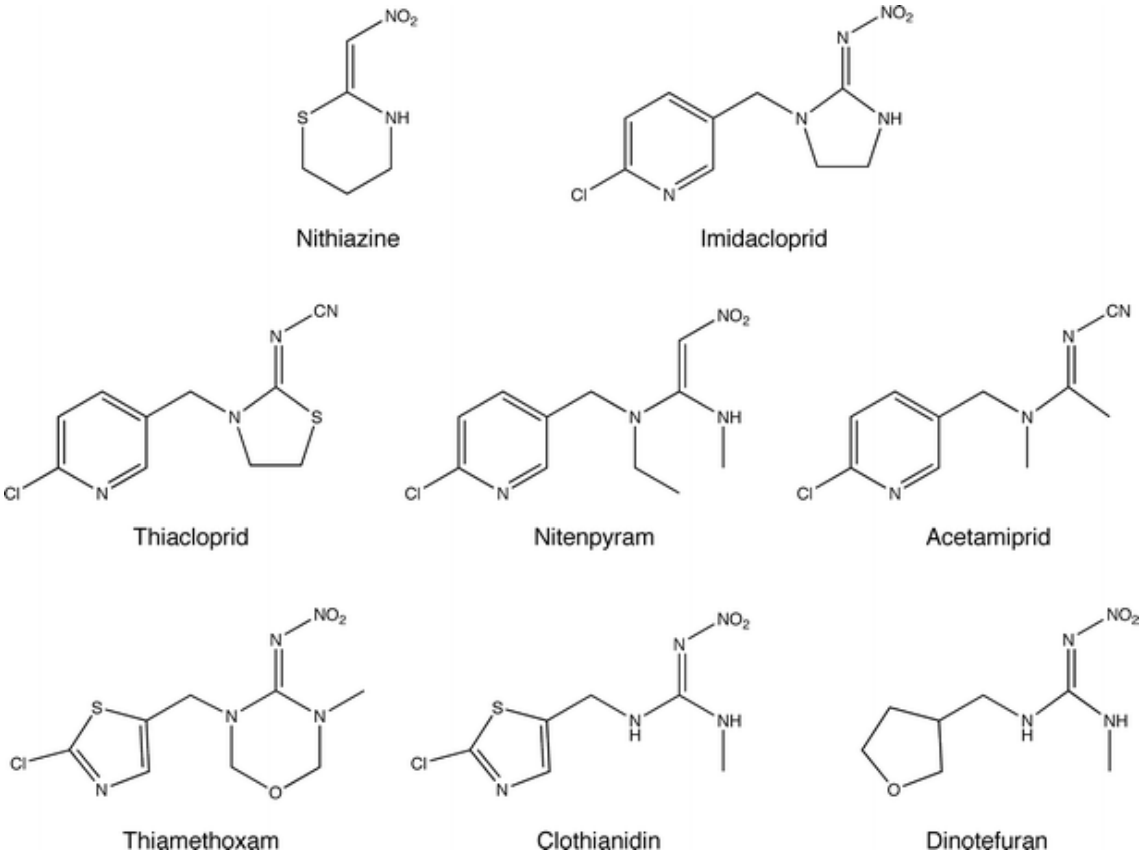

Figure 1.4 Chemical structure of nithiazine and neonicotinoid insecticides. Nithiazine is a synthetic compound with insecticidal activity on nAChRs which was a lead compound for the development of neonicotinoid insecticides. The neonicotinoid insecticides include chloronicotinyl compounds (imidacloprid, nitenpyram, acetamiprid and thiacloprid), thianicotinyl compounds (thiamethoxam and clothianidin) and the furanicotinyl compound (dinotefuran) from (Millar and Denholm, 2007).

Spinosad was developed in 1997 and is a combination of spinosyn A and spinosyn D from soil bacterium, *Saccharopolyspora spinosa* (Millar and Denholm, 2007; Jones and Sattelle, 2010; Galm and Sparks, 2016; Thompson, Dutton and Sparks, 2000). It acts as an agonist and positive allosteric modulator of the α6 nAChR (Hawkins, Mitchell and Jones, 2022; Sparks *et al.*, 2021). Spinosad only appears to act on the α6 nAChR subunit (Perry *et al.*, 2015; Somers *et al.*, 2015) and thus various species have developed resistance either by mutations in the α6 binding site (Puinean *et al.*, 2012; Hiruta *et al.*, 2018; Ureña *et al.*, 2019; Silva *et al.*, 2016) or by producing non-functional α6 subunits, as this subunit appears to be redundant (Berger *et al.*, 2016; Wan *et al.*, 2018). This has been further confirmed by systematic knockouts of insect nAChRs in *D. melanogaster*, where only the α6 knockouts displayed resistance to spinosad (Table 1.2) (Perry *et al.*, 2021; Lu *et al.*, 2022; Zhang *et al.*, 2022b).

1.9 Knockout Studies of nAChR in Insects

Knockout studies of nAChRs can give insights into their functional role and through resistance in the knockouts, which insecticides interact with which subunits. Most of the knockout studies have been carried out in the model organism *D. melanogaster* (Perry *et al.*, 2021; Lu *et al.*, 2022; Zhang *et al.*, 2022b), summarised in Table 1.2. These studies vary slightly in the insecticides they tested, the level of detail in the results and how they categorised the level of resistance (Perry *et al.*, 2021; Lu *et al.*, 2022; Zhang *et al.*, 2022b).

Table 1.2 A summary table of the results of knocking out nAChR subunits in D. melanogaster. Both the α4 and β1 homozygous knockouts appear to be lethal so any information about these subunits has to be deduced from heterozygous knockouts or other mutants (Perry et al.*, 2021; Lu* et al.*, 2022). In the case of the β1 subunit this was a somatic knockout using a GAL4-UAS driver (Perry* et al.*, 2021).*

Subunit	**Behavioural Effects**	**References**	**Resistance**	**References**
α1	Decreased courtship, change in sleep patterns, decreased longevity, decreased fertility	(Somers *et al.*, 2017; Zhang *et al.*, 2022b)	High: Imidacloprid, thiacloprid, acetamiprid, triflumezopyrim; Moderate: thiamethoxam, clothianidin, dinotefuran, nitenpyram Low: spinetoram	(Perry *et al.*, 2021; Lu *et al.*, 2022; Zhang *et al.*, 2022b)
α2	Decreased fertility, decreased climbing	(Zhang *et al.*, 2022b)	High: Imidacloprid, thiacloprid, triflumezopyrim, thiamethoxam Low: dinotefuran, sulfoxaflor, spinetoram	(Perry *et al.*, 2021; Lu *et al.*, 2022; Zhang *et al.*, 2022b)

α3	Decreased climbing	(Zhang *et al.*, 2022b)	Moderate: thiamethoxam, clothianidin, dinotefuran, nitenpyram, sulfoxaflor, flupyradifurone, imidacloprid, triflumezopyrim Low: spinetoram	(Lu *et al.*, 2022; Zhang *et al.*, 2022b)
α4	Lethal	(Lu *et al.*, 2022)	Mutant: Moderate: imidacloprid	(Lu *et al.*, 2022)
α5	None detected	(Zhang *et al.*, 2022b)	Moderate: Imidacloprid, nitenpyram, thiamethoxam, sulfoxaflor Low: dinotefuran, spinetoram	(Zhang *et al.*, 2022b)
α6	None detected	(Homem *et al.*, 2020)	High: Spinosad, spinetoram Moderate: nitenpyram, thiamethoxam, triflumezopyrim Low: dinotefuran, sulfoxaflor	(Perry *et al.*, 2021; Lu *et al.*, 2022; Zhang *et al.*, 2022b)
α7	Decreased climbing	(Zhang *et al.*, 2022b)	Moderate: imidacloprid, acetamiprid, nitenpyram, thiamethoxam, dinotefuran, sulfoxaflor	(Perry *et al.*, 2021; Lu *et al.*, 2022; Zhang *et al.*, 2022b)

β1	Knockout lethal. Mutant: reduced locomotion, fertility and longevity	(Perry *et al.*, 2021; Lu *et al.*, 2022; Homem *et al.*, 2020)	Mutant: Imidacloprid, nitenpyram, sulfoxaflor R81T: imidacloprid, thiacloprid, acetamiprid, thiamethoxam, clothianidin, dinotefuran, nitenpyram, sulfoxaflor, flupyradifurone, triflumezopyrim	(Perry *et al.*, 2021; Lu *et al.*, 2022)
β2	Decreased fertility, decreased climbing, decreased longevity	(Zhang *et al.*, 2022b)	Moderate: Imidacloprid, nitenpyram, thiamethoxam, sulfoxaflor, triflumezopyrim Low: dinotefuran, spinetoram	(Perry *et al.*, 2021; Zhang *et al.*, 2022b)
β3	Decreased fertility	(Zhang *et al.*, 2022b)	Moderate: Imidacloprid, nitenpyram, thiamethoxam, triflumezopyrim, spinosad, spinetoram Low: dinotefuran, sulfoxaflor	(Zhang *et al.*, 2022b)

1.10 *Myzus persicae*

M. persicae (Figure 1.5), also known as the green peach aphid or peach potato aphid, is considered the most important global pest aphid with over 400 host plant species and a global distribution (Bass *et al.*, 2014; Capinera, 2001; Fenton, Woodford and Malloch, 1998). Most damage to crops occurs through the transmission of plant viruses (Capinera, 2001). During the

spring and summer wingless adults reproduce by clonal parthenogenesis and the rate of reproduction is correlated with temperature. Winged adults are occasionally produced when host plants become too overcrowded (Capinera, 2001). In the autumn winged females and males are produced, the winged females birth egg-laying females (oviparae) on peach trees (genus: *Prunus*), these then mate with the males to produce eggs that overwinter on the peach tree (Capinera, 2001). In the UK, where peach trees are rare, *M. persicae* overwinter parthenogenetically and so all the *M. persicae* found in the UK are clones (Fenton, Woodford and Malloch, 1998).

Figure 1.5 M. persicae David Cappaert, Bugwood.org.

Over time *M. persicae* has developed resistance to most insecticides, with eight independent mechanisms of resistance described (Troczka *et al.*, 2021). For example, a neonicotinoid-resistant strain (FRC) of *M. persicae* was discovered in Southern France (Bass *et al.*, 2011), and has spread throughout the Mediterranean and across the Mediterranean sea to Tunisia (Charaabi *et al.*, 2017; Slater *et al.*, 2012; Panini *et al.*, 2014). The resistance is due to a target site mutation in the β1 nAChR subunit, with some contribution from enhanced metabolism (Bass *et al.*, 2011) and is semirecessive (Mottet *et al.*, 2016). The resistance mutation, R81T, is in loop D and is a key determinant in neonicotinoid binding. The lack of an arginine residue gives the receptor a more vertebrate-like ligand binding site, that does not bind neonicotinoids as well (Ihara *et al.*, 2014). The equivalent mutation in *D. melanogaster*, generated using

CRISPR/Cas9, lead to deficits in fertility and locomotion as well as neonicotinoid resistance (Table 1.2) (Homem *et al.*, 2020). This mutation was also found in laboratory selected and field strains of the aphid, *Aphis gossypii* showing resistance to thiamethoxam, imidacloprid, acetamiprid and sulfoxaflor (Zhang *et al.*, 2022a; Wang *et al.*, 2020; Chen *et al.*, 2017). The resistance derived from the R81T mutation in the FRC strain has never been found without additional metabolic resistance; alone R81T induces modest resistance but it acts synergistically with the overexpression of cytochrome P450 enzymes to produce strong resistance (Troczka *et al.*, 2021). There is also a subspecies of *M. persicae* from Greece that has adapted to a tobacco host, that has resistance to nicotine and neonicotinoids that pre-exists the development of neonicotinoids (Bass *et al.*, 2013; Troczka *et al.*, 2021). This resistance is entirely due to metabolism with many more copies of cytochrome P450 enzymes (Bass *et al.*, 2013).

1.11 *Apis mellifera*

The European honeybee, *A. mellifera* is a eusocial insect and as beekeeping is well established, it is used as a model organism for social behaviour (Robinson, Fahrbach and Winston, 1997). However, as it is a eusocial insect it is difficult to extrapolate changes in behaviour from the model organism *D. melanogaster*, for which knockout studies of nAChRs have been done (Zhang *et al.*, 2022b). Thus, when comparing the effect of knockout studies in *D. melanogaster* (Zhang *et al.*, 2022b) and the sublethal effects of neonicotinoids in bees (Table 1.3), they do not seem to have related effects because different behaviours are being measured (opposite effects would be expected as neonicotinoids are nAChR agonists). Bees are agriculturally important pollinators, pollinating nearly 75% of crop species according to the UN Food and Agriculture Organisation (*FAO's Global Action on Pollination Services for Sustainable Agriculture*). Therefore, it is an important non-target species to study so insecticides can be developed that have a lower impact on this beneficial insect.

A. mellifera are potentially vulnerable to pesticides as they have fewer detoxifying enzymes (Claudianos *et al.*, 2006). However, *A. mellifera* has not been found to be more sensitive to insecticides compared to other insects (Hardstone and Scott, 2010). Usually the field dose of neonicotinoids bees are exposed to is not lethal (Cresswell, 2011), however a larger lethal dose can be acquired if neonicotinoids accumulate in leaf guttation drops which bees may drink (Girolami *et al.*, 2009). The emergence of colony collapse disorder in the USA in 2006

(Oldroyd, 2007) has led to concern about the sustainable availability of *A. mellifera* colonies for agricultural pollination. Colony collapse disorder is a phenomenon where overwintering hives are found empty with few dead bees and no obvious signs of infection or other problems. There are contradicting results from studies over the role of neonicotinoids in colony collapse disorder (Lu, Hung and Cheng, 2020). As bees are not directly exposed to lethal doses of neonicotinoids, effects caused by sublethal doses may be the cause of negative consequences of neonicotinoids on bee populations. There is a good synopsis of the effects of sublethal doses in (Lu, Hung and Cheng, 2020). Table 1.3 contains a summary of some of the effects low doses of neonicotinoids have in bees, which tend to lead to impairments of learning, memory, locomotion and reproduction. There may be greater consequences of using neuroactive pesticides on eusocial insects, as opposed to controlling *Varroa destructor* mites that afflict bees (Abbo *et al.*, 2016), as the health of the entire colony is more dependent on complex behaviours such as navigation and communication from certain individuals (Lu, Hung and Cheng, 2020).

Table 1.3 The sublethal effects of neonicotinoids on bees

Species	**Insecticide**	**Effect**	**Reference**
All	Any	More energy required to detoxify insecticides	(Colgan *et al.*, 2019; Abbo *et al.*, 2016)
A. mellifera, B. terrestris	Thiamethoxam, imidacloprid, clothianidin	Difficulties foraging, particularly navigation	(Lu, Hung and Cheng, 2020; Lämsä *et al.*, 2018; Yang *et al.*, 2008; Henry *et al.*, 2012; Gill, Ramos-Rodriguez and Raine, 2012; Kumar, Singh and Pramod Kodigenahalli Nagarajaiah, 2020)
A. mellifera	Imidacloprid, acetamiprid	Decreased capacity for learning	(Lu, Hung and Cheng, 2020; Han *et al.*, 2010; Zhang *et al.*, 2020)

Osmia bicornis	Thiamethoxam	Difficulties in reproduction and raising larvae	(Lu, Hung and Cheng, 2020)
A. mellifera	Imidacloprid, thiamethoxam, clothianidin, thiacloprid	Reduce acetylcholine in brood food, developmental impairments	(Grünewald and Siefert, 2019)
A. mellifera	Thiamethoxam	Locomotor deficits	(Charreton *et al.*, 2015)
A. mellifera (Africanised)	Imidacloprid	Damaged midgut and Kenyon cells	(Catae *et al.*, 2018)
B. terrestris	Imidacloprid	Less pollen foraging	(Feltham, Park and Goulson, 2014)
A. mellifera	Imidacloprid	Reduce density micro-glomerulus in mushroom bodies.	(Peng and Yang, 2016)
A. mellifera	Clothianidin	Memory impairment	(Tison *et al.*, 2019)

1.12 Aim of Thesis

As nAChRs are the targets of efficient and widely used insecticides it is important to study them in detail in order to provide a basis for developing improved insecticides with less specificity towards non-target and beneficial organisms. Whilst the recent use of chaperone proteins have provided a breakthrough in enabling heterologous expression of nAChRs from *D. melanogaster*, *A. mellifera* and *B. terrestris* (Ihara et al., 2020), a nAChR from a crop pest has yet to be robustly expressed.

The aim of this thesis, therefore is to clone and functionally characterise nAChR subunits from a major pest species, *M. persicae*, using the *X. laevis* oocyte expression system. Also, a nAChR from a beneficial species, *A. mellifera*, will be similarly characterised. Findings from these studies will enhance our understanding of functional and pharmacological properties of nAChRs from diverse insect species.

Part of the aim of my project in studying nAChRs from a pest species and a beneficial species is that a greater understanding of insect nAChRs will assist in the development of pest-specific insecticides. This will allow the use of insecticides to increase crop yield and require less land to produce crops, while reducing the negative effects of insecticides on biodiversity.

Chapter 2 Methods

2.1 Reagents

Agarose, neomycin, antibiotic antimycotic solution, collagenase type I from *Clostridium histolyticum*, ampicillin, amikacin, imidacloprid, thiacloprid, clothianidin, acetylcholine chloride, spinosad, choline chloride, dopamine hydrochloride, potassium phosphate, acetic acid (Acros Organics), tyramine, amitraz, GABA, glycine and α-bungarotoxin were purchased from Sigma-Aldrich (Gillingham, UK). Luria-Bertani (LB) medium capsules were from MP Biomedicals (Irvine, CA, USA). Glycerol was from Fisher Bioreagents; Tris-Base and LB Agar were from Fisher Scientific (both Loughborough, UK). Calcium chloride and sodium chloride are from VWR Amresco Life Sciences (Lutterworth, UK) and potassium chloride from VWR Prolabo Chemicals (Lutterworth, UK). Magnesium chloride, histamine dihydrochloride, sodium L-glutamate monohydrate and octopamine hydrochloride were from Merck (Gillingham, UK). Chloroform and ethanol were from Honeywell (Charlotte, NC, USA). HEPES and ampicillin were from Melford (Ipswich, UK). Atropine was from Scientific Laboratory Supplies (Nottingham, UK). Serotonin (5-hydroxytryptamine) hydrochloride was from Alfa Aesar (Heysham, UK). Isopropanol was from Serva (Heidelberg, Germany). Dimethyl sulfoxide (DMSO) and EDTA were from BDH Laboratory Supplies (Poole, UK). Nicotine di-d-tartrate was from Research Biochemicals International (Natick, MA, USA). 1-(m-chlorophenyl)-biguanide (mCPBG) hydrochloride and quipazine dimaleate were from Tocris (Abingdon, UK).

2.2 Animals

Oocytes were either obtained ready to inject from Ecocyte Europe (https://ecocyte-us.com/products/xenopus-oocyte-delivery-service/) or ovary tissue from adult female *X. laevis* was purchased from The European Xenopus Resource Centre based at Portsmouth University, (Portsmouth, UK) or *X. laevis* frogs were purchased from Xenopus 1, Dexter, Michigan, USA. Frogs were handled strictly adhering to the guidelines of the Scientific Procedure Act, 1986, of the United Kingdom.

2.3 DNA sequencing

DNA sequences were verified at SourceBioscience (https://www.sourcebioscience.com/home). Primers used for sequencing subunits cloned into the pCI vector were usually pCIfor: 5' CTTACTGACATCCACTTTGC 3' and pCIrev: 5' AGCTTATAATGGTTACAAATAAAGC 3', which recognise the pCI vector.

2.4 Molecular Biology

2.4.1 RNA Extraction and Reverse Transcription

50 snap frozen *M. persicae* were provided by Syngenta. These were the Braveheart clone, first identified in Scotland in 1997 (Fenton, Woodford and Malloch, 1998). This is sensitive to all insecticides, a possible consequence of adaption to the cold (Fenton, Woodford and Malloch, 1998). Total RNA was extracted from *M. persicae* using TRIzol™ according to the manufacturer's protocol (Invitrogen, Waltham, MA, USA). mRNA (at 225.6ng/µl) was then reverse transcribed to cDNA using the GoScript™ Reverse Transcription System (Promega, Madison, WI, USA).

RNA from *A. mellifera* had been previously extracted (Jones *et al.*, 2006).

2.4.2 Cloning Protocol

A flowchart illustrating the process of cloning the *M. persicae* nAChR subunits (and the *A. mellifera* α5 subunit) is shown in Figure 2.1.

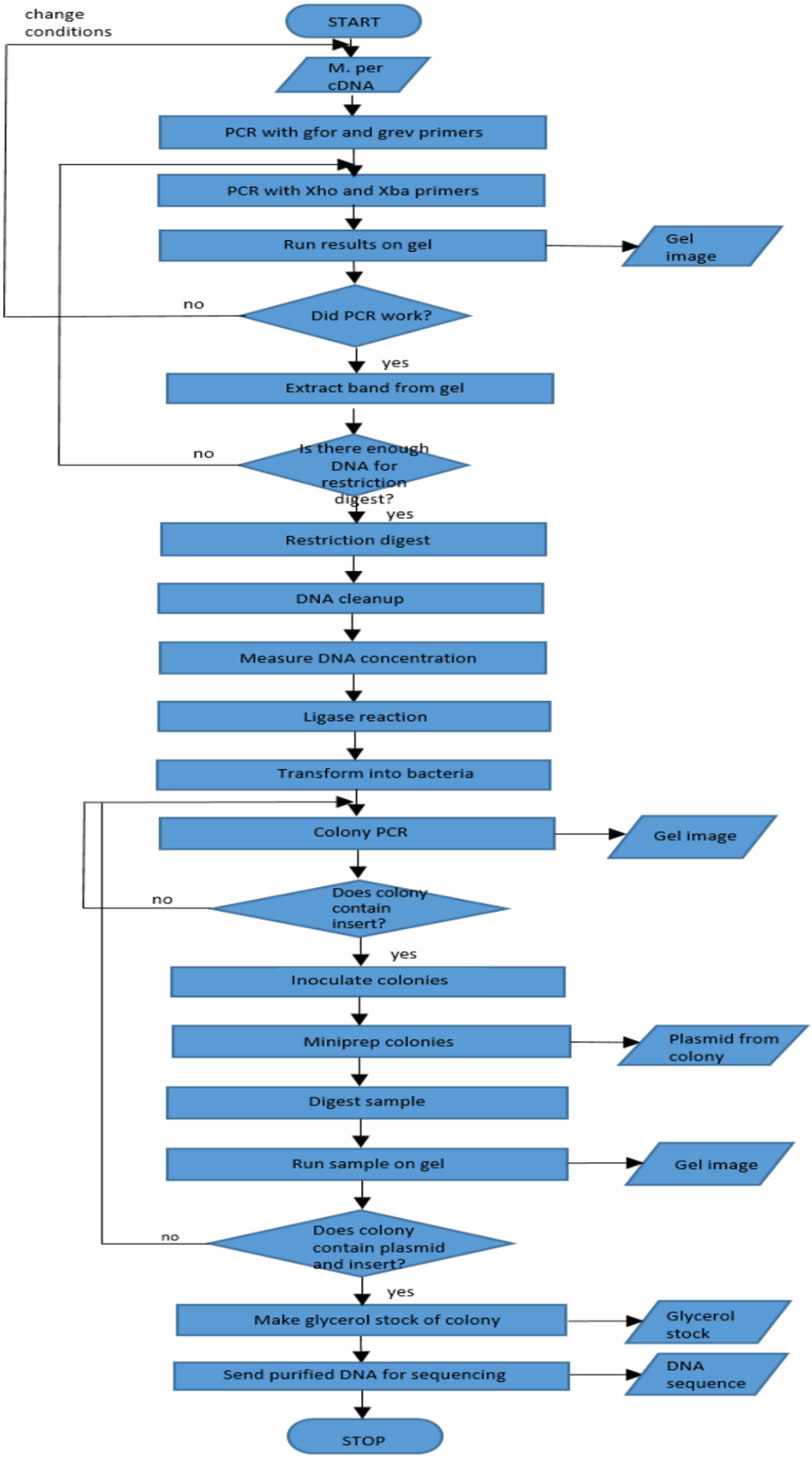

Figure 2.1 A flowchart of the cloning process for M. persicae nAChR subunits.

2.4.2.1 PCR

A nested PCR was used to clone the nAChR subunits using the primers in Table 2.1. The first reaction used the gfor and grev primers based on the 5' and 3' untranslated regions respectively. The second reaction used the *Xho* and *Xba* primers incorporating start and stop codons and *Xho* and *Xba* restriction sites respectively. Amplification products from the first reaction were used at a dilution of 1:100 as a template for the second PCR reaction. PCR used the Q5® High-Fidelity 2X Master Mix (New England Biolabs, Ipswich, MA, USA) according to the manufacturer's protocol with a 50 µl reaction, a 55°C annealing temperature was used unless there was too much amplification of non-specific DNA then the annealing temperature was increased to 60°C, other conditions are in Table 2.2.

Table 2.1 Primers used for cloning; restriction sites underlined. Primers are written in the 5' to 3' direction.

Primer	**Sequence**
Mper_a1gfor	GGTCCAATTGCCGTCTCGAG
Mper_a1Xho	ATCGCTCGAGATGAAAATCATTTGCGCGATATTC
Mper_a1Xba	CGATCGTCTAGATCATAAAATGGCTTGCAGTTTCTT
Mper_a1grev	GAGCTTTGTATTGTTGTGGTGTC
Mper_a2gfor	ATTCAGTCGACCGCCGCCG
Mper_a2Xho	ATCGCTCGAGCGCGATGCCGTCCGTCGC
Mper_a2Xba	CGATCGTCTAGAGACTATTCCAAATCGGACGTTG
Mper_a2grev	CATCAACCGTTTAACGCCGAG
Mper_a3gfor	GTGACCTTTGATATGGTCACCG
Mper_a3Xho	ATCGCTCGAGATGAAGACGTTGGCCGGCGC
Mper_a3Xba	CGATCGTCTAGATTACATAATGTTATTATAATTCTGTTTC
Mper_a3grev	CTGGCCTGTCCAATGTTGACC
Mper_a4gfor	CCGTCAACAGCCGGATCGG
Mper_a4Xho	ATCGCTCGAGCAGATATGTGGCCG
Mper_a4Xba	CGATCGTCTAGATTTATGAGGTTTGGTATTCGCTG
Mper_a4grev	TAAAAGGCGTCCTCCAATCGG
Mper_a6gfor	CGCCGCGAGCGTACCATCC
Mper_a6Xho	ATCGCTCGAGATGACGTCGTCCACATCAAAG
Mper_a6Xba	CGATCGTCTAGATCACTCAACGATTATGTGAGGC
Mper_a6grev	CATGACTGCCATATCGACATCC
Mper_a7gfor	CCGCCGCCGCTGAATGGG
Mper_a7Xho	ATCGCTCGAGATGGGAATACTCCCGTATCTGC
Mper_a7Xba	CGATCGTCTAGATCACGTGACGATGACATGCGG

Mper_a7grev	GACGCAATGACGTCGGTGGC
Mper_a8gfor	GTCTTACTAGTTTCAAACGGCG
Mper_a8Xho	ATCGCTCGAGATGAATATCTTATACATCCTCCCG
Mper_a8Xba	CGATCGTCTAGACTAGTTGGCACCGTAAGTGCG
Mper_a8grev	GCCGCGTAGTCATATAAAGTTG
Mper_a9gfor	GTGCCAATATTGCCACCAGAC
Mper_a9Xho	ATCGCTCGAGGATGGACGGTCTACGGTCGG
Mper_a9Xba	CGATCGTCTAGACTAAAACACAAAGCGAGATAGAAG
Mper_a9grev	TCGTACATATCAGGCCCAATTG
Mper_a10gfor	TAGATTGTTGTTGCTCGTGGTG
Mper_a10Xho	ATCGCTCGAGATGTTGGGCACTCGTCATATTG
Mper_a10Xba	CGATCGTCTAGACTACGGCATGAGCCTCAAGAG
Mper_a10grev	TGCCTTTATTGAAGAGGATGCG
Mper_b1gfor	GTACAAGTGCCAAAGGCCGC
Mper_b1Xho	ATCGCTCGAGATGAACACTTCCGTTGGACTAC
Mper_b1Xba	CGATCGTCTAGATTATTTTCCGCCGTAGATTTCG
Mper_b1grev	CAGTAACAAAATTGTACGTACACC
Mper_b2gfor	TAGGCATATATATCCGCCGCC
Mper_b2Xho	ATCGCTCGAGATCTACTGTACTCTACTTGTATTC
Mper_b2Xba	CGATCGTCTAGATATTCACTTCAGAAAATAAATCACC
Mper_b2grev	GATCTTTGGTGAAATATTGTTTTCG
Mper_b3gfor	TTACAGCTTTCGGCTTTAGTTAG
Mper_b3Xho	ATCGCTCGAGTTTATGTTGAACACGATGGGTG
Mper_b3Xba	CGATCGTCTAGAAATTCACAAGTAAATCTAATTAGGG
Mper_b3grev	TAAAATATAAATTAAATTAAAGTTATCATTG
Amel_a5gfor	TCTCGCGTTTAAGTGGTCCATCAA
Amel_a5Xho	ATCGCTCGAGATGTCGCCTTTGGTCCTGTTC
Amel_a5Xba	CGATCGTCTAGATTAACCCTCTTTGGCAATGTTCG
Amel_a5grev	CCGTATTTCTACCATCGTCCATT
Mper_nachogfor	CGTAAAAGTAGCTGCAGTGTAG
Mper_nachoXho	ATCGCTCGAGGATATGGGATCAATAGTTCTAAAG
Mper_nachoXba	CGATCGTCTAGACTATTCTTGTTTTTGAGCTTTAGG
Mper_nachogrev	AATGAGCTAAGTTTGGGAAAATTG
Mper_RIC3gfor	AAATTGGTTGACGAAGTTCGGC
Mper_RIC3Xho	ATCGCTCGAGGACATGGCGACAGAGATAAGT
Mper_RIC3Xba	CGATCGTCTAGACCATATGTTTATATTTTCATTTTTCG
Mper_RIC3grev	TTTTAAAACCGTGCATGTACATTG
Amel_RIC3gfor	AGTTATACGAACGAAAAATTTACG
Amel_RIC3Xho	ATCGCTCGAGATGGCTGAAATAACAGATTTCGG
Amel_RIC3Xba	CGATCGTCTAGATTTTTATATGTTTTTGCTATTATTCTC
Amel_RIC3grev	CAATGATTTAACACGAAATATAATG

Mper_UNC50gfor	TAACAAATCTTAAAATTGAAGTTACAC
Mper_UNC50Xho	ATCGCTCGAGTAATGCCAAGCAGCGTAAATTCC
Mper_UNC50Xba	CGATCGTCTAGATTATAGAATTCTGTACTTGTATATGG
Mper_UNC50grev	CATAAAATTTCTATAAACATATAATTGG
Mper_TMX3gfor	GTAATTTGAGAAATGTGTATAATCTG
Mper_TMX3Xho	ATCGCTCGAGATGATGATCTCTAATATATTTACTAC
Mper_TMX3Xba	CGATCGTCTAGATGAATATTTTAATGAGTAGTTTTATTC
Mper_TMX3grev	CATCTGTTAATAAATCAATACGCC

Table 2.2 PCR protocol

Step	**Temperature (°C)**	**Time (s)**
1	98	30
2	98	10
3	55/60	20
4	72	30
5	Go to step 2	x35
6	72	120
7	12	∞

The PCR products were then run on a 1% agarose gel with SYBR Safe (Life Technologies, Carlsbad, CA, USA) or Diamond™ Nucleic Acid dye (Promega, Madison, WI, USA) in TAE buffer, using a Power Pcc300 Bio-rad, E143 Consort. The band, identified by size using the 1 kb plus ladder (New England Biolabs, Ipswich, MA, USA) (Figure 2.2), from the second PCR was then cut out and purified using the Monarch® DNA Gel Extraction Kit (New England Biolabs). The concentration of the purified PCR product was measured using a NanoDrop One (Thermo Scientific, Waltham, MA, USA) and if there was less than 1 µg of DNA the second PCR was repeated in order to generate enough DNA for the restriction digest.

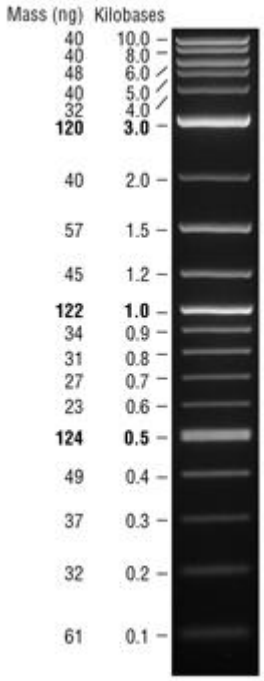

Figure 2.2 1 kb plus ladder used for gels from https://international.neb.com/products/n3200-1-kb-plus-dna-ladder#Product%20Information

2.4.2.2 Restriction Digest

The restriction digest of PCR products was set up with *Xho*I and *Xba*I from New England Biolabs, using the manufacturer's protocol and incubated at 37°C for 1 hour. Either Monarch® PCR and DNA Cleanup Kit (New England Biolabs, Ipswich, MA, USA) or SmartPure PCR (Eurogentec, Seraing, Belgium) was use to purify the digested DNA for the ligation.

2.4.2.3 Ligation

A 10 µl ligase reaction was set up with T4 ligase (Promega, Madison, WI, USA) and appropriate buffer with 50 ng pCI pre-digested as above with *Xho*I and *Xba*I and the digested DNA insert in a 3:1 ratio insert to PCI. This was then left at 4°C overnight.

2.4.2.4 Transformation

For transformation, 4 µl of the ligation reaction (50 ng DNA) was incubated with 100 µl competent bacteria (*Escherichia coli* DH5α, competent cells generated at Oxford Brookes University) on ice for 10 min. They were then placed in a 42°C water bath for 45 s, after recovery for 2 min on ice, 1 ml LB was added and the cells were incubated for 1 hour at 37°C. 100 µl culture was then spread on plates with 100 µg/ml ampicillin and incubated at 37°C overnight.

2.4.2.5 Colony PCR

A colony PCR was then used to determine which colonies contained the insert. This used Q5® High-Fidelity 2X Master Mix (New England Biolabs, Ipswich, MA, USA) in a 25 µl reaction with the conditions in Table 2.3 and pCIfor and pCIrev primers. The colony was transferred to the PCR reaction using a pipette tip. The PCRs were then run on an agarose gel as above to see if they contained the insert.

Table 2.3 Colony PCR protocol

Step	**Temperature (°C)**	**Time (s)**
1	98	30
2	98	10
3	55	20
4	72	30
5	Go to step 2	x29
6	72	120
7	12	∞

2.4.2.6 Minipreps

A selection of colonies that contained inserts were then used to inoculate 2.5 ml LB containing 100 µg/ml ampicillin overnight at 37°C. DNA was extracted from 1.5 ml of these cultures using the E. Z. N. A.® Plasmid DNA Mini Kit (Omega Bio-tek, Norcross, GA, USA). A 5 µl sample of the

purified plasmid was then digested with *Xho*I and *Xba*I as above and run on an agarose gel as above to confirm the presence of the insert. The miniprep was then sent for sequencing as described above. The remaining 1 ml of culture was used to make a 20% glycerol stock, which was then stored in a -80°C freezer.

2.4.3 Midipreps

In order to increase the concentration of DNA for injection; colonies were plated from the glycerol stocks and then used to inoculate 100 ml LB with 100 µg/ml ampicillin overnight. DNA was then purified using the PureYield™ Plasmid Midiprep System (Promega, Madison, WI, USA).

2.4.4 Maxipreps

In order to increase the concentration of DNA for injection; colonies were plated from the glycerol stocks and then used to inoculate 100 ml LB with 100 µg/ml ampicillin overnight. DNA was then purified using the E. N. Z. A.® Plasmid Maxi Kit (Omega Bio-Tek, Norcross, GA, USA).

2.4.5 *In vitro* Transcription

To prepare the DNA for transcription it was either amplified by PCR (with pCIfor and the relevant rev primer) (*M. persicae* α1 and α2) or pCI was linearised with *Xba*I (*M. persicae* α3, α8, β1, RIC-3, UNC-50, TMX3 and NACHO). The DNA was then transcribed using the mMESSAGE mMACHINE® Kit (Life Technologies, Carlsbad, CA, USA) according to the manufacturer's protocol. The mRNA was purified using the lithium chloride protocol provided and stored in nuclease free water.

2.4.6 Site-Directed Mutagenesis

Site directed mutagenesis was attempted to fix a PCR error near the C-terminus of the *M. persicae* α2 subunit, where two bases were skipped and to introduce the R81T point mutation to the *M. persicae* β1 subunit (Table 2.4). The Q5® Site-Directed Mutagenesis Kit (New England Biolabs, Ipswich, MA, USA) was used according to the manufacturer's protocol. Primers were designed using NEBase Changer (https://nebasechanger.neb.com/) (Table 2.5).

Table 2.4 The sequences for site-directed mutagenesis.

Key: insertion, substitution.	**Sequence**
M. persicae α2 original	TCCTGTGCGAAGCACCGGCTCTACGACGACACGAAGCCAATCGACC GGGACCTGTCGTTCATCGCTAG
M. persicae α2 target	TCCTGTGCGAAGCACCGGCGCTCTACGACGACACGAAGCCAATCGA CCGGGACCTGTCGTTCATCGCTAG
M. persicae β1 original	ATAATGAAATCAAACGTTTGGTTGAGACTTGTATGGAGGGACTATCA ATTACAATGGGACGAGGCAGA
M. persicae β1 R81T	ATAATGAAATCAAACGTTTGGTTGACACTTGTATGGAGGGACTATCA ATTACAATGGGACGAGGCAGA

Table 2.5 Primers for site-directed mutagenesis

Primer	**Sequence**
Mperalpha2_endfor	GCGCTCTACGACGACACGAAG
Mperalpha2_endrev	CGGTGCTTCGCACAGGAT
Mperbeta1PCIR81Tfor	GTTTGGTTGACACTTGTATGGAG
Mperbeta1PCIR81Trev	GTTTGATTTCATTATTTGACTCTTTTC

2.4.7 Acquiring *M. persicae* β1 R81T Mutant from Twist Bioscience

After site-directed mutagenesis was unsuccessful in producing the *M. persicae* β1 R81T mutant, Syngenta provided the mutant subunit DNA from Twist Bioscience (San Francisco, CA, USA). This was then cloned into pCI, using *Xho*I and *Xba*I restriction sites.

2.4.8 Sequence Analysis

Unless otherwise specified signal peptides were predicted using (http://www.cbs.dtu.dk/services/SignalP/) and transmembrane helices were predicted using (https://embnet.vital-it.ch/software/TMPRED_form.html) (website no longer available). All alignments use ClustalW and MEGAX (Kumar *et al.*, 2018). Peptide sequences were used to construct the phylogenetic tree with MEGAX software (Kumar *et al.*, 2018) using the Maximum Likelihood method and Jones-Taylor-Thornton matrix model (Jones, Taylor and Thornton, 1992). The trees with the highest log likelihood after 1000 bootstrap replications are shown.

2.5 Electrophysiology

Functional studies on insect nAChRs were performed using the *X. laevis* oocyte expression system and two-electrode voltage-clamp electrophysiology.

2.5.1 Preparing Oocytes

Oocytes were obtained as above (2.2 Animals). Oocytes from Ecocyte arrived ready for injection. Otherwise, ovaries were dissected from culled *X. laevis* by making an incision in the abdomen and removing the ovarian lobes which are then placed in oocyte dissecting solution (OR2) (sodium chloride 82 mM, potassium chloride 2 mM, magnesium chloride 2 mM, HEPES 5 mM, pH 7.6). Oocytes were either prepared for injection by incubation with collagenase type I at 2 mg/ml in OR2 for 45 min at room temperature with shaking at 150 RPM or the protocol in

Chapter 11 (Xiong and Gendelman, 2014); which involves incubating with 2 mg/ml collagenase type I for 30 min at 30 RPM, then defolliculating with 0.1 m potassium phosphate pH 6.5 for 10 min or by manual defolliculation followed by incubation with 0.5 mg/ml collagenase type I in OR2 for 6 min at room temperature at 150 RPM.

2.5.2 Injecting DNA or RNA

Oocytes were injected using a Nanoject II (Drummond Scientific Company, Broomall, PA, USA) with 23 nl of DNA at concentrations in Table 2.6 or Table 2.7 or 50.6 nl RNA at specified concentrations. The α1 subunit from *D. melanogaster* was previously cloned by Alexandra Cuevas at 97 ng/µl (NM_079757.4), the nAChR subunits from *A. mellifera* apart from α5 were cloned by Dr Joseph Hawkins. All combinations were injected at a 1:1 ratio molar ratio (except *M. persicae* α6, α7, NACHO and RIC-3 2:2:1:1 ratio). Oocytes were stored in Ca^{2+} OR2 (sodium chloride 82 mM, potassium chloride 2 mM, calcium chloride 2 mM, HEPES 5 mM, pH 7.6), supplemented with 1 × antibiotic antimycotic solution and 0.05 mg/ml neomycin or in standard oocyte saline solution (SOS; 100 mM sodium chloride, 2 mM potassium chloride, 1.8 mM calcium chloride, 1 mM magnesium chloride, 5 mM HEPES, pH 7.4) supplemented with 1 x antibiotic antimycotic solution, 0.1 mg/ml amikacin and 0.05 mg/ml neomycin.

Table 2.6 Concentrations of A. mellifera nAChR subunits in pCI injected into X. laevis oocytes

***A. mellifera* nAChR subunit**	**DNA concentration (ng/µl)**
α5	498.1
α6	455.2
α7	604.2
α1	331.9
α2	430.1
α3	337.6
α8	323.8
α9	504.5
β1	115

Table 2.7 Concentrations of M. persicae nAChR subunits and chaperones in pCI injected into X. laevis oocytes

***M. persicae* nAChR subunit or chaperone**	**DNA concentration (ng/µl)**
α6 (miniprep)	120.4
α7 isoform 7a (miniprep)	93.3
NACHO (miniprep)	77.1
human NACHO	277.6
RIC-3 (c23) (miniprep)	114.0
α6 (midiprep)	764.8
NACHO (midiprep)	388.1
RIC-3 (c30) (midiprep)	1171.1
α6 (maxiprep)	3854.0
α7 (maxiprep)	4503.3
NACHO (maxiprep)	1523.0
RIC-3 (c21) (maxiprep)	4998.7
α1 (miniprep)	104.1
α3 (miniprep)	118.7
α8 (miniprep)	110.5
β1 (miniprep)	210.1
UNC-50 (miniprep)	89.5
TMX3 (miniprep)	132.1
α1 (maxiprep)	296.9
α3 (maxiprep)	353.7
α8 (maxiprep)	291.8
β1 (maxiprep)	390.9
UNC-50 (maxiprep)	214.7
TMX3 (maxiprep)	248.4
α2	151.7

2.5.3 Two-Electrode Voltage-Clamp Electrophysiology

Oocytes were tested for responses 2-5 days after injection using two-electrode voltage-clamp electrophysiology; one of the electrodes in the oocyte and one of the electrodes in the bath are used to hold the potential difference across the membrane at a specified voltage, using a negative feedback amplifier, when channels in the membrane open the movement of ions across the membrane can be measured as a current by the other electrode in the oocyte (Figure 2.3) (Rettinger, Schwarz and Schwarz, 2016; Bretschneider and de Weille, 2006). This used borosilicate glass microelectrodes (Harvard Apparatus, Holliston, MA, USA) filled with 3 mM potassium chloride (resistance 2-20 MΩ) and an Oocyte Clamp OC-725C amplifier (Warner Instruments, CT, USA). Oocytes were clamped at −80 mV and responses were recorded on a flatbed chart recorder (Kipp & Zonen BD-11E, Delft, The Netherlands). The oocytes were continuously perfused with SOS at a flow rate of 10 ml/min. Oocytes were selected for experiments if responses were consistent for two or more applications of the normalising concentration of agonist.

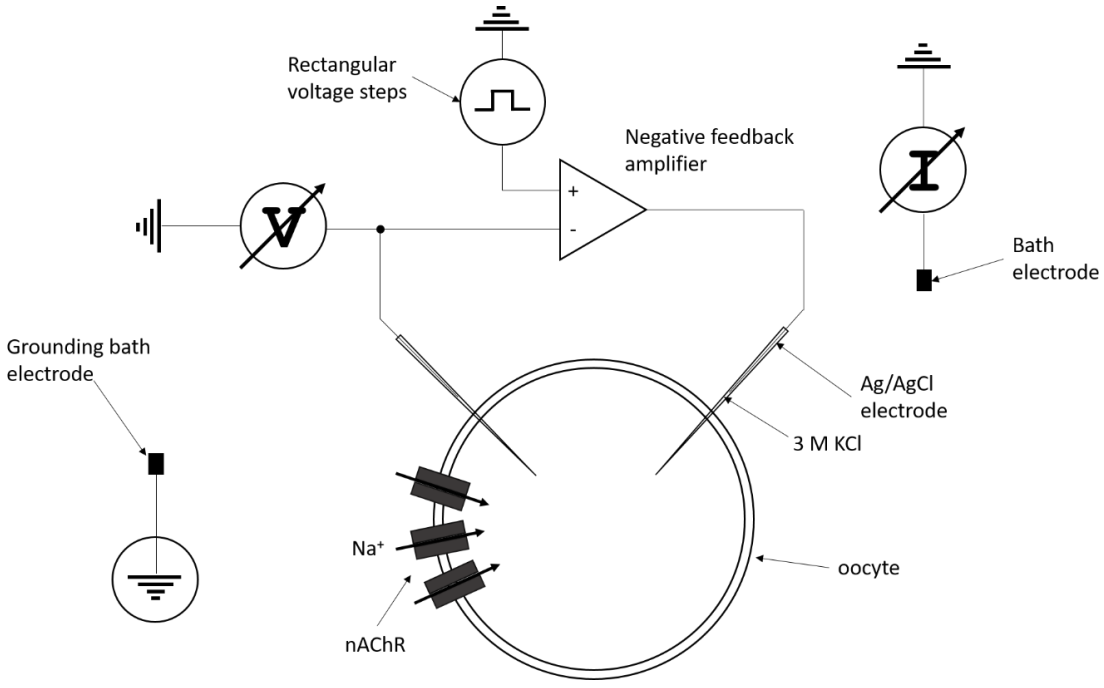

Figure 2.3 Circuit diagram of the two-electrode voltage clamp system. Mitchell personal figure.

2.5.4 Dose-Response Curves

Agonist EC_{50} concentration was determined using agonist concentration response curves, which were generated by challenging oocytes to different concentrations of agonist in SOS for 5 s, with 3 min between challenges which was tested as adequate time to allow for desensitisation. Curves were calculated by normalising the current response to maximal responses induced by the agonist (see 2.6).

2.5.5 Testing Chemicals

Spinosad (10 mM), imidacloprid (100 mM), thiacloprid (100 mM) and amitraz (10 mM) were initially dissolved in DMSO then diluted to working concentrations in a 1:1000 ratio in SOS. The working DMSO concentration did not affect electrophysiological readings. All other chemicals were either dissolved in distilled water to make frozen stocks (100 mM) then dissolved to working concentrations in SOS or dissolved directly in SOS (10 mM) on the day of use. Test chemicals in SOS were applied at 3 min intervals.

2.6 Statistical Analysis

Concentration-response data were fitted with the Hill equation to estimate the EC_{50} and Hill coefficient:

$y = Imax/(\frac{1}{\left(\frac{EC50}{[agonist]}\right)^{nH}})$ where y is the normalised current amplitude, Imax is the maximal response, EC50 is the agonist concentration at half-maximal efficacy, [agonist] is the agonist concentration, and nH is the Hill coefficient. Curve fitting was carried out using GraphPad software version 8 (GraphPad Software, La Jolla, CA, United States). All curves were plotted as log(agonist) vs response – Variable slope. The peak of the current responses was normalised to the agonist concentration that gave a maximal response. Error bars on concentration-response curve graphs show standard error, 'n' indicates the number of oocytes and 'N' indicates the number of frogs these oocytes came from. EC_{50} values and Hill coefficients are

shown as mean ± 95% confidence limits whilst other values are shown as mean ± standard error unless specified. Original data given to a maximum of three significant figures.

Chapter 3 Cloning of *Myzus persicae* Nicotinic Acetylcholine Receptor Subunits and Chaperones

3.1 Introduction

3.1.1 Cloning of Insect Nicotinic Acetylcholine Receptor Families

The complete nAChR subunit gene families have been identified from several insect species such as *A. gambiae*, *A. mellifera*, *B. mori*, *B. terrestris*, *Bombus impatiens*, *P. americana*, *B. germanica* and *T. castaneum* (Jones, Grauso and Sattelle, 2005; Jones *et al.*, 2006; Shao, Dong and Zhang, 2007; Sadd *et al.*, 2015; Jones *et al.*, 2020; Jones and Sattelle, 2007) (see Chapter 1.3). The core subunits have over 60% identity between orthologues from different insect species whereas the divergent subunits have less than 29% identity to other nAChR subunits (Jones and Sattelle, 2010). The complete nAChR gene family from *M. persicae* has yet to be reported, although several nAChR from *M. persicae* have been cloned; the α1 subunit (X81888), α2 subunit (incomplete) (X81887), α3 subunit (AJ236786), α8 subunit (AJ236787), β1 subunit (AJ251838), α6 subunit (AJ880086), a partial α7 subunit (AJ880085) and a partial α4 subunit (AJ236788), since publication some of these subunits have been renamed in light of phylogenetic analysis (Sgard *et al.*, 1998; Huang *et al.*, 1999; Jones *et al.*, 2005; Huang *et al.*, 2000; Kirwan, 2003). However, nAChR subunits have been characterised from another aphid *A. pisum* (Dale *et al.*, 2010; Liu *et al.*, 2013). *A. pisum* possesses 11 nAChR subunit genes (α1-α4, α6-α8 and β1). Interestingly, no α5 subunit was found. It was suggested that since the aphid's nAChR gene family is the most ancient to be described, the α5 subunit appeared later on in the evolution of insects (Dale *et al.*, 2010). As with other insects alternative splicing was found for the α4 (exon 4) and α6 (exon 8) subunits and α7 subunit had unusual tandem duplications of exons 6 and 7, speculated to represent early genome duplication events that would give rise to α5 subunits in more evolutionarily advanced insects (Dale *et al.*, 2010). The divergent *A. pisum* nAChR subunits consisted of one β subunit (β2) and two α subunits (α9 and α10). Neither of the divergent α subunits have the two-cysteines forming the cys-loop, although they do possess aromatic amino acids commonly conserved in this region (Dale *et al.*, 2010). No A to I editing was found in any of the *A. pisum* nAChR subunits.

3.1.2 Cloning of Insect Nicotinic Acetylcholine Receptor Chaperones

3.1.2.1 NACHO

In the paper that originally identified NACHO as a nAChR chaperone (Gu *et al.*, 2016) NACHO from *D. melanogaster* was cloned. It had 37% sequence identity with the human NACHO and could also fully augment the functional surface expression of the human α7 nAChR in HEK293T cells. More recently in the Jones laboratory, NACHO from *A. mellifera* was cloned and used to enable the expression of the homomeric *A. mellifera* α6 nAChR in *X. laevis* oocytes (Hawkins, Mitchell and Jones, 2022). Another study also reported the cloning of the *A. mellifera* NACHO (Brunello *et al.*, 2022), this increased the acetylcholine current from human α4β2 nAChRs expressed in *X. laevis* oocytes.

3.1.2.2 UNC-50 and TMX3

UNC-50 and TMX3 genes were cloned from *D. melanogaster*, *A. mellifera* and *B. terrestris* (Ihara *et al.*, 2020) to facilitate the expression of nAChRs from the respective species in *X. laevis* oocytes. UNC-50 and TMX3 genes were also cloned from *L. salmonis* (a crustacean) to enable the expression of nAChRs (Rufener *et al.*, 2020). *A. mellifera* UNC-50 and TMX3 were also cloned in (Brunello *et al.*, 2022) where the UNC-50 gene encoded a 268 amino acid protein with 44% sequence identity to *C. elegans* UNC-50 and the TMX3 gene encoded 432 amino acids and had 30% sequence identity with *C. elegans* UNC-74 (Brunello et al., 2022).

3.1.2.3 RIC-3

11 alternatively spliced isoforms of *D. melanogaster* RIC-3 were cloned and characterised (Lansdell *et al.*, 2008). These were created by either including or excluding exon 2, exon 6 or exon 9 or by alternative versions of exon 7. Exon 7 contains the entire coiled-coil domain but this does not seem to contribute to the expression of the human α7 nAChR (Lansdell *et al.*, 2008). In some conditions RIC-3 lacking exon 2, in the proline-rich domain, lead to larger surface expression of human α7 and a hybrid nAChR of *D. melanogaster* α2 and rat β2

(Lansdell *et al.*, 2008). In *D. melanogaster* S2 cell lines RIC-3 from *D. melanogaster* enhanced nAChR maturation to a greater extent than human RIC-3 but the converse was the case in human tsA201 cell lines (Lansdell *et al.*, 2008). RIC-3 genes were cloned from *D. melanogaster*, *A. mellifera* and *B. terrestris* (Ihara *et al.*, 2020) and from *L. salmonis* (Rufener *et al.*, 2020) to facilitate nAChR expression. The *A. mellifera* RIC-3 has a very long proline-rich domain and no detected coiled-coil domain (Figure 3.17) (Ihara *et al.*, 2020). In contrast the *B. terrestris* RIC-3 is very short lacking the second transmembrane helix (Ihara *et al.*, 2020). The *A. mellifera* RIC-3 was also cloned (Brunello *et al.*, 2022), where five isoforms were found (Figure 3.1). All the isoforms contained two transmembrane helices; some had an extra section between the two transmembrane helices. Only two isoforms contained the exon with the coiled-coil domain (and these did not have the extra section in the proline-rich domain). Two isoforms were missing most of the C-terminal domain due to premature stop codons.

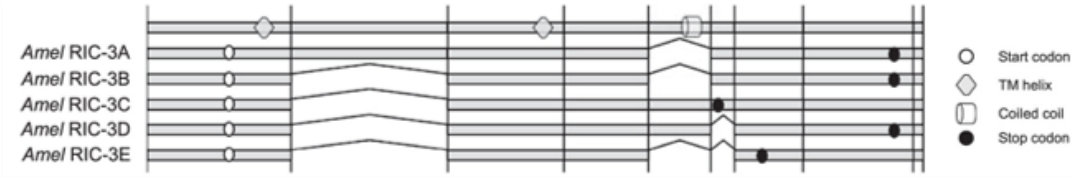

Figure 3.1 Schematic representation of the alternatively spliced A. mellifera RIC-3 variants. Adapted from (Brunello et al., 2022).

3.2 Aim

The aim of the study described in this chapter was to clone all the nAChR subunits and protein chaperones that could potentially contribute to the expression of nAChRs from the aphid, *M. persicae*, which would be the first robust heterologous expression of receptors consisting wholly of nAChR subunit from an insect pest species.

3.3 Results

3.3.1 Sequence Predictions

Putative *M. persicae* nAChR subunit sequences were predicted by tBLASTn using the *A. pisum* nAChR peptide sequences (Dale *et al.*, 2010) against the *M. persicae* database on the AphidBase website (https://bipaa.genouest.org/sp/myzus_persicae/).

3.3.2 Cloning of *M. persicae* β1 and β2 Subunits

The process of cloning the *M. persicae* nAChR subunits and chaperones is outlined in Chapter 2, Figure 2.1. Here, the cloning of the *M. persicae* β1 and β2 subunits is used as an example to illustrate the cloning process that was used to clone the other nAChR subunits and chaperones.

After the nested PCRs, both PCR1 and PCR2 products were run on an agarose gel and the band from the second PCR, if it was at approximately the expected size (commonly around 1.5 kb), was excised for further purification (Figure 3.2). Purified nAChR subunit chaperones were then cloned into the pCI plasmid (Chapter 2.4.2.2-3), which were then used to transform competent *E. coli* (Chapter 2.4.2.4).

Well	1	2	3	4	5	6	7
	1 kb plus ladder	β1-PCR1	β2-PCR1		β1-PCR2		β2-PCR2

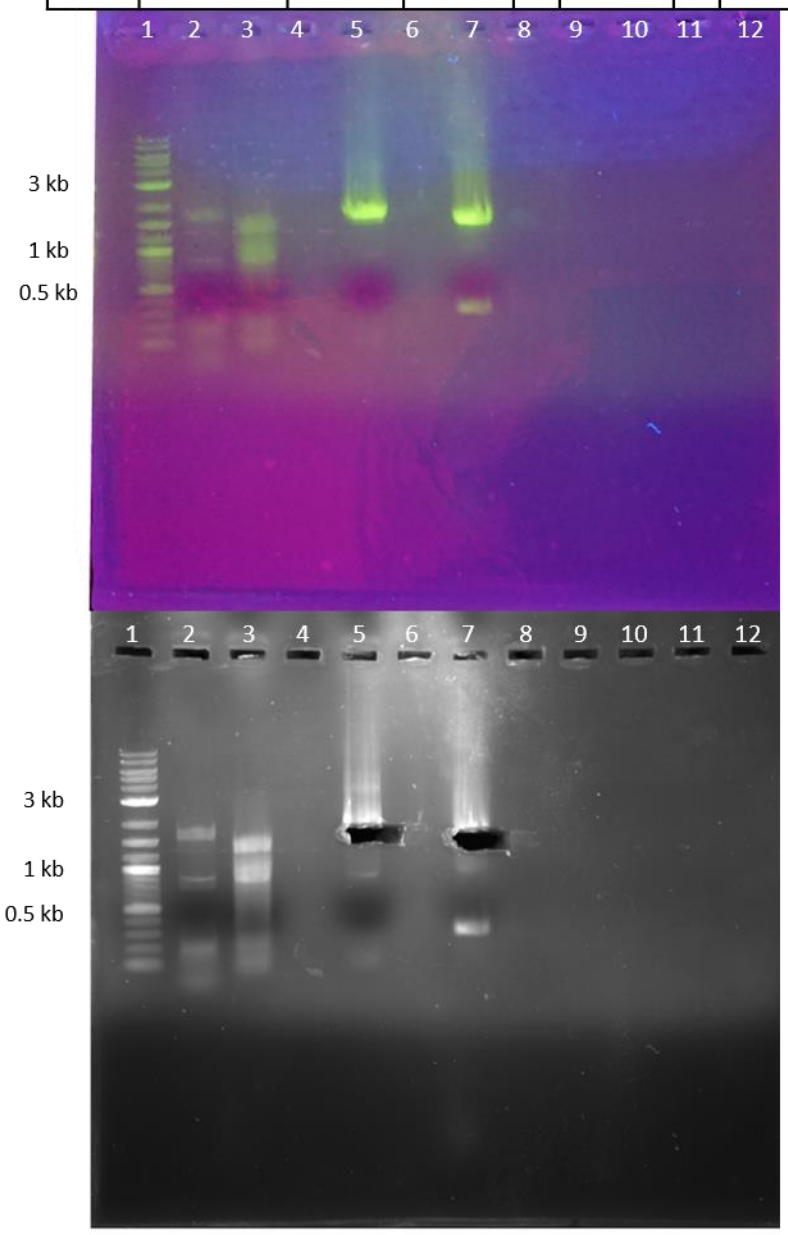

Figure 3.2 Example agarose gels showing amplification products after reverse transcription and PCR. Well numbers in table correspond to labelled well numbers on gel. Gel images of amplification products of M. persicae β1 and β2 nAChR subunits before and after band excision. The photograph of the top gel was taken with low UV before excision on a Transilluminator Model MUV2020-312 (Major Science, Saratoga, CA, USA). The bottom gel photograph was taken, after excision using a Bio-rad Gel imager (Hercules, CA, USA). The 1kb NEB plus ladder (Figure 2.2.) was used.

After colony PCRs were carried out on *E. coli* transformants (see Chapter 2.4.2.5), amplification products were run on an agarose gel to identify which colonies contained an insert. In the case of β1 colonies 1, 2, 3, 4, 5, 6, 7 contain the cloned subunit and for β2 colonies 11, 13, 14

and 18 contain the cloned subunit, indicated by amplification products of the expected size of ~1.5 kbp and ~1.3 kbp for β1 and β2, respectively (Figure 3.3).

Well	1	2	3	4	5	6	7	8	9	10	11	12
Row 1 β1	1 kb plus ladder	1	2	3	4	5	6	7	8	9		
Row 2 β2	1 kb plus ladder	10	11	12	13	14	15	16	17	18		

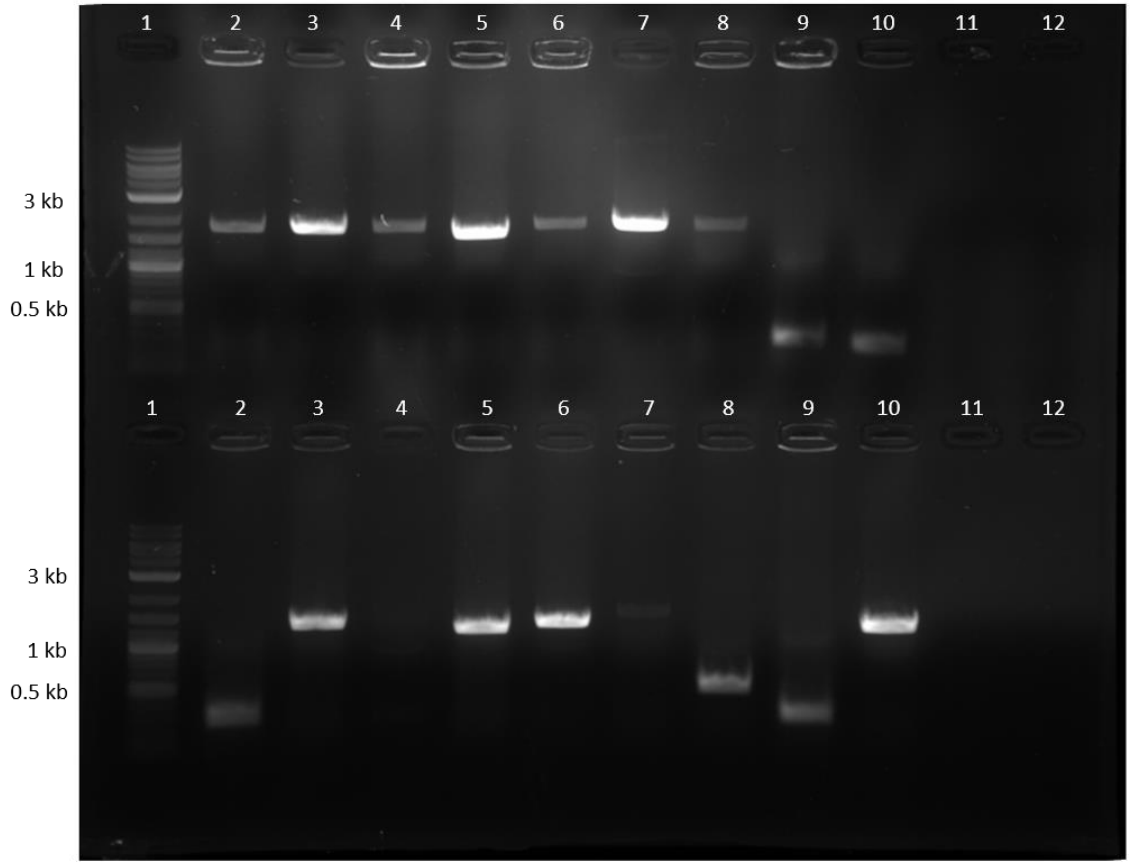

Figure 3.3 Agarose gel of colony PCR to detect the cloning of M. persicae β1 and β2 nAChR subunits from transformed E. coli *colonies. Well numbers in table correspond to labelled well numbers on gel. The top row shows β1 colonies and the bottom row β2 colonies. The image taken using a Bio-rad Gel imager. The 1kb NEB plus ladder (Figure 2.2) was used.*

Colonies identified as containing the pCI plasmid with a cloned insert were used to inoculate LB medium for purification of the plasmid by miniprep (Chapter 2.4.2.6). After the minipreps a 5 µl sample was digested with *Xho*I and *Xba*I. The digests were then run on a gel to confirm that the minipreps contained the insert (Figure 3.4).

Well	1	2	3	4	5
	1 kb plus ladder	β1 c4	β1 c6	β2 c11	β2 c18

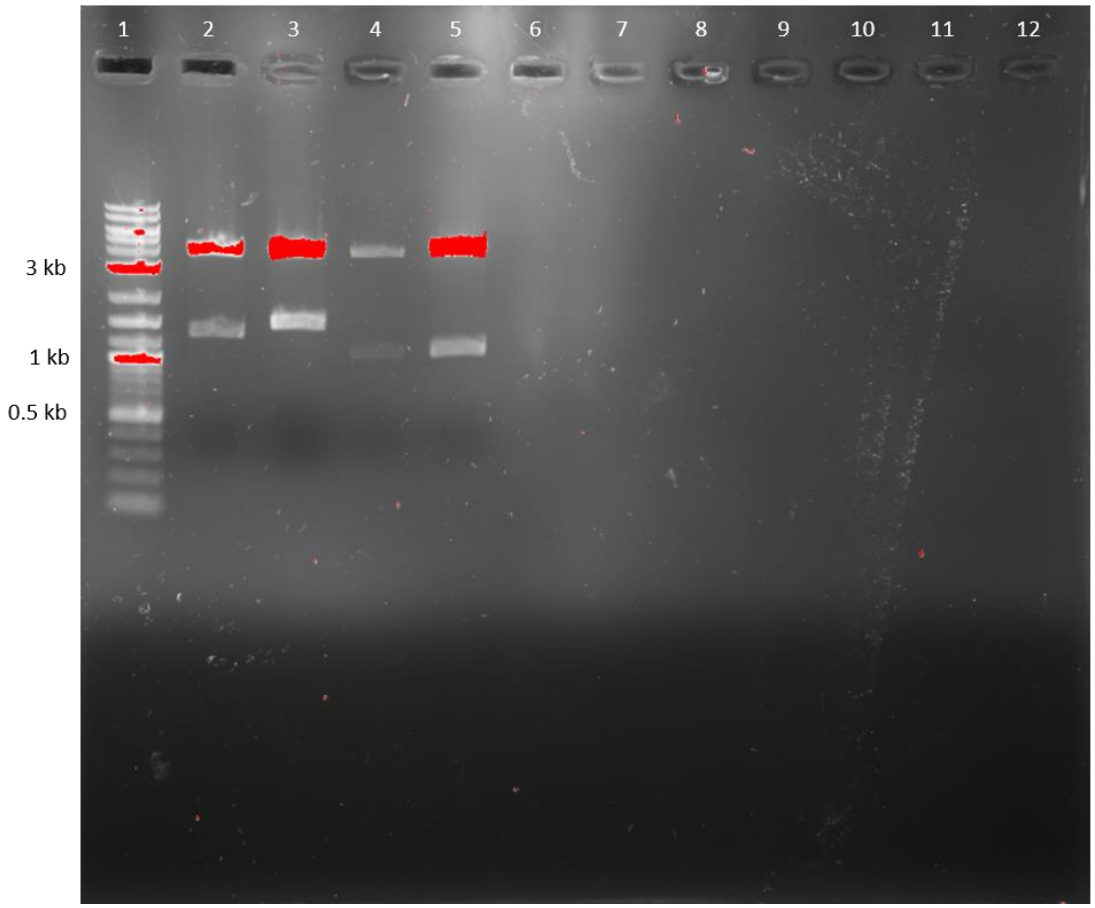

Figure 3.4 An agarose gel showing the digest of the minipreps of M. persicae β1 and β2 with XhoI and XbaI. Well numbers in table correspond to labelled well numbers on gel. Both the pCI plasmid (~3 kb) and insert (1-1.8 kb) can be seen. The image taken using a Bio-rad Gel imager and the red bands were a result of overexposure. The 1 kb plus ladder (Figure 2.2) was used.

3.3.3 Sequences of Cloned *M. persicae* Nicotinic Acetylcholine Receptor Subunits

The α1, α2, α3, α6, α7, α8, α9, α10 and β1 *M. persicae* nAChR subunits were successfully cloned into the pCI vector and sequenced. Phylogenetic analysis of the resulting peptide sequences confirmed their orthologous relationships with subunits from other insect species (Figure 3.20 and 3.3.5). For the α4 and β2 subunits, only splice variants with incomplete predicted open reading frames were cloned (Figures 3.8 and 3.14). The α3 and α8 sequences were identical to the predicted and previously cloned sequences (Huang *et al.*, 1999) and had all the features expected of nAChRs (Figure 3.5). The α3 subunit has a slight variation of the cation selectivity sequence preceding the second transmembrane region, NEK, instead of GEK

(Figure 3.5) (Corringer, Novère and Changeux, 2000; Jensen, Schousboe and Ahring, 2005). The α1, α4 and β1 subunits have splice variants. Both the α6 and α7 subunits have alternative exons and different splice variants have been obtained for each of these.

Mper_a3

```
  1 mktlagaiilcimlviisgcSMNPDAKRLYDDLLSNYNKLVRPVLNNTDPLPVRIKLKLSQLIDINLK
 69 NQIMTTNLWVEQYWYDYKLTWNPDEYGGVEGLHVPSEHVWRPDIVLYNNADGNFEVTLATKAMLHYSG
137 RVEWKPPAIYKSSCEIDVEFFPFDEQTCVMKFGSWTYDGFQVDLRHANEVSGSRVVDVGVDLSEFYAS
205 VEWDILEVPAIRNEKYYTCCEEPYLDITFNITMRRKTLFYTVNLIIPCMGISFLTILVFYLPSDSNEK
273 VSLSISILLSLTVFFLLLAEIIPPTSLVVPLLGKFVLFTMILDTLSICVTVVVLNIHFRSPTTHVMSP
341 WVRRVFIHILPRMLIMRRPHYQMERKSLMGTCHRIMVRTCNGLELRDQESADQLLHSNDVFPARDLES
409 GVIGCCEIHGPIIALPSSSEINLNAPVPKGRKHWHDCPELHKAVEGAAYIADYIKKEEEEKKIKEDWK
477 YVAMVLDRLFLWIFTLAVTMGSAGIILQAPTLYDNRLPINVRLSEILAHTPTVKQNYNNIM
```

Mper_a8

```
  1 mnilyilplllplsycEFALNNTKFEGNPYKKHLFDDLLSNYNRLIRPVQNHSENLTVWMGLKLTQLT
 69 EMNLKSQVMTTSVWLIQKWFDCNLKWDPKDYGGLDKLYVPSDHIWLPDIVLFNNADGNYEVTLMTKAV
137 LKYTGEVLWSPPAIYKSYCEINVLYFPFDEQNCYMMFGSWTYNGNQVDLRHIDQSQGRNRVDVGIDLS
205 EFYLSVEWDLLEVPAVRNEEFYSCCSESYTDITFNIKMRRKTLFYTVNLIIPCVGLTFMTVLVFYLPS
273 DSGEKVTLCSNILVSLTVFFLLLAEIIPPTSLAVPLLGKYLLFTMVLVSMSIGMTVVVLNIHFRSPST
341 HTLSPWVRTVFLHMMPQILMMRRPPYSLMTNDGFQSSPGYFNELDYSRDSISDSGGTEQKPPSLTQRH
409 WSFKKIQSVQPHNYPENVMPKTMSPDLLKALQGVCYIAQHIKDADKDKEVIEDWKYVSMVFDRFFLWV
477 FTLACIVGTCAIIFQAPSLYDQRQPIDFQLSSIPRRRSNLALPHEIDFYERTYGAN
```

Figure 3.5 Peptide sequences of cloned M. persicae α3 and α8 nAChR subunits, which are identical to accession numbers AJ236786 and AJ236787 when translated respectively. The predicted signal peptide is in lowercase, predicted transmembrane helices in bold, the cys-loop cysteines underlined and the consecutive cysteines present in α subunits double underlined.

3.3.3.1 The α1 Subunit.

Two clones for the *M. persicae* α1 subunit were identified. The α1 sequences of both clones had all the features associated with nAChRs (Figure 3.6). One clone, c22, is identical to the predicted and previously cloned sequence (Sgard *et al.*, 1998). The other clone, c21, is missing 20 amino acids when compared to c22 (Figure 3.6) (OQ102299), most likely a result of alternative splicing. The missing amino acids are located in the intracellular loop, between TM3 and TM4, which is commonly variable in nAChR subunits (Jones and Sattelle, 2010). The missing sequence contains a putative protein kinase C (PKC) phosphorylation site (S415) and another kinase site (S416) (Figure 3.6), predicted using NetPhos 3.1

(https://services.healthtech.dtu.dk/service.php?NetPhos-3.1). Alternative splicing in the TM3-TM4 intracellular loop leading to the inclusion/exclusion of potential phosphorylation sites have been observed in other subunits, for example, the *A. mellifera* α3 nAChR subunit (Jones *et al.*, 2006). The clone containing the complete sequence (c22) was used for further experiments.

```
Mper_a1c22   1 mkiicaifasvivgqlampYASVYGSADAKRLYDDLLSNYNRLIRPVGNNSDRLTVK
Mper_a1c21   1 mkiicaifasvivgqlampYASVYGSADAKRLYDDLLSNYNRLIRPVGNNSDRLTVK

Mper_a1c22  58 MGLKLSQIIEVNLRNQIMTTNVWVEQEWNDYKLKWNPEDYGGVDTLHVPSEHIWLPD
Mper_a1c21  58 MGLKLSQIIEVNLRNQIMTTNVWVEQEWNDYKLKWNPEDYGGVDTLHVPSEHIWLPD

Mper_a1c22 115 IVLYNNADGNYEVTIMTKAILHYTGKVVWKPPAIYKSFCEINVEYFPFDEQTCSMKF
Mper_a1c21 115 IVLYNNADGNYEVTIMTKAILHYTGKVVWKPPAIYKSFCEINVEYFPFDEQTCSMKF

Mper_a1c22 172 GSWTYDGYMMDLRHISQAPDSDVIEVGIDLQDYYLSVEWDIMGVPAVRHEKFYVCCE
Mper_a1c21 172 GSWTYDGYMMDLRHISQAPDSDVIEVGIDLQDYYLSVEWDIMGVPAVRHEKFYVCCE

Mper_a1c22 229 EPYLDIFFNITLRRKTLFYTVNLIIPCVGISFLSVLVFYLPSESGEKVSLCISILLS
Mper_a1c21 229 EPYLDIFFNITLRRKTLFYTVNLIIPCVGISFLSVLVFYLPSESGEKVSLCISILLS

Mper_a1c22 286 LTVFFLLLVEIIPPTSLTVPLLGKYLLFTMVLVTLSVFVTVAVLNVNFRSPVTHKMR
Mper_a1c21 286 LTVFFLLLVEIIPPTSLTVPLLGKYLLFTMVLVTLSVFVTVAVLNVNFRSPVTHKMR

Mper_a1c22 343 PWVVKLFIQILPKVLFIERPKKGDSIDEDDDDDDEKHGEILSGVFNVPSEIDKYLGY
Mper_a1c21 343 PWVVKLFIQILPKVLFIERPKKGDSIDEDDDDDDEKHGEILSGVFNVPSEIDKYLGY

Mper_a1c22 400 NRGYSFDYDVPPPLPSSRYCGARAVCAGGVNGGAGVSAGAGAVTGSNDTVVNMASDE
Mper_a1c21 400 NRGYSFDYDV----------NGGAGVSAGAGAVTGSNDTVVNMASDE

Mper_a1c22 457 DEDAIELDAEDEYDDMFSPTTTTDDGLASPTFESHHHHHQHQHGCPVDQQPRHDPAM
Mper_a1c21 437 DEDAIELDAEDEYDDMFSPTTTTDDGLASPTFESHHHHHQHQHGCPVDQQPRHDPAM

Mper_a1c22 514 QTIQDAKFIAQHVKNQDKFDEIIEDWQYVAMVLDRLFLWIFTCACLIGTALIIFQAP
Mper_a1c21 494 QTIQDAKFIAQHVKNQDKFDEIIEDWQYVAMVLDRLFLWIFTCACLIGTALIIFQAP

Mper_a1c22 571 ALYDKTKPIDVVYSKIAKKKLQAIL
Mper_a1c21 551 ALYDKTKPIDVVYSKIAKKKLQAIL
```

Figure 3.6 The aligned sequences of two clones (a1c22 and a1c21) of M. persicae α1 nAChR subunits. The predicted signal peptide is in lowercase, predicted transmembrane helices in bold, the cys-loop cysteines underlined, the consecutive cysteines present in α subunits double underlined and putative phosphorylation sites that differ between the two isoforms circled, predicted using NetPhos 3.1 (https://services.healthtech.dtu.dk/service.php?NetPhos-3.1).

3.3.3.2 The α2 Subunit

We were initially unable to find from AphidBase (https://bipaa.genouest.org/sp/myzus_persicae/) a complete transcript of the α2 subunit with the N-terminus required to design primers, the previously cloned α2 subunit had not included the N-terminus (Sgard *et al.*, 1998). However, by 2020 updates to the website allowed us to find a predicted complete transcript (LOC111030749). Neither the transcript nor any of the

clones contained a detectable signal peptide (using SignalP-5.0 https://services.healthtech.dtu.dk/service.php?SignalP-5.0) (Figure 3.7). Starting at the 17th amino acid there is a series of asparagine residues encoded by a repeated sequence, the number of these asparagine residues varies with each PCR possibly due to the DNA polymerase slipping on the repeated sequence (Figure 3.7) (Viguera, Canceill and Ehrlich, 2001). The initial cloning of the α2 subunit had a frame shift mutation near the C-terminus, this was corrected using site-directed mutagenesis using the protocol in Chapter 2. The c31 and c37 clones were cloned using the corrected α2 clone as a template. Otherwise, the α2 sequences cloned had features commonly associated with nAChRs (Figure 3.7). There was a slight variation in the cation selecting GEK motif from GEK to KEK (Corringer, Novère and Changeux, 2000). The site-directed mutagenesis-corrected clone was used in DNA expression experiments and the transcribed c37 clone was used in RNA expression experiments.

```
Mper_a2       1 MPSVAPAAAHDGDIRHNNNNNNNNNNNNNNAGTGSSNYNSKKFRGRRRRRGCAQLT
Mper_a2c2o    1 MPSVAPAAAHDGDIRHNNNNNNNNNN----AGTGSSNYNSKKFRGRRRRRGCAQLT
Mper_c2c31    1 MPSVAPAAAHDGDIRHNNNNNNNNN-----AGTGSSNYNSKKFRGRRRRRGCAQLT
Mper_c2c37    1 MPSVAPAAAHDGDIRHNNNNNNNNNNN---AGTGSSNYNSKKFRGRRRRRGCAQLT

Mper_a2      56 SSLPLLLLSAVGCLCNPDAKRLYDDLLSNYNRLIRPVSNNTDTVLVKLGLRLSQL
Mper_a2c2o   52 SSLPLLLLSAVGCLCNPDAKRLYDDLLSNYNRLIRPVSNNTDTVLVKLGLRLSQL
Mper_a2c31   51 SSLPLLLLSAVGCLCNPDAKRLYDDLLSNYNRLIRPVSNNTDTVLVKLGLRLSQL
Mper_a2c37   53 SSLPLLLLSAVGCLCNPDAKRLYDDLLSNYNRLIRPVSNNTDTVLVKLGLRLSQL

Mper_a2     111 IELNLKDQILTTNVWLEHEWADHKFIWEPLEYGGVKELYVPSEHIWLPDIVLYNN
Mper_a2co   107 IELNLKDQILTTNVWLEHEWADHKFIWEPLEYGGVKELYVPSEHIWLPDIVLYNN
Mper_a2c31  106 IELNLKDQILTTNVWLEHEWADHKFIWEPLEYGGVKELYVPSEHIWLPDIVLYNN
Mper_a2c37  108 IELNLKDQILTTNVWLEHEWADHKFIWEPLEYGGVKELYVPSEHIWLPDIVLYNN

Mper_a2     166 ADGEYVVTTMTKAVLHHSGKVMWTPPAIFKSSCEIDVRYFPFDQQTCFMKFGSWS
Mper_a2co   162 ADGEYVVTTMTKAVLHHSGKVMWTPPAIFKSSCEIDVRYFPFDQHTCFMKFGSRS
Mper_a2c31  161 ADGEYVVTTMTKAVLHHSGKVMWTPPAIFKSSCEIDVRYFPFDQQTCFMKFGSWS
Mper_a2c37  163 ADGEYVVTTMTKAVLHHSGKVMWTPPAIFKSSCEIDVRYFPFDQQTCFMKFGSWS

Mper_a2     221 YDGNQINLKHIGQLVGTNKVDVGIDLSAYYPSVEWDILGVPAERHEKYYSCCAEP
Mper_a2co   217 YDGNQINLKHIGQLVGTNKVDVGIDLSAYYPSVEWDILGVPAERHEKYYSCCAEP
Mper_a2c31  216 YDGNQINLKHIGQLVGTNKVDVGIDLSAYYPSVEWDILGVPAERHEKYYSCCAEP
Mper_a2c37  218 YDGNQINLKHIGQLVGTNKVDVGIDLSAYYPSVEWDILGVPAERHEKYYSCCAEP

Mper_a2     276 YIDIFFNITLRRRTLFYTVNLIVPCVGISYLSVLVFYLPADSKEKISLCITILLS
Mper_a2c2o  272 YIDIFFNITLRRRTLFYTVNLIVPCVGISYLSVLVFYLPADSKEKISLCITILLS
Mper_a2c31  271 YIDIFFNITLRRRTLFYTVNLIVPCVGISYLSVLVFYLPADSKEKISLCITILLS
Mper_a2c37  273 YIDIFFNITLRRRTLFYTVNLIVPCVGISYLSVLVFYLPADSKEKISLCITILLS

Mper_a2     331 QTMFFLLISEIIPSTSLSLPLLGKYLLFTMLLVALCVVVTIIINIHYRQPSTHK
Mper_a2co   327 QTMFFLLISEIIPSTSLSLPLLGKYLLFTMLLVALCVVVTIIINIHYRQPSTHK
Mper_a2c31  326 QTMFFLLISEIIPSTSLSLPLLGKYLLFTMLLVALCVVVTIIINIHYRQPSTHK
Mper_a2c37  328 QTMFFLLISEIIPSTSLSLPLLGKYLLFTMLLVALCVVVTIIINIHYRQPSTHK

Mper_a2     386 IPSWMRTVFIRALPKMLLMRVPEQLLADSAMKQKQMKTCKKLNLNLARLNAASVG
Mper_a2c2o  382 IPSWMRTVFIRALPKMLLMRVPEQLLADSAMKQKQMKTCKKLNLNLARLNAASVG
Mper_a2c31  381 IPSWMRTVFIRALPKMLLMRVPEQLLADSAMKQKQMKTCKKLNLNLARLNAASVG
Mper_a2c37  383 IPSWMRTVFIRALPKMLLMRVPEQLLADSAMKQKQMKTCKKLNLNLARLNAASVG

Mper_a2     441 ATLNVPPAPVASPPPGHRSPTDSLRRFVAATGRTGCNGTAAAAGAASRLVNAAVS
Mper_a2c2o  437 ATLNVPPAPVASPPPGHRSPTDSLRRFVAATGRTGCNGTAAAAGAASRLVNAAVS
Mper_a2c31  436 ATLNVPPAPVASPPPGHRSPTDSLRRFVAATGRTGCNGTAAAAGAASRLVNAAVS
Mper_a2c37  438 ATLNVPPAPVASPPPGHRSPTDSLRRFVAATGRTGCNGTAAAAGAASRLVNAAVS

Mper_a2     496 SIDDTLNEVPAAIRKKYPFELEKAIHNVKFIQHHLQRQDEYNTEDQDWGFVAMVL
Mper_a2co   492 SIDDTLNEVPAAIRKKYPFELEKAIHNVKFIQHHLQRQDEYNTEDQDWGFVAMVL
Mper_a2c31  491 SIDDTLNEVPAAIRKKYPFELEKAIHNVKFIQHHLQRQDEYNTEDQDWGFVAMVL
Mper_a2c37  493 SIDDTLNEVPAAIRKKYPFELEKAIHNVKFIQHHLQRQDEYNTEDQDWGFVAMVL

Mper_a2     551 DRLFLWIFTVASIMGTILILCEAPALYDDTKPIDRDLSFIARKQFSPTSDLE
Mper_a2co   547 DRLFLWIFTVASIMGTILILCEAPALR--RHEANRPGPVVHR----------
Mper_a2c31  546 DRLFLWIFTVASIMGTILILCEAPALYDDTKPIDRDLSFIARKQFSPTSDLE
Mper_a2c37  548 DRLFLWIFTVASIMGTILILCEAPALYDDTKPIDRDLSFIARKQFSPTSDLE
```

Figure 3.7 The aligned sequences of the predicted sequence and three clones (α2c2o, α2c31 and a2c37) of M. persicae α2 nAChR subunits. Predicted transmembrane helices are shown in bold, the cys-loop cysteines underlined and the consecutive cysteines present in α subunits double underlined.

3.3.3.3 The α4 Subunit

Four clones of the *M. persicae* α4 subunit were obtained, none of which had the complete predicted sequence (Figure 3.8), only a partial sequence had previously been cloned (Huang *et al.*, 1999). Two clones, c7 and c18, had a splice variant that was missing amino acids 116-212 of the predicted sequence without a frame shift (Figure 3.8). This removes several essential ligand-binding loops, as well as the cys-loop, so this protein is predicted to be non-functional. The clones through do possess all of four transmembrane domains and a C-terminal extracellular domain. The other two α4 clones, c5 and c13, have a splice variant that introduces a frame shift, producing truncated proteins of only 114 amino acids that ends within the N-terminal region (Figure 3.8).

```
Mper_a4      1 mwpkfaflglviirlmvsaNPDAKRLYDDLLSSYNKLVRPVVNTSDVLRVSIKLK
Mper_a4c7    1 mwpkfaflglviirlmvsaNPDAKRLYDDLLSSYNKLVRPVVNTSDVLRVSIKLK
Mper_a4c5    1 mwpkfaflglviirlmvsaNPDAKRLYDDLLSSYNKLVRPVVNTSDVLRVSIKLK

Mper_a4     56 LSQLIDVNLKNQIMTTNVWVEQAWNDYKLQWDPKEYGGVQMLHVPSDHIWRPDIV
Mper_a4c7   56 LSQLIDVNLKNQIMTTNLWVEQAWNDYKLQWDPKEYGGVQMLHVPSDHIWRPDIV
Mper_a4c5   56 LSQLIDVNLKNQIMTTNLWVEQAWNDYKLQWDPKEYGGVQMLHVPSDHIWRPDIV

Mper_a4    111 LYNNADGNFDVTPATKATIYHVGLVEWKPPAIFKSSCEIDVEFFPFDEQTCVLKF
Mper_a4c7  111 LYNK----------------------------------------------------
Mper_a4c5  111 LYNK----------------------------------------------------

Mper_a4    166 GSWTYDGFKVDLRHMDEKVGSNIVDVGVDLSEFYMSVEWDILEVPAVRNEKIYPC
Mper_a4c7      ------------------------------------------------NEKIYPC
Mper_a4c5      ------------------------------------------------------

Mper_a4    221 CDEPYLDITFNITMRRKTLFYTVNIIIPCMGISFLTVLTFYLPSDSGEKVTLSIS
Mper_a4c7  122 CDEPYLDITFNITMRRKTLFYTVNIIIPCMGISFLTVLTFYLPSDSGEKVTLSIS
Mper_a4c5      ------------------------------------------------------

Mper_a4    276 ILISLHVFFLLVVEIIPPTSLVVPLLGKYLIFAMILVSISICVTVVVLNVHFRSP
Mper_a4c7  177 ILISLHVFFLLVVEIIPPTSLVVPLLGKYLIFAMILVSISICVTVVVLNVHFRSP
Mper_a4c5      ------------------------------------------------------

Mper_a4    331 QTHKMAPWVKRVFIHILPRLLVMRRPQYQFEPNKFNAGSIMLKGRDIHPCFFQAG
Mper_a4c7  232 QTHKMAPWVKRVFIHILPRLLVMRRPQYQFEPNKFNAGSIMLKGRDIHPCFFQAG
Mper_a4c5      ------------------------------------------------------

Mper_a4    386 CGYDSTEPGRDKGRRQTDDSSVSKGTRETSKEDLSSDGEGGSCQIHGVAQSLISD
Mper_a4c7  287 CGYDSTEPGRDKGRRQTDDSSVSKGTRETSKEDLSSDGEGGSCQIHGVAQSLISD
Mper_a4c5      ------------------------------------------------------

Mper_a4    441 EISVTEMTTDCSKSSILLRSPGFLHSSCPPAMHKSCFCIRFIAEHTKITDDATKV
Mper_a4c7  342 EISVTEMTTDCSKSSILLRSPGFLHSSCPPAMHKSCFCIRFIAEHTKITDDATKV
Mper_a4c5      ------------------------------------------------------

Mper_a4    496 KEDWKYVAMVLDRLFLWIFTLAVFAGTAGIILQAPTLYDDRIPIDKKFSEYQTS
Mper_a4c7  397 KEDWKYVAMVLDRLFLWIFTLAVFAGTAGIILQAPTLYDDRIPIDKKFSEYQTS
Mper_a4c5      ------------------------------------------------------
```

Figure 3.8 Alignment of the predicted sequence and two clones (a4c7 and a4c5) of M. persicae α4 nAChR subunits. The predicted signal peptide is in lowercase, predicted transmembrane helices in bold, the cys-loop cysteines underlined and the consecutive cysteines present in α subunits double underlined.

3.3.3.4 The α6 Subunit

The *M. persicae* α6 nAChR subunit is thought to have at least two splice variants with two alternatives for exon 8, from the predicted sequences (Dale *et al.*, 2010). We have cloned a complete coding sequence containing exon 8a (c3 and c4) (which had previously been cloned (Kirwan, 2003)) but the clones containing exon 8b (c6 and c8) had a nonsense mutation later in the clone, most likely due to an error in the PCR (Figure 3.9). Thus, the complete clone (c3) with exon 8a was used for further experiments. All the α6 sequences cloned had all the features associated with nAChRs (Figure 3.9).

```
Mper_a6c3     1mtsstskfvavlfllaavkikesvqGKFERQLLDDLLIEYNPLERPVSNESDPLE
Mper_a6c6     1mtsstskfvavlfllaavkikesvqGKFERQLLDDLLIEYNPLERPVSNESDPLE

Mper_a6c3    56VTFGITLQQIIDVDEKNQIVITNAWLNMEWVDYNMRWNISEYGGVKDLRLNPNRL
Mper_a6c6    56VTFGITLQQIIDVDEKNQIVITNAWLNMEWVDYNMRWNISEYGGVKDLRLNPNRL

Mper_a6c3   111WKPDILMYNSADEKFDGTYQTNVVVRHNGTCLYVPPGIFKSTCKIDITWFPFDDQ
Mper_a6c6   111WKPDILMYNSADEKFDGTYQTNVVVRHNGTCLYVPPGIFKSTCKIDITWFPFDDQ

Mper_a6c3   166NCLMKFGSWTYNGFQIDLVLKSDGGDLSDFTTNGEWYLLGMPGKKNVINYACCPE
Mper_a6c6   166NCLMKFGSWTYNGFQIDLVLKSDGGDLSDFTTNGEWYLLGMPGKKNVINYACCPE

Mper_a6c3   221PYVDITFTIKIRRRTLYYFFNLIVPCVLISSMALLGFTLPPDCGEKLTL------
Mper_a6c6   221PYVDITFTIKIRRRTLYYFFNLIVPCVLISSMALLGFTLPPDCGEKLTLGHKNKL

Mper_a6c3   267---EITILLSLTVFLNLVAESMPTTSEAVPLIGTYFNCIMFMVASSVVLTLVVLN
Mper_a6c6   276VVTGVTILLSLTVFLNLVAETLPQVSDAIPLLGTYFNCIMFMVASSVVLTLVVLN

Mper_a6c3   322YHHRTADIHTMGPWVKCFFLLWLPWILCMQRPGKDISFKAIRSRYTDRRGIELRE
Mper_a6c6   331YHHRTADIHTMGPWVKCFSCYGCHGSYVCKGQVKTYRSRPSEVDIQIEEASNSES

Mper_a6c3   377RSSRSLLANVLDIDDDFRASVLSHRVYNSGAASSSSPASESRSVCNYSARELQLI
Mper_a6c6   386DRQEVY----------------------------------------------
------

Mper_a6c3   432LQEVRYITDHMRKQQDDQEVINDWKYAAMVVDRFCLIVFTFFTLVATVAVMYSAP
Mper_a6c6     ------------------------------------------------------

Mper_a6c3   487HIIVE
Mper_a6c6     -----
```

Figure 3.9 The aligned sequences of two clones (a6c3 and a6c6) of M. persicae α6 nAChR subunits. The predicted signal peptide is in lowercase, predicted transmembrane helices in bold, the cys-loop cysteines underlined and the consecutive cysteines present in α subunits double underlined. Exon 8a is highlighted in light grey and exon 8b is highlighted in dark grey.

3.3.3.4 The α7 Subunit

The *M. persicae* α7 subunit was anticipated to have two alternative exons (exon 6 and exon 7) based on the α7 subunit identified in the aphid, *A. pisum* (Dale *et al.*, 2010), where exon 6 includes some of the ligand-binding loops and the first transmembrane helix, whilst exon 7 includes the second transmembrane helix. The *M. persicae* α7 clones identified in this study contain exon6a and exon7a (c10, c11 and c13) (OQ102300) or exon6a and exon7b (c12) (OQ102301) (Figure 3.10), thus two out of the four theorised isoforms were cloned. The c11 clone with exon 6a and 7a was used for expression experiments. All the α7 sequences cloned possessed features associated with nAChRs subunits (Figure 3.10).

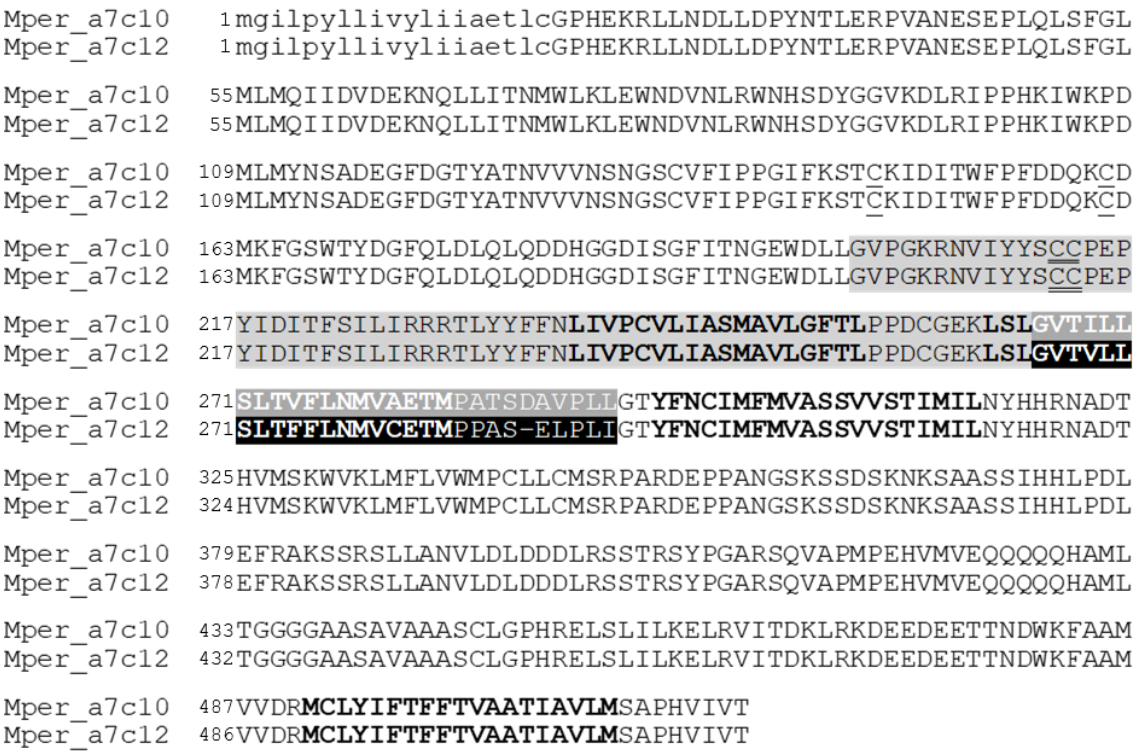

Figure 3.10 The aligned sequences of two clones (a7c10 and a7c12) of M. persicae α7 nAChR subunits. The predicted signal peptide is in lowercase, predicted transmembrane helices in bold, the cys-loop cysteines underlined and the consecutive cysteines present in α subunits double underlined. Exon 6a is highlighted in light grey shading. Exon 7a is highlighted in medium grey shading with white text and exon 7b in dark grey shading with white text.

3.3.3.5 The β1 Subunit

Two clones for the *M. persicae* β1 nAChR subunit were identified. One clone (c6) was identical to the complete predicted β1 sequence and previously cloned sequence (Huang *et al.*, 2000), lacking the adjacent cysteines that defines α subunits (Figure 3.11). The other clone (c4)

contains the first 325 amino acids then there is a frame shift which results in a premature stop codon. This variant is missing the fourth transmembrane helix and most of the intracellular loop (Figure 3.11). The c6 sequence clone had all the features associated with nAChRs (Figure 3.11) and was used for expression studies.

```
Mper_b1c6    1 mntsvgllmavffvcsqfirgcwcSEDEERLVRDLFRGYNKLIRPVQNMTEKVNV
Mper_b1c4    1 mntsvgllmavffvcsqfirgcwcSEDEERLVRDLFRGYNKLIRPVQNMTEKVNV

Mper_b1c6   56 QFGLAFVQLINVNEKSQIMKSNVWLRLVWRDYQLQWDEADYGGIQVLRLPPDKVW
Mper_b1c4   56 QFGLAFVQLINVNEKSQIMKSNVWLRLVWRDYQLQWDEADYGGIQVLRLPPDKVW

Mper_b1c6  111 KPDIVLFNNADGNYEVRYKSNVLIRPNGELLWIPPAIYQSSCTIDVTYFPFDQQT
Mper_b1c4  111 KPDIVLFNNADGNYEVRYKSNVLIRPNGELLWIPPAIYQSSCTIDVTYFPFDQQT

Mper_b1c6  166 CIMKFGSWTFNGDQVSLALYNDKQFVDLSDYWKSGTWDIIEVPAYLNVYQESPTQ
Mper_b1c4  166 CIMKFGSWTFNGDQVSLALYNDKQFVDLSDYWKSGTWDIIEVPAYLNVYQESPTQ

Mper_b1c6  221 TDITFYIVIRRKTLFYTVNLILPTVLISFLCVLVFYLPAEAGEKVTLGISILLSL
Mper_b1c4  221 TDITFYIVIRRKTLFYTVNLILPTVLISFLCVLVFYLPAEAGEKVTLGISILLSL

Mper_b1c6  276 VVFLLLVSKILPPTSLVLPLIAKYLLFTFIMNTVSILVTVIIINWNFRGPRTHRM
Mper_b1c4  276 VVFLLLVSKILPPTSLVLPLIAKYLLFTFIMNTVSILVTVIIINWNFRGPTRACA

Mper_b1c6  331 PPWIRTVFLYYLPACMFMKRPKKTRLRWMMEMPGMSGPPHPHHTSPSDLPAPAPP
Mper_b1c4  331 PEFRDAVQTQDGGNGAGRPASSQLQDQPKGKRREERE----------------

Mper_b1c6  386 SSATPSKHKMEAMELADLHHPNCKINRKASAERRESESSDSLILSPEASKATEAV
Mper_b1c4      ------------------------------------------------------

Mper_b1c6  441 EFIAEHLRNEDQYIQIREDWKYVAMVIDRLQLYLFFFVTTAGTLGILMDAPHIFE
Mper_b1c4      ------------------------------------------------------

Mper_b1c6  496 TVDQDKIIEIYGGK
Mper_b1c4      --------------
```

Figure 3.11 The aligned sequences of two clones (β1c6 and β1c4) of M. persicae β1 nAChR subunits. The predicted signal peptide is in lowercase, predicted transmembrane helices in bold and the cys-loop cysteines underlined. R81, which has been found mutated in strains of M. persicae resistant to neonicotinoids (Bass et al., 2011), is highlighted in grey.

3.3.3.6. The Divergent Subunits

A. pisum possesses three divergent nAChR subunits, α9, α10 and β2 (Dale *et al.*, 2010) (Figure 3.20). To our knowledge, *M. persicae* divergent nAChR subunits had not been previously reported. Our BLAST analysis showed that *M. persicae* also possesses three divergent subunits, which we denoted as α9, α10 and β2 (Figure 3.20). Complete clones of the α9 (OQ102302) and α10 (OQ102303) subunits were obtained that were identical to predicted transcripts from AphidBase (Figures 3.12 and 3.13). There was also an α9 clone (c2) with point mutations compared to the predicted sequence, R181S (AGA to AGC) and D223Y (UAC to GAC),

neither of these are consistent with A to I editing. As with *A. pisum* (Dale et al., 2010), neither the *M. persicae* α9 nor α10 subunits have both of the two cysteine residues forming the cys-loop but they do have other features associated with nAChRs such as the YXCC motif characteristic of α subunits and four TM domains. Neither *M. persicae* α9 nor α10 possesses the GEK motif preceding the second transmembrane domain, which is associated with cation selectivity but this is not unusual for divergent insect subunits (Corringer, Novère and Changeux, 2000; Jensen, Schousboe and Ahring, 2005; Jones and Sattelle, 2010; Dale *et al.*, 2010). No β2 subunit clone contained the complete predicted sequence. Two clones (c14 and c18) were missing the first 83 amino acids and a third clone (c13) was missing the first 192 amino acids (Figure 3.14). There was also no GEK motif, with the sequence TEK instead.

```
Mper_a9c7    1 mdglrsglfliflaaycaagDTTNSRLPDENITAGHELRKQLLKNYDKVVVPATS
Mper_a9c2    1 mdglrsglfliflaaycaagDTTNSRLPDENITAGHELRKQLLKNYDKVVVPATS

Mper_a9c7   56 KKRVPMKVNTVFNSVELNYESSHMIIYAWLKVTWIDDRLTWNPNDYDQVNYITFE
Mper_a9c2   56 KKRVPMKVNTVFNSVELNYESSHMIIYAWLKVTWIDDRLTWNPNDYDQVNYITFE

Mper_a9c7  111 HFEIWHPDLMAYNNIEANTIVDGNTRSIVFNTGDVLWVQPVQYRIYCRADMTHWP
Mper_a9c2  111 HFEIWHPDLMAYNNIEANTIVDGNTRSIVFNTGDVLWVQPVQYRIYCRADMTHWP

Mper_a9c7  166 YDTQTGMLKIGSWVYRTNSINMTDTAHEIEIHSPQSEWQILRISSEKITKLYSCC
Mper_a9c2  166 YDTQTGMLKIGSWVYSTNSINMTDTAHEIEIHSPQSEWQILRISSEKITKLYSCC

Mper_a9c7  221 PNDPDSHVEYNITVHRNSNTYHPVVFVPALCTALLNLLVFWLSLDDYRYKLIISL
Mper_a9c2  221 PNDPYSHVEYNITVHRNSNTYHPVVFVPALCTALLNLLVFWLSLDDYRYKLIISL

Mper_a9c7  276 FNALIVVVVLQILYSKIPLILSTVPLISLYYTYSLALIVLTAIISVVVKNMTIIR
Mper_a9c2  276 FNALIVVVVLQILYSKIPLILSTVPLISLYYTYSLALIVLTAIISVVVKNMTIIR

Mper_a9c7  331 KPLSKPISSIVQSKFMEFLAMEVNEPSSSNRIQNEDKEIDLQYIEFNKRQIFAKI
Mper_a9c2  331 KPLSKPISSIVQSKFMEFLAMEVNEPSSSNRIQNEDKEIDLQYIEFNKRQIFAKI

Mper_a9c7  386 IDKICFIIFSIIYVILLSRFVF
Mper_a9c2  386 IDKICFIIFSIIYVILLSRFVF
```

Figure 3.12 The aligned sequences of two clones (a9c7 and a9c2) of M. persicae α9 nAChR subunits. The predicted signal peptide is in lowercase, predicted transmembrane helices in bold and the consecutive cysteines present in α subunits double underlined. Single amino acid changes between the α9 clones are highlighted in grey.

```
Mper_a10

   1 mlgtrhiglfiiiiatqatplwaFFSTVQLYNHNSTVEHILRKNIFKNYDKIVKPYAPQDKNSLE
  66 VSMKMLVKSAELNYEKSQMILSTWFIANWIDDRLTWNPSEYEHLNSIIVDHREIWHPDIMAFNNV
 131 DANMEDDRTHVNSVVNRSGGVIWVEPVQYIIHCKTDTTNWPHDTQTGVLKLGSWLYLGRDLNLTI
 196 DEGHEVEMASSHSEWDITNVSKERNIRYYDCCPDEQYIDIEYNITIRRKVHPYKSVLYIPALCSI
 261 SFNLLTFWLPYTDNQSKLFVNLFNALFVTLAIMVVYTKVPIVTSTVPLIVVYYTYSLGLIATTAV
 326 LSMAVKSMSAVSKPLPHGITWFLHSDYLVYLGIEINGSTTDCHMLCESEEMIAQAADLNERQKLA
 391 KVIDRICFVVFAFVYLVLLLRLMP
```

Figure 3.13 The cloned sequence of the M. persicae α10 subunit. The predicted signal peptide is in lowercase, predicted transmembrane helices in bold and the consecutive cysteines present in α subunits double underlined.

Figure 3.14 The aligned predicted sequence and sequences of two clones (β2c18 and β2c13) of M. persicae β2 nAChR subunits. The predicted signal peptide is in lowercase, predicted transmembrane helices in bold and the cys-loop cysteines underlined.

3.3.3 Description of Cloned *M. persicae* Nicotinic Acetylcholine Receptor Chaperones

Four potential chaperones of *M. persicae* nAChRs were identified and cloned; NACHO, UNC-50, TMX3 and RIC-3.

3.3.4.1 NACHO

The *A. mellifera* NACHO peptide sequence previously cloned in the laboratory (UKN32600) (Hawkins, Mitchell and Jones, 2022) was used to tBLASTn search AphidBase (https://bipaa.genouest.org/sp/myzus_persicae/) and a sequence with 60% identity was identified (MYZPE13164_0_v1.0_000097510.1) (Figure 3.15). The open reading frame of the predicted *M. persicae* NACHO was amplified by RT-PCR, then cloned into the pCI vector

(Chapter 2.4.2). The sequence of the clone was identical to what was predicted and contains a signal peptide and three transmembrane helices (Figure 3.15) (OQ181221).

```
Mper_NACHO    1mgsivlkslsvllgifflfvgtlkmspvisKELHKDLRKDYVKYAKVFPLSKM
Amel_NACHO    1mgsvvlkslsvllgiffvfvgtmkltshisKDLHKDLRKEYVKYAKVFPLSGT

Mper_NACHO   54IDFKVPAKWYRRAVGGTEVLSGVCLAFVPYRNVKQGANITLLMSHLLAVYTHY
Amel_NACHO   54LDFKVPSKWYRRVVGSLEIICGLAMAIVPSHKIKNASNTVLLLLMLMAVYSHY

Mper_NACHO  107AAKDKFERMAPALVFLFMLAGRLVIDYQLRRKELAEIAEP----KAQKQE
Amel_NACHO  107MVNDKFERIAPALVFFFMLTGRLVIDWQLRREDTQPVTANGVDDKTKKQD
```

Figure 3.15 The aligned sequences of NACHO from M. persicae and A. mellifera (UKN32600) (Hawkins, Mitchell and Jones, 2022). The predicted signal peptide is in lowercase and predicted transmembrane helices in bold.

3.3.4.2 UNC-50

The predicted protein sequence for *M. persicae* UNC-50 (XP_022181810.1) was retrieved from NCBI (https://www.ncbi.nlm.nih.gov/) by text search and then used to tBLASTn search AphidBase to find the corresponding transcript from which primers were designed to amplify the full coding region before cloning into pCI (Chapter 2.4.2). The cloned sequence was identical to the predicted sequence. No signal peptide was found for UNC-50 but it was predicted to have six transmembrane helices (Figure 3.16).

```
  Mper_UNC50

  1MPSSVNSFRSTSSLTYLPSPVTQRTCMSAAVKRYRYLRKLTNFKQMDFEFALWQMTFLFINPQKVYRN
 69FQHRKETKLQFARDDPAFLVLLSGLLCVSSIAFTYVLRLGFVEEFLKFLLYIVTVDCLLSGVIISTVLW
137LVANRYLIKSNYKGQDVEWAYAFDIHLNAFVPTLVISHIFQLFFYHIFLRHDWFLPLFIGNTLWLIAI
205GYYLYITFLGYSCLPILQKTEVLLTPFILLFFLYILSFAINWNISDNVMSIYKYRIL
```

Figure 3.16 The cloned sequence of M. persicae UNC-50. Predicted transmembrane helices are in bold.

3.4.4.3 TMX3

The predicted protein sequence for *M. persicae* TMX3 (XP_022177952.1) was retrieved from NCBI (https://www.ncbi.nlm.nih.gov/) by text search and then used to tBLASTn search AphidBase to find the corresponding transcript from which primers were designed to amplify the full coding region. The cloned sequence was identical to the predicted sequence. TMX3 contains a putative signal peptide and one transmembrane helix (Figure 3.17).

Mper_TMX3

```
  1mmisniftttlgfivsvillkdvrsSRVLELSDGFIEMKNDGHWFIMFYAPWCGHCKKLEPIWRHVAQ
 69ALHHSDIRVGKIDCTRYKRVVSEFGLSGYPTIMFFRDREGEFKFNSERSTEEMVHFAKRLARPPVQEV
137TDSKDIEMLKQTKKNFFMFIGKSVGHTWDLFYDLAKQYQAHSYFYITPEITGKQHFVFGETPAVVVYK
205EEQHYSFNADEWDMDFNTSLTQWINTERFDTFVKVTRSNIHHMLETNKYLVLALVEENKIEKLPPHHS
273EFLQMVESVIVKNRERFHRNFQFGWIGSPEFASSITSSDVSLPSLIIYNSSTRHHHFPKEKPHELTPE
341SITIFLEAVRNQSVKAYGGSGVFIQMYRMYYETKKSLVNIWVNN PAVASVLFGLPIGFLLLICY STCC
409TDIMDASDDDEEDVHHEKKE
```

Figure 3.17 The cloned sequence of M. persicae TMX3. The predicted signal peptide is in lowercase and predicted transmembrane helices in bold.

3.3.4.4 RIC-3

The predicted protein sequence of *M. persicae* RIC-3 was retrieved from AphidBase (Accession number: g23094.p2) by text search. This sequence information was used to design primers to amplify and clone the *M. persicae* RIC-3 open reading frame (Chapter 2.4.2). As with RIC-3 from other species (Lansdell *et al.*, 2008; Ben-Ami *et al.*, 2005; Halevi *et al.*, 2003; Treinin, 2008) *M. persicae* RIC-3 appears to have multiple isoforms. Two clones were identical to the predicted sequence (c23 and c30) (Figure 3.18), which has most of the features associated with RIC-3, including two transmembrane domains flanking a proline-rich region and a coiled-coil domain (Treinin, 2008; Halevi *et al.*, 2003). As with *D. melanogaster* and *A. mellifera* (Lansdell *et al.*, 2008; Ihara *et al.*, 2020), no signal peptide was identified but the first transmembrane helix starts only 11 amino acids from the N-terminus. In human RIC-3 the signal peptide is not cleaved (Castelán *et al.*, 2008) so the first transmembrane helix likely remains attached.

Another *M. persicae* RIC-3 isoform was cloned (c21) which contains a splice variant that appears to remove the coiled-coil domain (Figure 3.18) (predicted using https://bcf.isb-sib.ch/cgi-bin/webmarcoil/webmarcoilC1.cgi). In other species, variants which lack the coiled-coil domain are found but this appears to have no effect on function (Lansdell *et al.*, 2008; Halevi *et al.*, 2003; Ben-Ami *et al.*, 2005; Castelán *et al.*, 2008). Further variation is increased by a potential A to I editing site which converts M291 (ATG) (numbers from the predicted peptide sequence) to V291 (GTG) (c25 and c21) (Figure 3.19), this is the only A to I editing identified in in any of the *M. persicae* nAChR subunits or chaperones studied here.

Comparing RIC-3 from *M. persicae* and from other species (Figure 3.18), the RIC-3 from *D. melanogaster* (BCD56240.1) is fairly similar to the *M. persicae* RIC-3 except for some variation in the middle. The sequence of RIC-3 from *A. mellifera* is only similar to the other RIC-3 sequences at the N terminus and the C terminus and has a very different sequence for most of the protein. However, the sequence identity between RIC-3 from *M. persicae* and RIC-3 from *D. melanogaster* or *A. mellifera* is similar (28%).

Figure 3.18 The aligned sequences of three clones (RIC3c23, RIC3c25 and RIC3c21) from M. persicae, DmRIC-3[6,7,9] from D. melanogaster (Lansdell et al., 2008) (AM902271 translated using ExPASy https://web.expasy.org/translate/), also from (Ihara et al., 2020) and Amel RIC-3 from A. mellifera (Ihara et al., 2020) (BCD56240.1). Bold shows predicted transmembrane helices, underlined predicted coiled-coil domains and boxed putative A to I editing. Dmel RIC-3 and Amel RIC-3 transmembrane helices predicted with MemBrain 3.1

(Feng et al., 2020), coiled-coil domains predicted with DeepCoil (Zimmermann et al., 2018; Gabler et al., 2020; Ludwiczak et al., 2019).

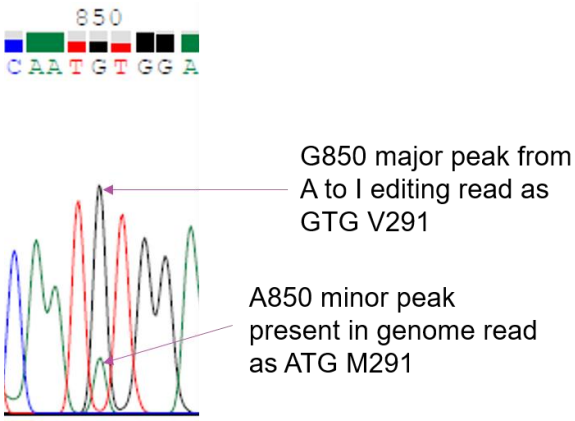

Figure 3.19 A section of the chromatogram of the PCR product of M. persicae RIC-3, showing potential A to I editing. AB1 file displayed using Chromas (Technelysium, South Brisbane, Australia).

3.3.5 Phylogenetic Analysis of the Cloned *M. persicae* Nicotinic Acetylcholine Receptor Subunits

A phylogenetic tree of insect nAChRs was constructed using the cloned *M. persicae* peptide sequences (Figure 3.20), unless there was sequence variation or there was no complete cloned sequence in which case the predicted sequence was used (α4 and β2). Also included in the phylogenetic tree are nAChR sequences from the aphid *A. pisum*, the fruit fly *D. melanogaster* and the honeybee *A. mellifera.* The nAChR subunit sequences cloned from *M. persicae* are in monophyletic groups with orthologous subunits from other species. The orthologous *A. pisum* and *M. persicae* sequences are very close together on the tree, reflecting the high sequence similarity due to the fact both species belong to the same order. The tree shows that the nAChR subunits from *D. melanogaster* and *A. mellifera* expressed in (Ihara *et al.*, 2020) are in the same monophyletic groups as the nAChR subunits from *M. persicae* we are expressing, these groups are outlined in black (Figure 3.20). Three divergent subunits from *M. persicae* were cloned, a fourth divergent subunit (β3) was predicted (Jones personal communication) but was not identified from cDNA.

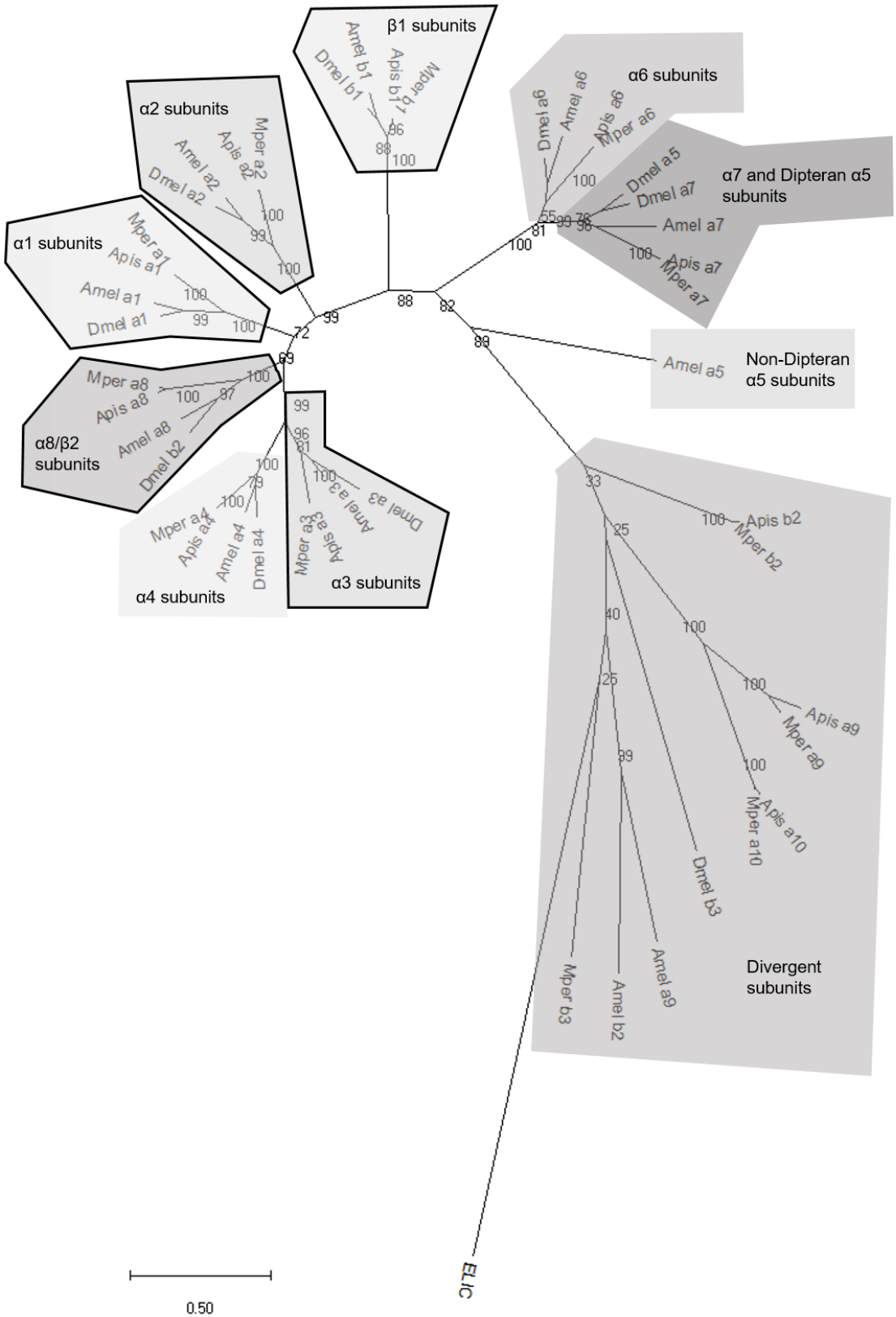

Figure 3.20 Tree showing the relationship of M. persicae (Mper) subunits with those of A. pisum (Apis), A. mellifera (Amel) and D. melanogaster (Dmel), ELIC was used as an outgroup. For accession numbers for A. pisum, D. melanogaster and A. mellifera see Figure 5.1 in Chapter 5.

3.4 Discussion

3.4.1 *M. persicae* nAChR Subunits

In this chapter we identified the complete nAChR subunit gene family from the aphid *M. persicae*. 11 *M. persicae* nAChR subunit genes were identified similar to the *A. pisum* genome (Dale *et al.*, 2010). As shown in Figure 3.19, *M. persicae* possesses α1-4, α6-8 and β1 nAChR subunits, which are core subunits with clear orthologous relationships with subunits from different insect species. As with *A. pisum*, *M. persicae* does not possess an α5 subunit (a *M. persicae* nAChR subunit previously denoted as α5 has since been shown to be orthologous to α4 subunits (Huang *et al.*, 1999; Jones *et al.*, 2005)). This is speculated to be because Hemiptera are a more ancient order of insects and the α5 subunit evolved more recently (Dale *et al.*, 2010). There are three divergent subunits α9, α10 and β2 which are closely related to the orthologous *A. pisum* subunits but have no *D. melanogaster* or *A. mellifera* orthologues.

The open reading frame of nine of the *M. persicae* nAChR subunits were amplified and cloned into the pCI vector to enable heterologous expression studies. All the complete cloned *M. persicae* subunits have the features expected of nAChRs; a signal peptide and four transmembrane helices. All the nAChR subunits possess the cys-loop apart from α9 and α10, which lack one of the cysteines, the same as in *A. pisum* α9 and α10 subunits (Dale *et al.*, 2010; Liu *et al.*, 2013). Lacking the cysteines may reflect more ancestral subunits such as those found in bacteria (ELIC) (Tasneem *et al.*, 2004). There was variation in the cation selective GEK motif in α2, α3, α4 and β2 subunits. The α9 and α10 subunits lack the GEK motif entirely, which is not unusual for insect divergent subunits (Corringer, Novère and Changeux, 2000; Jensen, Schousboe and Ahring, 2005; Jones and Sattelle, 2010). However, variation in the core α2 and α3 subunits is only found in aphids (Dale *et al.*, 2010; Liu *et al.*, 2013). A signal peptide was also not detected for the α2 subunit and thus it was initially difficult to find the N-terminus on AphidBase, this is similar to in *A. pisum* where the complete reading frame was not found for the α2 subunit (Liu *et al.*, 2013).

Splice variants were discovered in the *M. persicae* α1, α4, α6, α7 and β1 nAChR subunits. For *A. pisum* only the α4, α6 and α7 subunits were found to have alternative splicing, there was also tandem duplications of exons 6 and 7 in the α7 subunit (Dale *et al.*, 2010; Liu *et al.*, 2013).

The alternative splicing in the α1 subunit is interesting as it leads to 20 amino acids being removed from the intracellular loop (Figure 3.5), an area of high variability between nAChRs (Jones and Sattelle, 2010). Such splicing has not been observed in α1 nAChR subunits of other insects (Liu *et al.*, 2013; Jones *et al.*, 2020; Shao, Dong and Zhang, 2007; Jones *et al.*, 2010; Jones, Grauso and Sattelle, 2005) although in the *A. mellifera* α3 subunit alternative splicing leads to variation in this region which is suspected to affect phosphorylation (Jones *et al.*, 2006). For the *M. persicae* α1 subunit two putative phosphorylation sites are absent in one of the splice variants (Figure 3.5). Phosphorylation has a possible role in desensitisation (Changeux, 2012). Two splice variants leading to truncations of the *M. persicae* α4 subunit were cloned (Figure 3.7), similar to a previous report where a partial version of the aphid α4 subunit (originally denoted as the α5 subunit) had been cloned (Huang *et al.*, 1999). In one of our *M. persicae* α4 clones lack of splicing to the next exon results in the introduction of a premature stop codon so only the first 114 amino acids are translated; this is similar to alternative splicing in the *D. melanogaster* and *L. migratoria* α4 subunit (Figure 3.7) (Lansdell and Millar, 2000a; Zhang *et al.*, 2017). The other splice variant remains in frame and is missing amino acids 116-212 from the predicted sequence, which removes the cys-loop and several essential acetylcholine binding loops so this protein is predicted to be non-functional. This does not fit with previous theories regarding truncated versions of nAChR, which were postulated to act as a binding protein soaking up excess acetylcholine in the extracellular space (Sattelle *et al.*, 2005). In *A. pisum* α4 there was alternative splicing of exon 4, between exon 4 and exon 4' (Liu *et al.*, 2013). This splicing of α4 is highly conserved in several insect species (Jones and Sattelle, 2010; Jones *et al.*, 2020; Zhang *et al.*, 2017). Splicing of the α6 subunit is also common in insects (Liu *et al.*, 2013; Shao, Dong and Zhang, 2007; Jones, Brown and Sattelle, 2007; Zhang *et al.*, 2017; Jones *et al.*, 2020). The *M. persicae* α6 subunit has two versions of exon 8 (Figure 3.8), similar to *A. pisum* which has alternative splicing of exon 8 in the α6 subunit (Liu *et al.*, 2013; Dale *et al.*, 2010). Alternative splicing of the α6 subunit introduces variation around TM2, which forms the pore and so may affect ion conductance (Corringer, Novère and Changeux, 2000). Alternative splicing of the α7 nAChR subunit has been observed in a small number of insects, *A. pisum*, *B. germanica* and *P. americana* (Dale *et al.*, 2010; Jones *et al.*, 2020). Two splice variants of the *M. persicae* α7 subunit were successfully cloned containing exon6a and exon7a or exon6a and exon7b, so there are two further predicted isoforms containing exon6b that were not detected. This introduces variation at the C-terminal section of the N-terminal extracellular domain and TM1 (exon 6) or in the TM2 region (exon 7) (Figure 3.9), which may alter ion conductance as TM2 forms the

pore lining (Corringer, Novère and Changeux, 2000). Splicing of the α7 subunit, only found so far in aphids and cockroaches (Dale *et al.*, 2010; Jones *et al.*, 2020), is theorised to reflect stages of gene duplication events leading to the generation of a separate subunit, α5 (Dale *et al.*, 2010).

Several insect nAChRs undergo RNA editing, in particular the α6 subunit (Jones and Sattelle, 2010). However, when analysing amplified cDNA no A to I editing was identified in any of the *M. persicae* nAChR subunits, similar to *A. pisum* (Liu *et al.*, 2013).

3.4.2 *M. persicae* nAChR Chaperones

3.4.2.1 NACHO, UNC-50 and TMX3

The cloned *M. persicae* NACHO had 60% amino acid sequence identity to the previously cloned *A. mellifera* NACHO (Hawkins, Mitchell and Jones, 2022). Both NACHO sequences share the same predicted structure of four transmembrane helices (including the signal peptide), which was also the same as human NACHO (Gu *et al.*, 2016). Previously, *D. melanogaster* NACHO was found to substitute for human NACHO in fully augmenting human α7 expression in human cells despite sharing only 37% identity (Gu *et al.*, 2016), indicating that the function of NACHO is even more conserved than sequence identity. Thus, it is expected that *M. persicae* NACHO will fulfil the same functions as *A. mellifera* NACHO with 60% identity. *A. mellifera* NACHO permitted the expression of the *A. mellifera* α6 nAChR in *X. laevis* oocytes (Hawkins, Mitchell and Jones, 2022). Perhaps *M. persicae* NACHO may have a similar effect with the *M. persicae* α6 nAChR subunit.

The percentage sequence identities of UNC-50 and TMX3 cloned from *M. persicae* compared to the sequences of UNC-50 and TMX3 from *D. melanogaster*, *A. mellifera* and *B. terrestris* (Ihara *et al.*, 2020), are displayed in Table 3.1. These chaperone proteins were found to permit expression of nAChRs consisting of a variety of subunits in *X. laevis* oocytes (Ihara *et al.*, 2020; Brunello *et al.*, 2022; Takayama *et al.*, 2022; Rufener *et al.*, 2020). *M. persicae* UNC-50 was predicted to have six transmembrane domains, in contrast to UNC-50 of *L. salmonis*, *C. elegans*, human, *A. mellifera* and *D. melanogaster* that are not predicted to have the first transmembrane helix (Rufener *et al.*, 2020; Brunello *et al.*, 2022) thus instead have five transmembrane domains. This may be an artefact of the transmembrane prediction software

or the *M. persicae* UNC-50, with the extra transmembrane domain, may have a different topology at the membrane. None of the UNC-50 sequences were predicted to have a signal peptide (Rufener *et al.*, 2020; Brunello *et al.*, 2022; Fitzgerald *et al.*, 2000). *M. persicae* TMX3 is predicted to have one transmembrane domain near the C-terminus and a signal peptide, the same as predicted in *L. salmonis*, *D. melanogaster*, *A. mellifera* and *C. elegans* (Rufener *et al.*, 2020; Brunello *et al.*, 2022). Some of the sequence before the transmembrane domain, near the N-terminus but after the signal peptide may contain the thioredoxin-like domain (Rufener *et al.*, 2020; Brunello *et al.*, 2022).

Table 3.1 The percentage identity of UNC-50 and TMX3 amino acid sequences cloned from M. persicae to the UNC-50 and TMX3 cloned from D. melanogaster, A. mellifera and B. terrestris (Ihara et al., 2020).

Species	**% identity of UNC-50 to *M. persicae* UNC-50**	**% identity of TMX3 to *M. persicae* TMX3**
D. melanogaster	52	49
A. mellifera	56	47
B. terrestris	57	46

3.4.2.2 RIC-3

Two RIC-3 isoforms were cloned from *M. persicae*, one containing two transmembrane helices and a coiled-coil domain, the other with the two transmembrane helices but without the coiled-coil domain (Figure 3.17). This matches the data from *D. melanogaster* and *A. mellifera* RIC-3 where the coiled-coil domain is in a single exon that is not in every isoform (Lansdell *et al.*, 2008; Brunello *et al.*, 2022). In human RIC-3 only the transmembrane domains and proline-rich domain (between the transmembrane helices) are required to enhance human α7 nAChR expression and this is similar for *D. melanogaster* (Castelán *et al.*, 2008; Lansdell *et al.*, 2008), so it is not clear what the roles of these isoforms are. Unlike in *D. melanogaster* and *A. mellifera* (Lansdell *et al.*, 2008; Brunello *et al.*, 2022) no variation was found in *M. persicae* RIC-3 between the two transmembrane helices (Figure 3.17). The variant with the longer section

between transmembrane domains from *D. melanogaster* lead to lower surface expression of some nAChRs (Lansdell *et al.*, 2008). This variant from *A. mellifera* was used to express nAChRs from *A. mellifera* in *X. laevis* oocytes but the RIC-3 from *D. melanogaster* used to express nAChRs from *D. melanogaster* did not contain this section (Ihara *et al.*, 2020) (Figure 3.17). A putative A to I editing site was identified in *M. persicae* RIC-3 (Figure 3.18) that converts a methionine to a valine in the C-terminal region of the protein. Not much is known about the function of this region (Treinin, 2008; Lansdell *et al.*, 2008) so it is not known what effect this will have on the actions of the protein.

3.5 Conclusion

Most of the nAChR subunits and several protein chaperones from *M. persicae* have been cloned to enable subsequent expression experiments.

Chapter 4 Functional Expression of Nicotinic Acetylcholine Receptors from *Myzus persicae* with the Assistance of Protein Chaperones

4.1 Introduction

Expression of nAChRs in *X. laevis* oocytes has been highly informative in studying their functional and pharmacological properties (Buckingham, Pym and Sattelle, 2006). Unfortunately, achieving functional expression of nAChRs consisting of insect subunits has proven frustratingly elusive over the past three decades (Sattelle *et al.*, 2005; Millar, 2009). Recently, robust expression of insect nAChRs was achieved through the use of chaperone proteins as outlined below.

4.1.1 The Expression of nAChRs Containing the Insect α6 Subunit

A nAChR consisting of the *D. melanogaster* α5 and α6 subunits was expressed in *X. laevis* oocytes, with RIC-3 from *C. elegans*, the ratio α6:α5:RIC-3 2:4:1 gave the largest response (Watson *et al.*, 2010). RIC-3 (from *C. elegans*) also enabled the expression of homomeric nAChRs consisting of *D. melanogaster* α5 or α7 subunits and a heteromeric nAChR containing *D. melanogaster* α5, α6 and α7 subunits, using *D. melanogaster* RIC-3 produced no significant difference in pharmacological properties (Lansdell *et al.*, 2012). Previously in the Jones laboratory, expression has been achieved of the *A. mellifera* homomeric α6 nAChR (Hawkins, Mitchell and Jones, 2022), with the chaperone protein, NACHO (Gu *et al.*, 2016; Hawkins, Mitchell and Jones, 2022), although expression was observed in only 33% of batches of oocytes injected, it is not clear what variation in the batches of oocytes leads to this frequency of expression. It has yet to be determined whether other chaperones or nAChRs are required for robust and more frequent expression.

4.1.2 The Expression of Ionotropic Acetylcholine Receptors from Nematodes in *X. laevis* Oocytes using RIC-3, UNC-50 and TMX3

In the nematode, *C. elegans*, the levamisole sensitive acetylcholine receptor (L-AChR) is a cys-LGIC very similar to nAChRs but does not respond to nicotine (Boulin *et al.*, 2008). L-AChRs are expressed at the neuromuscular junction and consist of UNC-29, UNC-38, LEV-1, UNC-63 and LEV-8 subunits, mutations in which gives rise to resistance to the anthelmintic levamisole (Fleming *et al.*, 1997; Culetto *et al.*, 2004; Towers *et al.*, 2005). To reconstitute functional L-AChRs in *X. laevis* oocytes eight proteins were required; LEV-8, UNC-38, UNC-63 (α subunits), LEV-1 and UNC-29 (non-α subunits) and three chaperone proteins RIC-3, UNC-50 and TMX3 (UNC-74) (Boulin *et al.*, 2008). This receptor responded to acetylcholine in a concentration-dependent manner with an EC_{50} of 26 µM (Boulin *et al.*, 2008). The use of RIC-3, UNC-50 and TMX3 allowed the expression of similar L-AChRs from a parasitic nematode *Haemonchus contortus*, although they had slightly different subunit combinations; ACR-8, UNC-29, UNC-38 and UNC-63 or UNC-29, UNC-38 and UNC-63 (Boulin *et al.*, 2011). To express the ACR-16 receptor, which responded to nicotine, in *X. laevis* oocytes only RIC-3 was required, UNC-50 and TMX3 did not increase expression (Boulin *et al.*, 2008).

4.1.3 The Expression of nAChRs from Insects and Crustaceans in *X. laevis* Oocytes using RIC-3, UNC-50 and TMX3

In 2020, two papers were published which used the combination of RIC-3, UNC-50 and TMX3 chaperones to express nAChRs from insects and crustaceans in *X. laevis* oocytes (Ihara *et al.*, 2020; Rufener *et al.*, 2020), extrapolating from the work previously carried out on nematode acetylcholine receptors. It was found that TMX3 was essential for the expression of a receptor containing the *D. melanogaster* α1 and β1 subunits, with the addition of UNC-50 and RIC-3 increasing expression (Ihara *et al.*, 2020; Takayama *et al.*, 2022). Expression of a combination of α2, α8 and β1 subunits from *A. mellifera* without chaperones could be achieved, but expression was very infrequent (Brunello *et al.*, 2022). However, it was found for the expression of a nAChR made up of a combination of subunits from the crustacean, *L. salmonis*, neither RIC-3 alone nor UNC-50 and TMX3 together were sufficient for expression (Rufener *et al.*, 2020). Thus, to increase the probability of robust and frequent expression we decided to use RIC-3, UNC-50 and TMX3 in each experiment.

Expression was achieved with a variety of subunit combinations from *D. melanogaster*, *A. mellifera*, *B. terrestris* and *L. salmonis* with RIC-3, UNC-50 and TMX3 protein chaperones (see Chapter 1, Table 1.1). A nAChR could be created using just α1 and β1 subunits but other nAChRs were expressed by the addition of the α2 and α8/β2 subunits (Ihara *et al.*, 2020; Rufener *et al.*, 2020). A nAChR made up of α3, β1 and β2 subunits from *L. salmonis* was also expressed (Rufener *et al.*, 2020). When there was an attempt to replicate the expression of a nAChR consisting of the *A. mellifera* α1, α8 and β1 subunits (in (Ihara *et al.*, 2020)), expression was not achieved unless an α1 variant containing a 26 amino acid-long sequence at the N-terminus was used (Brunello *et al.*, 2022). Changing the injection ratios of the *D. melanogaster* α1 and β1 subunits gave two different receptors which did not significantly differ in their affinity or efficacy for acetylcholine but did lead to a different affinity for imidacloprid (Takayama *et al.*, 2022).

Receptors made up of combinations of α1, α2, α3, α8/β2 and β1 subunits from *D. melanogaster*, *A. mellifera*, *B. terrestris* and *L. salmonis* had EC_{50}s for acetylcholine in the range 1-60 μM (Chapter 1, Table 1.1) (Ihara *et al.*, 2020; Rufener *et al.*, 2020; Takayama *et al.*, 2022). Receptors made up of combinations of α1, α2, α8/β2 and β1 subunits also responded to imidacloprid, thiacloprid and clothianidin with EC_{50}s in the range 5-3,000 nM, although the receptor from *L. salmonis* made up of α3, β1 and β2 subunits did not respond to imidacloprid and thiacloprid, only clothianidin (EC_{50} 81 nM) (Ihara *et al.*, 2020; Rufener *et al.*, 2020; Takayama *et al.*, 2022). Imidacloprid, thiacloprid and clothianidin acted as partial agonists, with lower maximal responses than acetylcholine, although the response to clothianidin was usually larger than the response to imidacloprid and thiacloprid (Ihara *et al.*, 2020; Rufener *et al.*, 2020). nAChRs made up of combinations of α1, α2, α8 and β1 subunits from *D. melanogaster*, *A. mellifera* or *B. terrestris* could be inhibited by neonicotinoids in a range too low for any agonist actions (10 pM-100 nM), although the amount of inhibition varied with the neonicotinoid and nAChR composition (Ihara *et al.*, 2020). The successful heterologous expression of a nAChR from a crop pest species is yet to be reported.

4.2 Aims

The aim of the work described in this chapter is to express a nAChR from a pest species, *M. persicae*, in *X. laevis* oocytes with the assistance of the protein chaperones RIC-3, UNC-50 and TMX3 and to functionally characterise this receptor.

4.3 Results

4.3.1 Expression of a nAChR Composed of the *M. persicae* α6 and α7 Subunits with NACHO and RIC-3 by Injection of DNA.

The *M. persicae* α6 and α7 subunit cDNAs were cloned into pCI and injected into *X. laevis* oocytes (Chapter 2.4.2 and Chapter 2.5.2). Based on previous reports successfully expressing α6 and α7 subunits (Lansdell *et al.*, 2012; Watson *et al.*, 2010; Hawkins, Mitchell and Jones, 2022), NACHO and RIC-3 cDNA (also cloned from *M. persicae*) were co-injected in various combinations but none responded to 1 mM acetylcholine, over several months of experiments (13 batches of oocytes). This included DNA from minipreps, midipreps and maxipreps (concentrations given in Chapter 2, Table 2.7).

4.3.2 Expression of a nAChR Composed of the *M. persicae* α1, α3, α8 and β1 Subunits with RIC-3, UNC-50 and TMX3 by Injection of DNA.

The *M. persicae* α1, α3, α8 and β1 subunit cDNAs were cloned and injected into *X. laevis* oocytes with RIC-3, UNC-50 and TMX3 cDNAs, in a 1:1 ratio with the concentrations given in Chapter 2, Table 2.7. There was a response to 300 µM acetylcholine in 9 out of 16 batches of oocytes and this was concentration dependent (Figure 4.1). However, the response was often too small (less than 100 nA) to measure a concentration response curve. Increasing the concentration of DNA injected (to the maxiprep concentrations given in Chapter 2, Table 2.7) did not seem to increase the response to acetylcholine.

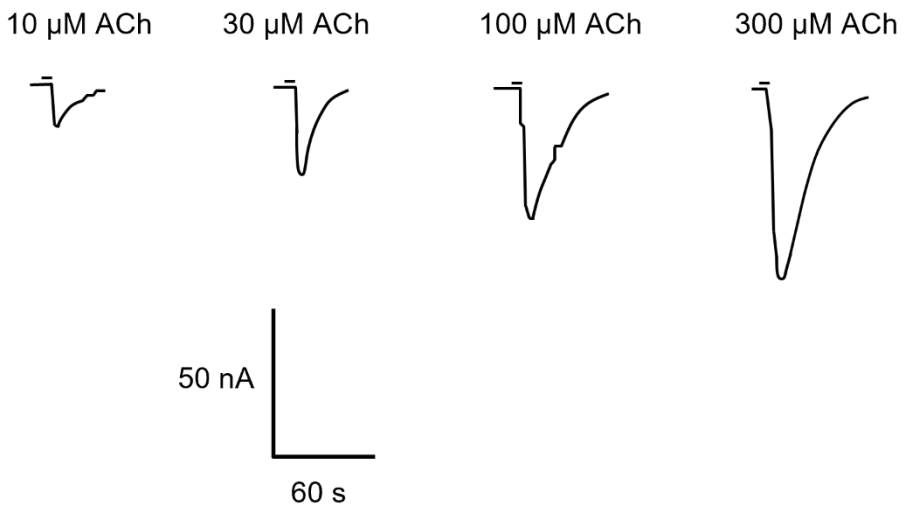

Figure 4.1 Representative current traces showing the response to different concentrations of acetylcholine (10 -300 µM) of X. laevis oocytes injected with M. persicae α1, α3, α8 and β1 nAChR subunit cDNAs and M. persicae RIC-3, UNC-50 and TMX3 cDNAs.

4.3.3 Expression of a nAChR Composed of the *M. persicae* α1, α2, α8 and β1 Subunits with RIC-3, UNC-50 and TMX3 by Injection of DNA.

A response to 1 mM acetylcholine was found in one batch of *X. laevis* oocytes injected with *M. persicae* α1, α2, α8 and β1 subunit cDNAs with RIC-3, UNC-50 and TMX3 cDNAs out of the two batches in which expression was attempted (2 out of 12 oocytes, when DNA was injected, expression was not expected in 100% of oocytes due to difficulty injecting DNA into the nucleus) (Figure 4.2).

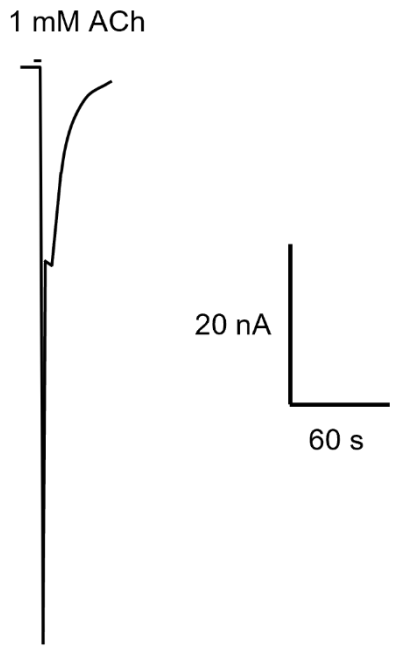

Figure 4.2 Traces showing the response to 1 mM acetylcholine of X. laevis oocytes injected with M. persicae α1, α2, α8 and β1 nAChR subunit cDNAs and M. persicae RIC-3, UNC-50 and TMX3 cDNAs.

4.3.4 Expression of a nAChR Composed of the *M. persicae* α1, α3, α8 and β1 Subunits with RIC-3, UNC-50 and TMX3 by Injection of RNA.

In an attempt to increase the consistency of expression, cRNA generated *in vitro* of *M. persicae* nAChR subunits and chaperones (Chapter 2.4.5) was injected into *X. laevis* oocytes. Expression of a nAChR consisting of α1, α3, α8 and β1 nAChR subunits from *M. persicae* with the *M. persicae* RIC-3, UNC-50 and TMX3 chaperones was detected in one out of the 17 batches of oocytes tested (2 out of 23 oocytes, when RNA was injected the number of oocytes with expression per batch was expected to be higher than when DNA was injected). These oocytes responded in a concentration-dependent manner but there was not enough data to create a concentration response curve (requires n = 5) (Figure 4.3). Seven batches were injected with RNA at a concentration of 100 ng/µl as in (Ihara *et al.*, 2020) and ten with RNA at a concentration of 200 ng/µl, the increase in concentration of RNA made no difference to the success of expression. The addition of NACHO did not lead to successful expression (tried in two batches of oocytes). Neither the use of different RIC-3 variants (c21 and c25) nor the α1 variant (c21) lead to expression (tried in two batches each).

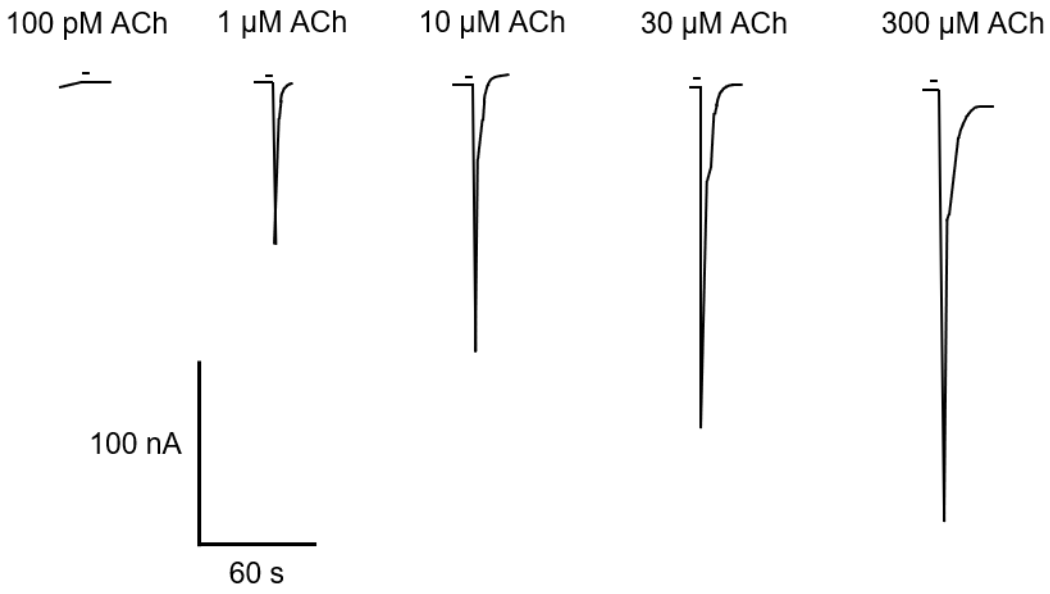

Figure 4.3 Representative current traces showing the response to different concentrations of acetylcholine (100 pM - 300 µM) of X. laevis oocytes injected with M. persicae α1, α3, α8 and β1 nAChR subunit RNA and M. persicae RIC-3, UNC-50 and TMX3 RNA.

4.3.5 Expression of a nAChR Composed of the *M. persicae* α1, α2, α8 and β1 Subunits with RIC-3, UNC-50 and TMX3 by Injection of RNA.

Out of the five batches of oocytes injected with *M. persicae* α1, α2, α8 and β1 nAChR subunit RNA plus RIC-3, UNC-50 and TMX3 RNA, one responded to acetylcholine (3 out of 21 oocytes), in a concentration-dependent manner (Figure 4.4). However, expression was too small for an accurate concentration response curve to be measured. The addition of NACHO RNA did not lead to expression, in fact expression was achieved in oocytes without NACHO in the same batch.

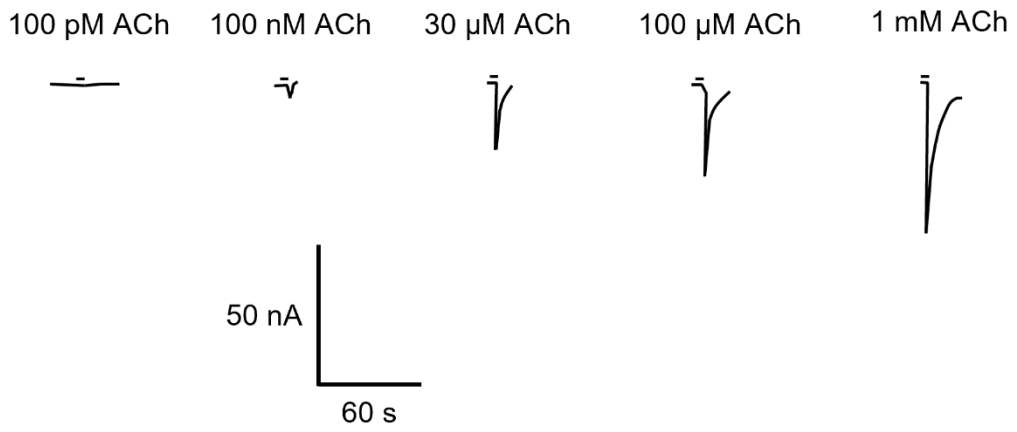

Figure 4.4 Representative current traces showing the response to different concentrations of acetylcholine (100 pM - 1 mM) of X. laevis oocytes injected with M. persicae α1, α2, α8 and β1 nAChR subunit RNA and M. persicae RIC-3, UNC-50 and TMX3 RNA.

4.3.6 Expression of a nAChR Composed of the *D. melanogaster* α1 and *M. persicae* α3, α8 and β1 nAChR Subunits with *M. persicae* RIC-3, UNC-50 and TMX3 by Injection of DNA.

With limited success expressing nAChRs containing the α1 subunit from *M. persicae*, the α1 subunit from *D. melanogaster* was used instead, as receptors containing this subunit had successfully been expressed (Ihara *et al.*, 2020; Takayama *et al.*, 2022). Injecting oocytes with the *D. melanogaster* α1 subunit cDNA and the *M. persicae* α3, α8 and β1 subunit cDNAs with RIC-3, UNC-50 and TMX3 cDNA (from *M. persicae*) robustly responded to acetylcholine in four out of five batches of oocytes tested. This response was concentration dependent and a concentration response curve was generated giving an EC_{50} of 123 (78.1-193) µM (Figure 4.5). It was observed with all of the expressed receptors in this chapter that oocytes expressing the receptor also responded to pressure (when SOS alone was applied) (Figure 4.5 (A)) but to a much smaller extent than the maximal response to acetylcholine. Whereas oocytes that had no response to acetylcholine or water injected controls did not respond to pressure (or any chemicals) (Figure 4.7). These effects may represent the opening of endogenous calcium-dependent ion channels activated by calcium ions (in SOS) entering through the constitutively open nAChR, as some nAChRs are permeable to calcium ions (Barish, 1983; Vernino *et al.*, 1992) or these nAChRs may be activated by pressure (although this response does not appear in every expressing oocyte). This made it difficult to find the concentration of acetylcholine

that was too low to produce a response from the receptor and so to start the concentration response curve at zero (Figures 4.5 and 4.7).

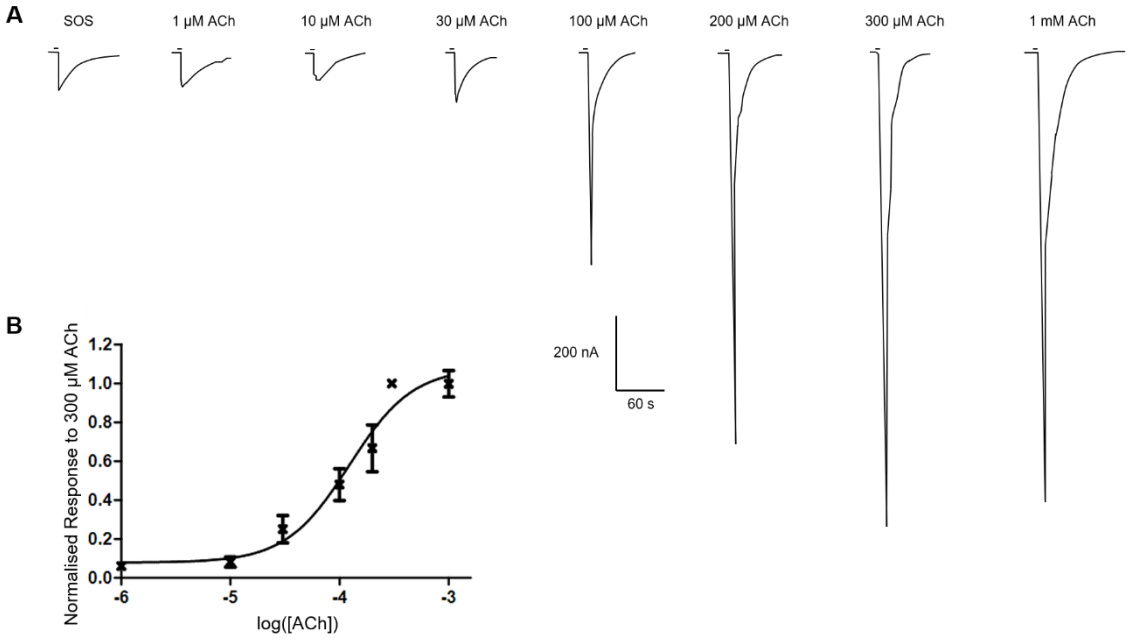

Figure 4.5 Reponses to acetylcholine in X. laevis oocytes injected with the D. melanogaster α1 nAChR subunit and M. persicae α3, α8 and β1 nAChR subunits with M. persicae RIC-3, UNC-50 and TMX3. A. Representative current traces showing responses to different concentrations of acetylcholine (1–1000 µM). The first trace shows the effect of applied SOS only indicating a response to pressure. B. Acetylcholine concentration response curve. Data are normalised to the maximal response (300 µM acetylcholine) and have a mean EC_{50} of 123 (78.1-193) µM from 5 oocytes from 3 different batches of oocytes.

When plotted separately, the individual concentration response curves appeared to show considerable variation with EC_{50s} ranging from 56.0-235 µM (Figure 4.6). This indicates that different stoichiometries or combinations of subunits may be expressed, giving varying affinities for acetylcholine.

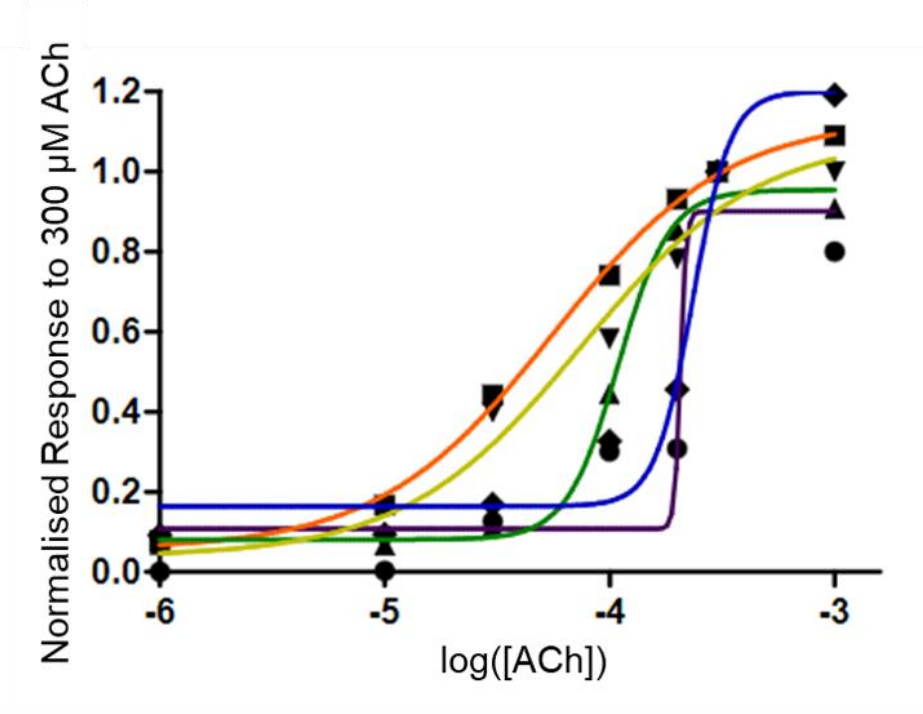

Figure 4.6 Reponses to acetylcholine in X. laevis oocytes injected with the D. melanogaster α1 nAChR subunit and M. persicae α3, α8 and β1 nAChR subunits with M. persicae RIC-3, UNC-50 and TMX3. Acetylcholine concentration response curves plotted separately of the data from Figure 4.5 (B). Data are normalised to the maximal response (300 µM acetylcholine).

4.3.7 Expression of a nAChR Composed of the *D. melanogaster* α1 and *M. persicae* β1 with *M. persicae* RIC-3, UNC-50 and TMX3 by Injection of DNA.

In order to determine the minimum number of nAChR subunits required to form a functional receptor, *D. melanogaster* α1 and *M. persicae* β1 with *M. persicae* RIC-3, UNC-50 and TMX3 were injected into *X. laevis* oocytes. A response to acetylcholine 3-4 days later (Figure 4.7) was observed in every batch of oocytes (5 batches). Whereas no response was detected when oocytes were injected with *D. melanogaster* α1 alone with *M. persicae* RIC-3, UNC-50 and TMX3.

Concentration response curves were generated for the nAChR consisting of *D. melanogaster* α1 and *M. persicae* β1 from which an EC_{50} of 91.1 (67.7-123) µM for acetylcholine was calculated (Figure 4.7). Plotting the curves separately did not seem to show multiple populations of receptors (Figure 4.8), in line with a recent study showing that expression of different ratios of the *D. melanogaster* α1 and β1 subunits does not affect the affinity for acetylcholine (Takayama *et al.*, 2022).

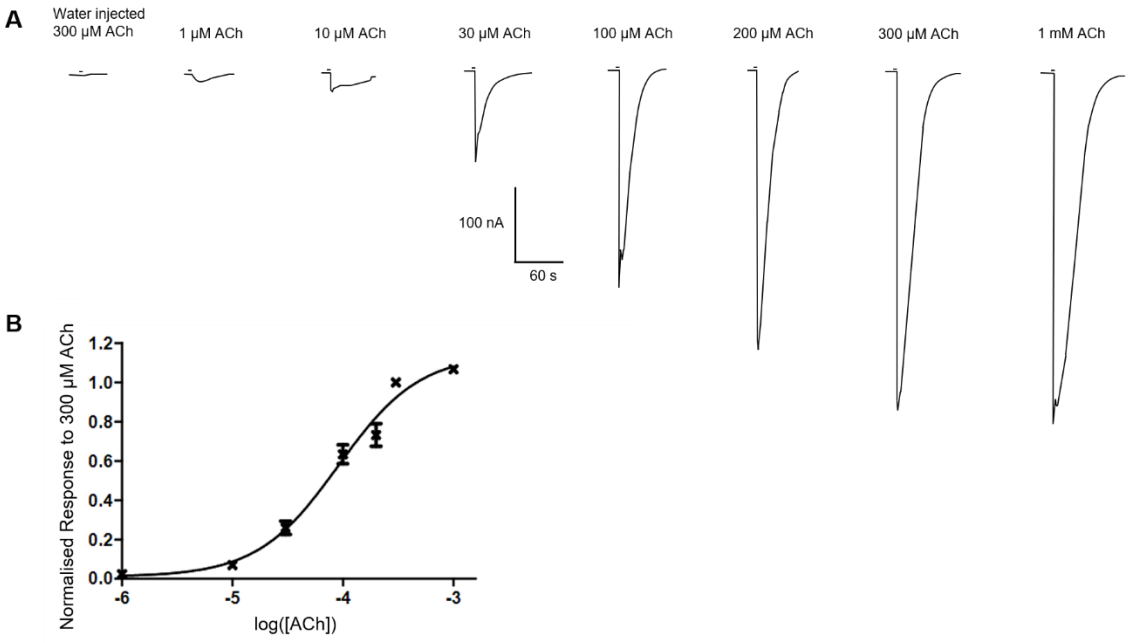

Figure 4.7 Reponses to acetylcholine in X. laevis oocytes injected with the D. melanogaster α1 nAChR subunit and M. persicae β1 nAChR subunits with M. persicae RIC-3, UNC-50 and TMX3. A. Representative current traces showing responses to different concentrations of acetylcholine (1–1000 µM). The first trace shows the response of an oocyte injected with water alone whilst the remaining traces show responses from oocytes injected with nAChR subunits. B. Acetylcholine concentration response curve. Data are normalised to the maximal response (300 µM acetylcholine) and have a mean EC_{50} of 91.1 (67.7-123) µM from 5 oocytes from 3 different batches of oocytes.

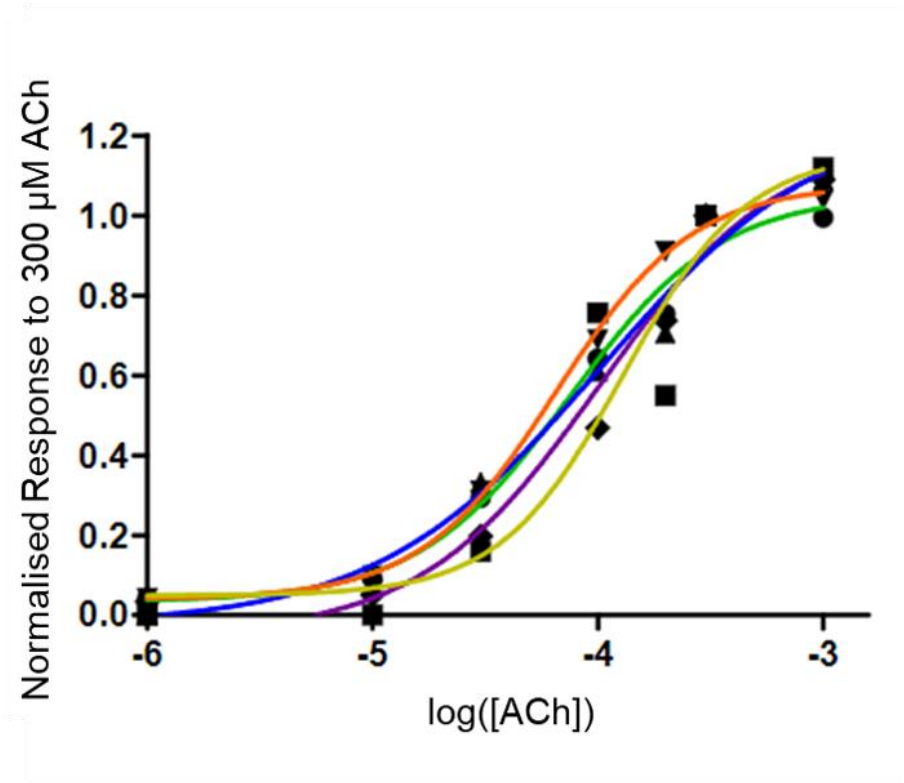

Figure 4.8 Reponses to acetylcholine in X. laevis oocytes injected with the D. melanogaster α1 subunit and M. persicae β1 subunit with M. persicae RIC-3, UNC-50 and TMX3. Acetylcholine concentration response curves plotted separately of the data from Figure 4.7 (B). Data are normalised to the maximal response (300 µM acetylcholine).

In order to ensure that the response to acetylcholine was not caused by endogenous muscarinic acetylcholine receptors, 1 µM atropine, an inhibitor of muscarinic acetylcholine receptors (Dale, 1914), was co-applied to the oocytes with 300 µM acetylcholine, following pre-incubation with 1 µM atropine. The acetylcholine response was slightly reduced to 94.1% of the maximum but not completely ablated, demonstrating that the response is not muscarinic (Figure 4.9) and is likely due to the injected subunits.

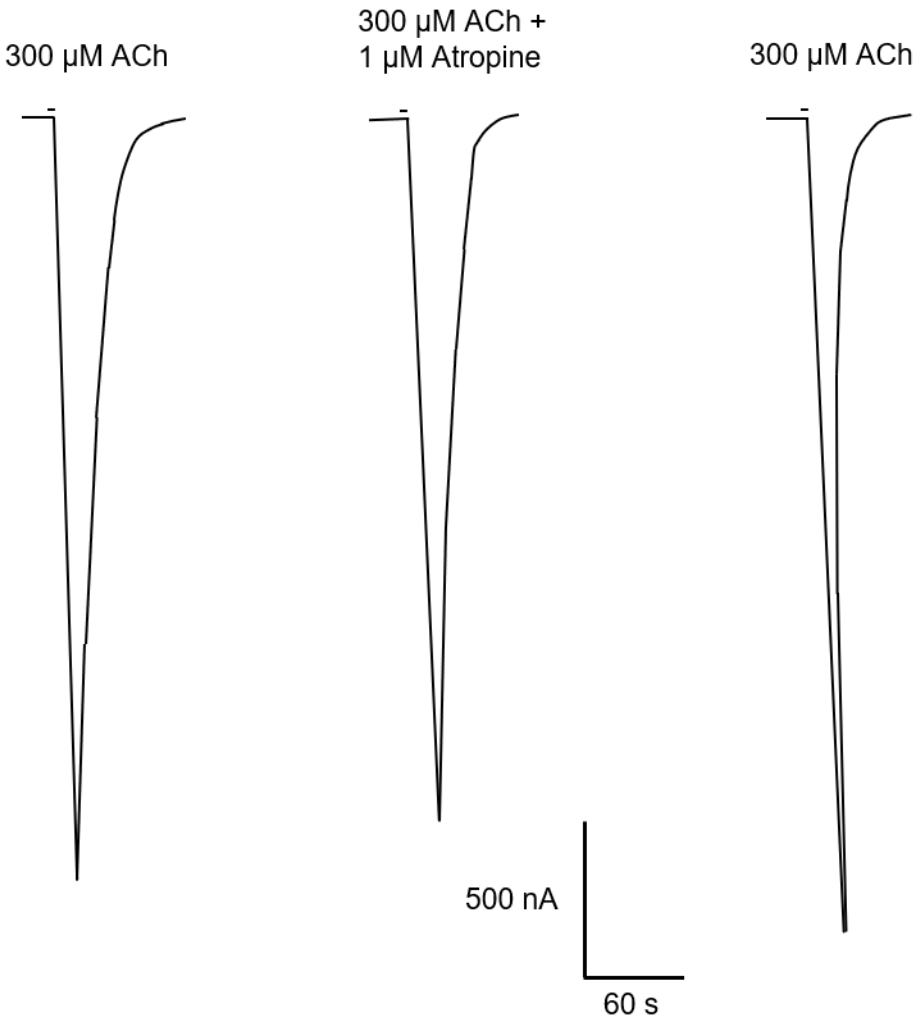

Figure 4.9 Traces showing the nAChR composed of D. melanogaster α1 and M. persicae β1 with M. persicae RIC-3, UNC-50 and TMX3 expressed in X. laevis oocytes in response to 300 µM acetylcholine (ACh), then the response to 300 µM acetylcholine and 1 µM atropine following pre-incubation with 1 µM atropine for 3 min 29 s followed by the response to 300 µM acetylcholine only after a wash with SOS solution for 5 min.

When 100 µM imidacloprid was applied to oocytes injected with the *D. melanogaster* α1 and *M. persicae* β1 subunits, it acted as a partial agonist, with a small initial response compared to 300 µM acetylcholine. However, the response does not return to the baseline as quickly as with acetylcholine (Figure 4.10) and subsequent responses to 300 µM acetylcholine were reduced and did not fully recover after an hour (Figure 4.10). Similar responses were seen with imidacloprid concentrations from 100 nM to 10 µM (not shown). When 100 µM thiacloprid was applied it also acted as a partial agonist with the response not returning to baseline as quickly and a similar inhibitory effect on subsequent acetylcholine responses was observed (Figure 4.11).

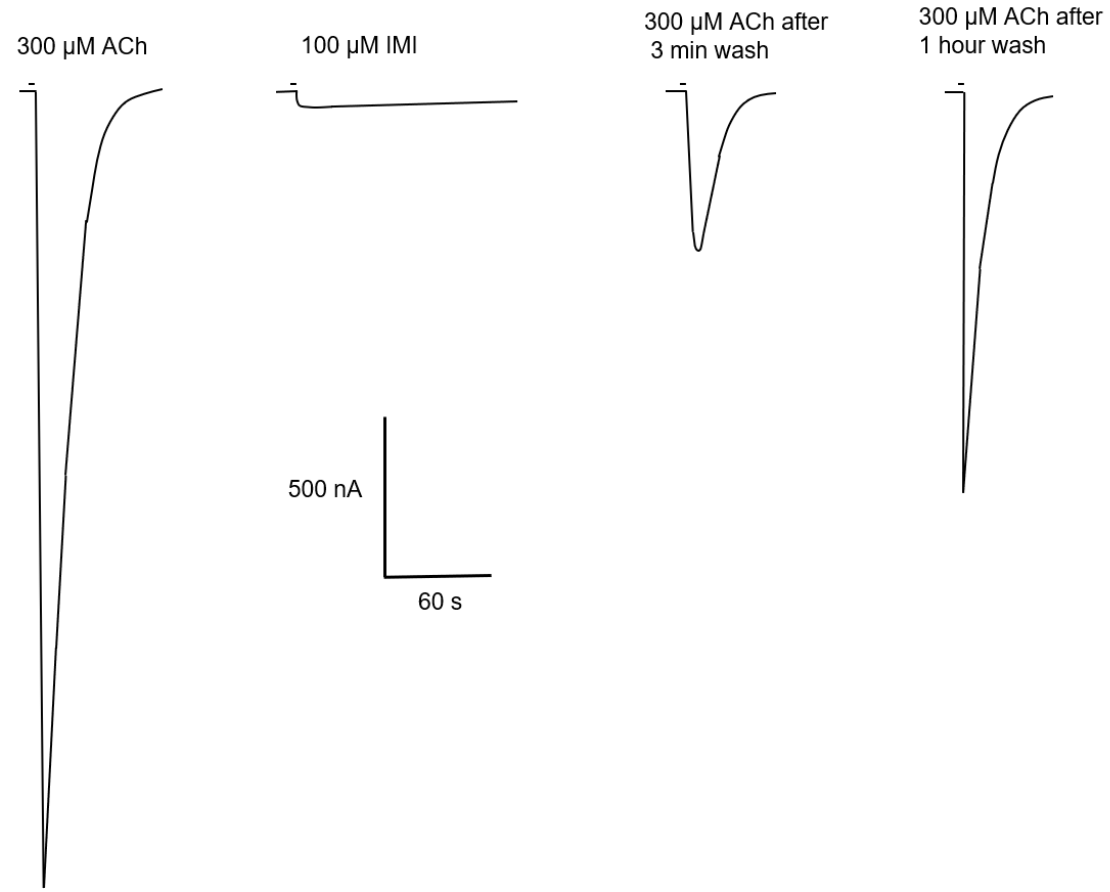

Figure 4.10 Traces showing the nAChR composed of D. melanogaster α1 and M. persicae β1 with M. persicae RIC-3, UNC-50 and TMX3 expressed in X. laevis oocytes in response to 300 µM acetylcholine (ACh), then 100 µM imidacloprid, then 300 µM acetylcholine after 3 min, then 300 µM acetylcholine after over 1 hour washing.

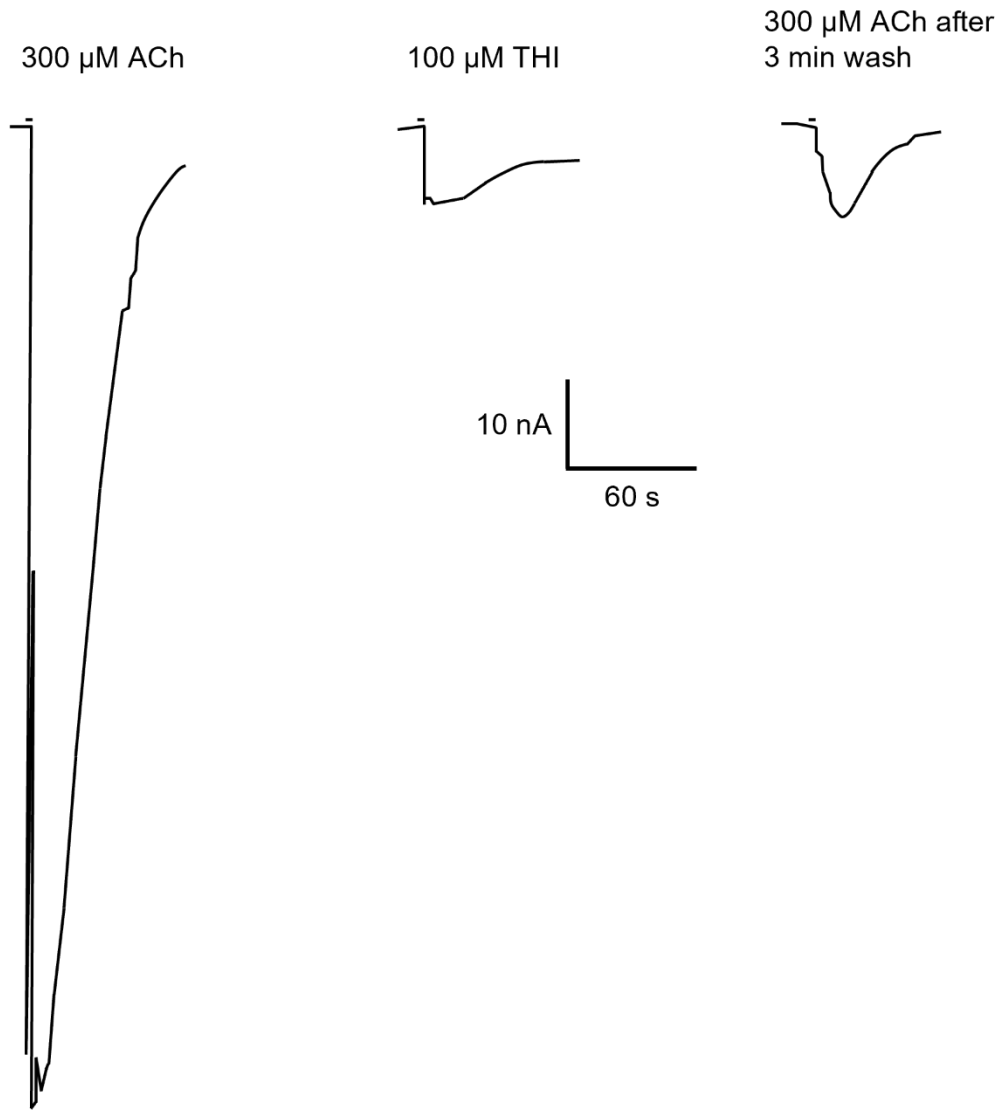

Figure 4.11 Traces showing the nAChR composed of D. melanogaster α1 and M. persicae β1 with M. persicae RIC-3, UNC-50 and TMX3 expressed in X. laevis oocytes in response to 300 µM acetylcholine (ACh), then 100 µM thiacloprid, then 300 µM acetylcholine after 3 min.

4.4 Discussion

4.4.1 Expression of *M. persicae* nAChRs with Chaperones

Expression of *M. persicae* α6 and α7 subunits with the assistance of NACHO and RIC-3 from *M. persicae* was not achieved. These experiments were based on the successful expression of the *A. mellifera* α6 subunit with NACHO (Hawkins, Mitchell and Jones, 2022) but this could not be

extrapolated to work with *M. persicae* subunits. It is not clear why expression can be achieved with nAChR subunit and chaperones from one insect species but not with subunits and chaperones from another species.

Expression could be achieved with the DNA injection of *M. persicae* α1, α3, α8 and β1 subunits with RIC-3, UNC-50 and TMX3 and with *M. persicae* α1, α2, α8 and β1 subunits with RIC-3, UNC-50 and TMX3, however it was infrequent and not robust. Thus, the injection of RNA of these subunits and chaperones was tried using the same conditions as for the successful expression of nAChRs from *D. melanogaster*, *A. mellifera* and *B. terrestris* (Ihara *et al.*, 2020). This led to more robust but more infrequent expression, which still did not allow for complete functional characterisation. It is not clear why the robust and frequent expression of nAChRs from other species with RIC-3, UNC-50 and TMX3 as chaperones was not achieved with nAChRs from *M. persicae*. A variant of the α1 subunit was tried but it did not lead to expression, the variation between the α1 splice variants was not in the N-terminal region that seems to be important for expression (Chapter 3, Figure 3.5) (Brunello *et al.*, 2022). RIC-3 variants were also tried but there was no expression from any of these batches. The longer RIC-3 variant (c23) that was originally used is most similar to the *D. melanogaster* RIC-3 used to express *D. melanogaster* nAChRs (Chapter 3, Figure 3.17) (Ihara *et al.*, 2020). It is also not certain what effect changing the RIC-3 variant used would have on expression as it does not appear to be essential for the expression of nAChR made up of these subunits (Ihara *et al.*, 2020). The addition of *M. persicae* NACHO RNA to either *M. persicae* α1, α3, α8 and β1 subunits with RIC-3, UNC-50 and TMX3 or *M. persicae* α1, α2, α8 and β1 subunits with RIC-3, UNC-50 and TMX3 RNA did not lead to expression, in fact there was expression in the same batch of oocytes without NACHO but not with NACHO. Although NACHO can act synergistically with RIC-3 (Gu *et al.*, 2016), there is not much data on the effects of combining NACHO with RIC-3, UNC-50 and TMX3 upon nAChR expression.

4.4.2 Expression of nAChRs Composed of *D. melanogaster* and *M. persicae* Subunits with Chaperones

Robust and frequent expression was achieved with combinations of subunits (*M. persicae* α3, α8 and β1 or *M. persicae* β1 alone) that included the addition of the *D. melanogaster* α1 subunit to produce hybrid receptors with *M. persicae* RIC-3, UNC-50 and TMX3. Since receptors had been successfully expressed using the *D. melanogaster* α1 subunit (Ihara *et al.*,

2020; Takayama *et al.*, 2022), thus this subunit was selected to produce a hybrid receptor to express. As the *M. persicae* β1 subunit has a neonicotinoid resistance mutation (Bass *et al.*, 2011), this was prioritised for study as it was thought that useful information could be gained by the expression of a hybrid receptor containing the *M. persicae* β1 subunit.

The nAChRs consisting of the *D. melanogaster* α1 subunit and the *M. persicae* α3, α8 and β1 subunits had an EC_{50} for acetylcholine of 123 (78.1-193) μM and the nAChR consisting of *D. melanogaster* α1 subunit and *M. persicae* β1 subunit had an EC_{50} for acetylcholine of 91.1 (67.7-123) μM, these are not significantly different as the 95% confidence limits (from the GraphPad analysis) overlap. This is higher than the EC_{50} for acetylcholine than from other insect nAChRs expressed in *X. laevis* oocytes (Chapter 1, Table 1.1) (Sgard *et al.*, 1998; Lansdell *et al.*, 2012; Ihara *et al.*, 2020; Hawkins, Mitchell and Jones, 2022; Takayama *et al.*, 2022). The EC_{50}s for all the *M. persicae* nAChRs seem to be in the same range as those for the *D. melanogaster* and *M. persicae* hybrid receptors (Figures 4.1, 4.3 and 4.4). Plotting the acetylcholine concentration response curves separately for oocytes injected with *D. melanogaster* α1 and the *M. persicae* α3, α8 and β1 cDNAs appear to form three separate groups (with EC_{50}s 56.0-75.0 μM, 109 μM and 206-234 μM), potentially indicating nAChRs with different subunit combinations or stoichiometries. Using *D. melanogaster* subunits, nAChRs can be formed of just the α1 and β1 subunits or the α1, β1 and β2 (α8) subunits (Ihara *et al.*, 2020; Takayama *et al.*, 2022) so potentially these nAChRs could be formed, a mixture of different nAChRs or nAChRs involving the α3 subunit. Thus, as we were unsure which subunits made nAChRs in oocytes injected with the *D. melanogaster* α1 subunit and the *M. persicae* α3, α8 and β1 subunits cDNAs, oocytes injected just with the *D. melanogaster* α1 subunit and the *M. persicae* β1 subunits cDNAs were used for further study. We are not certain of the stoichiometry of the receptor formed by injecting *D. melanogaster* α1 subunit and the *M. persicae* β1 subunits cDNAs in a 1:1 ratio. However, in nAChRs formed of the *D. melanogaster* α1 and β1 subunits in different ratios no difference in the affinity of acetylcholine was found (Takayama *et al.*, 2022) so our experiments so far may not show any difference due to different stoichiometries.

The nAChR consisting of *D. melanogaster* α1 and *M. persicae* β1 subunits with *M. persicae* RIC-3, UNC-50 and TMX3 was only inhibited slightly by 1 μM atropine (5.9% inhibition). As the response was not completely ablated as expected for mAChRs (Dale, 1914) this confirms the response to acetylcholine was not due to muscarinic acetylcholine receptors that may be endogenously expressed in the oocytes. In other similar experiments, 0.5 μM atropine was

included in the perfusion buffer so the response was not ablated by atropine but there is no numerical data on its effects on nAChR responses (Ihara *et al.*, 2020; Takayama *et al.*, 2022).

4.4.3 The Interactions of Neonicotinoids with the nAChR Composed of the *D. melanogaster* α1 and *M. persicae* β1 Subunits

Similar to other nAChRs imidacloprid and thiacloprid acted as partial agonists on the *D. melanogaster* α1 and *M. persicae* β1 nAChR (Figures 4.10 and 4.11) (Ihara *et al.*, 2020; Rufener *et al.*, 2020; Takayama *et al.*, 2022). However, the application of 100 µM imidacloprid or thiacloprid lead to a subsequent reduction in the response to 300 µM acetylcholine which never fully recovered (Figure 4.10 and 4.11). This has not been mentioned in other papers, which normalise the neonicotinoid response to the acetylcholine response (Ihara *et al.*, 2020; Takayama *et al.*, 2022). The mechanism of this effect is not known. It may be that at 100 µM the neonicotinoids cause channel block, however lower concentrations of imidacloprid also had inhibitory effect. Other studies on the inhibitory effects of neonicotinoids on acetylcholine responses have used concentrations that were too low for an agonistic effect (10-100 pM) (Ihara *et al.*, 2020). As the response to clothianidin was usually larger than the response to imidacloprid and thiacloprid from nAChRs (Ihara *et al.*, 2020; Rufener *et al.*, 2020), it may be easier to characterise the response of the *D. melanogaster* α1 and *M. persicae* β1 to clothianidin.

4.4.4 Further Work

It appears sequences in the N-terminal region are important for the expression of insect nAChRs containing the α1 subunit; the *A. mellifera* α1, α8, β1 nAChR could only be expressed with RIC-3, UNC-50 and TMX3 if it included a 26 amino acid sequence at the N-terminus of the α1 subunit (Brunello *et al.*, 2022). Thus, it would be worth comparing the sequences of the *M. persicae* α1 subunit and the *D. melanogaster* α1 subunit (Figure 4.12), which expresses with other *M. persicae* subunits, to see if any modifications could be made to the *M. persicae* α1 subunit that could result in increased expression of nAChRs made up entirely of *M. persicae* subunits. These two subunits have a very similar sequence in the N-terminal ligand-binding domain and the transmembrane regions, with 67% identity overall (Figure 4.12). As the

extracellular N-terminal domain is very similar (Figure 4.12), the signal peptide from the *D. melanogaster* α1 could be inserted into the *M. persicae* α1 subunit to see if this improved expression.

Figure 4.12 The aligned peptide sequences of the α1 subunits from D. melanogaster and M. persicae. Identical amino acids highlighted in grey. The predicted signal peptide is in lowercase, predicted transmembrane helices in bold, the cys-loop cysteines underlined and the consecutive cysteines present in α subunits double underlined. Structural motifs were predicted as in Chapter 2.4.8.

Different subunit combinations could be attempted from the *D. melanogaster* α1 subunit and the *M. persicae* α2, α3, α8 and β1 subunits. This would allow better identification of the subunits forming particular nAChR subtypes when the *D. melanogaster* α1 and *M. persicae* α3, α8 and β1 subunits are injected (Figure 4.6). Injecting the *M. persicae* α2 nAChR subunit may lead to the expression of different nAChR subtypes, orthologous to nAChRs studied in (Ihara *et al.*, 2020). Changing the injection ratios of the *D. melanogaster* α1 and the *M. persicae* β1

subunits would give more control over the stoichiometry of the receptor and allow analysis of any change in properties caused by the different stoichiometries, similar to the experiments in (Takayama *et al.*, 2022), which observed a different in imidacloprid affinity.

Further study is required on the interaction of neonicotinoids with the *D. melanogaster* α1, *M. persicae* β1 nAChR. The creation of concentration response curves for imidacloprid, thiacloprid and clothianidin would allow numerical analysis and comparison of their partial agonism and potency. Potentially, a way to quantify the reduction of the acetylcholine response after the application of neonicotinoids (Figures 4.10 and 4.11) could allow the investigation of different neonicotinoid actions. It may also be useful to replicate experiments in (Ihara *et al.*, 2020) and study the inhibitory effects of pM neonicotinoid concentrations, especially if these turn out to have some relevance to field conditions.

As mentioned in Chapter 2, the *M. persicae* β1 subunit with the R81T mutation has already been obtained and cloned into pCI ready for expression. The expression of a nAChR containing the R81T neonicotinoid resistance mutation in the *M. persicae* β1 subunit would allow comparison with wildtype nAChRs and direct quantification of the mutation's effects on neonicotinoid potency for the first time. This could then be used to screen for potentially novel compounds that 'break' resistance and therefore would be effective on aphids with the R81T mutation.

4.5 Conclusion

Although the robust and frequent expression of a nAChR consisting entirely of subunits from *M. persicae* with the assistance of the protein chaperones RIC-3, UNC-50 and TMX3 was difficult to achieve, using the α1 subunit from *D. melanogaster* allowed nAChRs containing some *M. persicae* subunits to be robustly expressed. A nAChR composed of the *D. melanogaster* α1 and *M. persicae* β1 subunits responded to imidacloprid and thiacloprid both as partial agonists and by a reduction in the response to acetylcholine.

Chapter 5 Functional Characterisation of the Homomeric *Apis mellifera* α5 Nicotinic Acetylcholine Receptor

5.1 Introduction

Most of the results in this chapter were published in (Mitchell *et al.*, 2022) (Appendix), apart from some of the phylogenetic analysis and the effects of α-bungarotoxin. The interactions of serotonin (5-HT) from (Mitchell *et al.*, 2022) with the *A. mellifera* α5 nAChR have been included in Chapter 6 with the interactions of other biogenic amines and related compounds.

5.1.1 Expression of α5, α6 and α7 Insect Nicotinic Acetylcholine Receptors

The insect α5, α6 and α7 subunits were all first identified in *D. melanogaster* and grouped together phylogenetically (Grauso *et al.*, 2002). The sequences were identified as being similar to vertebrate α7 (22-23% sequence identity) and *C. elegans* ACR-16 (Ce21) subunits, which can form homomeric receptors (Grauso *et al.*, 2002; Ballivet *et al.*, 1996), and thus were considered to represent more ancestral nAChRs (Corringer, Novère and Changeux, 2000).

A nAChR has been expressed in *X. laevis* oocytes made up of *D. melanogaster* α5 and α6 subunits with the *C. elegans* chaperone protein, RIC-3 (Watson *et al.*, 2010). Expression was inconsistent but the ratio Dα6: Dα5: RIC-3 2:4:1 gave the largest agonist responses. The nAChR responded to nicotine (1 mM), acetylcholine (100 µM), spinetoram (10 µM) and spinosyn A in a concentration-dependent manner (nM range) but 100 µM imidacloprid did not induce an agonistic response. A spinosyn A-induced current could be blocked by 40 µM d-tubocurarine.

Success was also achieved in expressing *D. melanogaster* homomeric α5 or α7 nAChRs and a heteromeric nAChR made up of a combination of α5, α6 and α7 in *X. laevis* oocytes, all requiring the presence of RIC-3 (from *C. elegans*) (Lansdell *et al.*, 2012). However, expression was not consistent; not all batches of oocytes had expression. Acetylcholine EC_{50}s were 8.8 µM for the homomeric α5 nAChR, 6.7 µM for the homomeric α7 nAChR and 13.5 nM for the heteromeric nAChR. All three receptors were completely inhibited by 0.1 µM α-bungarotoxin.

The α7 nAChR subunit from the cockroach, *P. americana*, was expressed, in *X. laevis* oocytes as a homomeric receptor without a chaperone protein, although the currents were too small to measure the affinity of acetylcholine and carry out instructive characterisation studies (Cartereau *et al.*, 2020). Thus, other nAChR subunits or chaperone proteins are likely required to achieve robust expression of the α7 subunit. The EC_{50} of nicotine was 790 μM and 0.5 μM atropine was applied at all times in the saline solution, showing the response was not from mAChRs. At 5 mM and 10 mM nicotine there was a response from non-injected and water injected oocytes, but this was smaller than the response in oocytes expressing the α7 nAChR and control oocytes did not respond to lower concentrations of nicotine (Cartereau *et al.*, 2020). The nicotine-induced current was not inhibited by 10 μM α-bungarotoxin after 5 min incubation. Further experiments revealed that imidacloprid had no agonist actions but thiacloprid was a partial agonist (Cartereau *et al.*, 2021). When coapplied with nicotine 10 μM imidacloprid acted as a positive modulator but 10 μM thiacloprid acted as an antagonist (Cartereau *et al.*, 2021).

Previously in the Jones laboratory, expression of the *A. mellifera* homomeric α6 nAChR had been achieved in *X. laevis* oocytes (Hawkins, Mitchell and Jones, 2022), with the chaperone protein, NACHO (Gu *et al.*, 2016; Hawkins, Mitchell and Jones, 2022), although expression was observed in only 33% of batches of oocytes injected. It has yet to be determined whether other chaperones or nAChRs are required for robust expression. The α6 nAChR had an EC_{50} of 0.88 μM for acetylcholine and was completely inhibited by α-bungarotoxin but not atropine (Hawkins, Mitchell and Jones, 2022). Spinosad acts as an agonist and when co-applied with 3 μM acetylcholine the channel did not close, highlighting the α6 nAChR subunit as a molecular target for the spinosyn class of insecticides.

The expression of the *A. mellifera* α7 homomeric nAChR in *X. laevis* oocytes was achieved in a very small proportion of oocytes when the α7 subunit was expressed alone, with human RIC-3, human NACHO or with human RIC-3 and NACHO and in a higher proportion of oocytes when expressed with *C. elegans* RIC-3, UNC-50 and TMX3 (Brunello *et al.*, 2022). No response to acetylcholine was seen in any oocytes when the α7 was expressed with *A. mellifera* RIC-3, UNC-50 and TMX3 or *A. mellifera* NACHO. Responses were to 100 μM acetylcholine.

5.1.2 The Insect α5 Nicotinic Acetylcholine Receptor Subunit

The insect α5 nAChR subunit has always been phylogenetically grouped with the α6 and α7 subunits (Jones *et al.*, 2010; Jones and Sattelle, 2010), even though non-Dipteran α5 subunits do not appear to be as closely related to other insect α6 and α7 subunits (Jones and Sattelle, 2010) (Chapter 1, Figure 1.2). Aphids do not have an α5 subunit (Dale *et al.*, 2010), (Chapter 3). This is speculated to be because the α5 subunit evolved recently after the divergence of aphids and other insects, possibly from gene duplication of the α7 subunit (Dale *et al.*, 2010; Wang *et al.*, 2015). Based on phylogenetic analysis, the α5 subunit of Diptera (flies and mosquitoes) and non-Diptera (cockroaches, bees, beetles and butterflies) may belong to distinct monophyletic groups (Cartereau *et al.*, 2020). Our further phylogenetic analysis and functional characterisation may help resolve this.

The α5 subunit from the locust *L. migratoria* was not found to form functional nAChRs, when injected alone, but did form a functional receptor with the rat β2 subunit with an EC_{50} for acetylcholine of 335 μM (Zhang *et al.*, 2017).

The α5 subunit is not known to be the specific target for any class of insecticides. Spinosad is thought to act on only the α6 subunit as shown by heterologous expression of the *A. mellifera* α6 subunit (Hawkins, Mitchell and Jones, 2022; Watson *et al.*, 2010) and mutations in the α6 binding site (Puinean *et al.*, 2012; Hiruta *et al.*, 2018; Ureña *et al.*, 2019; Silva *et al.*, 2016) or non-functional α6 subunits (Berger *et al.*, 2016; Wan *et al.*, 2018; Perry *et al.*, 2021; Lu *et al.*, 2022) leading to spinosad resistance. Neonicotinoids have been found to act on receptors made up of α1, α2, α3, β1 and/or β2/α8, either through heterologous expression (Ihara *et al.*, 2020; Rufener *et al.*, 2020) or through knockout studies of nAChRs (Perry *et al.*, 2021; Lu *et al.*, 2022). However, most of these studies have been carried out on *D. melanogaster* which appears to have an α5 subunit that is particular to Dipteran species (Cartereau *et al.*, 2020; Jones and Sattelle, 2010). Thus, as Dipteran and non-Dipteran α5 may represent different nAChR subclasses it is worth testing a non-Dipteran α5 nAChR to identify if it has different properties from a Dipteran α5 nAChR.

5.2 Chapter Aim

The aim of this chapter was to achieve functional expression of a non-Dipteran α5 nAChR and use this to test the actions of compounds that target nAChRs. To this end the *A. mellifera* α5 nAChR subunit was cloned and expressed in *X. laevis* oocytes. Co-expression with other *A. mellifera* nAChR subunits was evaluated to see if they combined with the α5 subunit to produce a nAChR with an altered affinity for acetylcholine.

5.3 Results

5.3.1 Phylogenetic analysis of the *A. mellifera* α5 nicotinic acetylcholine receptor subunit

As discussed earlier, the *A. mellifera* α5 nAChR subunit was previously classified as a member of the 'α7 group' bearing notable resemblance with the vertebrate α7 subunits (Jones and Sattelle, 2010) and therefore considered closely related to the *A. mellifera* α6 subunit as well as the *D. melanogaster* α5, α6 and α7 subunits, which had previously been expressed with chaperones (Lansdell *et al.*, 2012; Hawkins, Mitchell and Jones, 2022). However, with the cloning of nAChR subunits from more insect species analysis indicated that the α5 subunit of *A. mellifera* and other non-Dipteran insects was not orthologous to the Dipteran α5 subunit (Jones and Sattelle, 2010). In order to further study the relationship between the Dipteran and non-Dipteran α5 subunits we performed phylogenetic analysis to identify if the *A. mellifera* and *D. melanogaster* α5 subunit are true orthologues. A phylogenetic tree was constructed with nAChR subunits from different insects; *A. pisum, A. gambiae*, *A. mellifera*, *B. terrestris*, *B. mori*, *D. melanogaster*, *P. americana*, *T. castaneum*; as well as various cys-LGICs from vertebrates (Figure 5.1). This shows that the non-Dipteran (beetle, bee, cockroach and moth) α5 subunits form a distinct group from the α6, α7 and Dipteran (fruit fly and mosquito) α5 subunits. The non-Dipteran α5 subunits have not previously been studied as there is no equivalent subunit in the model organism *D. melanogaster* and it is not known whether it is targeted by insecticides.

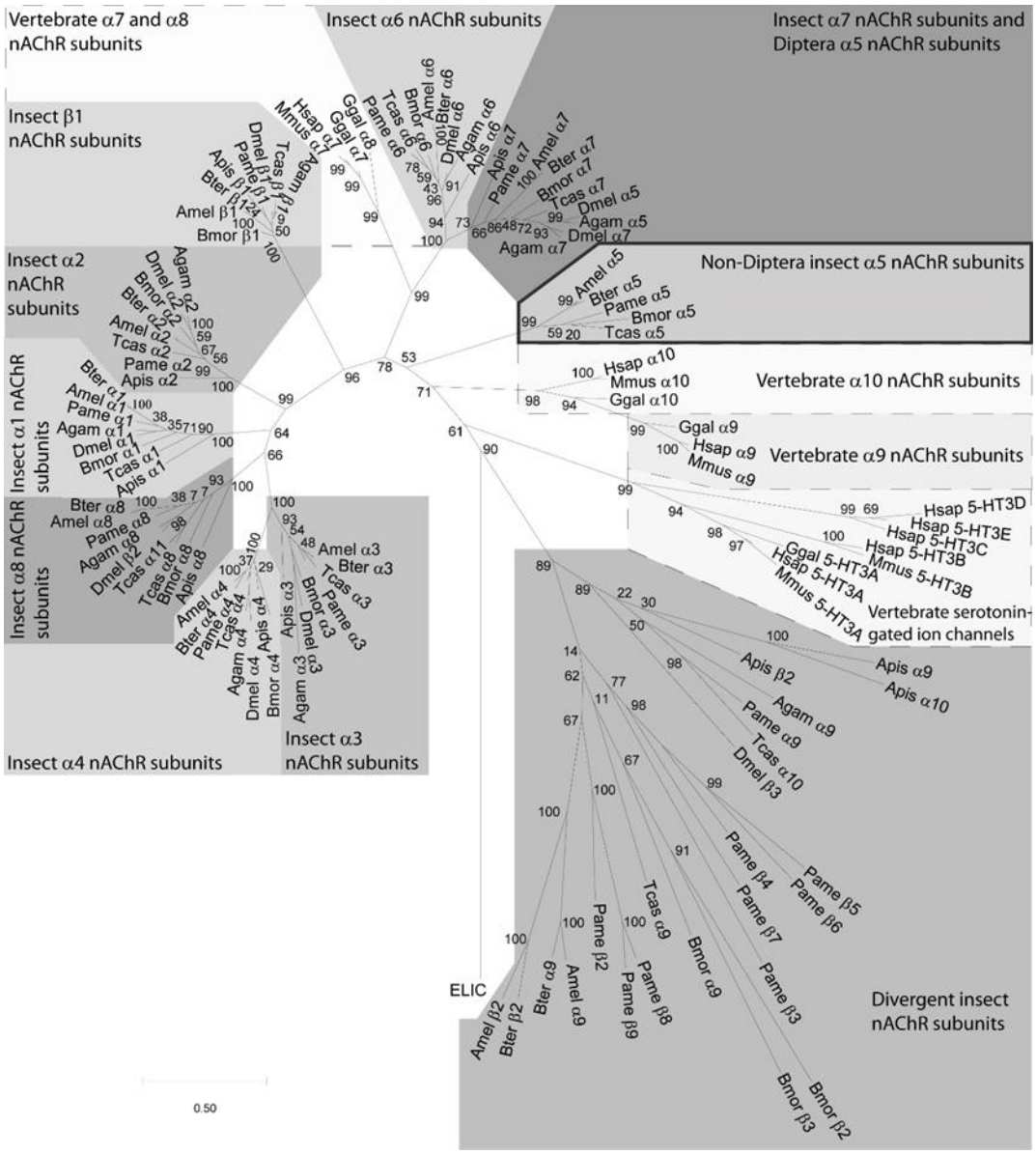

Figure 5.1 Tree showing relationships of insect and vertebrate α7–10 nAChR subunit protein sequences as well as vertebrate 5-HT3 subunits. Numbers at each node signify bootstrapping 1000 times represented as a percentage of trees in which the associated taxa clustered together and the scale bar represents substitutions per site. ELIC (Accession number P0C7B7), from Dickeya chrysanthemi, a bacterial ancestor of cysLGICs, was used as an outgroup. Species subunit sequences used in the tree are as follows: Agam (A. gambiae) see (Jones, Grauso and Sattelle, 2005); Amel (A. mellifera) α5 (AJE70263) otherwise see (Jones et al., 2006); Apis (A. pisum) see (Dale et al., 2010); Bmor (B. mori) see (Shao, Dong and Zhang, 2007); Bter (B. terrestris) see (Sadd et al., 2015); Dmel (D. melanogaster); Pame (P. americana) see (Jones et al., 2020); Tcas (T. castaneum) see (Jones and Sattelle, 2007); Ggal (Gallus gallus) α7 (NP989512), α8 (CAA36544), α9 (NP990091), α10 (NP001094506), 5-HT3A (XP040508006); Hsap (Homo sapiens) α7 (CAA69697), α9 (NP060051), α10 (CAC20435), 5-HT3A (NP998786), 5-HT3B (NP006019.), 5-HT3C (AF459285), 5-HT3D (AY159812), 5-HT3E (AY159813); Mmus (Mus musculus) α7 (AAF35885), α9 (NP001074573), α10 (NP001074893), 5-HT3A (6Y59_A), 5-HT3B (NP064670).

Analysis of gene duplication events indicate that the Dipteran α5 nAChR subunit appears to have evolved from a gene duplication of the α7 subunit (Figure 5.2) but the non-Dipteran α5 arises from a much earlier gene duplication before the core subunit groups branch off.

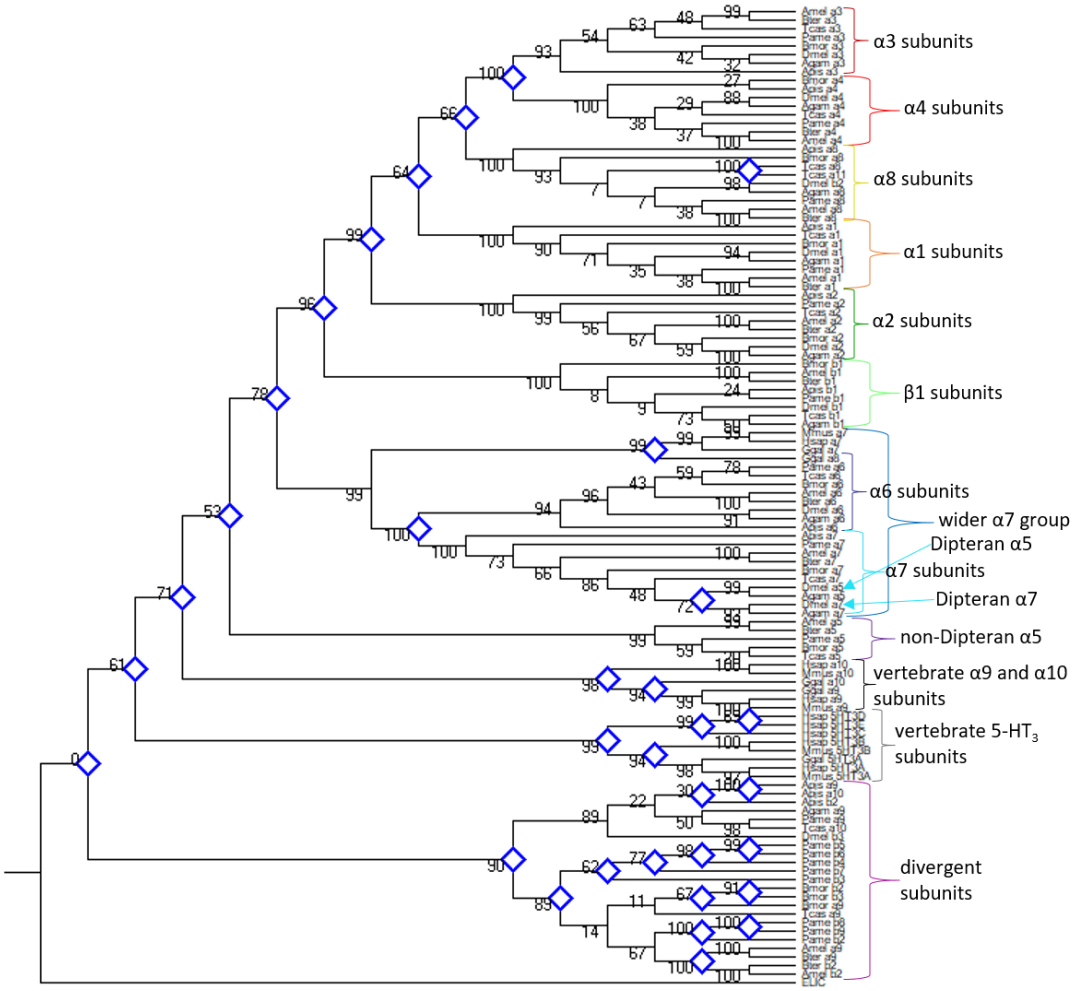

Figure 5.2 Gene duplications from the phylogenetic tree in Figure 5.1, blue squares indicate a gene duplication event, created in MEGA X (Kumar et al., 2018).

The exon-intron boundaries were also mapped from several species to see if they were different between the non-Dipteran α5, Dipteran α5 and the wider α7 group. There were a few boundaries shared by all the nAChRs and some boundaries shared by the majority of the α7 group but not non-Dipteran α5 (Figure 5.3, green arrows). The average number of

boundaries shared between the subunits in the α7 group (α6, α7 and Dipteran α5) was 7.41 ± 0.262 and between the non-Dipteran α5 and the α7 group 3.31 ± 0.419 (95% confidence limits calculated using the two-tailed t test) indicating that the non-Dipteran α5 are not as closely related to subunits in the α7 group as those within the group. This, taken together with the phylogenetic analysis, suggests that the α5 subunits of Diptera and non-Diptera are in fact members of different nAChR subgroups. The α5 nAChR of *A. mellifera* was cloned to enable heterologous expression studies to determine whether non-Dipteran α5 nAChRs possess distinct functional characteristics.

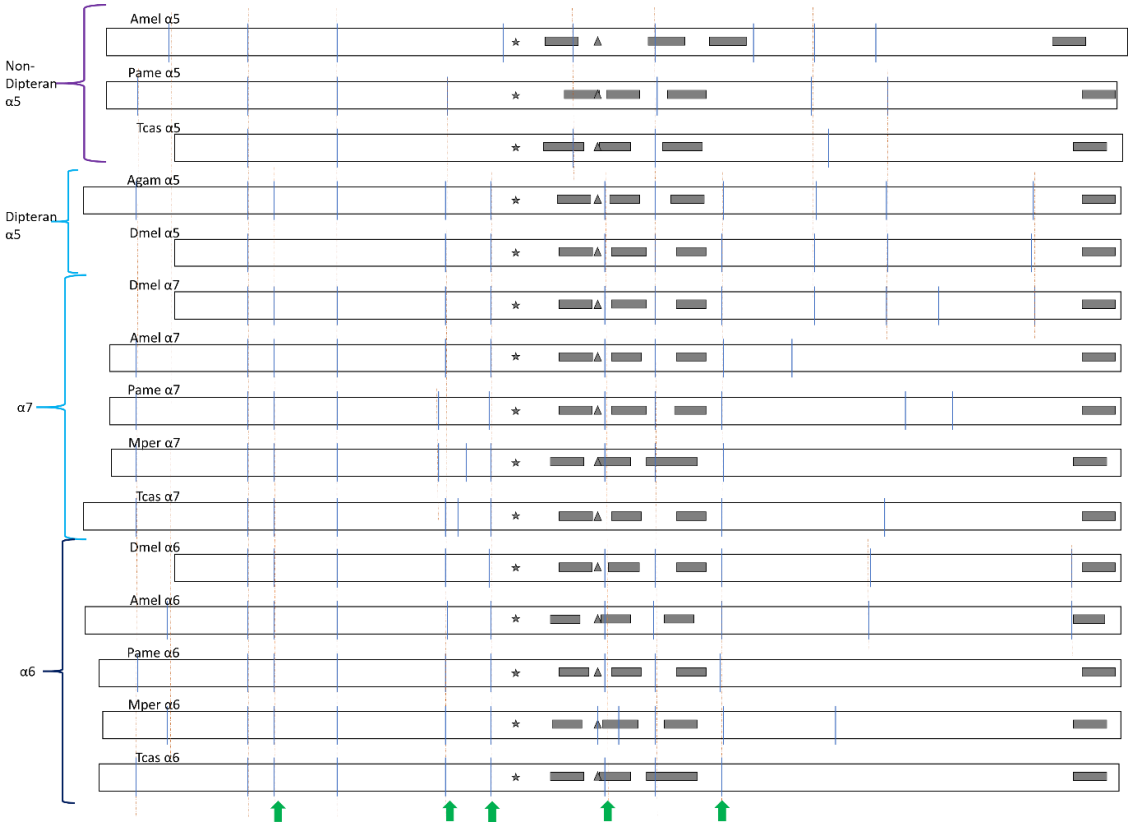

Figure 5.3 Exon composition of a selection of insect α5, α6 and α7 nAChR subunits. Transmembrane regions are indicated as grey boxes, a star marks the adjacent cysteines denoting an α subunit and triangles the GEK sequence preceding TM2 that is important for cation selection (Corringer, Novère and Changeux, 2000; Jensen, Schousboe and Ahring, 2005). Exon boundaries are in blue. Exon boundaries shared between most α6, α7 and Dipteran α5 but not a majority of non-Dipteran α5 are indicated by a green arrow

5.3.2 Cloning the *A. mellifera* α5 Nicotinic Acetylcholine Receptor Subunit

The *A. mellifera* α5 subunit was cloned into the pCI plasmid using the method and primers outlined in Chapter 2.4.2. The α5 insert was sequenced and found to match the predicted *A. mellifera* α5 subunit sequence (Accession number AJE70263) and the reported sequence in (Jones *et al.*, 2006).

5.3.3 Expression of the *A. mellifera* α5 Nicotinic Acetylcholine Receptor Subunit in *X. laevis* Oocytes

Two-electrode voltage-clamp electrophysiology on *X. laevis* oocytes injected with pCI plasmid encoding the *A. mellifera* α5 nAChR subunit responded to acetylcholine in a concentration-dependent manner, 2-5 days after injection (Figure 5.4 (A)). Expression was robust and consistent, with responses observed in 100% of batches of oocytes injected and maximal currents up to about 2.30 µA. A concentration response curve was generated (Figure 5.4 (B)), which gave an EC_{50} of 2.65 (2.41-2.93) mM (Table 5.1) indicating a low affinity for acetylcholine compared to other nAChRs, where EC_{50}s in the µM or nM range were observed (Hawkins, Mitchell and Jones, 2022; Thomsen *et al.*, 2015; Lansdell *et al.*, 2012; Ihara *et al.*, 2020). The Hill coefficient was 2.30 (1.89-2.72) indicating cooperative activity as it was greater than one (Weiss, 1997).

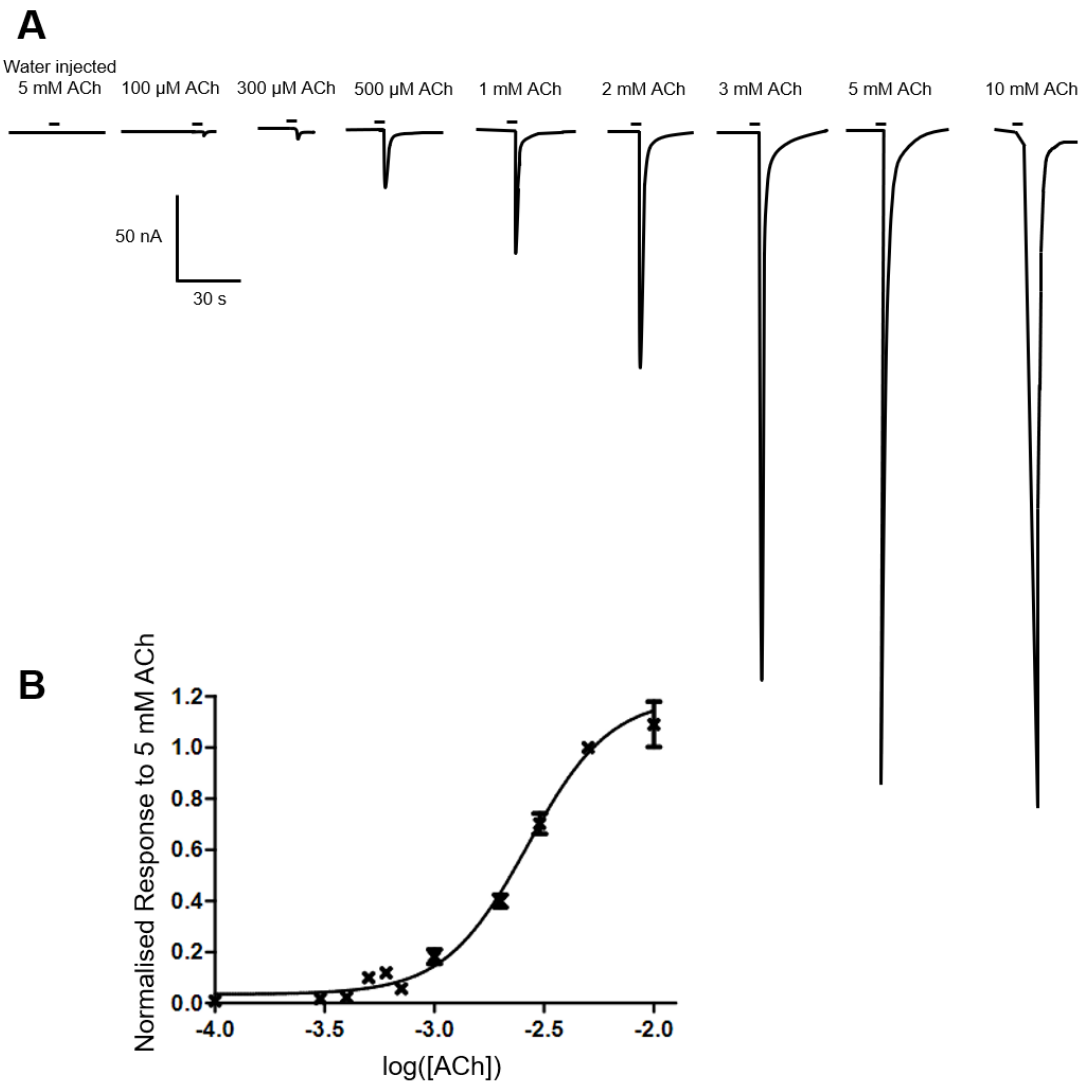

Figure 5.4 Reponses to acetylcholine in X. laevis oocytes expressing the A. mellifera α5 nAChR subunit. A. Representative current traces showing responses to different concentrations of acetylcholine (0.1–10 mM). The first trace shows the response of an oocyte injected with water alone whilst the remaining traces show responses from oocytes injected with α5. B. Acetylcholine concentration response curve. Data are normalised to the maximal response (5 mM acetylcholine) and have a mean EC_{50} of 2.65 (2.41-2.93) mM from 15 oocytes from 7 different batches of oocytes.

In order to ensure that the response to acetylcholine was not caused by endogenous muscarinic acetylcholine receptors, atropine, an inhibitor of muscarinic acetylcholine receptors, was applied to the oocytes. The response was reduced to 68.4% of the maximum but not completely ablated, demonstrating that the response is not muscarinic (Figure 5.5) and is likely due to the injected α5 subunit.

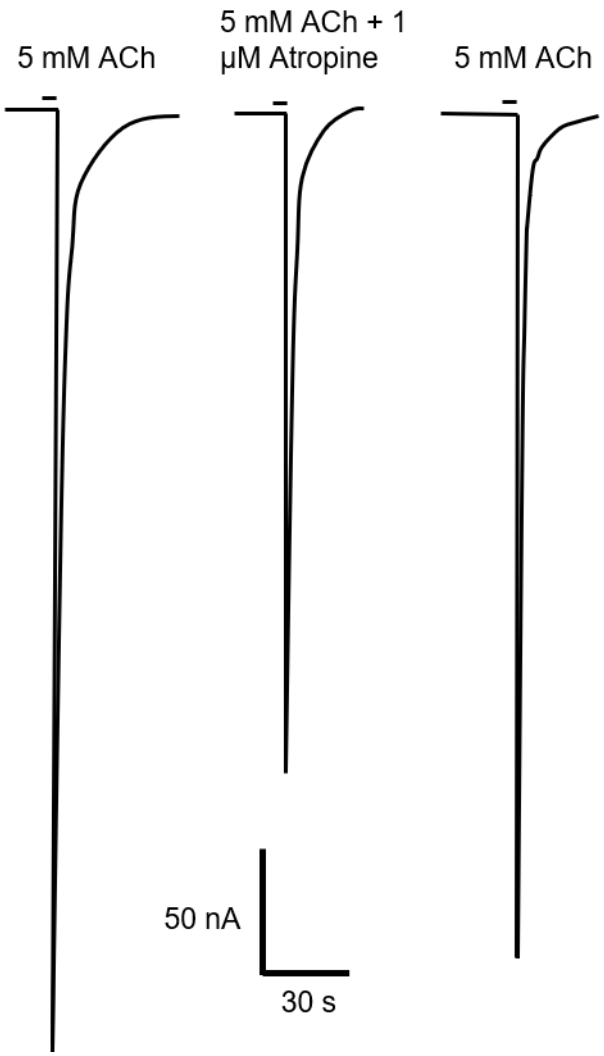

Figure 5.5 Traces showing A. mellifera α5 nAChR expressed in X. laevis oocytes in response to 5 mM acetylcholine (ACh), then with 1 µM atropine following pre-incubation with 1 µM atropine for 5 min followed by ACh only again after a wash with SOS solution for 5 min.

The low sensitivity of α5 to acetylcholine with an EC_{50} in the mM range indicates that the receptor is unlikely to respond to acetylcholine *in vivo*. In order to identify another endogenous ligand of the homomeric *A. mellifera* α5 nAChR, we analysed the actions of choline on the receptor, as it has been found to be a full agonist on human α7 nAChR (Papke, Bencherif and Lippiello, 1996; Mandelzys, De Koninck and Cooper, 1995; Thomsen *et al.*, 2015; Alkondon *et al.*, 1997). Choline was determined to be a full agonist, having the same maximal response as acetylcholine and responded in a concentration-dependent manner (Figure 5.6), with an EC_{50} of 9.07 (4.48-18.4) mM (N = 4, n = 5). This high EC_{50} value suggests that choline is also not an endogenous ligand of the *A. mellifera* α5 nAChR.

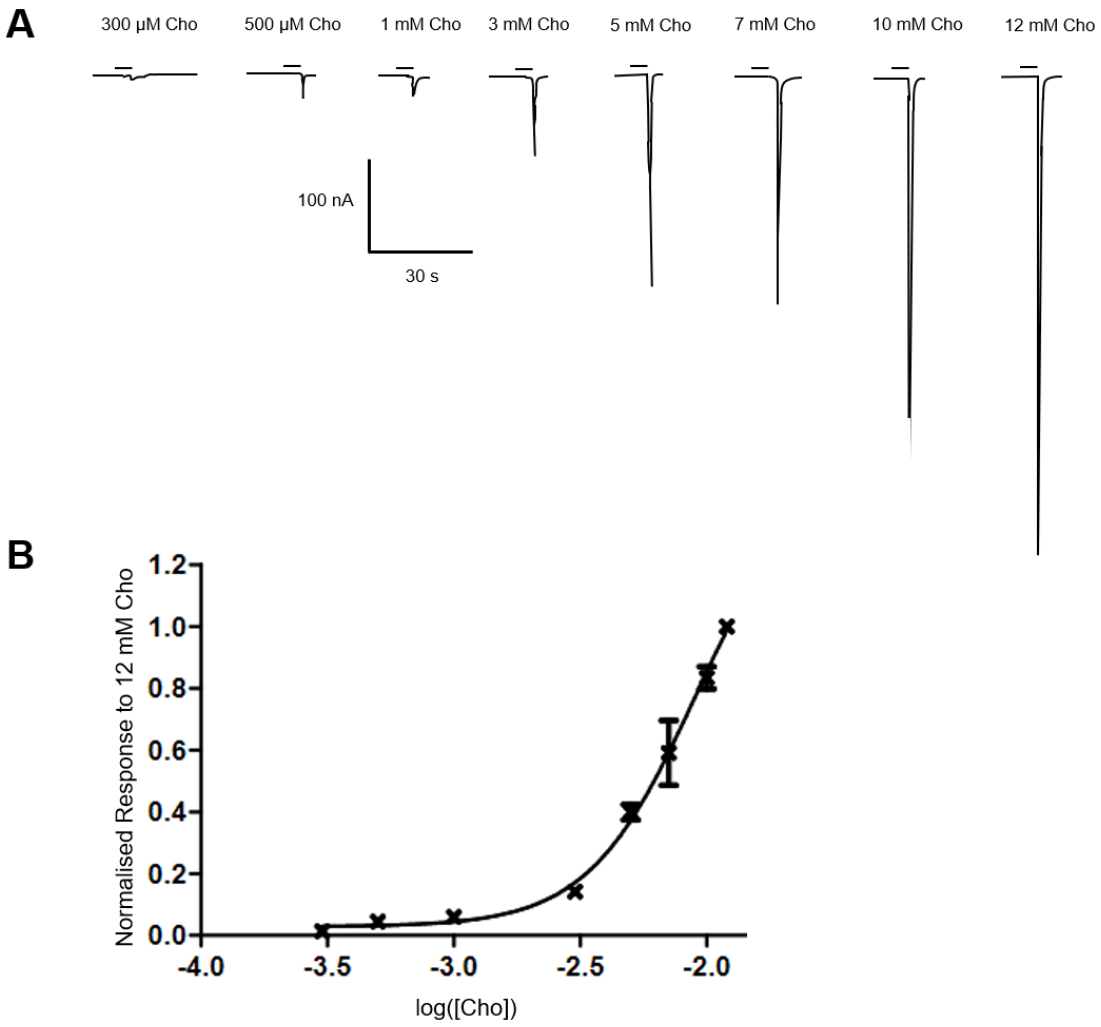

Figure 5.6 Reponses to choline in X. laevis oocytes expressing the A. mellifera α5 nAChR subunit. A. Representative current traces showing responses to different concentrations of choline (0.3–12 mM). B. Choline concentration response curve. Data are normalised to the response to 12 mM choline and have a mean EC_{50} of 9.07 (4.48-18.4) mM from 5 oocytes from 4 different batches of eggs.

5.3.4 Co-expression of the *A. mellifera* α5 Nicotinic Acetylcholine Receptor Subunit with other *A. mellifera* Nicotinic Acetylcholine Receptor Subunits

The *A. mellifera* α5 subunit was co-expressed with other *A. mellifera* nAChR subunits to see if this increased the affinity for acetylcholine (Table 5.1, Figure 5.7 (B)). Traces from *A. mellifera* α5 + α3 + α8 are shown as an example (Figure 5.7 (A)). None of the EC_{50} values from the combinations tried were significantly different from the EC_{50} value of *A. mellifera* α5 subunit expressed alone (Table 5.1) and neither were the Hill coefficients. This included the combination of α5 + α6 + α7, which for *D. melanogaster* expressed as a heteromeric receptor

with an acetylcholine EC_{50} of 13.5 nM (Lansdell *et al.*, 2012). There was no response to 5 mM acetylcholine with either the combinations of *A. mellifera* α5 + α2 (N = 1), *A. mellifera* α5 + α1 + α2 (N = 3) or *A. mellifera* α5 + α1 + α2 + α3 + α8 + α9 + α6 + α7 (N = 2), although in the latter case it may be due to the concentration of *A. mellifera* α5 DNA injected being too small for expression due to dilution with other subunits.

Table 5.1 Effect of acetylcholine on membrane currents from X. laevis oocytes expressing A. mellifera α5 and other A. mellifera nAChR subunits. EC_{50} and Hill coefficient values are displayed as the mean ± 95% confidence limits.

Receptor	**Acetylcholine EC_{50} (mM)**	**Hill Coefficient**	**n = oocytes, N = frogs**
α5	2.65 (2.41-2.93)	2.30 (1.89-2.72)	n = 15, N = 7
α5 + α3 + α8	2.94 (2.07-4.17)	2.47 (1.16-3.79)	n = 3, N = 2
α5 + α1	2.94 (2.49-3.47)	2.86 (1.97-3.75)	n = 6, N = 4
α5 + α9	2.33 (1.89-2.86)	2.97 (1.34-4.59)	n = 3, N = 2
α5 + β1	2.13 (1.88-2.41)	5.33 (1.40-9.26)	n = 3, N = 2
α5 + α6 + α7	2.31 (1.70-3.14)	2.43 (0.956-3.91)	n = 3, N = 2

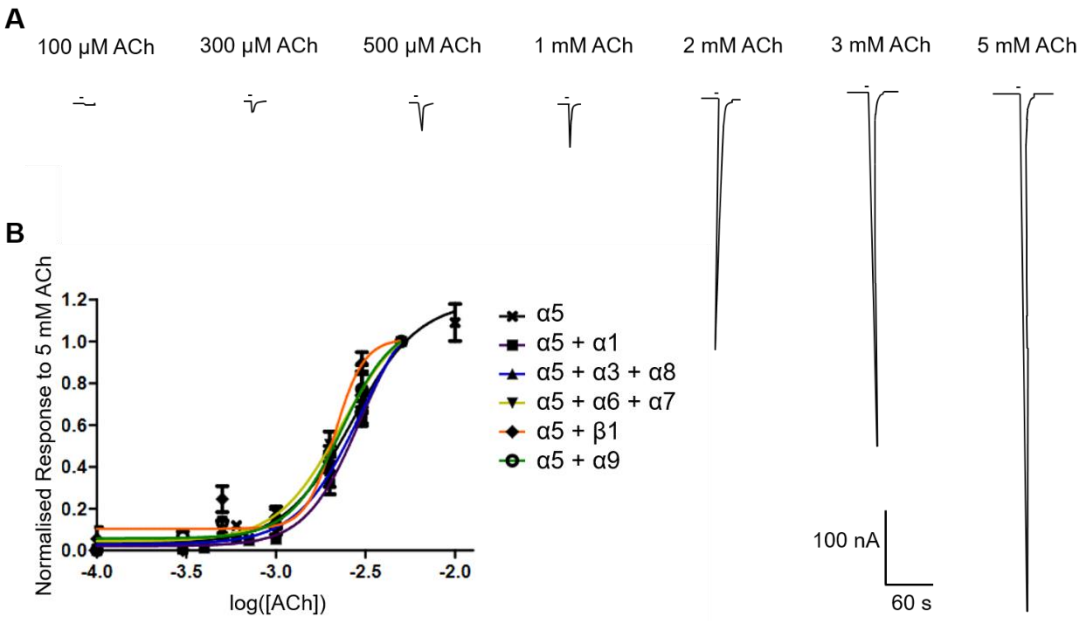

Figure 5.7 A. Responses to acetylcholine in X. laevis oocytes injected with A. mellifera α5 + α3 + α8 nAChR DNA. B. Acetylcholine concentration response curves for all A. mellifera nAChR combinations tested. Data are normalised to the maximal response (5 mM acetylcholine).

5.3.5 Actions of Insecticides and Other Nicotinic Acetylcholine Receptor Targeting Compounds on the *A. mellifera* α5 Nicotinic Acetylcholine Receptor

In order to determine whether the *A. mellifera* α5 nAChR is a potential target of currently used insecticides the actions of representative compounds from two major classes of pesticides (spinosyns and neonicotinoids) were tested.

Spinosad at 10 µM did not elicit an agonistic response from *X. laevis* oocytes expressing the *A. mellifera* α5 subunit (Figure 5.8 (A)) and did not act as an antagonist or modulator when 1-10 µM was applied with 1-5 mM acetylcholine (Figure 5.8 (B) and (C)). Unlike the response on *X. laevis* oocytes expressing the *A. mellifera* α6 subunit with NACHO, where spinosad acted as an agonist and modulator of the acetylcholine response (Hawkins, Mitchell and Jones, 2022).

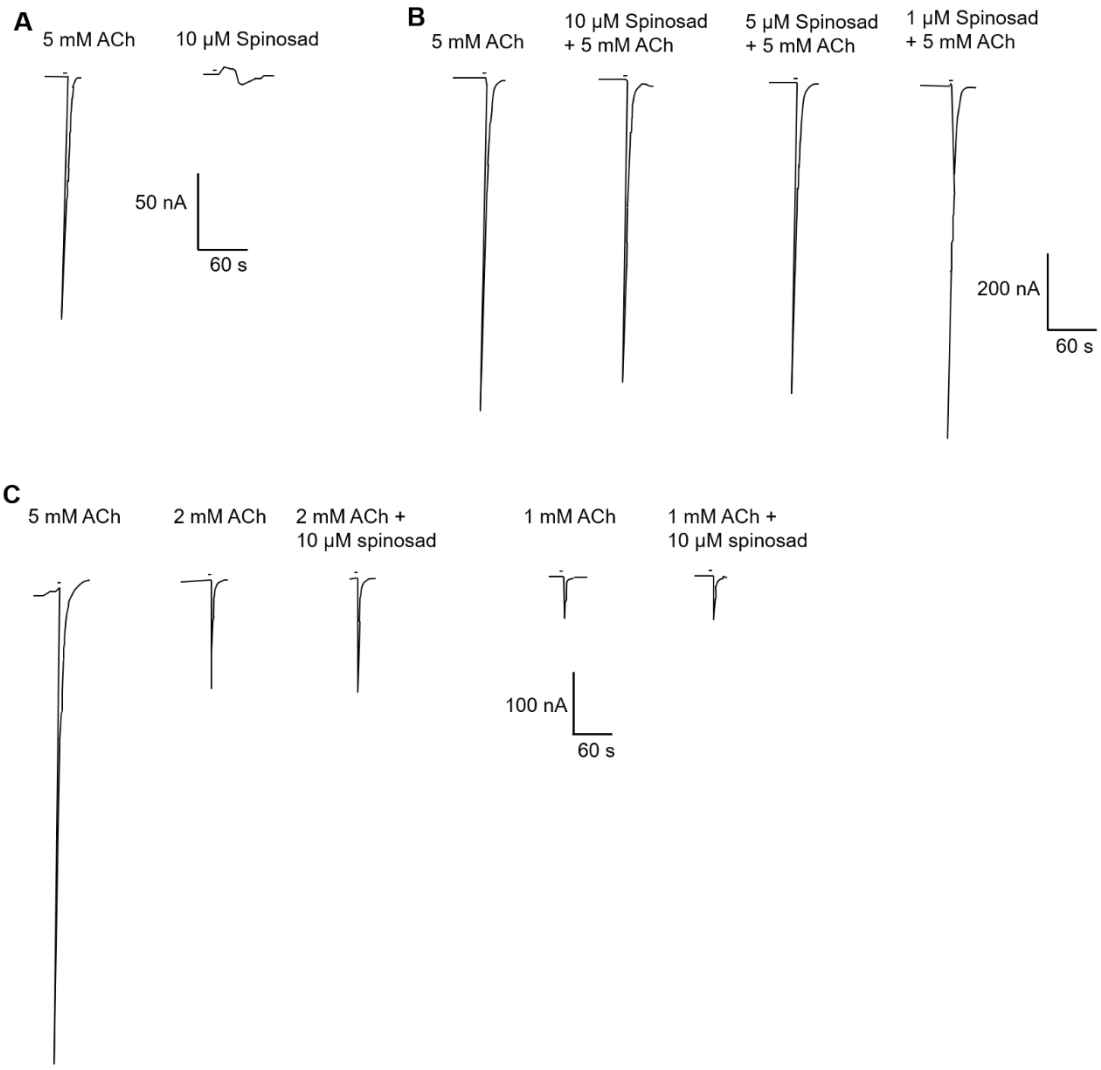

Figure 5.8 Traces of effects of spinosad on A. mellifera α5 subunit expressed in X. laevis oocytes. A. 10 µM spinosad applied 3 min after 5 mM acetylcholine (ACh) B. Co-application of 10 µM spinosad + 5 mM acetylcholine, 5 µM spinosad + 5 mM acetylcholine, 1 µM spinosad + 5 mM acetylcholine C. 2 mM acetylcholine compared to 2 mM acetylcholine + 10 µM spinosad and 1 mM acetylcholine compared to 1 mM acetylcholine + 10 µM spinosad. 3 min wash between applications.

Imidacloprid (a prototypical N-nitroguanidine neonicotinoid) and thiacloprid (a prototypical N-cyanoamidine neonicotinoid) (Millar and Denholm, 2007) did not have any agonistic activities on *X. laevis* oocytes expressing the *A. mellifera* α5 subunit at 100 µM (Figure 5.9), despite responses being recorded when 10 µM or lower concentrations were applied to other *A. mellifera* nAChRs consisting of α1, α2, α8 and β1 subunits (Ihara *et al.*, 2020). They did, however, act as antagonists when 100 µM was coapplied with 2 mM acetylcholine (Figure 5.9) with imidacloprid reducing the response to 57.4 ± 2.4% (n = 3 oocytes, N = 3 frogs) and thiacloprid to 58.6 ± 2.6% (n = 3, N = 3) of the response when compared to 2 mM acetylcholine alone. Using imidacloprid, it was shown that this inhibition was dose dependent (Figure 5.9

(A)) with 10 µM coapplication reducing the response to 76.3 ± 2.3% (n = 3, N = 3) whereas 1 µM coapplication appeared to slightly positively modulate the response as was 107.3% ± 1.5% (n = 3, N = 3).

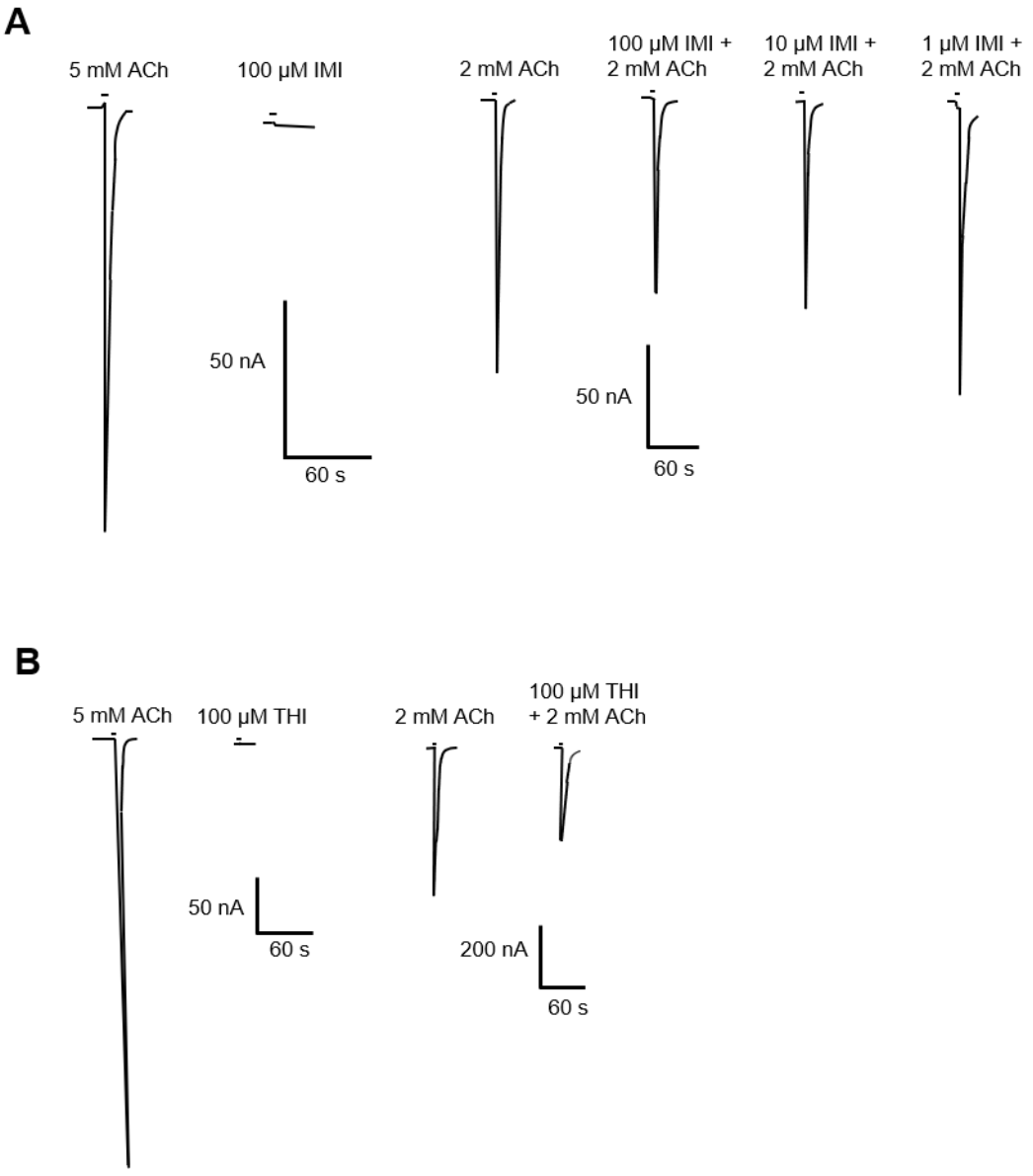

Figure 5.9 Traces of effects of neonicotinoids on A. mellifera α5 subunit expressed in X. laevis oocytes. A. Imidacloprid (IMI) showed no agonist actions when 100 µM was applied 3 min after 5 mM acetylcholine (ACh). Imidacloprid showed antagonistic actions when coapplied with 2 mM acetylcholine (EC_{50} concentration) in a dose dependent manner. B. Thiacloprid (THI) showed no agonist actions when 100 µM was applied 3 min after 5 mM acetylcholine. Thiacloprid showed antagonistic actions when 100 µM was coapplied with 2 mM acetylcholine.

Nicotine acts as an agonist on *A. mellifera* α5 expressed in *X. laevis* oocytes (Figure 5.10), the response is concentration dependent but requires high (mM) concentrations of nicotine so an EC_{50} was not calculated.

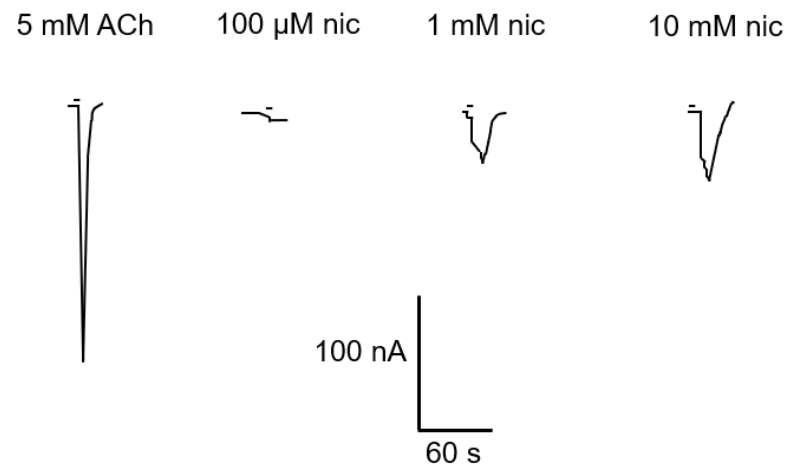

Figure 5.10 Current traces showing responses to high concentrations of nicotine (nic) applied 3 min after 5 mM acetylcholine (ACh) from X. laevis oocytes expressing the A. mellifera α5 nAChR subunit.

To identify if the *A. mellifera* α5 nAChR is sensitive to α-bungarotoxin *X. laevis* oocytes were pre-incubated with 0.1 µM α-bungarotoxin for 3 min 20 s before co-application of 2 mM acetylcholine with 0.1 µM α-bungarotoxin. This nearly completely inhibited the response (Figure 5.11). After washing for over 26 min, the response to 2 mM acetylcholine was restored. So, in common with some other insect nAChRs (from *D. melanogaster*, *A. mellifera* and *S. gregaria*) (Lansdell *et al.*, 2012; Hawkins, Mitchell and Jones, 2022; Marshall *et al.*, 1990) the *A. mellifera* α5 nAChR is α-bungarotoxin sensitive.

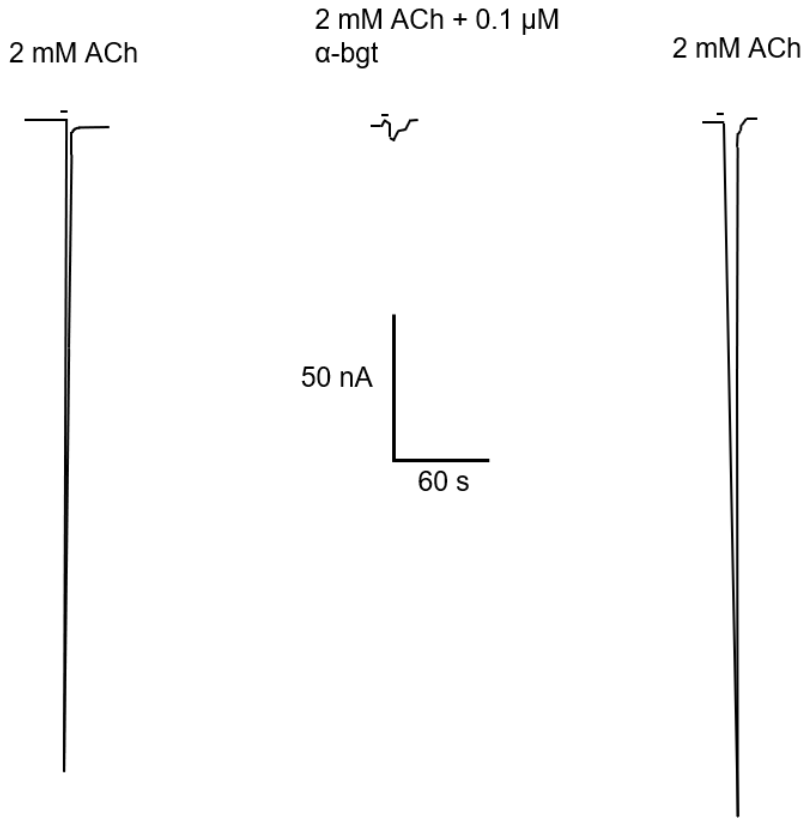

Figure 5.11 Representative traces showing responses from X. laevis oocytes expressing the A. mellifera α5 nAChR subunit to 2 mM acetylcholine (ACh) (EC_{50} concentration), 2 mM acetylcholine coapplied with 0.1 µM α-bungarotoxin (α-bgt) after 3 min 20s incubation with 0.1 µM α-bungarotoxin, normal response to 2 mM acetylcholine restored after 26 min washing with SOS.

5.4 Discussion

5.4.1 The Non-Dipteran α5 Subunits are a Phylogenetically Distinct Group from Other Insect Nicotinic Acetylcholine Receptor Subunits.

Originally the *A. mellifera* α5 nAChR subunit was grouped with the α6 and α7 subunits, as well as other α5 subunits as part of a larger group including the vertebrate α7 and α8 subunits (Jones *et al.*, 2010; Jones and Sattelle, 2010). Our phylogenetic analysis shows the *A. mellifera* α5 subunit is in a separate monophyletic group, along with α5 subunits from Blatteria (*P. americana*), Coleoptera (*T. castaneum*), Lepidoptera (*B. mori*) and other Hymenoptera (*B. terrestris*) but not the α5 subunit from Diptera (*D. melanogaster* and *A. gambiae*) (Figure 5.1), in agreement with other previous analysis (Cartereau *et al.*, 2020). This is further underlined

by the presence of exon boundaries in common between α6, α7 and Dipteran α5 subunits that are not shared by non-Dipteran α5 subunits (Figure 5.3). It appears that the Dipteran α5 subunit arises from a gene duplication of the α7 subunit (Figure 5.2), whereas the non-Dipteran α5 subunits arose from a separate event. Interestingly, aphids do not possess an α5 subunit, leading to the suggestion that the α5 subunit is the last of the core subunits to have evolved (Dale *et al.*, 2010). Our phylogenetic analysis suggests that the α5 subunit arose differently in the Dipteran and non-Dipteran lineages of insects more recently evolved than aphids.

5.4.2 The Properties of the *A. mellifera* α5 as a Homomeric Nicotinic Acetylcholine Receptor

The sequence of the *A. mellifera* α5 subunit unit has all the predicted features associated with an α nAChR subunit: four transmembrane helices, a large extracellular domain, a cys-loop and two adjacent cysteines in loop C considered important for acetylcholine binding (Jones *et al.*, 2006; Jones and Sattelle, 2010; Corringer, Novère and Changeux, 2000). So it was expected that if it could be expressed it would have pharmacological characteristics similar to other nAChRs (Dale, 1914). The *A. mellifera* α5 sequence contains the GEK motif just before the second transmembrane domain, which is important for cation selectivity and thus is assumed to be a cation channel (Corringer, Novère and Changeux, 2000; Jensen, Schousboe and Ahring, 2005).

When expressed in *X. laevis* oocytes the *A. mellifera* α5 nAChR does respond to acetylcholine (Figure 5.4) but with a much lower affinity than other homomeric insect nAChRs (Lansdell *et al.*, 2012; Hawkins, Mitchell and Jones, 2022; Brunello *et al.*, 2022) and heteromeric insect nAChRs (Lansdell *et al.*, 2012; Ihara *et al.*, 2020) as shown by a considerably higher EC_{50}. None of these receptors were from the same monophyletic group as the *A. mellifera* α5, so it remains to be seen if other non-Dipteran α5 nAChR have a similar affinity for acetylcholine. A hybrid receptor of *L. migratoria* α5 and rat β2 had an EC_{50} (335 μM) that was lower than the *A. mellifera* α5 nAChR but higher than other non-hybrid nAChRs (Zhang *et al.*, 2017). However, expression of the *A. mellifera* α5 was much more consistent and robust than for other insect nAChRs (Lansdell *et al.*, 2012; Hawkins, Mitchell and Jones, 2022; Cartereau *et al.*, 2020; Brunello *et al.*, 2022), without the need for chaperone proteins to achieve expression.

Co-expression of the *A. mellifera* α5 subunit with various combinations of *A. mellifera* subunits did not produce nAChRs with a significantly different EC_{50} for acetylcholine indicating that the subunits that were tested were not assembling with the α5 subunit to generate receptors with altered acetylcholine sensitivity. This included combinations that are co-localised with the α5 subunit in honeybees; the α2 and α7 subunits with the α5 subunit are found in the outer compact Kenyon cells, antennal lobes and dorsal lobes among other regions at the same stages of development (Thany *et al.*, 2005). Several combinations did not produce any expression at all. We did not try expressing with the rat β2 subunit, which produced successful expression with the *L. migratoria* α5 subunit (Zhang *et al.*, 2017). It was also seen that rat RIC-3 made no difference to the expression of the *P. americana* α7 nAChR (Cartereau *et al.*, 2020). It may be a particular combination of subunits and chaperones is required to achieve expression of an *A. mellifera* nAChR with a higher affinity for acetylcholine containing the α5 subunit, as chaperones can have differential effects on different subunit combinations (Matta *et al.*, 2017; Halevi *et al.*, 2003; Ben-Ami *et al.*, 2005).

In order to investigate the possible causes of the low acetylcholine affinity of the *A. mellifera* α5 nAChR the scientific literature was searched for any amino acids involved in agonist binding in nAChRs (Table 5.2). The *A. mellifera* α5 has almost all the amino acids thought to be important for agonist binding, including the YXCC motif in loop C (Table 5.2). The few labelled amino acids not possessed by *A. mellifera* α5 were mostly from the γ subunit in *Torpedo californica*. Therefore, there is no obvious mechanism for the low affinity for acetylcholine at the single amino acid level.

Table 5.2 Table of Amino Acids Important for Agonist Binding in nAChRs, Method of Identification and if the Amino Acid is Present in A. mellifera α5. Amino acid numbers refers to an amino acid sequence alignment of all the sequences constructed using ClustalW (Kumar et al., 2018).

nAChR	**Species**	**ACh binding Amino acids**	**Method**	**Reference**	**In Amel α5**
α7	chicken	L118	Model AChBP	(Amiri *et al.*, 2008)	Yes (155)
AChBP	*Aplysia californica*	Y195	Photoaffinity labelling	(Tomizawa *et al.*, 2007)	Yes (246)
AChBP	*A. californica*	M116	Photoaffinity labelling	(Tomizawa *et al.*, 2007)	No V (153)
α4	chicken	Y225	Photoaffinity labelling	(Tomizawa *et al.*, 2007)	Yes (246)
$(\alpha1)_2\beta1\gamma\delta$	*T. californica*	αY198	Photoaffinity labelling APFBzCho	(Nirthanan *et al.*, 2005)	Yes (246)
$(\alpha1)_2\beta1\gamma\delta$	*T. californica*	γL109/δL111	Photoaffinity labelling APFBzCho	(Nirthanan *et al.*, 2005)	No I (145)
$(\alpha1)_2\beta1\gamma\delta$	*T. californica*	γY111	Photoaffinity labelling APFBzCho	(Nirthanan *et al.*, 2005)	No S (147)
$(\alpha1)_2\beta1\gamma\delta$	*T. californica*	γY117	Photoaffinity labelling APFBzCho	(Nirthanan *et al.*, 2005)	No V (153)
$(\alpha4)_3(\beta2)_2$	human	αW156	X-ray crystallography structure nicotine	(Morales-Perez, Noviello and Hibbs, 2016)	Yes (185)
$(\alpha1)_2\beta1\gamma\delta$	human	αW149	Trp derivatives, cation-π modelling	(Zhong *et al.*, 1998)	Yes (185)
$(\alpha1)_2\beta1\gamma\delta$	*T. californica*	αC192 and αC193	[^{3}H]Bromoacetyl-choline, reducing label	(Dunn, Conti-Tronconi and Raftery, 1993)	Yes (240-241)

$(\alpha1)_2\beta1\gamma\delta$	*T. californica*	αY93	[^{3}H]ACh mustard	(Cohen, Sharp and Liu, 1991)	Yes (128)
$(\alpha1)_2\beta1\gamma\delta$	*T. californica*	γW55	[^{3}H]nicotine photoaffinity labelling	(Chiara, Middleton and Cohen, 1998)	Yes (90)
$(\alpha1)_2\beta1\gamma\delta$	*T. californica*	αY198	[^{3}H]nicotine photoaffinity labelling	(Middleton and Cohen, 1991)	Yes (246)
$(\alpha1)_2\beta1\gamma\delta$	*T. californica*	αY190	[^{3}H]*d*-Tubocurarine photoaffinity labelling	(Chiara and Cohen, 1997)	Yes (238)
$(\alpha1)_2\beta1\gamma\delta$	*T. californica*	γW55/δW57	[^{3}H]*d*-Tubocurarine photoaffinity labelling	(Chiara and Cohen, 1997)	Yes (90)
$(\alpha1)_2\beta1\gamma\delta$	mouse	αD152	point mutation carbCh binding	(Osaka, Sugiyama and Taylor, 1998)	Yes (188)
$(\alpha1)_2\beta1\gamma\delta$	mouse	αD200	point mutation carbCh binding	(Osaka, Sugiyama and Taylor, 1998)	Yes (248)
$(\alpha1)_2\beta1\gamma\delta$	mouse	γD174/ δD180	point mutation carbCh binding	(Osaka, Sugiyama and Taylor, 1998)	Yes (214)
$(\alpha1)_2\beta1\gamma\delta$	mouse	αY93	point mutation carbCh binding	(Sine *et al.*, 1994)	Yes (128)
$(\alpha1)_2\beta1\gamma\delta$	mouse	αY190	point mutation carbCh binding	(Sine *et al.*, 1994)	Yes (238)
$(\alpha1)_2\beta1\gamma\delta$	mouse	αY198	point mutation carbCh binding	(Sine *et al.*, 1994)	Yes (246)

α7	chicken	Y92	point mutation ACh action	(Galzi *et al.*, 1991)	Yes (128)
α7	chicken	Y187	point mutation ACh action	(Galzi *et al.*, 1991)	Yes (238)
α7	chicken	W148	point mutation ACh	(Galzi *et al.*, 1991)	Yes (185)
$(\alpha 1)_2\beta 1\gamma\delta$	human	αG153	slow-channel congenital myasthenic syndrome	(Croxen *et al.*, 1997)	Yes (189)
α7	chicken	W54	point mutation ACh binding and action	(Corringer *et al.*, 1995)	Yes (90)

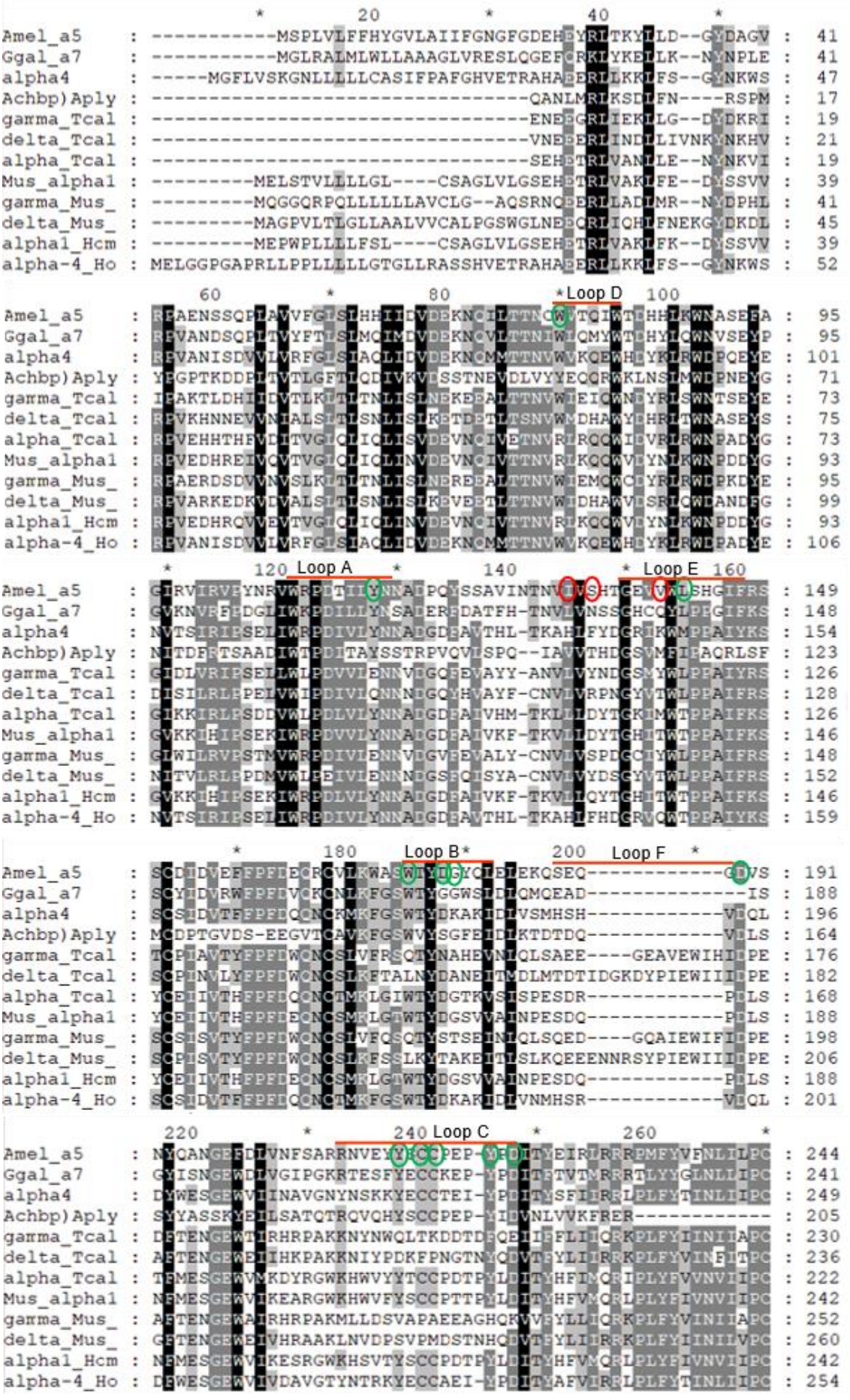
Loop D
Loop A
Loop E
Loop B
Loop F
Loop C

Figure 5.12 An alignment showing the N-terminal domain (where acetylcholine binding occurs) for the A. mellifera nAChR α5 subunit and subunits from Table 2: the α7 subunit from chicken, the α4 subunit from chicken, AChBP from A. californica, γ subunit from T. californica, δ subunit from T. californica, α subunit from T. californica, α1 subunit from mouse, γ subunit from mouse, δ subunit from mouse, α1 subunit from human, α4 subunit from human. Aligned using ClustalW Identical amino acids in A. mellifera α5 from Table 2 are circled in green whilst non-matching amino acids are circled in red. Binding loops are indicated by an orange line.

As expected for nAChRs (Dale, 1914), atropine did not completely ablate the response of the *A. mellifera* α5 nAChR (Figure 5.5) and thus the response to acetylcholine is not due to endogenous mAChRs in the oocytes (Zwart and Vijverberg, 1997) but rather to the expression of the α5 nAChR. Atropine did inhibit the response by 31.6%, comparable to the 46.7% inhibition of the rat α7 nAChR (Zwart and Vijverberg, 1997). In contrast, the *A. mellifera* α6 nAChR was not inhibited by atropine at all (Hawkins, Mitchell and Jones, 2022). In some experiments (Lansdell *et al.*, 2012) the effects of atropine were not studied. Other experiments (Cartereau *et al.*, 2020; Cartereau *et al.*, 2021; Ihara *et al.*, 2020) were carried out in 0.5 µM atropine so the response was not ablated by atropine but there is no numerical data on its effects.

Choline was found to be a full agonist on the *A. mellifera* α5 nAChR expressed in *X. laevis* oocytes, as it is on the human α7 (Papke, Bencherif and Lippiello, 1996; Mandelzys, De Koninck and Cooper, 1995; Alkondon *et al.*, 1997; Thomsen *et al.*, 2015). The EC_{50} for choline (9.07 (4.48-18.4) mM) is 3.42 fold larger than the EC_{50} for acetylcholine (2.65 (2.41-2.93) mM), in common with the human α7 (Thomsen *et al.*, 2015) the EC_{50} for choline (972 (888-1064) µM) is also higher than the EC_{50} for acetylcholine (113 (78-163) µM) but by a much larger ratio (8.60). This is in contrast to the DEG-3 subfamily in *C. elegans*, which all have a higher affinity for choline over acetylcholine when expressed in *X. laevis* oocytes (Treinin and Jin, 2021) including the DEG-3/DES-2 receptor in *C. elegans* in which choline (EC_{50} 1.8 ± 0.7 mM) acts as a superagonist compared to acetylcholine (EC_{50} 2.9 ± 0.5 mM) and the EC_{50} ratio is 0.621 (Yassin *et al.*, 2001). With EC_{50}s in the mM range, it is likely that neither acetylcholine nor choline is the endogenous ligand of the *A. mellifera* α5 nAChR, assuming that the receptor is homomeric *in vivo*.

Nicotine acts as an agonist on the *A. mellifera* nAChR in a concentration-dependent manner (Figure 5.10), as is expected for a nAChR (Dale, 1914). High concentrations of nicotine (10 mM) were not able to produce the same response as the maximal response to acetylcholine, in contrast to what was found for *P. americana* α7 nAChR (Cartereau *et al.*, 2020), where the acetylcholine response was too small to measure the affinity but the response to nicotine was much larger (EC_{50} 790 µM). The nAChR composed of the *D. melanogaster* α5 and α6 subunits

responded to 1 mM nicotine, as with the *A. mellifera* α5 nAChR (Watson *et al.*, 2010). The response to nicotine was not tested for *D. melanogaster* α5 and α7 homomeric nAChRs or the heteromeric nAChR composed of α5, α6 and α7 subunits (Lansdell *et al.*, 2012), nAChRs consisting of combinations of α1, α2, β1 and β2/α8 subunits from *D. melanogaster*, *A. mellifera* and *B. terrestris* (Ihara *et al.*, 2020) or for *A. mellifera* α6 nAChR (Hawkins, Mitchell and Jones, 2022).

α-bungarotoxin has long been used to investigate nAChRs (Changeux, 2012). It is known that insects have α-bungarotoxin sensitive and insensitive nAChRs (Courjaret and Lapied 2001; Buckingham *et al.*, 1997; Lansdell and Millar, 2000b; Dacher, Lagarrigue and Gauthier, 2005). However, it does not appear that this sensitivity is consistent between orthologous nAChRs in different species as in (Lansdell *et al.*, 2012) the α7 nAChR from *D. melanogaster* was completely inhibited by 0.1 μM α-bungarotoxin but in (Cartereau *et al.*, 2020) the (nicotine-induced) current from the *P. americana* α7 nAChR was not inhibited by 10 μM α-bungarotoxin. The homomeric vertebrate α7 is inhibited by α-bungarotoxin (Peng *et al.*, 1994). In common with *D. melanogaster* homomeric α5 and α7 nAChRs and the heteromeric α5, α6 and α7 nAChR (Lansdell *et al.*, 2012) and the *A. mellifera* α6 nAChR (Hawkins, Mitchell and Jones, 2022), the *A. mellifera* α5 nAChR was almost completely inhibited by 0.1 μM α-bungarotoxin. Recovery of *A. mellifera* α5 after α-bungarotoxin application took over 25 min, which is slower than for the *D. melanogaster* α5 nAChR, which took about 15 min to recover (Lansdell *et al.*, 2012) and for the *A. mellifera* α6 nAChR, which took 10 min (Hawkins, Mitchell and Jones, 2022). In *A. mellifera* α-bungarotoxin impairs long-term memory after multi-trial learning but not the memory retrieval or acquisition impaired by mecamylamine (MLA), a broad-spectrum nAChR antagonist, indicating both α-bungarotoxin sensitive and insensitive nAChRs have a role in memory (Dacher, Lagarrigue and Gauthier, 2005). It appears both the *A. mellifera* α5 and α6 homomeric nAChRs are α-bungarotoxin sensitive with a possible role in long-term memory but not memory retrieval or acquisition (Dacher, Lagarrigue and Gauthier, 2005; Hawkins, Mitchell and Jones, 2022). Other papers expressing insect nAChRs in *X. laevis* oocytes studying combinations of α1, α2, β1 and β2/α8 from *D. melanogaster*, *A. mellifera* and *B. terrestris* did not investigate α-bungarotoxin activity (Ihara *et al.*, 2020).

5.4.3 The Interactions of the A. mellifera α5 nAChR with Insecticides

Spinosad does not appear to act on the *A. mellifera* α5 nAChR (Figure 5.8), with neither agonistic nor antagonistic effects. This agrees with previous research which only identified the α6 subunit as a spinosad target through rescue of spinosad sensitivity in resistant strains by introduction of the α6 subunit or α6 chimeras (Perry *et al.*, 2015; Somers *et al.*, 2015). Thus various species have developed resistance either by mutations in the binding site of α6 (Puinean *et al.*, 2012; Hiruta *et al.*, 2018; Ureña *et al.*, 2019; Silva *et al.*, 2016) or by producing non-functional α6 subunits, as this subunit appears to be redundant (Berger *et al.*, 2016; Wan *et al.*, 2018). Knockouts of the α6 subunit in *D. melanogaster* are also resistant to spinosad (Lu *et al.*, 2022; Perry *et al.*, 2021). Heterologous expression of the α6 homomeric nAChR (Hawkins, Mitchell and Jones, 2022) or heteromeric nAChR containing α6 (Watson *et al.*, 2010) responded to spinosad as an agonist and it also acted as a modulator of the acetylcholine response (Hawkins, Mitchell and Jones, 2022).

Neither imidacloprid nor thiacloprid acted as agonists on *A. mellifera* α5 (Figure 5.9). This is not surprising as neonicotinoids are used to target many pests that do not have a non-Dipteran α5 subunit (such as aphids) (Millar and Denholm, 2007; Casida, 2018). They have been shown to act on nAChRs containing α1, α2, α3, β1 and β2/α8 combinations from expression studies (Ihara *et al.*, 2020; Rufener *et al.*, 2020) and knockout studies (Lu *et al.*, 2022; Perry *et al.*, 2021). The neonicotinoids did have a concentration-dependent inhibitory effect but at much higher concentrations than agonistic effects found in other studies (Ihara *et al.*, 2020; Rufener *et al.*, 2020) in the nM range. Thus, at high concentrations neonicotinoids can inhibit the nAChR as has been found for other nAChRs (Crossthwaite *et al.*, 2017) but whether the mechanism is competition for the active site or channel block is unclear. There appears to be no difference in activity between a N-nitroguanidine neonicotinoid (imidacloprid) and a N-cyanoamidine neonicotinoid (thiacloprid). Bees are more sensitive to N-nitroguanidine neonicotinoids (Casida, 2018) but this appears to be due to metabolic not target site effects (Manjon *et al.*, 2018). The interactions with neonicotinoids of the *A. mellifera* α5 nAChR partially matches what was found for the *P. americana* α7 nAChR (Cartereau *et al.*, 2021), where imidacloprid also had no agonist actions but thiacloprid acted as a partial agonist. Thiacloprid acted similarly as an antagonist (with nicotine), however imidacloprid acted as a positive modulator (with nicotine) (Cartereau *et al.*, 2021), unlike the *A. mellifera* α5 nAChR.

5.5 Conclusion

This is the first robust heterologous expression of an insect nAChR without chaperone proteins. The low sensitivity of this nAChR to acetylcholine and choline suggests that non-Dipteran α5 nAChR subunits have unusual pharmacological properties and that it may respond to another ligand *in vivo*. Therefore, we will test other known insect neurotransmitters on the *A. mellifera* α5 nAChR expressed in *X. laevis* oocytes.

Chapter 6 The Functional Characterisation of the *Apis mellifera* α5 nAChR with Biogenic Amines and Other Neurotransmitters

6.1 Introduction

The *A. mellifera* α5 nAChR expressed in *X. laevis* oocytes responded to acetylcholine but with a low affinity compared to other nAChRs (Chapter 5). Thus, we decided to test whether other possible neurotransmitters, such as biogenic amines (5-HT, dopamine, octopamine, tyramine and histamine), act as more potent agonists. It has been assumed that the effects of these biogenic amines in insects are mediated through GPCRs and histamine-gated chloride ion channels (Roeder, 1994; Kita *et al.*, 2017). The response of the *A. mellifera* α5 nAChR to 5-HT has been published (Mitchell *et al.*, 2022).

6.1.1 Cys-loop Ligand Gated Ion Channels Activated by Other Biogenic Amines

Vertebrates have a cationic cys-LGIC that responds to 5-HT, the 5-HT_{3A}R, that is closely related to nAChRs (Chapter 5, Figure 5.1), which can also respond to dopamine but at a much lower affinity (EC_{50}s for 5-HT in the range 123 nM-1.8 µM for mammals and EC_{50} for dopamine 135 µM in humans) (Thompson and Lummis, 2006). A hybrid receptor can also be formed between 5-HT_{3A}R subunits and nAChR α4 subunits that also responds to 5-HT and dopamine, with a very small response to cytisine (van Hooft *et al.*, 1998). Compared to insects and vertebrates, the nematode, *C. elegans* has a considerably extended cys-LGIC family responding to a diverse array of ligands (Jones and Sattelle, 2008). As mentioned in Chapter 5, all the nAChRs in the *C. elegans* DEG-3 subfamily have a higher efficacy and affinity for choline than acetylcholine (Treinin and Jin, 2021). In addition to this the ACR-23 member of this subfamily, which forms a homomeric receptor, responds to betaine (trimethylglycine), a metabolite from the pathway converting choline to glycine, also available from the diet, with a much higher affinity and efficacy than choline (Rufener *et al.*, 2013; Peden *et al.*, 2013). There are multiple anion channels gated by biogenic amines in *C. elegans* (Table 6.1) with receptors found that are gated by acetylcholine, 5-HT, dopamine and tyramine (Rodriguez Araujo *et al.*, 2022; Ringstad,

Abe and Horvitz, 2009; Morud *et al.*, 2021). GABA, histamine and glutamate, which act on anion channels, are considered typical inhibitory neurotransmitters in insects (Osborne, 1996). As shown in Table 6.1, many cys-LGICs respond to neurotransmitters other than their primary neurotransmitter, albeit at often a much lower affinity and efficacy. In particular, one of the histamine-gated chloride channels (HisClB) from *Musca domestica* responds to choline, 5-HT, tyramine, octopamine, dopamine and noradrenaline in addition to histamine (Kita *et al.*, 2017). Most characterised receptors have an EC_{50} for their primary agonist between about 100 nM-10 µM (see Chapter 1, Table 1.1) (Kita *et al.*, 2017; Thompson and Lummis, 2006; Ringstad, Abe and Horvitz, 2009; Morud *et al.*, 2021) but the relevance of an EC_{50} *in vivo* depends on the synaptic concentration of a neurotransmitter which is difficult to measure. Thus, to search for the possible primary agonist of the *A. mellifera* α5 nAChR we tested all the neurotransmitters used in an attempt to deorphanise a cys-loop chloride ion channel in insects (Feingold *et al.*, 2019) (GABA, glutamate, glycine, histamine, dopamine, tyramine and octopamine) plus 5-HT due to the reasonably close relationship of vertebrate 5-HT_3R subunits and non-Dipteran α5 nAChR subunits (Figure 5.1). We decided not to test noradrenaline and betaine as there is not good evidence they act as neurotransmitters in insects (Osborne, 1996).

There is evidence of a dopamine activated cationic ligand-gated ion channel in snail neurons (Green and Cottrell, 1996). This has an EC_{50} of 15 µM for dopamine and is inhibited by d-tubocurarine, strychnine, apomorphine, sulpiride and spiperone (Green and Cottrell, 1996). These experiments however, were carried out on whole neurons and so there is no information on the subunit composition of these channels (Green and Cottrell, 1996).

Table 6.1 A summary of cys-loop ligand gated ion channels gated by biogenic amines or with multiple neurotransmitter agonists.

Receptor	**Species**	**Primary Agonist**	**Other Agonists**	**Ion Permeability**	**Reference**
5-HT_{3A}R	Human, vertebrates	5-HT	dopamine	Na^+	(Thompson and Lummis, 2006)
5-HT_{3A}R-α4 hybrid	Human	5-HT	dopamine, cytisine	Na^+, Ca^{2+}	(van Hooft *et al.*, 1998)

muscle nAChR	Human	acetylcholine	GABA	Na^+	(Dionisio *et al.*, 2015)
HisClB	*M. domestica*	histamine	choline, 5-HT, tyramine, octopamine, dopamine, noradrenaline	Cl^-	(Kita *et al.*, 2017)
$GABA_AR$	Human	GABA	histamine	Cl^-	(Saras *et al.*, 2008)
MOD-1	*C. elegans*	5-HT	tryptamine	Cl^-	(Rodriguez Araujo *et al.*, 2022)
DEG-3/ DES-2	*C. elegans*	choline	acetylcholine	Na^+	(Yassin *et al.*, 2001)
ACR-23	*C. elegans*	betaine	choline, acetylcholine	Na^+	(Rufener *et al.*, 2013; Peden *et al.*, 2013)
LGC-53	*C. elegans*	dopamine		Cl^-	(Ringstad, Abe and Horvitz, 2009)
LGC-55	*C. elegans*	tyramine		Cl^-	(Ringstad, Abe and Horvitz, 2009)
LGC-40	*C. elegans*	choline	acetylcholine, 5-HT	Cl^-	(Ringstad, Abe and Horvitz, 2009)

LGC-52	*C. elegans*	dopamine	tyramine	Cl^-	(Morud *et al.*, 2021)
LGC-54	*C. elegans*	dopamine, tyramine	5-HT	Cl^-	(Morud *et al.*, 2021)
LGC-56	*C. elegans*	tyramine	dopamine	Cl^-	(Morud *et al.*, 2021)
LGC-50	*C. elegans*	5-HT		Cl^-	(Morud *et al.*, 2021)
LGC-52/ LGC-51	*C. elegans*	dopamine	tyramine	Cl^-	(Morud *et al.*, 2021)

6.1.2 Biogenic Amines in the Honeybee Brain

Acetylcholine, 5-HT, dopamine, octopamine, tyramine and histamine are all found in the central nervous system of the honeybee (Osborne, 1996; Bicker, 1999; Roeder, 1994; Mercer *et al.*, 1983). Earlier studies relied on histofluorescence to locate biogenic amines (Mercer *et al.*, 1983) but this cannot detect the non-fluorogenic amines; octopamine, tyramine and histamine. Later studies used immunoreactivity techniques that can detect all of the amines (Bicker, 1999; Schäfer and Rehder, 1989). HPLC has also been used to quantify the concentration of biogenic amines in specific honeybee brain regions (Mercer *et al.*, 1983). 5-HT was found in distinct clusters of neurons across the optic lobes, suboesophageal ganglia and mushroom bodies as well as connecting various brain regions, similar to other insects (Bicker, 1999; Mercer *et al.*, 1983). Dopamine was found in all the central brain and suboesophageal ganglia, including neurons of extrinsic origins in the mushroom bodies but not in the Kenyon cells (Bicker, 1999; Schäfer and Rehder, 1989). Dopamine was not found in neurons that process visual or olfactory information (Schäfer and Rehder, 1989). Immunoreactive neurons were not found in the optic lobes even though dopamine was isolated by HPLC from the optic lobes (Bicker, 1999; Mercer *et al.*, 1983; Schäfer and Rehder, 1989). Histamine is thought to be involved in the depolarising insect photoreceptors and, in *A. mellifera*, was found in five groups made up of 150 cell bodies, in areas including the optical

ganglia, central brain and the antennal lobes but not the mushroom bodies (Bicker, 1999). Octopamine was found in five groups of neurons, which was made up of about 100 cell bodies, in all the brain and suboesophageal ganglia, except the pedunculi of the mushroom bodies and some parts of the α and β lobes (Bicker, 1999). There has been less research on the location of tyramine as it was the last to be considered a neurotransmitter and is a precursor to octopamine so it is difficult to distinguish between octoapaminergic and tyraminergic neurons (Osborne, 1996; Roeder, 1994). However, it has become clear that tyramine has distinct effects from octopamine, including in the honeybee with opposing actions in vision (Roeder, 1994; Schilcher *et al.*, 2021) and there is a relatively high concentration of tyramine in insect brains (Roeder, 1994).

The *A. mellifera* α5 subunit (originally referred to as Apis α7-2) was located by *in situ* hybridisation to the dorsal lobes, optic lobes, mushroom bodies (outer compact Kenyon cells) and antennal lobes (Thany *et al.*, 2005). This overlaps largely with the locations of 5-HT, dopamine and octopamine found in the honeybee brain, although dopamine was not found in the Kenyon cells (Bicker, 1999; Schäfer and Rehder, 1989; Mercer *et al.*, 1983).

6.1.3 Biogenic Amines and Honeybee Behaviour

Biogenic amines have various diverse effects on honeybee behaviour, some examples of which are given below. There were two main techniques used to study behaviour and some studies used a combination of both; applying biogenic amines or antagonists and observing the outcomes on specific behaviours (Schilcher *et al.*, 2021; Linn *et al.*, 2020; Cook, Brent and Breed, 2017; Klappenbach, Kaczer and Locatelli, 2013; Agarwal *et al.*, 2011; Raza *et al.*, 2022; Arenas *et al.*, 2021; Hewlett *et al.*, 2018) or measuring a correlation between different behaviours and biogenic amine concentration (Huang *et al.*, 2022; Cook, Brent and Breed, 2017; Raza *et al.*, 2022; Arenas *et al.*, 2021; Mancini *et al.*, 2018; Hewlett *et al.*, 2018). However, these effects were assumed to be mediated by GPCRs and various studies of biogenic amine function used agonists or antagonists for specific GPCRs or measured specific GPCR expression, so the results of these experiments are likely to be due to the action of biogenic amines on GPCRs (Huang *et al.*, 2022; Klappenbach, Kaczer and Locatelli, 2013; Agarwal *et al.*, 2011; Mancini *et al.*, 2018; Hewlett *et al.*, 2018; Arenas *et al.*, 2021; Raza *et al.*, 2022).

6.1.3.1 Dopamine

Transient dopamine signalling is associated with wanting in honeybees, the equivalent of the mesolimbic dopamine system in mammals (Huang *et al.*, 2022). Dopamine levels increase during waggle dance initiation and starvation and the dopamine antagonist, fluphenazine, decreases foraging frequency (Huang *et al.*, 2022). The external application of dopamine also increases the initial waggle dance following (Linn *et al.*, 2020). Exposure to queen mandible pheromone decreases dopamine levels, this leads to downstream effects that prevent the production of new queens (Beggs *et al.*, 2007). Consumption of tyrosine in royal jelly increases dopamine and tyramine levels, this promotes the development of reproductive workers (Matsuyama, Nagao and Sasaki, 2015). There are mixed results for the effect of dopamine on appetitive (desire to meet bodily needs) learning and memory; it appears to improve learning and short-term memory (Raza *et al.*, 2022; Mancini *et al.*, 2018) but impair long-term memory (Klappenbach, Kaczer and Locatelli, 2013). Increased dopamine is associated with improved aversive (avoidance) learning (Agarwal *et al.*, 2011; Beggs *et al.*, 2007; Vergoz, Schreurs and Mercer, 2007). Higher concentrations of dopamine, octopamine and 5-HT are found in more social hive-kept bees than isolated bees and dopamine increases sociability (Hewlett *et al.*, 2018; Tsvetkov, Cook and Zayed, 2019). Lower dopamine levels associated with bees kept in smaller groups are correlated with decreased discrimination learning (Tsvetkov, Cook and Zayed, 2019). Increased dopamine levels are associated with a decreased threshold for defensive actions in response to alarm pheromones (Rittschof *et al.*, 2019; Nouvian *et al.*, 2018).

6.1.3.2 Octopamine and Tyramine

Octopamine and tyramine have functionally similar effects in *A. mellifera* by decreasing fanning behaviour (Cook, Brent and Breed, 2017), although it is difficult to distinguish the effect of tyramine as an octopamine precursor from the effect of tyramine itself and tyramine concentrations in the brain can be too low to measure (Braun and Bicker, 1992; Hewlett *et al.*, 2018). However, octopamine and tyramine have opposing action in honeybee vision, with octopamine decreasing the time taken to travel to a light and tyramine increasing the time

(Schilcher *et al.*, 2021). Thus, despite the fact that tyramine is a precursor to octopamine they can have different effects and presumably there must be different receptors that can sufficiently distinguish between the two. Octopamine seems to have a role in some decisions with honeybees given octopamine less likely to follow waggle dances and more likely to return to previously profitable resources and more likely to forage for pollen rather than nectar (Linn *et al.*, 2020; Arenas *et al.*, 2021). Octopamine slows aversive learning (Agarwal *et al.*, 2011) but increases appetitive learning and retention (Mancini *et al.*, 2018). Although more sociable hive-kept bees have higher concentrations of octopamine, injected octopamine decreases social interactions (Hewlett *et al.*, 2018).

6.1.3.3 5-HT

Enhancing or inhibiting 5-HT signalling impairs vision in honeybees so it is difficult to study the role of 5-HT in visual learning (Mancini *et al.*, 2018). Increased 5-HT is correlated with optimal appetitive learning and sociability and increased social interactions (Raza *et al.*, 2022; Hewlett *et al.*, 2018). 5-HT levels are higher in defensive colonies and increased 5-HT levels are associated with a decreased threshold for defensive actions in response to alarm pheromones, to a greater extent than dopamine (Nouvian *et al.*, 2018).

6.2 Chapter Aim

The aim of this chapter is to test the responses of the *A. mellifera* α5 nAChR expressed in *X. laevis* oocytes to insect neurotransmitters other than acetylcholine and related compounds, in particular biogenic amines.

6.3 Results

6.3.1 Response of the *A. mellifera* α5 nAChR to 5-HT

Due to the low affinity of acetylcholine, it was decided to test other neurotransmitters on the *A. mellifera* α5 nAChR expressed in *X. laevis* oocytes. 5-HT was the first candidate tried as the 5-HT_3 receptors in vertebrates are closely related to nAChRs (see Chapter 5 Figure 5.1) (Jones and Sattelle, 2010). The *A. mellifera* α5 nAChR responded to 5-HT in a concentration dependent manner (Figure 6.1 (A)). No response was observed in oocytes injected with water only, demonstrating that the currents are dependent upon the presence of the α5 nAChR subunit. 5-HT had an EC_{50} of 122 (111-134) µM (n = 7, N = 5) (Figure 6.1 (B)) and the mean maximum current response (at 1 mM) was 238 ± 24.0% (n = 18, N = 8) (± 95% confidence limits calculated using two-tailed t tests, for all the relative current responses in this chapter) of the maximum acetylcholine response (at 5 mM) (Figure 6.1 (C)). Thus 5-HT has a higher affinity and efficacy than acetylcholine for the *A. mellifera* α5 nAChR.

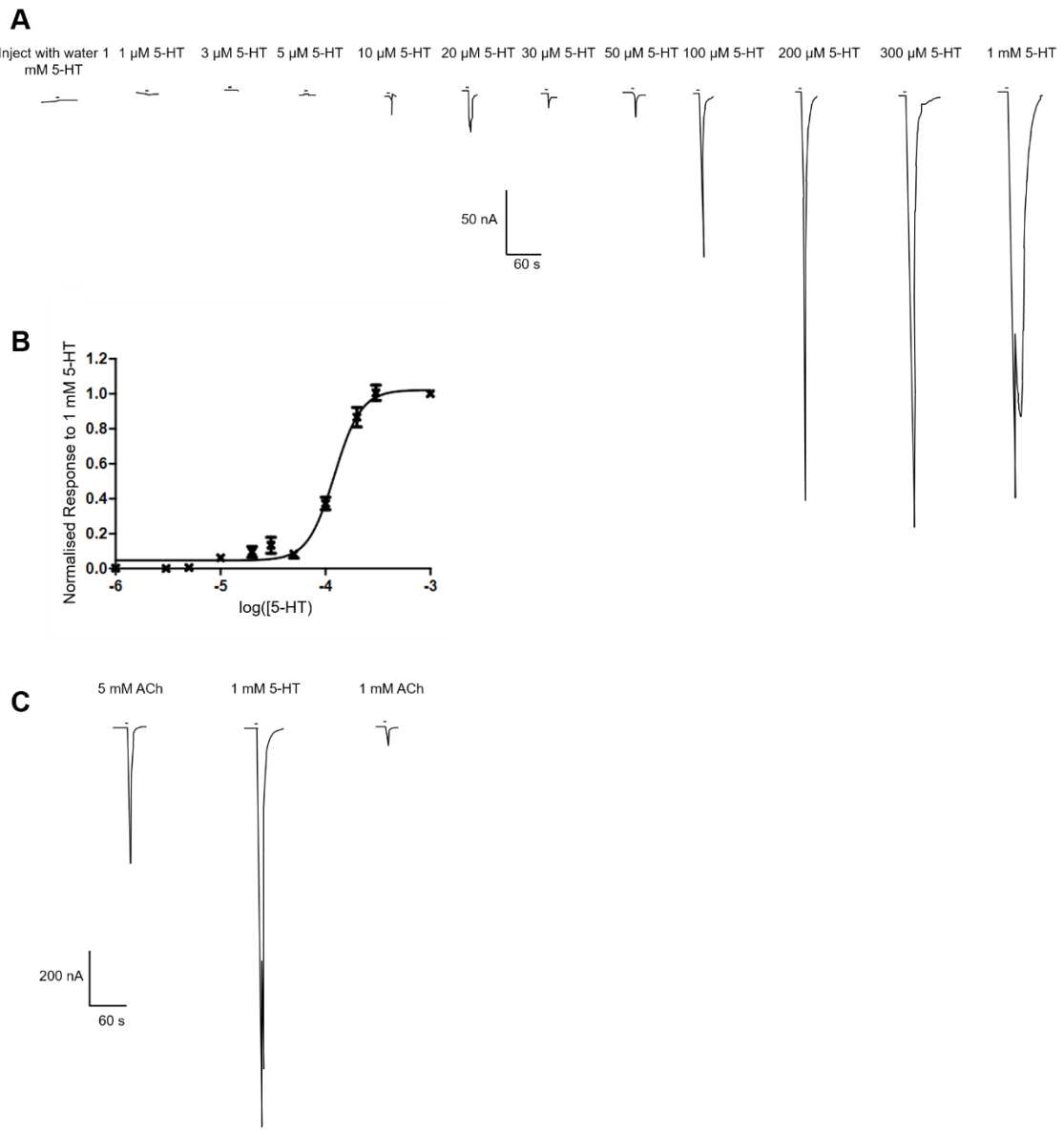

Figure 6.1 Reponses to 5-HT in X. laevis oocytes expressing the A. mellifera α5 nAChR subunit. A. Representative current traces showing responses to different concentrations of 5-HT (1–1000 µM). The lack of response from a control oocyte injected with water only is included. B. 5-HT concentration response curve. Data are normalised to the response to 1 mM 5-HT and have a mean EC_{50} 122 (111-134) µM from n = 7, N = 5. C. Sample traces comparing the response to maximal concentrations of acetylcholine (5 mM), 5-HT (1 mM) or 1 mM acetylcholine from the same oocyte, 3 min between applications.

Quipazine and mCPBG are potent $5HT_3R$ agonists (among many other chemicals) (Thompson and Lummis, 2006), mCPBG also activates $5HT_{3A}R$-nAChR α4 hybrid receptors and is a weak partial agonist, potentiator and channel blocker of vertebrate α9α10 receptors (van Hooft *et al.*, 1998; Rothlin *et al.*, 2003). No responses to 100 µM quipazine or mCPBG (Figure 6.2) or to lower concentrations (not shown) were observed.

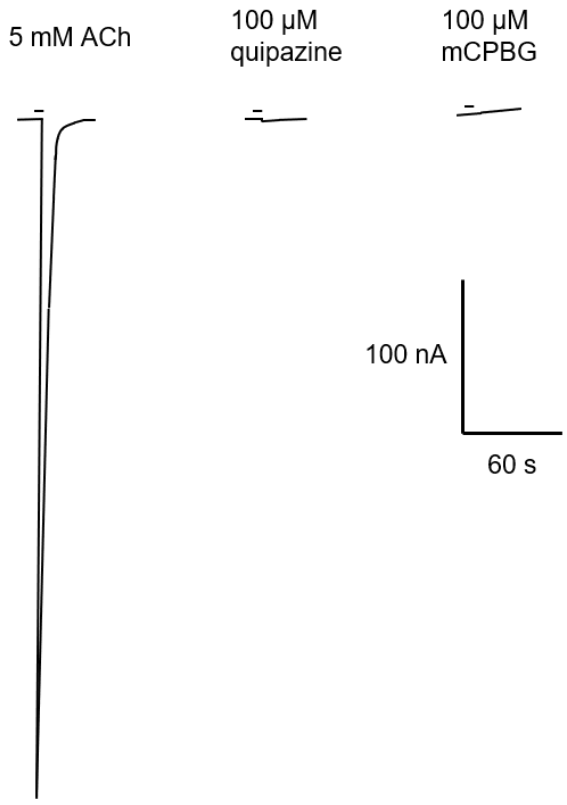

Figure 6.2 Trace showing that quipazine and mCPBG have no agonist actions when 100 µM was applied to X. laevis oocytes expressing the A. mellifera α5 nAChR 3 min after 5 mM acetylcholine application.

6.3.2 Response of the *A. mellifera* α5 nAChR to Dopamine

The *A. mellifera* α5 nAChR responded to dopamine in a concentration dependent manner (Figure 6.3 (A)). No response was observed in oocytes injected with water only, demonstrating that the currents are dependent upon the presence of the α5 nAChR subunit, in agreement with previous experiments on dopamine receptors in oocytes, which found no endogenous response to dopamine (Sakai *et al.*, 1990). Dopamine had an EC_{50} of 3.37 (2.93-3.89) µM (n = 5, N = 3) (Figure 6.3 (B)) and the mean relative maximum current response (at 100 µM) was 3,530 ± 1,900% (n = 7, N = 6) of the maximum acetylcholine response (at 5 mM) (Figure 6.3 (C)). Dopamine has the highest affinity and efficacy of the neurotransmitters tested for the *A. mellifera* α5 nAChR (Figure 6.9 and Table 6.2).

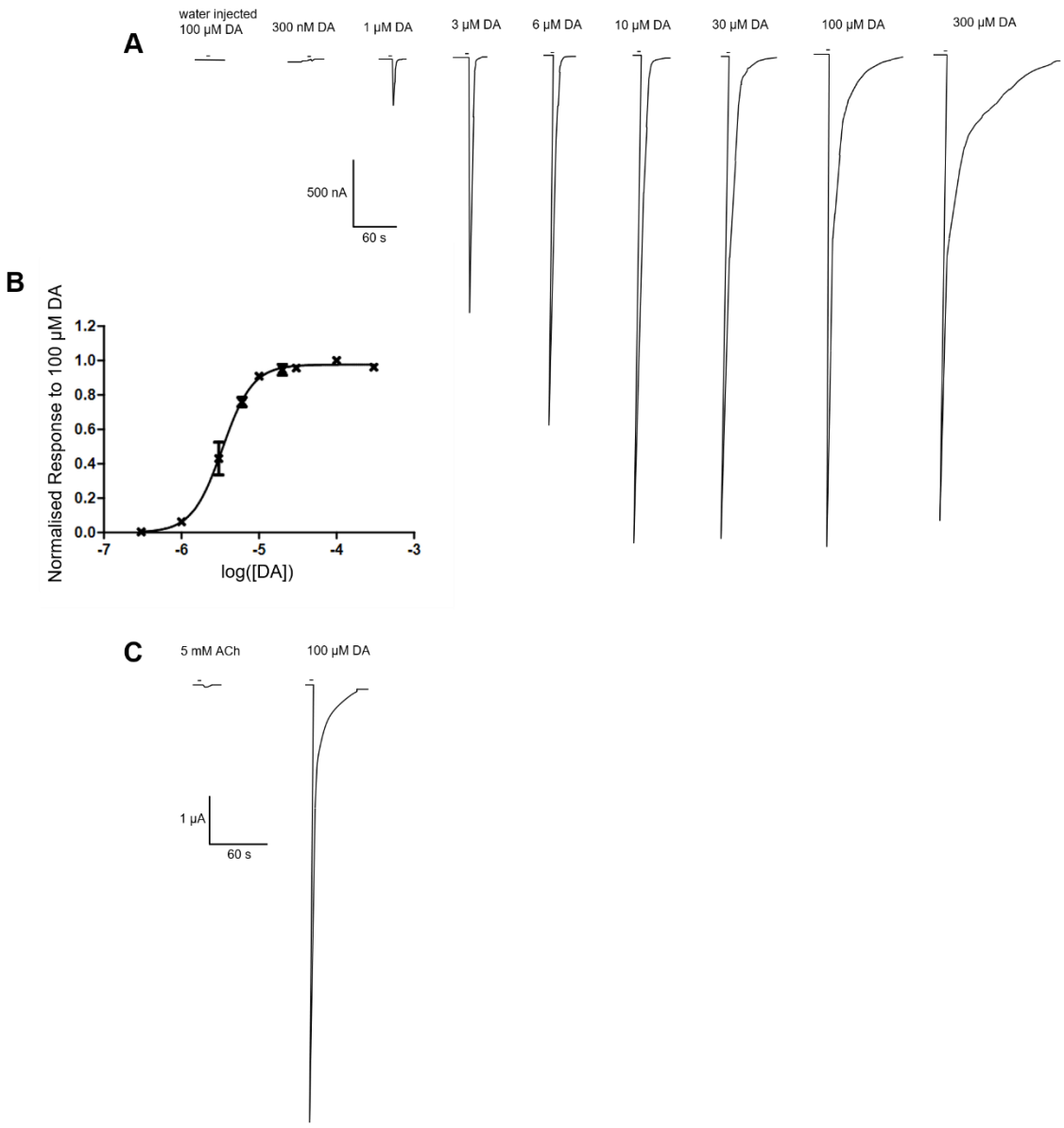

Figure 6.3 Response to dopamine (DA) in X. laevis oocytes expressing the A. mellifera α5 nAChR subunit. A. Representative current traces showing responses to different concentrations of dopamine (0.3-300 µM). The lack of response from a control oocyte injected with water only is included. B. Dopamine concentration response curve. Data are normalised to 100 µM dopamine and have an EC_{50} = 3.37 (2.93-3.89) µM n = 5, N = 3. C. Sample traces comparing the response to maximal concentrations of acetylcholine (5 mM) and DA (100 µM).

6.3.3 Response of the *A. mellifera* α5 nAChR to Octopamine

The *A. mellifera* α5 nAChR responded to octopamine in a concentration dependent manner (Figure 6.4 (A)). No response was observed in oocytes injected with water only, demonstrating that the currents are dependent upon the presence of the α5 nAChR subunit. Octopamine had an EC_{50} of 378 (354-404) µM (n = 6, N = 3) (Figure 6.4 (B)) and the mean maximum current

response (at 1 mM) was 899 ± 390% (n = 5, N = 5) of the maximum acetylcholine response (at 5 mM) (Figure 6.4 (C)).

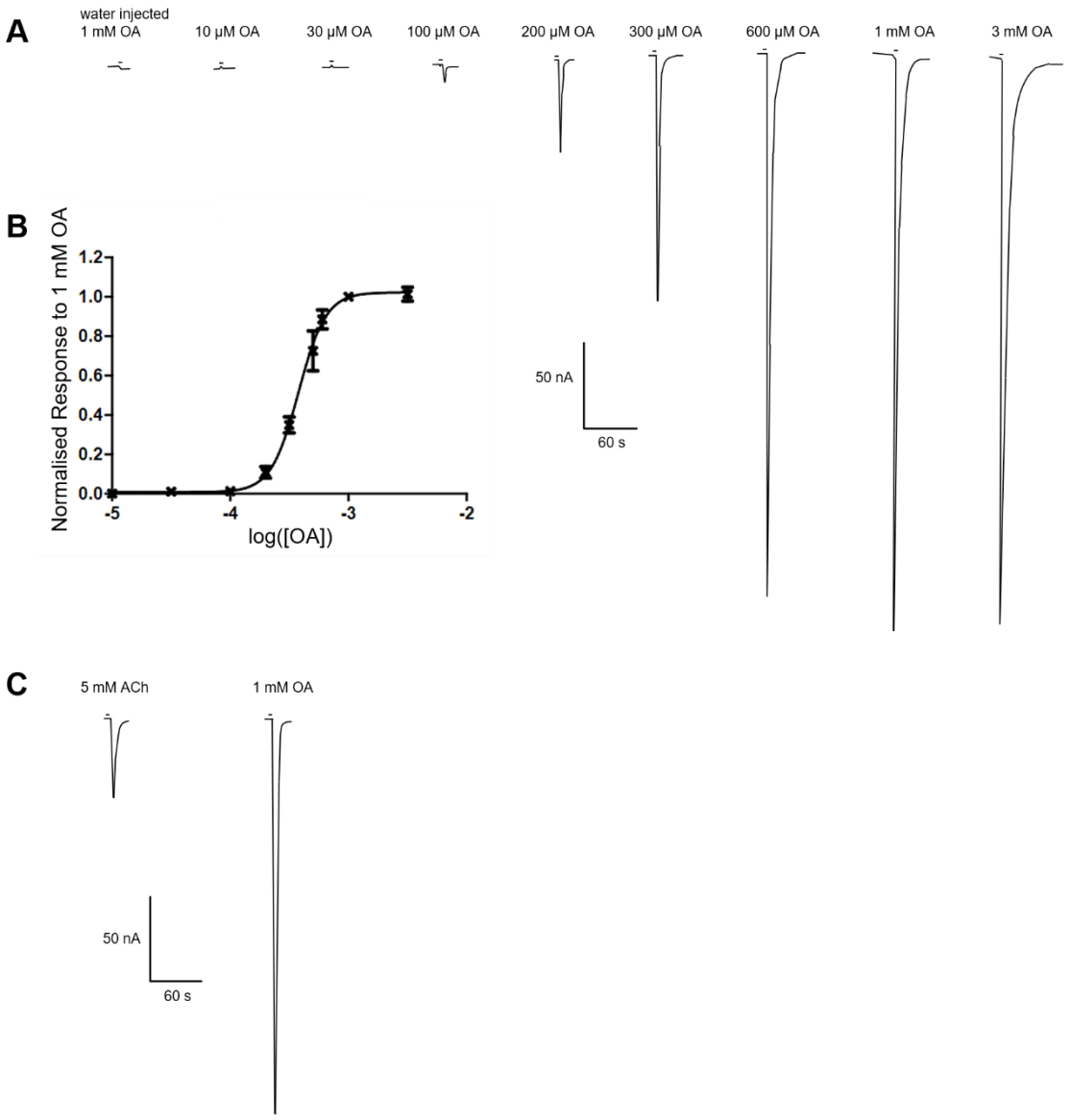

Figure 6.4 Response to octopamine (OA) in X. laevis oocytes expressing the A. mellifera α5 nAChR subunit. A. Representative current traces showing responses to different concentrations of octopamine (10-3000 µM). The lack of response from a control oocyte injected with water only is included. B. Octopamine concentration response curve. Data are normalised to 1 mM octopamine and have an EC_{50} = 378 (354-404) µM n = 6, N = 3. C. Sample traces comparing the response to maximal concentrations of acetylcholine (5 mM) and OA (1 mM).

Amitraz is an insecticide and arachnicide which is used to control *V. destructor* mites in beehives due to its low toxicity to honeybees (Guo *et al.*, 2021). Amitraz is an agonist of GPCRs which respond to octopamine, primarily Octβ2R (Guo *et al.*, 2021). Octβ2R from *A. mellifera* is much less sensitive to amitraz (EC_{50} 1.2 µM) than Octβ2R from *V. destructor* (EC_{50} 73 nM), thus

allowing its use in beehives without causing harm to honeybees (Guo *et al.*, 2021). We tested whether the *A. mellifera* α5 nAChR responds to amitraz as it responds to octopamine. The *A. mellifera* α5 nAChR expressed in *X. laevis* oocytes did not respond to 10 µM amitraz (Figure 6.5). Amitraz also had no antagonist actions at 10 µM when coapplied with 2 mM acetylcholine or 400 µM octopamine (Figure 6.5).

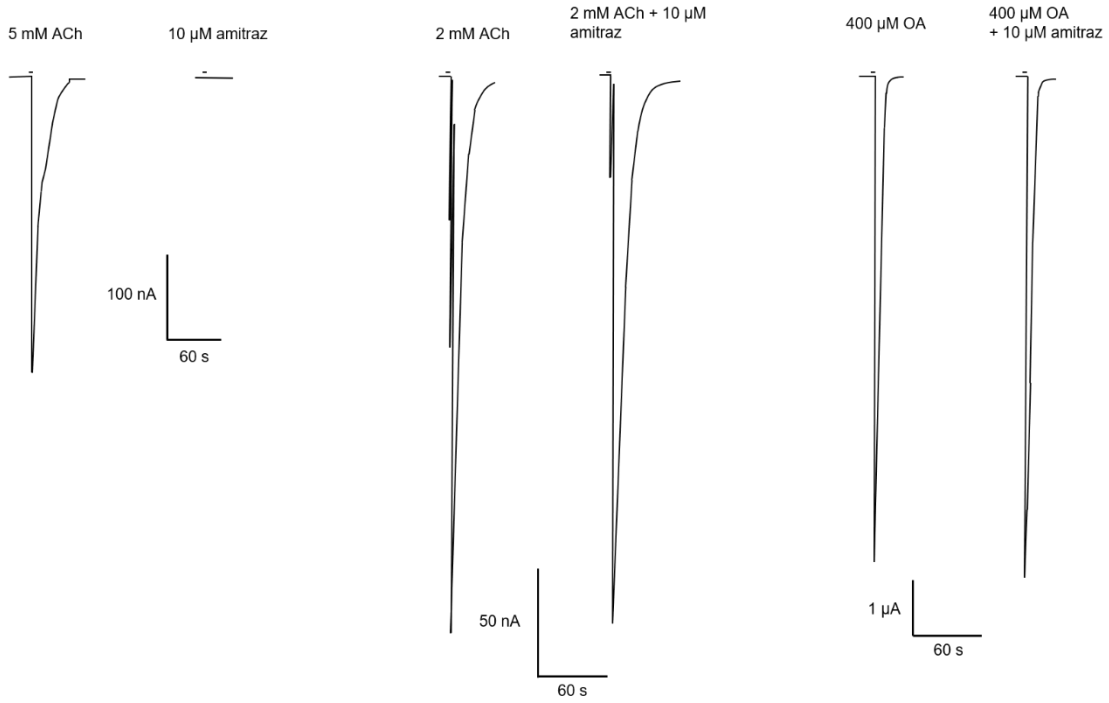

Figure 6.5 Traces showing that amitraz has no agonist actions when 10 µM was applied to X. laevis *oocytes expressing the A. mellifera α5 nAChR 3 min after 5 mM acetylcholine (ACh) application and that amitraz has no antagonist actions when 10 µM was coapplied with 2 mM acetylcholine or 400 µM octopamine (OA).*

6.3.4 Response of the *A. mellifera* α5 nAChR to Tyramine

The *A. mellifera* α5 nAChR responded to tyramine in a concentration dependent manner (Figure 6.6 (A)). No response was observed in oocytes injected with water only, demonstrating that the currents are dependent upon the presence of the α5 nAChR subunit. Tyramine had an EC_{50} of 91.1 (78.3-106) µM (n = 5, N = 3) (Figure 6.6 (B)) and the mean maximum current response (at 1 mM) was 770 ± 137% (n = 7, N = 4) of the maximum acetylcholine response (at 5 mM) (Figure 6.6 (C)).

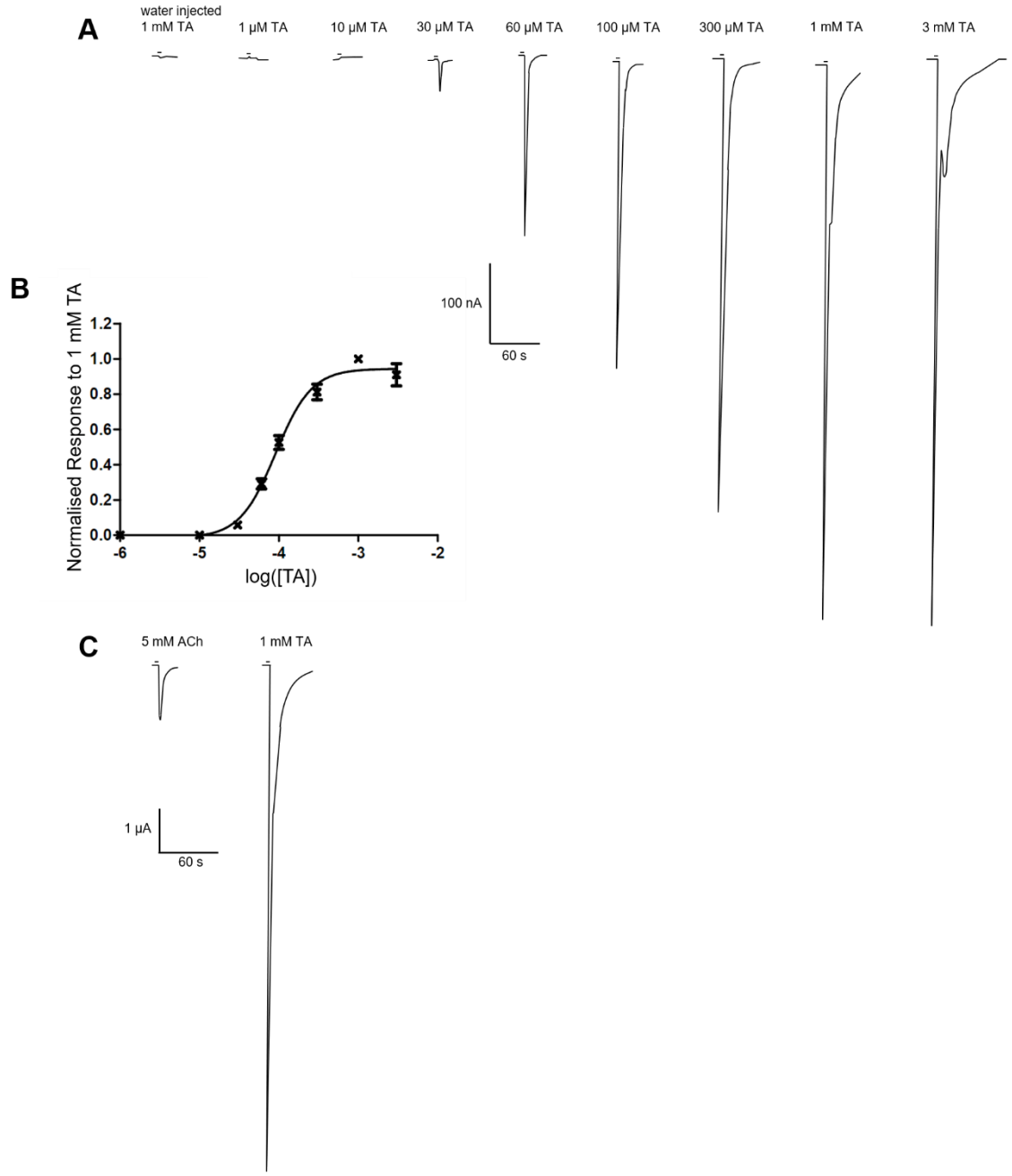

Figure 6.6 Response to tyramine (TA) in X. laevis oocytes expressing the *A. mellifera α5 nAChR subunit. A. Representative current traces showing responses to different concentrations of tyramine (1-3000 µM). The lack of response from a control oocyte injected with water only is included. B. Tyramine concentration response curve. Data are normalised to 1 mM tyramine and have an* EC_{50} *= 91.1 (78.3-106) µM n = 5, N = 3. C. Sample traces comparing the response to maximal concentrations of acetylcholine (5 mM) and TA (1 mM).*

6.3.5 Response of the *A. mellifera* α5 nAChR to Histamine

The *A. mellifera* α5 nAChR responded to histamine in a concentration dependent manner (Figure 6.7 (A)). Histamine had an EC_{50} of 3.36 (2.28-4.94) mM (n = 5, N = 4) (Figure 6.7 (B)) and the mean maximum current response (at 5 mM) was 45.3 ± 10.8% (n = 8, N = 5) of the maximum acetylcholine response (at 5 mM) (Figure 6.7 (C)). In oocytes injected with water only there was a slight response (-10 nA) to 5 mM histamine, but this was much less than the response of oocytes expressing the *A. mellifera* α5 nAChR (Figure 6.7 (A)).

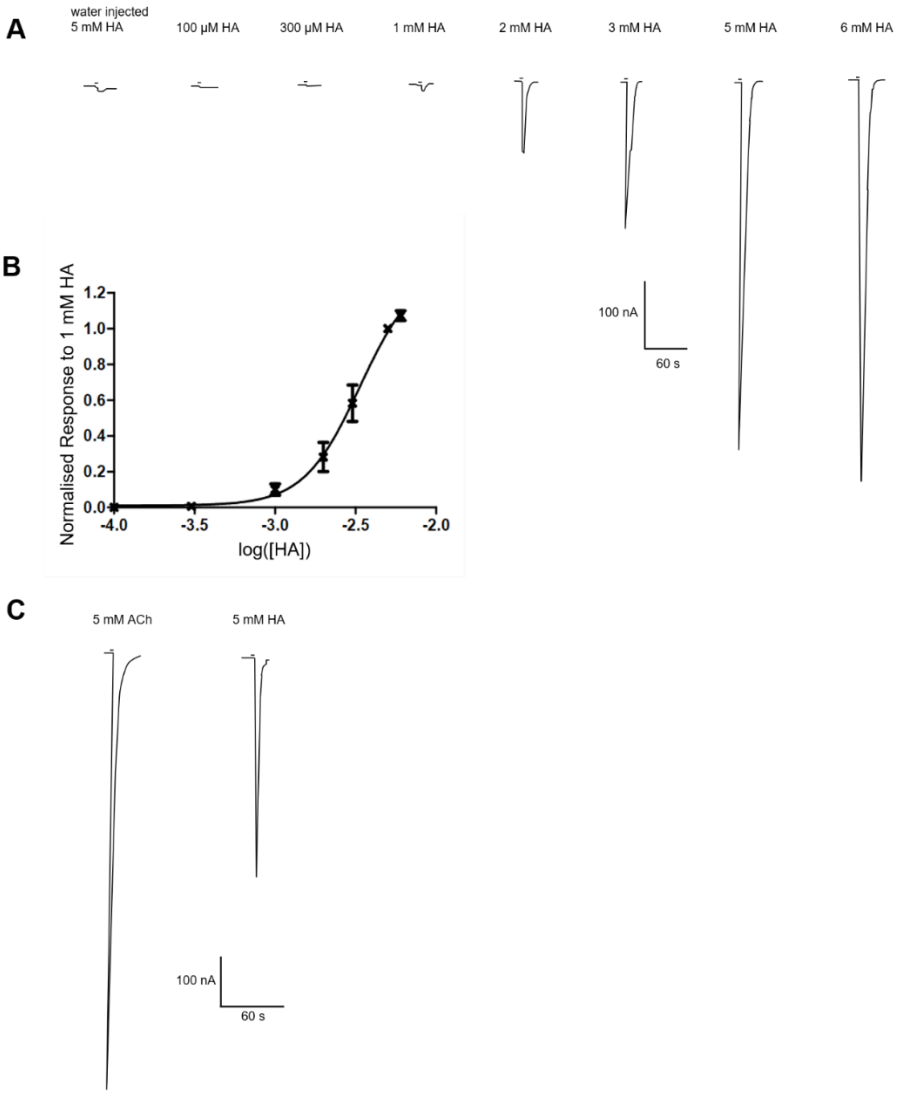

Figure 6.7 Response to histamine (HA) in X. laevis oocytes expressing the A. mellifera α5 nAChR subunit. A. Representative current traces showing responses to different concentrations of histamine (0.1-6 mM). The response from a control oocyte injected with water only is included. B. Histamine concentration response curve. Data are normalised to 5 mM histamine and have an EC_{50} = 3.36 (2.28-4.94) mM n = 5, N = 4. C. Sample traces comparing the response to maximal concentrations of acetylcholine (5 mM) and HA (5 mM).

6.3.6 Response of the *A. mellifera* α5 nAChR to GABA, Glycine and Glutamate

Oocytes injected with the *A. mellifera* α5 DNA, which responded to 5 mM acetylcholine, did not respond to 1 mM GABA, glycine or glutamate (Figure 6.8).

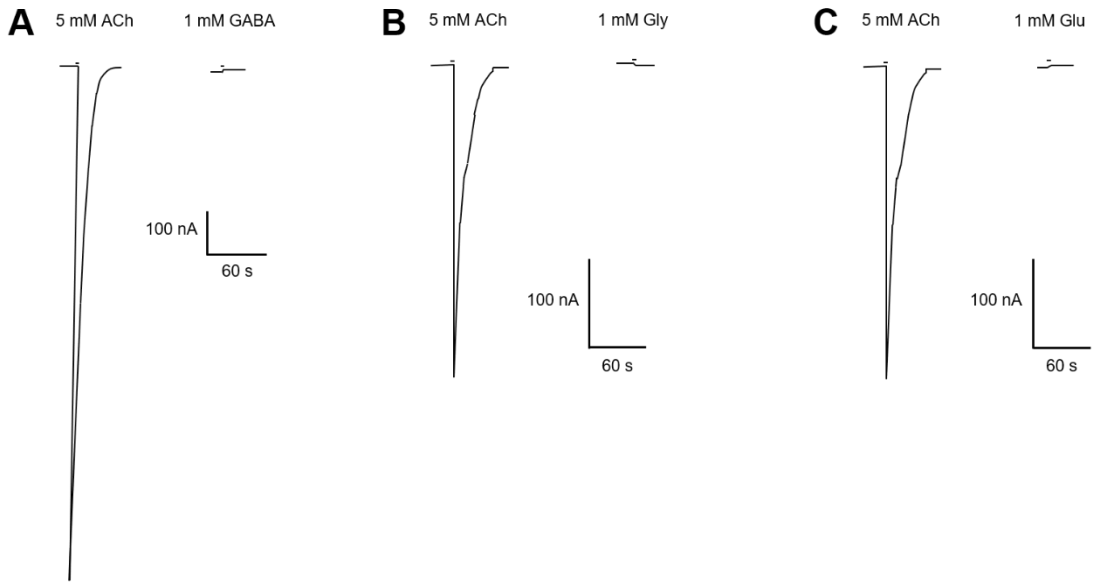

Figure 6.8 Traces showing that GABA (A), glycine (B) and glutamate (C) have no agonist actions when 1 mM was applied to X. laevis oocytes expressing the A. mellifera α5 nAChR 3 min after 5 mM acetylcholine application.

6.3.7 Comparing the Responses of the *A. mellifera* α5 nAChR to Different Neurotransmitters

Comparing the responses of the *A. mellifera* α5 nAChR to different biogenic amines reveals that dopamine has by far the highest affinity (EC_{50} 3.37 µM) and efficacy (3,530% the maximum acetylcholine response). Ranking the compounds in terms of affinity (EC_{50}) from highest to lowest gives: dopamine > tyramine > 5-HT > octopamine > acetylcholine > histamine > choline, although the confidence limits for acetylcholine and histamine and histamine and choline overlap so they are not significantly different. Ranking the compounds in terms of efficacy (relative maximum response) gives dopamine > octopamine > tyramine > 5-HT > acetylcholine/ choline > histamine, although the confidence limits for octopamine and tyramine overlap so they are not significantly different. Thus, compared to acetylcholine dopamine, octopamine, tyramine and 5-HT are superagonists whereas choline is a full agonist

and histamine is a partial agonist. Ranking the compounds using combined score for affinity and efficacy using the formula $Score = \frac{ACh\ EC50\ (\mu M)}{EC50\ (\mu M)} * \frac{Relative\ Maximum\ Response\ (\%)}{100}$, gives dopamine > tyramine > octopamine > 5-HT > acetylcholine > histamine > choline.

Table 6.2 Comparing the responses of the A. mellifera α5 nAChR expressed in X. laevis *oocytes to different neurotransmitters. EC_{50} values and Hill coefficients are displayed as the mean ± 95% confidence limits and maximum responses displayed as percentages ± 95% confidence limits calculated using a two-tailed t test.*

Neurotransmitter	**EC_{50} (µM)**	**Hill Coefficient**	**n = oocytes, N = frogs**	**Maximum Response Relative to 5 mM ACh (%)**	**n = oocytes, N = frogs**	**Combined Score**
Acetylcholine	2,650 (2,410-2,930)	2.30 (1.89-2.72)	n = 15, N = 7	100	n/a	1
Choline	9,070 (4,480-18,40)	2.04 (0.907-3.18)	n = 5, N = 4	100	n = 5, N = 4	0.293
5-HT	122 (111-134)	3.42 (2.50-4.34)	n = 7, N = 5	238 ± 24.0	n = 18, N = 8	51.9
Dopamine	3.37 (2.93-3.89)	2.22 (1.59-2.86)	n = 5, N = 3	3,530 ± 1,900	n = 7, N = 6	27,800
Octopamine	378 (354-404)	3.73 (3.00-4.46)	n = 6, N = 3	899 ± 390	n = 5, N = 5	63.1
Tyramine	91.1 (78.3-106)	1.92 (1.36-2.48)	n = 5, N = 3	770 ± 137	n = 7, N = 4	224

Histamine	3,360 (2,280-4,940)	2.50 (1.05-3.95)	n = 5, N = 4	45.3 ± 10.8	n = 8, N = 5	0.358

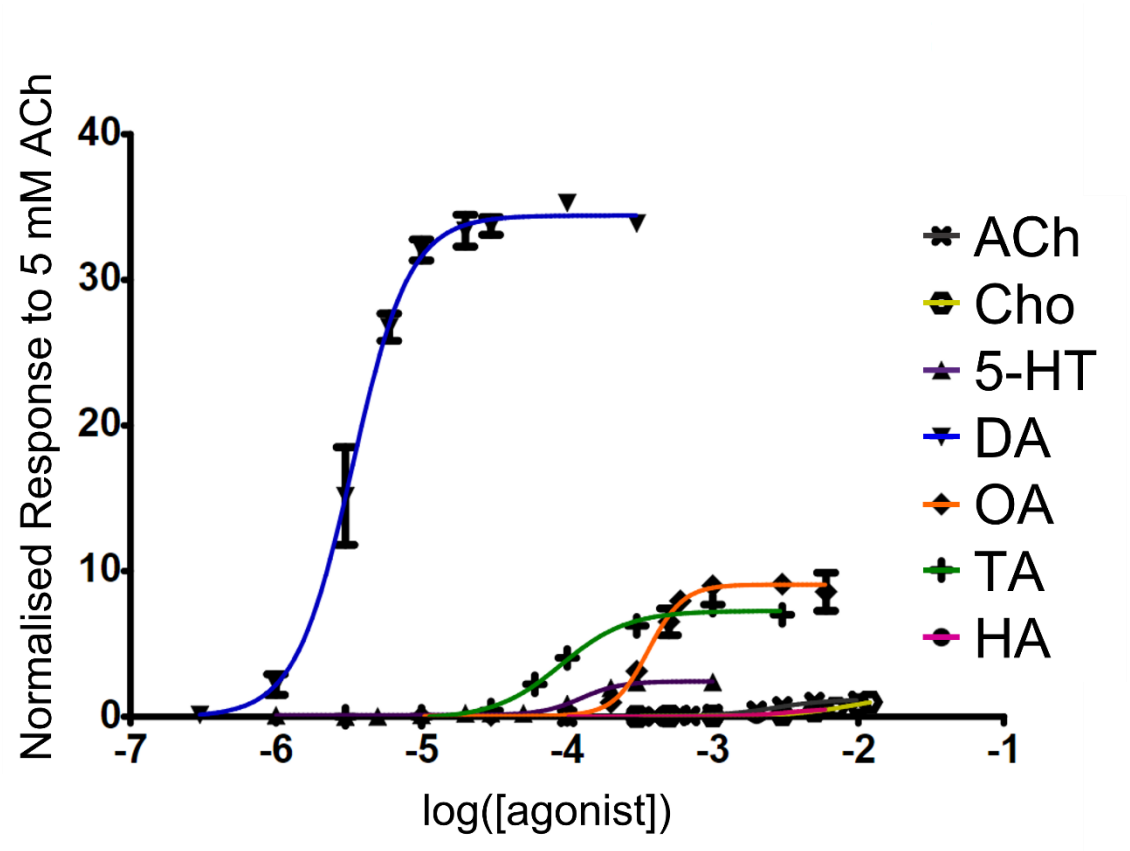

Figure 6.9 A concentration response graph comparing the responses of the A. mellifera α5 nAChR expressed in X. laevis *oocytes to acetylcholine, choline, 5-HT, dopamine, octopamine, tyramine and histamine.*

6.4 Discussion

6.4.1 The *A. mellifera* α5 nAChR is Primarily a Dopamine Receptor with Other Biogenic Amines Showing Agonist Actions

As can be seen in Figure 6.9 and Table 6.2, dopamine has a higher affinity and efficacy for the *A. mellifera* α5 nAChR than any of the other biogenic amines tested. The EC_{50} of dopamine,

3.37 (2.93-3.89) µM is within the range of EC_{50}s of many other cys-LGICs for their highest affinity agonist and neurotransmitter *in vivo* (Chapter 1, Table 1.1) (Lansdell *et al.*, 2012; Ihara *et al.*, 2020; Rufener *et al.*, 2020; Hawkins, Mitchell and Jones, 2022; Kita *et al.*, 2017; Thompson and Lummis, 2006; Ringstad, Abe and Horvitz, 2009; Morud *et al.*, 2021). Thus, the *A. mellifera* α5 nAChR is the first identified putative cationic cys-LGIC that has dopamine as a proposed endogenous agonist and the first potential ionotropic dopamine receptor in insects. Dopamine has been found in the honeybee brain and in most of the regions that overlap with the expression profile of the α5 subunit (Bicker, 1999; Thany *et al.*, 2005; Mercer *et al.*, 1983; Schäfer and Rehder, 1989). So, it is possible that the endogenous agonist of the *A. mellifera* α5 nAChR is dopamine, if it is expressed as a homomer *in vivo*. It remains to be seen if the ionotropic dopamine receptor in snails is related to the *A. mellifera* α5 nAChR (Green and Cottrell, 1996).

The *A. mellifera* α5 nAChR also responds to tyramine, 5-HT, octopamine, acetylcholine, histamine and choline but with a much lower affinity and efficacy than dopamine (Table 6.2, Figure 6.9). As shown in Table 6.1 there are multiple cys-LGICs expressed in *X. laevis* oocytes that respond to other neurotransmitters at higher concentrations and often lower efficacies than their proposed endogenous agonist (Thompson and Lummis, 2006; van Hooft *et al.*, 1998; Dionisio *et al.*, 2015; Saras *et al.*, 2008; Peden *et al.*, 2013; Ringstad, Abe and Horvitz, 2009; Morud *et al.*, 2021) including a histamine chloride channel from *M. domestica*, which also responds to choline, 5-HT, tyramine, octopamine, dopamine and noradrenaline (Kita *et al.*, 2017). This may be because the ligand binding site cannot sufficiently discriminate between different ligands. This may not have proved to be a problem from an evolutionary perspective as the synaptic concentrations of neurotransmitters other than the primary agonist may not be sufficiently high to affect signalling as the affinity for the receptor is too low. Thus, the *A. mellifera* α5 nAChR fits this pattern of having an agonist with an EC_{50} between 100 nM and 10 µM and then multiple other agonists with lower affinities and efficacies.

Most of the behavioural effects of dopamine and other biogenic amines have been assumed to be mediated by GPCRs, confirmed by the use of antagonists against specific dopamine receptors, flupenazine and pimozide (Huang *et al.*, 2022; Agarwal *et al.*, 2011; Raza *et al.*, 2022; Klappenbach, Kaczer and Locatelli, 2013; Mancini *et al.*, 2018; Nouvian *et al.*, 2018). GPCRs act on a slower timescale than ionotropic receptors (Albuquerque *et al.*, 2009), from research so far it is not clear what sort of honeybee behaviour would require a fast acting dopamine receptor. However, most of the behaviours studied revolve around learning and

memory and not fast reflexive behaviours (Klappenbach, Kaczer and Locatelli, 2013; Agarwal *et al.*, 2011; Raza *et al.*, 2022; Mancini *et al.*, 2018).

6.4.2 Amitraz Does Not Act on the *A. mellifera* α5 nAChR

As we had a receptor from *A. mellifera* that responded to octopamine we tested whether amitraz, a pesticide which is used in beehives to control *V. destructor* (Guo *et al.*, 2021) had any effects on the *A. mellifera* α5 nAChR. Amitraz at 10 µM had no effect on the *A. mellifera* α5 nAChR (Figure 6.5). This is not surprising as the targets of amitraz are well characterised as GPCRs that respond to octopamine (Guo *et al.*, 2021; Sparks *et al.*, 2021).

6.5 Conclusion

The *A. mellifera* α5 nAChR responds to 5-HT, dopamine, octopamine, tyramine and histamine as well as acetylcholine and choline, but not to GABA, glycine and glutamate. The response to dopamine has a higher affinity and efficacy than the responses to other neurotransmitters, with an EC_{50} in the range we have seen for endogenous agonists of other cys-LGICs, thus this may act as a dopamine receptor *in vivo*.

Chapter 7 Final Discussion

7.1 The Heterologous Expression of Insect nAChRs in *X. laevis* oocytes

As mentioned in the introduction, during the last few years there has been major progress in the heterologous expression of insect nAChRs in *X. laevis* oocytes and this has allowed their functional characterisation (Ihara *et al.*, 2020; Cartereau *et al.*, 2020; Rufener *et al.*, 2020; Hawkins, Mitchell and Jones, 2022; Brunello *et al.*, 2022; Takayama *et al.*, 2022). This thesis contributes to that progress by developing an expression system for a hybrid receptor consisting of the *D. melanogaster* α1 subunit and subunits from *M. persicae* with *M. persicae* RIC-3, UNC-50 and TMX3 and with the functional and pharmacological characterisation of the *A. mellifera* α5 nAChR. The expression of nAChRs from pest species and beneficial species will allow the development of more pest-specific insecticides, with fewer effects on beneficial species.

The cloning of the *M. persicae* nAChR subunits and chaperones means that they are prepared for any future expression experiments, such as those suggested in Chapter 4.4.4.

7.2 The Potential Functions of an Ionotropic Dopamine Receptor in *A. mellifera*

The *A. mellifera* α5 nAChR seems to be an ionotropic dopamine receptor (Chapter 6.4.1), whereas the *D. melanogaster* α5 nAChR has all the typical pharmacological properties of an acetylcholine receptor (Lansdell *et al.*, 2012). Why has the α5 nAChR subunit evolved differently in Diptera and non-Dipteran insects? Two of the key features that distinguish honeybees from some other insects (e.g. *D. melanogaster*) are their eusociality and their roles as pollinators, therefore a receptor that is not present in other insects may have a potential role in these processes. Biogenic amines have been co-opted to control social behaviours, but so far there has been no detected difference in biogenic amine receptor genes between solitary and social insects (Kamhi *et al.*, 2017). Dopamine is associated with increased sociability (Hewlett *et al.*, 2018). But some measures of sociability can be decreased by fluphenazine, an antagonist which specifically targets dopamine-activated GPCRs (Hewlett *et al.*, 2018), thus at least some of dopamine's role in sociability is due to these receptors.

Dopamine decreases the threshold for cooperative defensive behaviour, which may be a process that requires the fast action produced by ionotropic receptors but again this was decreased by antagonists acting on GPCRs and 5-HT has a greater effect on defensiveness (Nouvian *et al.*, 2018; Rittschof *et al.*, 2019). Nectar from different plants does contain neuroactive substances (octopamine, tyramine, caffeine, GABA, taurine, β-alanine, glutamate, glycine, nicotine and scopolamine) (Mustard, 2020; Muth *et al.*, 2022), that can have an effect on behaviour (Muth *et al.*, 2022) but there is no record of dopamine in nectar (Mustard, 2020). Also, neither dopamine, 5-HT nor octopamine has been detected in bee pollen (Zhao *et al.*, 2018).

7.3 The Possibility of Reclassifying the *A. mellifera* α5 as an Ionotropic Dopamine Receptor

As mentioned in Chapter 6.4.1, the experimental evidence suggests that the *A. mellifera* α5 nAChR is a dopamine receptor. This would be the first cationic cys-LGIC that has dopamine as a proposed endogenous agonist. However, little is known about the pharmacology of other non-Dipteran α5 receptors in this monophyletic group, as they have not been expressed. Expression of the α5 subunit from *L. migratoria* was attempted but was not successful with or without other nAChR subunits from *L. migratoria* (Zhang *et al.*, 2017). Thus, there may be variation within this group regarding expression and pharmacology serving species specific roles and it might be premature to consider reclassifying the group until more is known about the pharmacology of non-Dipteran α5 subunits from other species. Therefore, experiments characterising a different homomeric non-Dipteran α5 nAChR, would be very useful. A protein structure, especially with a ligand bound, would elucidate why the *A. mellifera* α5 nAChR has a higher affinity and efficacy for dopamine than acetylcholine at the molecular level. A homology model based on the human α7 nAChR has been created and acetylcholine and 5-HT have been docked into the binding site (Figure 7.1) (Mitchell *et al.*, 2022). The most notable differences between the *A. mellifera* α5 and human α7 that may contribute to ligand binding are on the complementary side of the binding site (Mitchell *et al.*, 2022). Further modelling exploring the possible interactions of dopamine with the binding site, may give insights into why dopamine is such a potent agonist of the *A. mellifera* α5 nAChR.

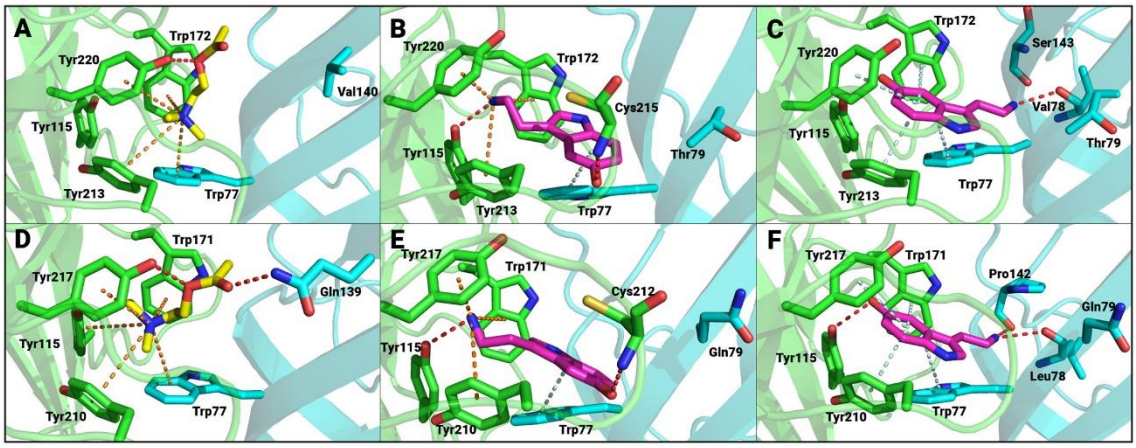

Figure 7.1 Homology modelling of the A. mellifera α5 nAChR based on the human α7 crystal structure (Zhao et al., 2021). Binding conformations generated by Autodock Vina with the interactions between acetylcholine (yellow) and serotonin (magenta) and the main binding site amino acids (red = hydrogen bond, orange = cation-π, and pale cyan = π-π) for A. mellifera α5 (A, and B, C) and human α7 (D, E, and F) from (Mitchell et al., 2022).

In future characterisation studies on cys-LGICs it may be worthwhile testing a range of neurotransmitters, especially if the predicted endogenous neurotransmitter has a low affinity, as has been done in previous research on HisClB in *M. domestica* and secCl in *D. melanogaster* (Kita *et al.*, 2017; Feingold *et al.*, 2019). This will allow the empirical detection of any unexpected agonists and further the understanding of the selectivity of these receptors by comparing the affinity and efficacy of different agonists.

Chapter 8 References

Abbo, P. M., Kawasaki, K., J., Hamilton, Michele, Cook, C., S., DeGrandi-Hoffman, Gloria, Li , Feng, W., Liu, Jie, Chen and Ping, Y. (2016) 'Effects of Imidacloprid and *Varroa destructor* on survival and health of European honey bees, *Apis mellifera*', *Insect Science,* 24(3), pp. 467-477.

Abiusi, E., D'Alessandro, M., Dieterich, K., Quevarec, L., Turczynski, S., Valfort, A. C., Mezin, P., Jouk, P. S., Gut, M., Gut, I., Bessereau, J. L. and Melki, J. (2017) 'Biallelic mutation of UNC50, encoding a protein involved in AChR trafficking, is responsible for arthrogryposis', *Human Molecular Genetics,* 26(20), pp. 3989-3994.

Agarwal, M., Giannoni Guzmán, M., Morales-Matos, C., Del Valle Díaz, R. A., Abramson, C. I. and Giray, T. (2011) 'Dopamine and Octopamine Influence Avoidance Learning of Honey Bees in a Place Preference Assay', *PLOS ONE,* 6(9), pp. e25371.

Albuquerque, E. X., Pereira, E. F. R., Alkondon, M. and Rogers, S. W. (2009) 'Mammalian Nicotinic Acetylcholine Receptors: From Structure to Function', *Physiological Reviews,* 89(1), pp. 73-120.

Alexander, J. K., Sagher, D., Krivoshein, A. V., Criado, M., Jefford, G. and Green, W. N. (2010) 'Ric-3 Promotes α7 Nicotinic Receptor Assembly and Trafficking through the ER Subcompartment of Dendrites', *Journal of Neuroscience,* 30(30), pp. 10112-10126.

Alkondon, M., Pereira, E. F. R., Cartes, W. S., Maelicke, A. and Albuquerque, E. X. (1997) 'Choline is a Selective Agonist of α7 Nicotinic Acetylcholine Receptors in the Rat Brain Neurons', *European Journal of Neuroscience,* 9(12), pp. 2734-2742.

Amiri, S., Shimomura, M., Vijayan, R., Nishiwaki, H., Akamatsu, M., Matsuda, K., Jones, A. K., Sansom, M. S. P., Biggin, P. C. and Sattelle, D. B. (2008) 'A Role for Leu118 of Loop E in Agonist Binding to the α7 Nicotinic Acetylcholine Receptor', *Molecular Pharmacology,* 73(6).

Arenas, A., Lajad, R., Peng, T., Grüter, C. and Farina, W. (2021) 'Correlation between octopaminergic signalling and foraging task specialisation in honeybees', *Genes, Brain and Behavior,* 20(4), pp. e12718.

Ballivet, M., Alliod, C., Bertrand, S. and Bertrand, D. (1996) 'Nicotinic Acetylcholine Receptors in the NematodeCaenorhabditis elegans', *Journal of Molecular Biology,* 258(2), pp. 261-269.

Bao, H., Xu, X., Liu, W., Yu, N. and Liu, Z. (2018) 'Dual effects of insect nAChR chaperone RIC-3 on hybrid receptor: Promoting assembly on endoplasmic reticulum but suppressing transport to plasma membrane on Xenopus oocytes', *Neurochemistry International,* 115, pp. 24-30.

Barish, M. E. (1983) 'A transient calcium-dependent chloride current in the immature Xenopus oocyte', *The Journal of Physiology,* 342(1), pp. 309-325.

Bass, C., Puinean, A. M., Andrews, M., Cutler, P., Daniels, M., Elias, J., Paul, V. L., Crossthwaite, A. J., Denholm, I., Field, L. M., Foster, S. P., Lind, R., Williamson, M. S. and Slater, R. (2011) 'Mutation of a nicotinic acetylcholine receptor β subunit is associated with resistance to neonicotinoid insecticides in the aphid *Myzus persicae*', *BioMed Central Neurocience,* 12(51).

Bass, C., Puinean, A. M., Zimmer, C. T., Denholm, I., Field, L. M., Foster, S. P., Gutbrod, O., Nauen, R., Slater, R. and Williamson, M. S. (2014) 'The evolution of insecticide resistance in the peach potato aphid, Myzus persicae', *Insect Biochemistry and Molecular Biology,* 51, pp. 41-51.

Bass, C., Zimmer, C. T., Riveron, J. M., Wilding, C. S., Wondji, C. S., Kaussmann, M., Field, L. M., Williamson, M. S. and Nauen, R. (2013) 'Gene amplification and microsatellite polymorphism underlie a recent insect host shift', *PNAS,* 110(48), pp. 19460-19465.

Beggs, K. T., Glendining, K. A., Marechal, N. M., Vergoz, V., Nakamura, I., Slessor, K. N. and Mercer, A. R. (2007) 'Queen pheromone modulates brain dopamine function in worker honey bees', *Proceedings of the National Academy of Sciences,* 104(7), pp. 2460-2464.

Ben-Ami, H. C., Yassin, L., Farah, H., Michaeli, A., Eshel, M. and Treinin, M. (2005) 'RIC-3 Affects Properties and Quantity of Nicotinic Acetylcholine Receptors via a Mechanism That Does Not Require the Coiled-coil Domains', *Journal of Biological Chemistry,* 280(30), pp. 28053-28060.

Berger, M., Puinean, A. M., Randall, E., Zimmer, C. T., Silva, W. M., Bielza, P., Field, L. M., Hughes, D., Mellor, I., Hassani-Pak, K., Siqueira, H. A. A., Williamson, M. S. and Bass, C. (2016) 'Insecticide resistance mediated by an exon skipping event', *Molecular Ecology,* 25(22), pp. 5692-5704.

Bicker, G. (1999) 'Biogenic amines in the brain of the honeybee: Cellular distribution, development, and behavioral functions', *Microscopy Research and Technique,* 44(2-3), pp. 166-178.

Boulin, T., Fauvin, A., Charvet, C. L., Cortet, J., Cabaret, J., Bessereau, J. L. and Neveu, C. (2011) 'Functional reconstitution of Haemonchus contortus acetylcholine receptors in Xenopus oocytes provides mechanistic insights into levamisole resistance', *British Journal of Pharmacology,* 164(5), pp. 1421-1432.

Boulin, T., Gielen, M., Richmond, J. E., Williams, D. C., Paoletti, P. and Bessereau, J.-L. (2008) 'Eight genes are required for functional reconstitution of the Caenorhabditis elegans

levamisole-sensitive acetylcholine receptor', *Proceedings of the National Academy of Sciences,* 105(47), pp. 18590-18595.

Bouzat, C. (2012) 'New insights into the structural bases of activation of Cys-loop receptors', *Journal of Physiology-Paris,* 106(1), pp. 23-33.

Braun, G. and Bicker, G. (1992) 'Habituation of an appetitive reflex in the honeybee', *Journal of Neurophysiology,* 67(3), pp. 588-598.

Breer, H. (1981) 'Characterization of synaptosomes from the central nervous system of insects', *Neurochem Int,* 3(2), pp. 155-63.

Bretschneider, F. and de Weille, J., R. (2006) *Introduction to Electrophysiological Methods and Instrumentation.* First edn. London: Elsevier.

Brunello, L., Ménard, C., Rousset, M., Vignes, M., Charnet, P. and Cens, T. (2022) 'Different efficiency of auxiliary/chaperone proteins to promote the functional reconstitution of honeybee Glutamate and Acetylcholine receptors in Xenopus laevis oocytes', *Insect Mol Biol*.

Buckingham, S., Lapied, B., Corronc, H. and Sattelle, F. (1997) 'Imidacloprid actions on insect neuronal acetylcholine receptors', *Journal of Experimental Biology,* 200(21), pp. 2685-2692.

Buckingham, S. D., Pym, L. and Sattelle, D. B. (2006) 'Oocytes as an Expression System for Studying Receptor/Channel Targets of Drugs and Pesticides', in Liu, X.J. (ed.) *Methods in Molecular Biology: Xenopus Protocols: Cell Biology and Signal Transduction*. Totowa, NJ: Humana Press Inc., pp. 331-345.

Capinera, J. L. (2001) *common name: green peach aphid, scientific name: Myzus persicae*. Featured Creatures: University of Florida. Available at: http://entnemdept.ufl.edu/creatures/veg/aphid/green_peach_aphid.htm#top (Accessed: 8/4/19 2019).

Carrington, D. (2019) 'Plummeting insect numbers 'threaten collapse of nature'', *The Guardian*. Available at: https://www.theguardian.com/environment/2019/feb/10/plummeting-insect-numbers-threaten-collapse-of-nature.

Cartereau, A., Taillebois, E., Le Questel, J.-Y. and Thany, S. H. (2021) 'Mode of Action of Neonicotinoid Insecticides Imidacloprid and Thiacloprid to the Cockroach Pameα7 Nicotinic Acetylcholine Receptor', *International journal of molecular sciences,* 22(18), pp. 9880.

Cartereau, A., Taillebois, E., Selvam, B., Martin, C., Graton, J., Le Questel, J.-Y. and Thany, S. H. (2020) 'Cloning and Expression of Cockroach α7 Nicotinic Acetylcholine Receptor Subunit', *Frontiers in Physiology,* 11, pp. 418.

Casida, J. E. (2018) 'Neonicotinoids and Other Insect Nicotinic Receptor Competitive Modulators: Progress and Prospects', *Annual Review of Entomology,* 63(1), pp. 125-144.

Castelán, F., Castillo, M., Mulet, J., Sala, S., Sala, F., Domínguez del Toro, E. and Criado, M. (2008) 'Molecular characterization and localization of the RIC-3 protein, an effector of nicotinic acetylcholine receptor expression', *Journal of Neurochemistry,* 105(3), pp. 617-627.

Catae, A. F., Roat, T. C., Pratavieira, M., Silva Menegasso, A. R. d., Palma, M. S. and Malaspina, O. (2018) 'Exposure to a sublethal concentration of imidacloprid and the side effects on target and nontarget organs of Apis mellifera (Hymenoptera, Apidae)', *Ecotoxicology,* 27(2), pp. 109-121.

Changeux, J.-P. (2012) 'The Nicotinic Acetylcholine Receptor: The Founding Father of the Pentameric Ligand-gated Ion Channel Superfamily', *Journal of Biological Chemistry,* 287(48), pp. 40207-40215.

Charaabi, K., Boukhris-Bouhachem, S., Makni, M. and Denholm, I. (2017) 'Occurrence of target-site resistance to neonicotinoids in the aphid *Myzus persicae* in Tunisia, and its status on different host plants', *Pest Management Science,* 74(6), pp. 1297-1301.

Charreton, M., Decourtye, A., Henry, M., Rodet, G., Sandoz, J.-C., Charnet, P. and Collet, C. (2015) 'A Locomotor Deficit Induced by Sublethal Doses of Pyrethroid and Neonicotinoid Insecticides in the Honeybee Apis mellifera', *PLOS ONE,* 10(12), pp. e0144879.

Chen, X., Li, F., Chen, A., Ma, K., Liang, P., Liu, Y., Song, D. and Gao, X. (2017) 'Both point mutations and low expression levels of the nicotinic acetylcholine receptor β1 subunit are associated with imidacloprid resistance in an Aphis gossypii (Glover) population from a Bt cotton field in China', *Pesticide Biochemistry and Physiology,* 141, pp. 1-8.

Chiara, D. C. and Cohen, J. B. (1997) 'Identification of Amino Acids Contributing to High and Low Affinity d-Tubocurarine Sites in the TorpedoNicotinic Acetylcholine Receptor', *Journal of Biological Chemistry,* 272(52), pp. 32940-32950.

Chiara, D. C., Middleton, R. E. and Cohen, J. B. (1998) 'Identification of tryptophan 55 as the primary site of [3H]nicotine photoincorporation in the γ-subunit of the Torpedo nicotinic acetylcholine receptor', *FEBS Letters,* 423(2), pp. 223-226.

Claudianos, C., Ranson, H., Johnson, R. M., Biswas, S., Schuler, M. A., Berenbaum, M. R., Feyereisen, R. and Oakeshott, J. G. (2006) 'A deficit of detoxification enzymes: pesticide

sensitivity and environmental response in the honeybee', *Insect Molecular Biology,* 15(5), pp. 615-636.

Cohen, J. B., Sharp, S. D. and Liu, W. S. (1991) 'Structure of the agonist-binding site of the nicotinic acetylcholine receptor. [3H]acetylcholine mustard identifies residues in the cation-binding subsite', *Journal of Biological Chemistry,* 266(34), pp. 23354-23364.

Colgan, J., T., Fletcher, K., I., Arce, N., A., Gill, J., R., Rodrigues, Ramos, A., Stolle, Eckart, Chittka, Lars, Wurm and Yannick (2019) 'Caste- and pesticide-specific effects of neonicotinoid pesticide exposure on gene expression in bumblebees', *Molecular Ecology*.

Cook, C. N., Brent, C. S. and Breed, M. D. (2017) 'Octopamine and tyramine modulate the thermoregulatory fanning response in honey bees (Apis mellifera)', *Journal of Experimental Biology,* 220(10), pp. 1925-1930.

Corringer, P.-J., Galzi, J.-L., Eiselé, J.-L., Bertrand, S., Changeux, J.-P. and Bertrand, D. (1995) 'Identification of a New Component of the Agonist Binding Site of the Nicotinic 7 Homooligomeric Receptor', *Journal of Biological Chemistry,* 270(20), pp. 11749-11752.

Corringer, P.-J., Novère, N. L. and Changeux, J.-P. (2000) 'Nicotinic Receptors at the Amino Acid Level', *Annual Review of Pharmacology and Toxicology,* 40(1), pp. 431-458.

Courjaret, R. and Lapied , B. (2001) 'Complex Intracellular Messenger Pathways Regulate One Type of Neuronal α-Bungarotoxin-Resistant Nicotinic Acetylcholine Receptors Expressed in Insect Neurosecretory Cells (Dorsal Unpaired Median Neurons)', *Molecular Pharmacology,* 60(1), pp. 80-91.

Cresswell, J. E. (2011) 'A meta-analysis of experiments testing the effects of a neonicotinoid insecticide (imidacloprid) on honey bees', *Ecotoxicology,* 20(1), pp. 149-157.

Crossley, M. S., Meier, A. R., Baldwin, E. M., Berry, L. L., Crenshaw, L. C., Hartman, G. L., Lagos-Kutz, D., Nichols, D. H., Patel, K., Varriano, S., Snyder, W. E. and Moran, M. D. (2020) 'No net insect abundance and diversity declines across US Long Term Ecological Research sites', *Nature Ecology & Evolution,* 4(10), pp. 1368-1376.

Crossthwaite, A. J., Bigot, A., Camblin, P., Goodchild, J., Lind, R. J., Slater, R. and Maienfisch, P. (2017) 'The invertebrate pharmacology of insecticides acting at nicotinic acetylcholine receptors', *Journal of Pesticide Science,* advpub.

Croxen, R., Newland, C., Beeson, D., Oosterhuis, H., Chauplannaz, G., Vincent, A. and Newsom-Davis, J. (1997) 'Mutations in Different Functional Domains of the Human Muscle Acetylcholine Receptor α Subunit in Patients with the Slow-Channel congenital Myasthenic Syndrome', *Human Molecular Genetics,* 6(5), pp. 767-774.

Culetto, E., Baylis, H. A., Richmond, J. E., Jones, A. K., Fleming, J. T., Squire, M. D., Lewis, J. A. and Sattelle, D. B. (2004) 'The Caenorhabditis elegans unc-63 Gene Encodes a Levamisole-sensitive Nicotinic Acetylcholine Receptor Subunit', *Journal of Biological Chemistry,* 279(41), pp. 42476-42483.

Dacher, M., Lagarrigue, A. and Gauthier, M. (2005) 'Antennal tactile learning in the honeybee: Effect of nicotinic antagonists on memory dynamics', *Neuroscience,* 130(1), pp. 37-50.

Dale, H. H. (1914) 'The Action of Certain Esters and Ethers of Choline, and their Relation to Muscarine', *Journal of Pharmacology and Experimental Therapeutics,* 6(2), pp. 147.

Dale, R. P., Jones, A. K., Tamborindeguy, C., Davies, T. G. E., Amey, J. S., Williamson, S., Wolstenholme, A., Field, L. M., Williamson, M. S., Walsh, T. K. and Sattelle, D. B. (2010) 'Identification of ion channel genes in the Acyrthosiphon pisum genome', *Insect Molecular Biology,* 19(s2), pp. 141-153.

Dalton, J. (2022) 'Bees will die as ministers approve toxic banned pesticide for second time, warn experts', *Independent* (15th January 2022 edn). Available at: https://www.independent.co.uk/climate-change/news/bees-pesticide-ban-sugar-neonicotinoid-b1993512.html.

Dau, A., Komal, P., Truong, M., Morris, G., Evans, G. and Nashmi, R. (2013) 'RIC-3 differentially modulates α4β2 and α7 nicotinic receptor assembly, expression, and nicotine-induced receptor upregulation', *BMC Neuroscience,* 14(1), pp. 47.

DEFRA (2022) 'Statement of reasons for the decision on the application for emergency authorisation for the use of Cruiser SB on sugar beet crops in 2022', London, United Kingdom: Department of Environment Food and Rural Affairs.

Dewhurst, S. A., Croker, S. G., Ikeda, K. and McCaman, R. E. (1972) 'Metabolism of biogenic amines in Drosophila nervous tissue', *Comp Biochem Physiol B,* 43(4), pp. 975-81.

Dionisio, L., Bergé, I., Bravo, M., Del Carmen Esandi, M. and Bouzat, C. (2015) 'Neurotransmitter GABA activates muscle but not α7 nicotinic receptors', *Molecular Pharmacology,* 87(3), pp. 391-400.

Dunn, S. M. J., Conti-Tronconi, B. M. and Raftery, M. A. (1993) 'A high-affinity site for acetylcholine occurs close to the .alpha.-.gamma. subunit interface of Torpedo nicotinic acetylcholine receptor', *Biochemistry,* 32(33), pp. 8616-8621.

Eimer, S., Gottschalk, A., Hengartner, M., Horvitz, H. R., Richmond, J., Schafer, W. R. and Bessereau, J.-L. (2007) 'Regulation of nicotinic receptor trafficking by the transmembrane Golgi protein UNC-50', *The EMBO Journal,* 26(20), pp. 4313-4323.

FAO's Global Action on Pollination Services for Sustainable Agriculture. Background. Rome, Italy: Food and Agricultural Organisation of the United Nations. Available at: http://www.fao.org/pollination/background/bees-and-other-pollinators/en/ (Accessed: 16/7/20 2020).

Feingold, D., Knogler, L., Starc, T., Drapeau, P., O'Donnell, M. J., Nilson, L. A. and Dent, J. A. (2019) 'secCl is a cys-loop ion channel necessary for the chloride conductance that mediates hormone-induced fluid secretion in Drosophila', *Scientific Reports,* 9(1), pp. 7464.

Feltham, H., Park, K. and Goulson, D. (2014) 'Field realistic doses of pesticide imidacloprid reduce bumblebee pollen foraging efficiency', *Ecotoxicology,* 23(3), pp. 317-323.

Feng, S. H., Zhang, W. X., Yang, J., Yang, Y. and Shen, H. B. (2020) 'Topology Prediction Improvement of α-helical Transmembrane Proteins Through Helix-tail Modeling and Multiscale Deep Learning Fusion', *J Mol Biol,* 432(4), pp. 1279-1296.

Fenton, B., Woodford, J. A. T. and Malloch, G. (1998) 'Analysis of clonal diversity of the peach–potato aphid, *Myzus persicae* (Sulzer), in Scotland, UK and evidence for the existence of a predominant clone', *Molecular Ecology,* 7(11), pp. 1475-1587.

Fitzgerald, J., Kennedy, D., Viseshakul, N., Cohen, B. N., Mattick, J., Bateman, J. F. and Forsayeth, J. R. (2000) 'UNCL, the mammalian homologue of UNC-50, is an inner nuclear membrane RNA-binding protein', *Brain Research,* 877(1), pp. 110-123.

Fleming, J. T., Squire, M. D., Barnes, T. M., Tornoe, C., Matsuda, K., Ahnn, J., Fire, A., Sulston, J. E., Barnard, E. A., Sattelle, D. B. and Lewis, J. A. (1997) '*Caenorhabditis elegans* Levamisole Resistance Genes *lev-1*, *unc-29*, and *unc-38* Encode Functional Nicotinic Acetylcholine Receptor Subunits', *The Journal of Neuroscience,* 17(15), pp. 5843.

Gabler, F., Nam, S.-Z., Till, S., Mirdita, M., Steinegger, M., Söding, J., Lupas, A. N. and Alva, V. (2020) 'Protein Sequence Analysis Using the MPI Bioinformatics Toolkit', *Current Protocols in Bioinformatics,* 72(1), pp. e108.

Galm, U. and Sparks, T. C. (2016) 'Natural product derived insecticides: discovery and development of spinetoram', *Journal of Industrial Microbiology & Biotechnology,* 43(2), pp. 185-193.

Galzi, J.-L., Bertrand, D., Devillers-Thiéry, A., Revah, F., Bertrand, S. and Changeux, J.-P. (1991) 'Functional significance of aromatic amino acids from three peptide loops of the α7 neuronal nicotinic receptor site investigated by site-directed mutagenesis', *FEBS Letters,* 294(3), pp. 198-202.

Gill, R. J., Ramos-Rodriguez, O. and Raine, N. E. (2012) 'Combined pesticide exposure severely affects individual- and colony-level traits in bees', *Nature,* 491(7422), pp. 105-108.

Girolami, V., Mazzon, L., Squartini, A., Mori, N., Marzaro, M., Di Bernardo, A., Greatti, M., Giorio, C. and Tapparo, A. (2009) 'Translocation of neonicotinoid insecticides from coated seeds to seedling guttation drops: a novel way of intoxication for bees', *J Econ Entomol,* 102(5), pp. 1808-15.

Grames, E. and Montgomery, G. (2022) *EntoGEM*: GitHub (Accessed: 29/7/22 2022).

Grauso, M., Reenan, R. A., Culetto, E. and Sattelle, D. B. (2002) 'Novel Putative Nicotinic Acetylcholine Receptor Subunit Genes, Dα5, Dα6 and Dα7, in Drosophila melanogaster Identify a New and Highly Conserved Target of Adenosine Deaminase Acting on RNA-Mediated A-to-I Pre-mRNA Editing', *Genetics,* 160(4), pp. 1519-1533.

Green, K. A. and Cottrell, G. A. (1996) 'Dopamine directly activates a ligand-gated channel in snail neurones', *Pflügers Archiv,* 431(4), pp. 639-644.

Grünewald, B. and Siefert, P. (2019) 'Acetylcholine and Its Receptors in Honeybees: Involvement in Development and Impairments by Neonicotinoids', *Insects,* 10(12).

Gu, S., Matta, Jose A., Lord, B., Harrington, Anthony W., Sutton, Steven W., Davini, Weston B. and Bredt, David S. (2016) 'Brain α7 Nicotinic Acetylcholine Receptor Assembly Requires NACHO', *Neuron,* 89(5), pp. 948-955.

Guo, L., Fan, X.-y., Qiao, X., Montell, C. and Huang, J. (2021) 'An octopamine receptor confers selective toxicity of amitraz on honeybees and Varroa mites', *eLife,* 10, pp. e68268.

Halevi, S., Yassin, L., Eshel, M., Sala, F., Sala, S., Criado, M. and Treinin, M. (2003) 'Conservation within the RIC-3 Gene Family: Effector of Mammalian Nicotinic Acetylcholine Receptor Expression', *Journal of Biological Chemistry,* 278(36), pp. 34411-34417.

Han, P., Niu, C.-Y., Lei, C.-L., Cui, J.-J. and Desneux, N. (2010) 'Use of an innovative T-tube maze assay and the proboscis extension response assay to assess sublethal effects of GM products and pesticides on learning capacity of the honey bee Apis mellifera L', *Ecotoxicology,* 19(8), pp. 1612-1619.

Hardstone, M. C. and Scott, J. G. (2010) 'Is Apis mellifera more sensitive to insecticides than other insects?', *Pest Management Science,* 66(11), pp. 1171-1180.

Haugstetter, J., Blicher, T. and Ellgaard, L. (2005) 'Identification and Characterization of a Novel Thioredoxin-related Transmembrane Protein of the Endoplasmic Reticulum *', *Journal of Biological Chemistry,* 280(9), pp. 8371-8380.

Hawkins, J., Mitchell, E. L. and Jones, A. K. (2022) 'NACHO permits functional heterologous expression of an insect homomeric α6 nicotinic acetylcholine receptor', *Pesticide Biochemistry and Physiology,* 181, pp. 105030.

Henry, M., Béguin, M., Requier, F., Rollin, O., Odoux, J.-F., Aupinel, P., Aptel, J., Tchamitchian, S. and Decourtye, A. (2012) 'A Common Pesticide Decreases Foraging Success and Survival in Honey Bees', *Science,* 336(6079), pp. 348.

Hewlett, S. E., Delahunt Smoleniec, J. D., Wareham, D. M., Pyne, T. M. and Barron, A. B. (2018) 'Biogenic amine modulation of honey bee sociability and nestmate affiliation', *PLOS ONE,* 13(10), pp. e0205686.

Hiruta, E., Aizawa, M., Nakano, A. and Sonoda, S. (2018) 'Nicotinic acetylcholine receptor α6 subunit mutation (G275V) found in a spinosad-resistant strain of the flower thrips, *Frankliniella intonsa* (Thysanoptera: Thripidae)', *Journal of Pesticide Science,* 43(4), pp. 272-276.

Holt, A. R., Alix, A., Thompson , A. and Maltby , L. (2016) 'Food production, ecosystem services and biodiversity: We can't have it all everywhere', *Science of the Total Environment,* 573, pp. 1422-1429.

Homem, R. A., Buttery, B., Richardson, E., Tan, Y., Field, L. M., Williamson, M. S. and Emyr Davies, T. G. (2020) 'Evolutionary trade-offs of insecticide resistance — The fitness costs associated with target-site mutations in the nAChR of Drosophila melanogaster', *Molecular Ecology,* 29(14), pp. 2661-2675.

Hou, C.-Y. (2019) 'EPA Cancels Registrations for 12 Neonicotinoid Pesticides', *The Scientist*.

Huang, J., Zhang, Z., Feng, W., Zhao, Y., Aldanondo, A., de Brito Sanchez, M. G., Paoli, M., Rolland, A., Li, Z., Nie, H., Lin, Y., Zhang, S., Giurfa, M. and Su, S. (2022) 'Food wanting is mediated by transient activation of dopaminergic signaling in the honey bee brain', *Science,* 376(6592), pp. 508-512.

Huang, Y., Williamson, M. S., Devonshire, A. L., Windass, J. D., Lansdell, S. J. and Millar, N. S. (1999) 'Molecular Characterization and Imidacloprid Selectivity of Nicotinic Acetylcholine Receptor Subunits from the Peach-Potato Aphid Myzus persicae', *Journal of Neurochemistry,* 73(1), pp. 380-389.

Huang, Y., Williamson, M. S., Devonshire, A. L., Windass, J. D., Lansdell, S. J. and Millar, N. S. (2000) 'Cloning, heterologous expression and co-assembly of Mpβ1, a nicotinic acetylcholine receptor subunit from the aphid Myzus persicae', *Neuroscience Letters,* 284(1), pp. 116-120.

Ihara, M., Buckingham, S. D., Matsuda, K. and Sattelle, D. B. (2017) 'Modes of Action, Resistance and Toxicity of Insecticides Targeting Nicotinic Acetylcholine Receptors', *Current Medicinal Chemistry,* 24(27), pp. 2925-2934.

Ihara, M., Furutani, S., Shigetou, S., Shimada, S., Niki, K., Komori, Y., Kamiya, M., Koizumi, W., Magara, L., Hikida, M., Noguchi, A., Okuhara, D., Yoshinari, Y., Kondo, S., Tanimoto, H., Niwa, R., Sattelle, D. B. and Matsuda, K. (2020) 'Cofactor-enabled functional expression of fruit fly, honeybee, and bumblebee nicotinic receptors reveals picomolar neonicotinoid actions', *Proceedings of the National Academy of Sciences*, pp. 202003667.

Ihara, M., Hikida, M., Matsushita, H., Yamanaka, K., Kishimoto, Y., Kubo, K., Watanabe, S., Sakamoto, M., Matsui, K., Yamaguchi, A., Okuhara, D., Furutani, S., Sattelle, D. B. and Matsuda, K. (2018) 'Loops D, E and G in the Drosophila Dα1 subunit contribute to high neonicotinoid sensitivity of Dα1-chicken β2 nicotinic acetylcholine receptor', *British Journal of Pharmacology,* 175(11), pp. 1999-2012.

Ihara, M., Okajima, T., Yamashita, A., Oda, T., Asano, T., Matsui, M., Sattelle, D. B. and Matsuda, K. (2014) 'Studies on an Acetylcholine Binding Protein Identify a Basic Residue in Loop G on the β1 Strand as a New Structural Determinant of Neonicotinoid Actions', *Molecular Pharmacology,* 86(6), pp. 736-746.

Ihara, M., Okajima, T., Yamashita, A., Oda, T., Hirata, K., Nishiwaki, H., Morimoto, T., Akamatsu, M., Ashikawa, Y., Kuroda, S. i., Mega, R., Kuramitsu, S., Sattelle, D. B. and Matsuda, K. (2008) 'Crystal structures of Lymnaea stagnalis AChBP in complex with neonicotinoid insecticides imidacloprid and clothianidin', *Invertebrate Neuroscience,* 8(2), pp. 71-81.

Jensen, M. L., Schousboe, A. and Ahring, P. K. (2005) 'Charge selectivity of the Cys-loop family of ligand-gated ion channels', *Journal of Neurochemistry,* 92(2), pp. 217-225.

Jones, A. K. (2018) 'Genomics, cys-loop ligand-gated ion channels and new targets for the control of insect pests and vectors', *Current Opinion in Insect Science,* 30, pp. 1-7.

Jones, A. K., Bera, A. N., Lees, K. and Sattelle, D. B. (2010) 'The cys-loop ligand-gated ion channel gene superfamily of the parasitoid wasp, Nasonia vitripennis', *Heredity,* 104(3), pp. 247-259.

Jones, A. K., Brown, L. A. and Sattelle, D. B. (2007) 'Insect nicotinic acetylcholine receptor gene families: from genetic model organism to vector, pest and beneficial species', *Invertebrate Neuroscience,* 7(1), pp. 67-73.

Jones, A. K., Buckingham, S. D., Brown, L. A. and Sattelle, D. B. (2009) 'Alternative splicing of the Anopheles gambiae nicotinic acetylcholine receptor, Agamαβ9, generates both alpha and beta subunits', *Invertebrate Neuroscience,* 9(2), pp. 77.

Jones, A. K., Goven, D., Froger, J.-A., Bantz, A. and Raymond, V. (2020) 'The cys-loop ligand-gated ion channel gene superfamilies of the cockroaches Blattella germanica and Periplaneta americana', *Pest Management Science,* 77, pp. 3787–3799.

Jones, A. K., Grauso, M. and Sattelle, D. B. (2005) 'The nicotinic acetylcholine receptor gene family of the malaria mosquito, Anopheles gambiae', *Genomics,* 85(2), pp. 176-187.

Jones, A. K., Marshall, J., Blake, A. D., Buckingham, S. D., Darlison, M. G. and Sattelle, D. B. (2005) 'Sgβ1, a novel locust (Schistocerca gregaria) non-α nicotinic acetylcholine receptor-like subunit with homology to the Drosophila melanogaster Dβ1 subunit', *Invertebrate Neuroscience,* 5(3), pp. 147-155.

Jones, A. K., Raymond-Delpech, V., Thany, S. H., Gauthier, M. and Sattelle, D. B. (2006) 'The nicotinic acetylcholine receptor gene family of the honey bee, Apis mellifera', *Genome Research,* 16, pp. 1422-1430.

Jones, A. K. and Sattelle, D. B. (2007) 'The cys-loop ligand-gated ion channel gene superfamily of the red flour beetle, Tribolium castaneum', *BMC Genomics,* 8(1), pp. 327.

Jones, A. K. and Sattelle, D. B. (2008) 'The cys-loop ligand-gated ion channel gene superfamily of the nematode, Caenorhabditis elegans', *Invertebrate Neuroscience,* 8(1), pp. 41-47.

Jones, A. K. and Sattelle, D. B. (2010) 'Diversity of Insect Nicotinic Acetylcholine Receptor Subunits', in Thany, S.H. (ed.) *Insect Niotinic Acetylcholine Receptors.* 1 ed: Landes Bioscience and Springer Science+Business Media, pp. 25-43.

Jones, D. T., Taylor, W. R. and Thornton, J. M. (1992) 'The rapid generation of mutation data matrices from protein sequences', *Bioinformatics,* 8(3), pp. 275-282.

Kamhi, J. F., Arganda, S., Moreau, C. S. and Traniello, J. F. A. (2017) 'Origins of Aminergic Regulation of Behavior in Complex Insect Social Systems', *Frontiers in Systems Neuroscience,* 11.

Kirwan, M. J. (2003) *Molecular characterisation of insect nicotinic acetylcholine receptors.* Ph.D., University College London United Kingdom.

Kita, T., Irie, T., Nomura, K., Ozoe, F. and Ozoe, Y. (2017) 'Pharmacological characterization of histamine-gated chloride channels from the housefly Musca domestica', *NeuroToxicology,* 60, pp. 245-253.

Klappenbach, M., Kaczer, L. and Locatelli, F. (2013) 'Dopamine interferes with appetitive long-term memory formation in honey bees', *Neurobiology of Learning and Memory,* 106, pp. 230-237.

Komonen, A., Halme, P. and Kotiaho, J. S. (2019) 'Alarmist by bad design: Strongly popularized unsubstantiated claims undermine credibility of conservation science', *Rethinking Ecology,* 4, pp. 17-19.

Kumar, G., Singh, S. and Pramod Kodigenahalli Nagarajaiah, R. (2020) 'Detailed Review on Pesticidal Toxicity to Honey Bees and Its Management ', in *Modern Beekeeping (Working Title)* [Online]. Version.

Kumar, S., Stecher, G., Li, M., Knyaz, C. and Tamura, K. (2018) 'MEGA X: Molecular Evolutionary Genetics Analysis across Computing Platforms', *Molecular Biology and Evolution,* 35(6), pp. 1547-1549.

Kweon, H.-J., Gu, S., Witham, E., Dhara, M., Yu, H., Mandon, E. D., Jawhari, A. and Bredt, D. S. (2020) 'NACHO Engages N-Glycosylation ER Chaperone Pathways for α7 Nicotinic Receptor Assembly', *Cell Reports,* 32(6), pp. 108025.

Lansdell, S. J., Collins, T., Goodchild, J. and Millar, N. S. (2012) 'The D*rosophila* nicotinic acetylcholine receptor subunits Dα5 and Dα7 form functional homomeric and heteromeric ion channels', *BMC Neuroscience,* 13(73).

Lansdell, S. J., Collins, T., Yabe, A., Gee, V. J., Gibb, A. J. and Millar, N. S. (2008) 'Host-cell specific effects of the nicotinic acetylcholine receptor chaperone RIC-3 revealed by a comparison of human and Drosophila RIC-3 homologues', *Journal of Neurochemistry,* 105(5), pp. 1573-1581.

Lansdell, S. J., Gee, V. J., Harkness, P. C., Doward, A. I., Baker, E. R., Gibb, A. J. and Millar, N. S. (2005) 'RIC-3 Enhances Functional Expression of Multiple Nicotinic Acetylcholine Receptor Subtypes in Mammalian Cells', *Molecular Pharmacology,* 68(5), pp. 1431-1438.

Lansdell, S. J. and Millar, N. S. (2000a) 'Cloning and heterologous expression of Dα4, a Drosophila neuronal nicotinic acetylcholine receptor subunit: identification of an alternative exon influencing the efficiency of subunit assembly', *Neuropharmacology,* 39(13), pp. 2604-2614.

Lansdell, S. J. and Millar, N. S. (2000b) 'The influence of nicotinic receptor subunit composition upon agonist, α–bungarotoxin and insecticide (imidacloprid) binding affinity', *Neuropharmacology,* 39(4), pp. 671-679.

Lewis, J. A., Wu, C. H., Berg, H. and Levine, J. H. (1980) 'The genetics of levamisole resistance in the nematode Caenorhabditis elegans', *Genetics,* 95(4), pp. 905-28.

Linn, M., Glaser, S. M., Peng, T. and Grüter, C. (2020) 'Octopamine and dopamine mediate waggle dance following and information use in honeybees', *Proceedings of the Royal Society B: Biological Sciences,* 287(1936), pp. 20201950.

Liu, Y.-p., Lin, K.-j., Liu, Y., Gui, F.-r. and Wang, G.-r. (2013) 'Nicotinic Acetylcholine Receptor Gene Family of the Pea Aphid, Acyrthosiphon pisum', *Journal of Integrative Agriculture,* 12(11), pp. 2083-2091.

Lu, C., Hung, Y.-T. and Cheng, Q. (2020) 'A Review of Sub-lethal Neonicotinoid Insecticides Exposure and Effects on Pollinators', *Current Pollution Reports,* 6(2), pp. 137-151.

Lu, W., Liu, Z., Fan, X., Zhang, X., Qiao, X. and Huang, J. (2022) 'Nicotinic acetylcholine receptor modulator insecticides act on diverse receptor subtypes with distinct subunit compositions', *PLOS Genetics,* 18(1), pp. e1009920.

Ludwiczak, J., Winski, A., Szczepaniak, K., Alva, V. and Dunin-Horkawicz, S. (2019) 'DeepCoil-a fast and accurate prediction of coiled-coil domains in protein sequences', *Bioinformatics,* 35(16), pp. 2790-2795.

Lämsä, J., Kuusela, E., Tuomi, J., Juntunen, S. and Watts, P. C. (2018) 'Low dose of neonicotinoid insecticide reduces foraging motivation of bumblebees', *Proceedings of the Royal Society B: Biological Sciences,* 285(1883), pp. 20180506.

Mancini, N., Giurfa, M., Sandoz, J.-C. and Avarguès-Weber, A. (2018) 'Aminergic neuromodulation of associative visual learning in harnessed honey bees', *Neurobiology of Learning and Memory,* 155, pp. 556-567.

Mandelzys, A., De Koninck, P. and Cooper, E. (1995) 'Agonist and toxin sensitivities of ACh-evoked currents on neurons expressing multiple nicotinic ACh receptor subunits', *Journal of Neurophysiology,* 74(3), pp. 1212-1221.

Manjon, C., Troczka, B. J., Zaworra, M., Beadle, K., Randall, E., Hertlein, G., Singh, K. S., Zimmer, C. T., Homem, R. A., Lueke, B., Reid, R., Kor, L., Kohler, M., Benting, J., Williamson, M. S., Davies, T. G. E., Field, L. M., Bass, C. and Nauen, R. (2018) 'Unravelling the Molecular Determinants of Bee Sensitivity to Neonicotinoid Insecticides', *Current Biology,* 28(7), pp. 1137-1143.e5.

Marshall, J., Buckingham, S. D., Shingai, R., Lunt, G. G., Goosey, M. W., Darlison, M. G., Sattelle, D. B. and Barnard, E. A. (1990) 'Sequence and functional expression of a single alpha subunit of an insect nicotinic acetylcholine receptor', *The EMBO Journal,* 9(13), pp. 4391-4398.

Matsuda, K., Ihara, M. and Sattelle, D. B. (2020) 'Neonicotinoid Insecticides: Molecular Targets, Resistance, and Toxicity', *Annual Review of Pharmacology and Toxicology,* 60(1), pp. 241-255.

Matsuyama, S., Nagao, T. and Sasaki, K. (2015) 'Consumption of tyrosine in royal jelly increases brain levels of dopamine and tyramine and promotes transition from normal to reproductive workers in queenless honey bee colonies', *General and Comparative Endocrinology,* 211, pp. 1-8.

Matta, J. A., Gu, S., Davini, W. B., Lord, B., Siuda, E. R., Harrington, A. W. and Bredt, D. S. (2017) 'NACHO Mediates Nicotinic Acetylcholine Receptor Function throughout the Brain', *Cell Reports,* 19(4), pp. 688-696.

Mazzaferro, S., Whiteman, S. T., Alcaino, C., Beyder, A. and Sine, S. M. (2020) 'NACHO and 14-3-3 promote expression of distinct subunit stoichiometries of the α4β2 acetylcholine receptor', *Cellular and Molecular Life Sciences*.

Mercer, A. R., Mobbs, P. G., Davenport, A. P. and Evans, P. D. (1983) 'Biogenic amines in the brain of the honeybee, Apis mellifera', *Cell and Tissue Research,* 234(3), pp. 655-677.

Middleton, R. E. and Cohen, J. B. (1991) 'Mapping of the acetylcholine binding site of the nicotinic acetylcholine receptor: [3H]nicotine as an agonist photoaffinity label', *Biochemistry,* 30(28), pp. 6987-6997.

Millar, N. S. (2009) 'A review of experimental techniques used for the heterologous expression of nicotinic acetylcholine receptors', *Biochemical Pharmacology,* 78(7), pp. 766-776.

Millar, N. S. and Denholm, I. (2007) 'Nicotinic acetylcholine receptors: targets for commercially important insecticides', *Invertebrate Neuroscience,* 7(1), pp. 53-66.

Miller, K. G., Alfonso, A., Nguyen, M., Crowell, J. A., Johnson, C. D. and Rand, J. B. (1996) 'A genetic selection for Caenorhabditis elegans synaptic transmission mutants', *Proceedings of the National Academy of Sciences,* 93(22), pp. 12593-12598.

Mitchell, E. L., Viscarra, F., Bermudez, I., Hawkins, J., Goodchild, J. A. and Jones, A. K. (2022) 'The Apis mellifera alpha 5 nicotinic acetylcholine receptor subunit expresses as a homomeric receptor that is sensitive to serotonin', *Pesticide Biochemistry and Physiology*, pp. 105055.

Morales-Perez, C. L., Noviello, C. M. and Hibbs, R. E. (2016) 'X-ray structure of the human α4β2 nicotinic receptor', *Nature,* 538, pp. 411.

Morton, D. B. and Evans, P. D. (1984) 'Octopamine Release from an Identified Neurone in the Locust', *Journal of Experimental Biology,* 113(1), pp. 269-287.

Morud, J., Hardege, I., Liu, H., Wu, T., Choi, M.-K., Basu, S., Zhang, Y. and Schafer, W. R. (2021) 'Deorphanization of novel biogenic amine-gated ion channels identifies a new serotonin receptor for learning', *Current Biology,* 31(19), pp. 4282-4292.e6.

Mottet, C., Fontaine, S., Caddoux, L., Brazier, C., Mahéo, F., Simon, J.-C., Micoud, A. and Roy, L. (2016) 'Assessment of the Dominance Level of the R81T Target Resistance to Two Neonicotinoid Insecticides in Myzus persicae (Hemiptera: Aphididae)', *Journal of Economic Entomology,* 109(5), pp. 2182-2189.

Mukherjee, J., Kuryatov, A., Moss, S. J., Lindstrom, J. M. and Anand, R. (2009) 'Mutations of cytosolic loop residues impair assembly and maturation of α7 nicotinic acetylcholine receptors', *Journal of Neurochemistry,* 110(6), pp. 1885-1894.

Mulcahy, M. J., Blattman, S. B., Barrantes, F. J., Lukas, R. J. and Hawrot, E. (2015) 'Resistance to Inhibitors of Cholinesterase 3 (Ric-3) Expression Promotes Selective Protein Associations with the Human α7-Nicotinic Acetylcholine Receptor Interactome', *PLOS ONE,* 10(8), pp. e0134409.

Mustard, J. A. (2020) 'Neuroactive nectar: compounds in nectar that interact with neurons', *Arthropod-Plant Interactions,* 14(2), pp. 151-159.

Muth, F., Philbin, C. S., Jeffrey, C. S. and Leonard, A. S. (2022) 'Discovery of octopamine and tyramine in nectar and their effects on bumblebee behavior', *iScience,* 25(8), pp. 104765.

Nirthanan, S., Ziebell, M. R., Chiara, D. C., Hong, F. and Cohen, J. B. (2005) 'Photolabeling the Torpedo Nicotinic Acetylcholine Receptor with 4-Azido-2,3,5,6-tetrafluorobenzoylcholine, a Partial Agonist', *Biochemistry,* 44(41), pp. 13447-13456.

Nouvian, M., Mandal, S., Jamme, C., xe, ne, Claudianos, C., d'Ettorre, P., Reinhard, J., Barron, A. B. and Giurfa, M. (2018) 'Cooperative defence operates by social modulation of biogenic amine levels in the honey bee brain', *Proceedings: Biological Sciences,* 285(1871), pp. 1-9.

Noviello, C. M., Gharpure, A., Mukhtasimova, N., Cabuco, R., Baxter, L., Borek, D., Sine, S. M. and Hibbs, R. E. (2021) 'Structure and gating mechanism of the α7 nicotinic acetylcholine receptor', *Cell*.

Oldroyd, B. P. (2007) 'What's Killing American Honey Bees?', *PLOS Biology,* 5(6), pp. e168.

Orchard, I. (1990) 'Tyrosine hydroxylase-like immunoreactivity in previously described catecholamine-containing neurones in the ventral nerve cord of Rhodnius prolixus', *Journal of Insect Physiology,* 36(8), pp. 593-600.

Osaka, H., Sugiyama, N. and Taylor, P. (1998) 'Distinctions in Agonist and Antagonist Specificity Conferred by Anionic Residues of the Nicotinic Acetylcholine Receptor', *Journal of Biological Chemistry,* 273(21), pp. 12758-12765.

Osborne, R. H. (1996) 'Insect neurotransmission: Neurotransmitters and their receptors', *Pharmacology & Therapeutics,* 69(2), pp. 117-142.

Outhwaite, C. L., McCann, P. and Newbold, T. (2022) 'Agriculture and climate change are reshaping insect biodiversity worldwide', *Nature*.

Panini, M., Dradi, D., Marani, G., Butturini, A. and Mazzoni, E. (2014) 'Detecting the presence of target-site resistance to neonicotinoids and pyrethroids in Italian populations of Myzus persicae', *Pest Management Science,* 70(6), pp. 931-938.

Papke, R. L., Bencherif, M. and Lippiello, P. (1996) 'An evaluation of neuronal nicotinic acetylcholine receptor activation by quaternary nitrogen compounds indicates that choline is selective for the α7 subtype', *Neuroscience Letters,* 213(3), pp. 201-204.

Peden, A. S., Mac, P., Fei, Y.-J., Castro, C., Jiang, G., Murfitt, K. J., Miska, E. A., Griffin, J. L., Ganapathy, V. and Jorgensen, E. M. (2013) 'Betaine acts on a ligand-gated ion channel in the nervous system of the nematode C. elegans', *Nature Neuroscience,* 16(12), pp. 1794-1801.

Pedersen, J. E., Bergqvist, C. A. and Larhammar, D. (2019) 'Evolution of vertebrate nicotinic acetylcholine receptors', *BMC Evolutionary Biology,* 19(1), pp. 38.

Peng, X., Katz, M., Gerzanich, V., Anand, R. and Lindstrom, J. (1994) 'Human alpha 7 acetylcholine receptor: cloning of the alpha 7 subunit from the SH-SY5Y cell line and determination of pharmacological properties of native receptors and functional alpha 7 homomers expressed in Xenopus oocytes', *Molecular Pharmacology,* 45(3), pp. 546.

Peng, Y.-C. and Yang, E.-C. (2016) 'Sublethal Dosage of Imidacloprid Reduces the Microglomerular Density of Honey Bee Mushroom Bodies', *Scientific Reports,* 6(1), pp. 19298.

Perry, T., Chen, W., Ghazali, R., Yang, Y. T., Christesen, D., Martelli, F., Lumb, C., Bao Luong, H. N., Mitchell, J., Holien, J. K., Parker, M. W., Sparks, T. C. and Batterham, P. (2021) 'Role of nicotinic acetylcholine receptor subunits in the mode of action of neonicotinoid, sulfoximine and spinosyn insecticides in Drosophila melanogaster', *Insect Biochemistry and Molecular Biology,* 131, pp. 103547.

Perry, T., Somers, J., Yang, Y. T. and Batterham, P. (2015) 'Expression of insect α6-like nicotinic acetylcholine receptors in Drosophila melanogaster highlights a high level of conservation of the receptor:spinosyn interaction', *Insect Biochemistry and Molecular Biology,* 64, pp. 106-115.

Prescott, D. J., Hildebrand, J. G., Sanes, J. R. and Jewett, S. (1977) 'Biochemical and developmental studies of acetylcholine metabolism in the central nervous system of the moth Manduca sexta', *Comparative Biochemistry and Physiology Part C: Comparative Pharmacology,* 56(2), pp. 77-84.

Puinean, M., A., Lansdell, J., S., Collins, Toby, Bielza, Pablo, Millar and S., N. (2012) 'A nicotinic acetylcholine receptor transmembrane point mutation (G275E) associated with resistance to spinosad in *Frankliniella occidentalis*', *Journal of Neurochemistry,* 124(5), pp. 590-601.

Puinean, A. M., Foster, S. P., Oliphant, L., Denholm, I., Field, L. M., Millar, N. S., Williamson, M. S. and Bass, C. (2010) 'Amplification of a Cytochrome P450 Gene Is Associated with Resistance to Neonicotinoid Insecticides in the Aphid Myzus persicae', *PLOS Genetics,* 6(6), pp. e1000999.

Raza, M. F., Wang, T., Li, Z., Nie, H., Giurfa, M., Husain, A., Hlaváč, P., Kodrik, M., Ali, M. A., Rady, A. and Su, S. (2022) 'Biogenic amines mediate learning success in appetitive odor conditioning in honeybees', *Journal of King Saud University - Science,* 34(4), pp. 101928.

Rettinger, J., Schwarz, S. and Schwarz, W. (2016) *Electrophysiology: Basics, Modern Approaches and Applications.* First edn. Switzerland: Springer International Publishing.

Rex, E. B., Shukla, N., Gu, S., Bredt, D. and DiSepio, D. (2016) 'A Genome-Wide Arrayed cDNA Screen to Identify Functional Modulators of α7 Nicotinic Acetylcholine Receptors', *SLAS DISCOVERY: Advancing the Science of Drug Discovery,* 22(2), pp. 155-165.

Ringstad, N., Abe, N. and Horvitz, H. R. (2009) 'Ligand-Gated Chloride Channels Are Receptors for Biogenic Amines in C. elegans', *Science,* 325(5936), pp. 96-100.

Rittschof, C. C., Vekaria, H. J., Palmer, J. H. and Sullivan, P. G. (2019) 'Biogenic amines and activity levels alter the neural energetic response to aggressive social cues in the honey bee Apis mellifera', *Journal of Neuroscience Research,* 97(8), pp. 991-1003.

Robinson, G. E., Fahrbach, S. E. and Winston, M. L. (1997) 'Insect societies and the molecular biology of social behavior', *BioEssays,* 19(12), pp. 1099-1108.

Rodriguez Araujo, N., Hernando, G., Corradi, J. and Bouzat, C. (2022) 'The nematode serotonin-gated chloride channel MOD-1: A novel target for anthelmintic therapy', *Journal of Biological Chemistry,* 298(9).

Roeder, T. (1994) 'Biogenic amines and their receptors in insects', *Comparative Biochemistry and Physiology Part C: Pharmacology, Toxicology and Endocrinology,* 107(1), pp. 1-12.

Rothlin, C. V., Lioudyno, M. I., Silbering, A. F., Plazas, P. V., Gomez Casati, M. E., Katz, E., Guth, P. S. and Elgoyhen, A. B. (2003) 'Direct interaction of serotonin type 3 receptor ligands with recombinant and native α9α10-containing nicotinic cholinergic receptors', *Molecular Pharmacology,* 63(5), pp. 1067-1074.

Rufener, L., Bedoni, N., Baur, R., Rey, S., Glauser, D. A., Bouvier, J., Beech, R., Sigel, E. and Puoti, A. (2013) 'acr-23 Encodes a Monepantel-Sensitive Channel in Caenorhabditis elegans', *PLOS Pathogens,* 9(8), pp. e1003524.

Rufener, L., Kaur, K., Sarr, A., Aaen, S. M. and Horsberg, T. E. (2020) 'Nicotinic acetylcholine receptors: Ex-vivo expression of functional, non-hybrid, heteropentameric

receptors from a marine arthropod, Lepeophtheirus salmonis', *PLOS Pathogens,* 16(7), pp. e1008715.

Sadd, B. M., Barribeau, S. M., Bloch, G., de Graaf, D. C., Dearden, P., Elsik, C. G., Gadau, J., Grimmelikhuijzen, C. J. P., Hasselmann, M., Lozier, J. D., Robertson, H. M., Smagghe, G., Stolle, E., Van Vaerenbergh, M., Waterhouse, R. M., Bornberg-Bauer, E., Klasberg, S., Bennett, A. K., Câmara, F., Guigó, R., Hoff, K., Mariotti, M., Munoz-Torres, M., Murphy, T., Santesmasses, D., Amdam, G. V., Beckers, M., Beye, M., Biewer, M., Bitondi, M. M. G., Blaxter, M. L., Bourke, A. F. G., Brown, M. J. F., Buechel, S. D., Cameron, R., Cappelle, K., Carolan, J. C., Christiaens, O., Ciborowski, K. L., Clarke, D. F., Colgan, T. J., Collins, D. H., Cridge, A. G., Dalmay, T., Dreier, S., du Plessis, L., Duncan, E., Erler, S., Evans, J., Falcon, T., Flores, K., Freitas, F. C. P., Fuchikawa, T., Gempe, T., Hartfelder, K., Hauser, F., Helbing, S., Humann, F. C., Irvine, F., Jermiin, L. S., Johnson, C. E., Johnson, R. M., Jones, A. K., Kadowaki, T., Kidner, J. H., Koch, V., Köhler, A., Kraus, F. B., Lattorff, H. M. G., Leask, M., Lockett, G. A., Mallon, E. B., Antonio, D. S. M., Marxer, M., Meeus, I., Moritz, R. F. A., Nair, A., Näpflin, K., Nissen, I., Niu, J., Nunes, F. M. F., Oakeshott, J. G., Osborne, A., Otte, M., Pinheiro, D. G., Rossié, N., Rueppell, O., Santos, C. G., Schmid-Hempel, R., Schmitt, B. D., Schulte, C., Simões, Z. L. P., Soares, M. P. M., Swevers, L., Winnebeck, E. C., Wolschin, F., Yu, N., Zdobnov, E. M., Aqrawi, P. K., Blankenburg, K. P., Coyle, M., Francisco, L., Hernandez, A. G., Holder, M., Hudson, M. E., Jackson, L., Jayaseelan, J., Joshi, V., Kovar, C., Lee, S. L., Mata, R., Mathew, T., Newsham, I. F., Ngo, R., Okwuonu, G., Pham, C., Pu, L.-L., Saada, N., Santibanez, J., Simmons, D., Thornton, R., Venkat, A., Walden, K. K. O., Wu, Y.-Q., Debyser, G., Devreese, B., Asher, C., Blommaert, J., Chipman, A. D., Chittka, L., Fouks, B., Liu, J., O'Neill, M. P., Sumner, S., Puiu, D., Qu, J., Salzberg, S. L., Scherer, S. E., Muzny, D. M., Richards, S., Robinson, G. E., Gibbs, R. A., Schmid-Hempel, P. and Worley, K. C. (2015) 'The genomes of two key bumblebee species with primitive eusocial organization', *Genome Biology,* 16(1), pp. 76.

Sakai, Y., Sekiguchi, M., Okamoto, K., Kuwano, R.-z. and Takahashi, Y. (1990) 'Dopamine receptors expressed in the Xenopus oocytes injected with bovine striatal mRNA', *Molecular Brain Research,* 7(2), pp. 183-187.

Saras, A., Gisselmann, G., Vogt-Eisele, A. K., Erlkamp, K. S., Kletke, O., Pusch, H. and Hatt, H. (2008) 'Histamine Action on Vertebrate $GABA_A$ Receptors: Direct Channel Gating and Potentiation of GABA Responses', *Journal of Biological Chemistry,* 283(16), pp. 10470-10475.

Sattelle, D. B. (1980) 'Acetylcholine receptors of insects.', *Adv. Insect. Physiol.,* 15, pp. 215-315.

Sattelle, D. B., Jones, A. K., Sattelle, B. M., Matsuda, K., Reenan, R. and Biggin, P. C. (2005) 'Edit, cut and paste in the nicotinic acetylcholine receptor gene family of Drosophila melanogaster', *BioEssays,* 27(4), pp. 366-376.

Savary, S., Willocquet, L., Pethybridge, S. J., Esker, P., McRoberts, N. and Nelson, A. (2019) 'The global burden of pathogens and pests on major food crops', *Nature Ecology & Evolution,* 3(3), pp. 430-439.

Sawruk, E., Schloss, P., Betz, H. and Schmitt, B. (1990) 'Heterogeneity of Drosophila nicotinic acetylcholine receptors: SAD, a novel developmentally regulated alpha-subunit', *The EMBO Journal,* 9(9), pp. 2671-2677.

Schilcher, F., Thamm, M., Strube-Bloss, M. and Scheiner, R. (2021) 'Opposing Actions of Octopamine and Tyramine on Honeybee Vision', *Biomolecules,* 11(9).

Schulz, R., Sawruk, E., Mülhardt, C., Bertrand, S., Baumann, A., Phannavong, B., Betz, H., Bertrand, D., Gundelfinger, E. D. and Schmitt, B. (1998) 'Dα3, a New Functional α Subunit of Nicotinic Acetylcholine Receptors from Drosophila', *Journal of Neurochemistry,* 71(2), pp. 853-862.

Schäfer, S. and Rehder, V. (1989) 'Dopamine-like immunoreactivity in the brain and suboesophageal ganglion of the honeybee', *Journal of Comparative Neurology,* 280(1), pp. 43-58.

Scott, C. and Bilsborrow, P. E. (2019) 'The impact of the EU neonicotinoid seed-dressing ban on oilseed rape production in England', *Pest Management Science,* 75(1), pp. 125-133.

Seeburg, P. H. (2002) 'A-to-I Editing: New and Old Sites, Functions and Speculations', *Neuron,* 35(1), pp. 17-20.

Selyunin, A. S., Iles, L. R., Bartholomeusz, G. and Mukhopadhyay, S. (2017) 'Genome-wide siRNA screen identifies UNC50 as a regulator of Shiga toxin 2 trafficking', *Journal of Cell Biology,* 216(10), pp. 3249-3262.

Sgard, F., Fraser, S. P., Katkowska, M. J., Djamgoz, M. B. A., Dunbar, S. J. and Windass, J. D. (1998) 'Cloning and Functional Characterisation of Two Novel Nicotinic Acetylcholine Receptor α Subunits from the Insect Pest Myzus persicae', *Journal of Neurochemistry,* 71(3), pp. 903-912.

Shao, Y.-M., Dong, K. and Zhang, C.-X. (2007) 'The nicotinic acetylcholine receptor gene family of the silkworm, Bombyx mori', *BMC Genomics,* 8(1), pp. 324.

Shelukhina, I., Spirova, E., Kudryavtsev, D., Ojomoko, L., Werner, M., Methfessel, C., Hollmann, M. and Tsetlin, V. (2017) 'Calcium imaging with genetically encoded sensor Case12: Facile analysis of α7/α9 nAChR mutants', *PLOS ONE,* 12(8), pp. e0181936.

Shimomura, M., Satoh, H., Yokota, M., Ihara, M., Matsuda, K. and Sattelle, D. B. (2005) 'Insect-vertebrate chimeric nicotinic acetylcholine receptors identify a region, loop B to the N-terminus of the Drosophila Dα2 subunit, which contributes to neonicotinoid sensitivity', *Neuroscience Letters,* 385(2), pp. 168-172.

Silva, W. M., Berger, M., Bass, C., Williamson, M., Moura, D. M. N., Ribeiro, L. M. S. and Siqueira, H. A. A. (2016) 'Mutation (G275E) of the nicotinic acetylcholine receptor α6 subunit is associated with high levels of resistance to spinosyns in T*uta absoluta* (Meyrick) (Lepidoptera: Gelechiidae)', *Pesticide Biochemistry and Physiology,* 131, pp. 1-8.

Sine, S. M., Quiram, P., Papanikolaou, F., Kreienkamp, H. J. and Taylor, P. (1994) 'Conserved tyrosines in the alpha subunit of the nicotinic acetylcholine receptor stabilize quaternary ammonium groups of agonists and curariform antagonists', *Journal of Biological Chemistry,* 269(12), pp. 8808-8816.

Slater, R., Paul, V. L., Andrews, M., Garbay, M. and Camblin, P. (2012) 'Identifying the presence of neonicotinoidresistant peach-potato aphid (Myzus persicae) in the peach-growing regions of southern France and northern Spain', *Pest Management Science,* 68(4), pp. 634-638.

Somers, J., Luong, H. N. B., Mitchell, J., Batterham, P. and Perry, T. (2017) 'Pleiotropic effects of loss of the Dα1 subunit in Drosophila melanogaster: Implications for insecticide resistance', *Genetics,* 205(1), pp. 263-271.

Somers, J., Nguyen, J., Lumb, C., Batterham, P. and Perry, T. (2015) 'In vivo functional analysis of the Drosophila melanogaster nicotinic acetylcholine receptor Dα6 using the insecticide spinosad', *Insect Biochemistry and Molecular Biology,* 64, pp. 116-127.

Sparks, T. C., Storer, N., Porter, A., Slater, R. and Nauen, R. (2021) 'Insecticide resistance management and industry: the origins and evolution of the Insecticide Resistance Action Committee (IRAC) and the mode of action classification scheme', *Pest Management Science,* 77(6), pp. 2609-2619.

Sánchez-Bayo, F. and Wyckhuys, K. A. G. (2019) 'Worldwide decline of the entomofauna: A review of its drivers', *Biological Conservation,* 232, pp. 8-27.

Takayama, K., Ito, R., Yamamoto, H., Otsubo, S., Matsumoto, R., Ojima, H., Komori, Y., Matsuda, K. and Ihara, M. (2022) 'Effects of cofactors RIC-3, TMX3 and UNC-50, together with distinct subunit ratios on the agonist actions of imidacloprid on Drosophila melanogaster Dα1/Dβ1 nicotinic acetylcholine receptors expressed in Xenopus laevis oocytes', *Pesticide Biochemistry and Physiology,* 187, pp. 105177.

Tasneem, A., Iyer, L. M., Jakobsson, E. and Aravind, L. (2004) 'Identification of the prokaryotic ligand-gated ion channels and their implications for the mechanisms and origins of animal Cys-loop ion channels', *Genome Biology,* 6(1), pp. R4.

Thany, S. H., Crozatier, M., Raymond-Delpech, V., Gauthier, M. and Lenaers, G. (2005) 'Apisα2, Apisα7-1 and Apisα7-2: three new neuronal nicotinic acetylcholine receptor α-subunits in the honeybee brain', *Gene,* 344, pp. 125-132.

Thomas, C. D., Jones, T. H. and Hartley, S. E. (2019) '"Insectageddon": A call for more robust data and rigorous analyses', *Global Change Biology,* 25(6), pp. 1891-1892.

Thompson, A. J. and Lummis, S. C. R. (2006) '5-HT3 receptors', *Current pharmaceutical design,* 12(28), pp. 3615-3630.

Thompson, G. D., Dutton, R. and Sparks, T. C. (2000) 'Spinosad – a case study: an example from a natural products discovery programme', *Pest Management Science,* 56(8), pp. 696-702.

Thomsen, M. S., Zwart, R., Ursu, D., Jensen, M. M., Pinborg, L. H., Gilmour, G., Wu, J., Sher, E. and Mikkelsen, J. D. (2015) 'α7 and β2 Nicotinic Acetylcholine Receptor Subunits Form Heteromeric Receptor Complexes that Are Expressed in the Human Cortex and Display Distinct Pharmacological Properties', *PLOS ONE,* 10(6), pp. e0130572.

Tison, L., Rößner, A., Gerschewski, S. and Menzel, R. (2019) 'The neonicotinoid clothianidin impairs memory processing in honey bees', *Ecotoxicology and Environmental Safety,* 180, pp. 139-145.

Tomizawa, M., Maltby, D., Medzihradszky, K. F., Zhang, N., Durkin, K. A., Presley, J., Talley, T. T., Taylor, P., Burlingame, A. L. and Casida, J. E. (2007) 'Defining Nicotinic Agonist Binding Surfaces through Photoaffinity Labeling', *Biochemistry,* 46(30), pp. 8798-8806.

Towers, P. R., Edwards, B., Richmond, J. E. and Sattelle, D. B. (2005) 'The Caenorhabditis elegans lev-8 gene encodes a novel type of nicotinic acetylcholine receptor alpha subunit', *J Neurochem,* 93(1), pp. 1-9.

Treinin, M. (2008) 'RIC-3 and nicotinic acetylcholine receptors: Biogenesis, properties, and diversity', *Biotechnology Journal,* 3(12), pp. 1539-1547.

Treinin, M. and Jin, Y. (2021) 'Cholinergic transmission in C. elegans: Functions, diversity, and maturation of ACh-activated ion channels', *Journal of Neurochemistry,* 158(6), pp. 1274-1291.

Troczka, B. J., Singh, K. S., Zimmer, C. T., Vontas, J., Nauen, R., Hayward, A. and Bass, C. (2021) 'Molecular innovations underlying resistance to nicotine and neonicotinoids in the aphid Myzus persicae', *Pest Management Science,* 77(12), pp. 5311-5320.

Tsvetkov, N., Cook, C. N. and Zayed, A. (2019) 'Effects of group size on learning and memory in the honey bee Apis mellifera', *Journal of Experimental Biology,* 222(9), pp. jeb193888.

Unwin, N. (1995) 'Acetylcholine receptor channel imaged in the open state', *Nature,* 373(6509), pp. 37-43.

Unwin, N. (2005) 'Refined Structure of the Nicotinic Acetylcholine Receptor at 4Å Resolution', *Journal of Molecular Biology,* 346(4), pp. 967-989.

Ureña, E., Guillem-Amat, A., Couso-Ferrer, F., Beroiz, B., Perera, N., López-Errasquín, E., Castañera, P., Ortego, F. and Hernández-Crespo, P. (2019) 'Multiple mutations in the nicotinic acetylcholine receptor *Cchα6* gene associated with resistance to spinosad in medfly', *Scientific Reports,* 9, pp. 2961.

van Hooft, J. A., Spier, A. D., Yakel, J. L., Lummis, S. C. and Vijverberg, H. P. (1998) 'Promiscuous coassembly of serotonin 5-HT3 and nicotinic alpha4 receptor subunits into Ca(2+)-permeable ion channels', *Proceedings of the National Academy of Sciences of the United States of America,* 95(19), pp. 11456-11461.

van Klink, R., Bowler, D. E., Gongalsky, K. B., Swengel, A. B., Gentile, A. and Chase, J. M. (2020a) 'Meta-analysis reveals declines in terrestrial but increases in freshwater insect abundances', *Science,* 368(6489), pp. 417.

van Klink, R., Bowler, D. E., Gongalsky, K. B., Swengel, A. B., Gentile, A. and M., C. J. (2020b) 'Erratum for the Report “Meta-analysis reveals declines in terrestrial but increases in freshwater insect abundances”', *Science,* 70(6515).

Vergoz, V., Schreurs, H. A. and Mercer, A. R. (2007) 'Queen Pheromone Blocks Aversive Learning in Young Worker Bees', *Science,* 317(5836), pp. 384-386.

Vernino, S., Amador, M., Luetje, C. W., Patrick, J. and Dani, J. A. (1992) 'Calcium modulation and high calcium permeability of neuronal nicotinic acetylcholine receptors', *Neuron,* 8(1), pp. 127-134.

Viguera, E., Canceill, D. and Ehrlich, S. D. (2001) 'Replication slippage involves DNA polymerase pausing and dissociation', *Embo j,* 20(10), pp. 2587-95.

Wagner, D. L. (2020) 'Insect Declines in the Anthropocene', *Annual Review of Entomology,* 65(1), pp. 457-480.

Wagner, D. L., Grames, E. M., Forister, M. L., Berenbaum, M. R. and Stopak, D. (2021) 'Insect decline in the Anthropocene: Death by a thousand cuts', *Proceedings of the National Academy of Sciences,* 118(2), pp. e2023989118.

Walstab, J., Hammer, C., Lasitschka, F., Möller, D., Connolly, C. N., Rappold, G., Brüss, M., Bönisch, H. and Niesler, B. (2010) 'RIC-3 Exclusively Enhances the Surface Expression of Human Homomeric 5-Hydroxytryptamine Type 3A (5-HT3A) Receptors Despite Direct Interactions with 5-HT3A, -C, -D, and -E Subunits', *Journal of Biological Chemistry,* 285(35), pp. 26956-26965.

Wan, Y., Yuan , G., He , B., Xu , B., Xie , W., Wang , S., Zhang , Y., Wu , Q. and Zhou , X. (2018) 'F*occα6,* a truncated nAChR subunit, positively correlates with spinosad resistance in the western flower thrips, F*rankliniella occidentalis* (Pergande)', *Insect Biochemistry and Molecular Biology,* 99, pp. 1-10.

Wang, X., Meng, X., Liu, C., Gao, H., Zhang, Y. and Liu, Z. (2015) 'Cys-loop ligand-gated ion channel gene discovery in the Locusta migratoria manilensis through the neuron transcriptome', *Gene,* 561(2), pp. 276-282.

Wang, Z.-H., Gong, Y.-J., Chen, J.-C., Su, X.-C., Cao, L.-J., Hoffmann, A. A. and Wei, S.-J. (2018) 'Laboratory selection for resistance to sulfoxaflor and fitness costs in the green peach aphid Myzus persicae', *Journal of Asia-Pacific Entomology,* 21(1), pp. 408-412.

Wang, Z.-J., Liang, C.-R., Shang, Z.-Y., Yu, Q.-T. and Xue, C.-B. (2020) 'Insecticide resistance and resistance mechanisms in the melon aphid, Aphis gossypii, in Shandong, China', *Pesticide Biochemistry and Physiology*, pp. 104768.

Watson, G. B., Chouinard, S. W., Cook, K. R., Geng, C., Gifford, J. M., Gustafson, G. D., Hasler, J. M., Larrinua, I. M., Letherer, T. J., Mitchell, J. C., Pak, W. L., Salgado, V. L., Sparks, T. C. and Stilwell, G. E. (2010) 'A spinosyn-sensitive Drosophila melanogaster nicotinic acetylcholine receptor identified through chemically induced target site resistance, resistance gene identification, and heterologous expression', *Insect Biochemistry and Molecular Biology,* 40(5), pp. 376-384.

Weiss, J. N. (1997) 'The Hill equation revisited: uses and misuses', *The FASEB Journal,* 11(11), pp. 835-841.

Welti, E. A. R., Joern, A., Ellison, A. M., Lightfoot, D. C., Record, S., Rodenhouse, N., Stanley, E. H. and Kaspari, M. (2021) 'Studies of insect temporal trends must account for the complex sampling histories inherent to many long-term monitoring efforts', *Nature Ecology & Evolution,* 5(5), pp. 589-591.

Williams, M. E., Burton, B., Urrutia, A., Shcherbatko, A., Chavez-Noriega, L. E., Cohen, C. J. and Aiyar, J. (2005) 'Ric-3 Promotes Functional Expression of the Nicotinic Acetylcholine Receptor α7 Subunit in Mammalian Cells', *Journal of Biological Chemistry,* 280(2), pp. 1257-1263.

Xiong, H. and Gendelman, H. E. (2014) *Current Laboratory Methods in Neuroscience Research. Springer Protocols Handbooks* New York: Springer Science+Business Media.

Yang, E. C., Chuang, Y. C., Chen, Y. L. and Chang, L. H. (2008) 'Abnormal Foraging Behavior Induced by Sublethal Dosage of Imidacloprid in the Honey Bee (Hymenoptera: Apidae)', *Journal of Economic Entomology,* 101(6), pp. 1743-1748.

Yassin, L., Gillo, B., Kahan, T., Halevi, S., Eshel, M. and Treinin, M. (2001) 'Characterization of the DEG-3/DES-2 Receptor: A Nicotinic Acetylcholine Receptor That Mutates to Cause Neuronal Degeneration', *Molecular and Cellular Neuroscience,* 17(3), pp. 589-599.

Zhang, H., Yang, H., Dong, W., Gu, Z., Wang, C., Chen, A., Shi, X. and Gao, X. (2022a) 'Mutations in the nAChR β1 subunit and overexpression of P450 genes are associated with high resistance to thiamethoxam in melon aphid, Aphis gossypii Glover', *Comparative Biochemistry and Physiology Part B: Biochemistry and Molecular Biology,* 258, pp. 110682.

Zhang, Y., Liu, Y., Bao, H., Sun, H. and Liu, Z. (2017) 'Alternative splicing in nicotinic acetylcholine receptor subunits from Locusta migratoria and its influence on acetylcholine potencies', *Neuroscience Letters,* 638, pp. 151-155.

Zhang, Y.-C., Pei, X.-G., Yu, Z.-T., Gao, Y., Wang, L.-X., Zhang, N., Song, X.-Y., Wu, S.-F. and Gao, C.-F. (2022b) 'Effects of nicotinic acetylcholine receptor subunit deletion mutants on insecticide susceptibility and fitness in Drosophila melanogaster', *Pest Management Science,* 78, pp. 3519–3527.

Zhang, Z. Y., Li, Z., Huang, Q., Yan, W. Y., Zhang, L. Z. and Zeng, Z. J. (2020) 'Honeybees (Apis mellifera) modulate dance communication in response to pollution by imidacloprid', *Journal of Asia-Pacific Entomology,* 23(2), pp. 477-482.

Zhao, L., Qi, S., Liang, X., Shan, J., Cao, W., Wu, L. and Xue, X. (2018) 'Determination and distribution of biogenic amines in bee pollen', *International Journal of Food Science & Technology,* 53(1), pp. 166-173.

Zhao, Y., Liu, S., Zhou, Y., Zhang, M., Chen, H., Eric Xu, H., Sun, D., Liu, L. and Tian, C. (2021) 'Structural basis of human α7 nicotinic acetylcholine receptor activation', *Cell Research,* 31(6), pp. 713-716.

Zhong, W., Gallivan, J. P., Zhang, Y., Li, L., Lester, H. A. and Dougherty, D. A. (1998) 'From ab initio quantum mechanics to molecular neurobiology: A cation-π binding site in the nicotinic receptor', *Proceedings of the National Academy of Sciences of the United States of America,* 95(21), pp. 12088-12093.

Zimmermann, L., Stephens, A., Nam, S.-Z., Rau, D., Kübler, J., Lozajic, M., Gabler, F., Söding, J., Lupas, A. N. and Alva, V. (2018) 'A Completely Reimplemented MPI Bioinformatics Toolkit with a New HHpred Server at its Core', *Journal of Molecular Biology,* 430(15), pp. 2237-2243.

Zwart, R. and Vijverberg, H. P. M. (1997) 'Potentiation and Inhibition of Neuronal Nicotinic Receptors by Atropine: Competitive and Noncompetitive Effects', *Molecular Pharmacology,* 52(5), pp. 886.

Chapter 9 Appendix

Mitchell, E. L., Viscarra, F., Bermudez, I., Hawkins, J., Goodchild, J. A. and Jones, A. K. (2022) 'The Apis mellifera alpha 5 nicotinic acetylcholine receptor subunit expresses as a homomeric receptor that is sensitive to serotonin', *Pesticide Biochemistry and Physiology*, pp. 105055.

Appendix has been removed for copyright reasons.